

NASA Contractor Report 172440

126p.

FINAL REPORT: Summary of Shuttle Data Processing
and Aerodynamic Performance Comparisons for the
First Eleven(11) Flights

John T. Findlay, G. Mel Kelly, Michael L. Heck,
Judy G. McConnell

ANALYTICAL MECHANICS ASSOCIATES, INC.
17 Research Road
Hampton, Virginia 23666

Contract NAS1-16087
September 1984

(NASA-CR-172440) SUMMARY OF SHUTTLE DATA N87-10884
PROCESSING AND AERODYNAMIC PERFORMANCE
COMPARISONS FOR THE FIRST 11 FLIGHTS Final
Report (Analytical Mechanics Associates, Inc.) 126 p
CSCL 22A G3/16 43860
Unclas



National Aeronautics and
Space Administration

Langley Research Center
Hampton, Virginia 23665

NASA Contractor Report 172440

**FINAL REPORT: Summary of Shuttle Data Processing
and Aerodynamic Performance Comparisons for the
First Eleven(11) Flights**

**John T. Findlay, G. Mel Kelly, Michael L. Heck,
Judy G. McConnell**

**ANALYTICAL MECHANICS ASSOCIATES, INC.
17 Research Road
Hampton, Virginia 23666**

**Contract NAS1-16087
September 1984**

The NASA logo, consisting of the word "NASA" in a bold, sans-serif font.

**National Aeronautics and
Space Administration**

**Langley Research Center
Hampton, Virginia 23665**

FOREWORD

Of the many persons and agencies necessarily involved in any large flight data reduction activity, the authors would, first and foremost, like to acknowledge the individual effort of Mr. Harold R. Compton of the NASA LaRC Aerothermodynamics Branch of the Space Systems Division. As Technical Monitor his management and expertise enabled establishment of the necessary coordination throughout the Shuttle community which ensured data receipt and dissemination of results. The authors would also like to thank Messrs. Robert Blanchard (AB/SSD) and James C. Young (Vehicle Analysis Branch/SSD) who served as technical monitors in Mr. Compton's absence while on assignment at NASA Headquarters.

Next, and by no means incidental, the efforts of Karen D. Brender, now with the Space Station Office, and JoAnn Hudgins, AB/SSD, are acknowledged. These individuals, with contractual support from Systems Development Corporation, were responsible for Shuttle data management. Their ever cooperative response to the many additional data requests was greatly appreciated. Ms. Brender, in particular, was instrumental in the initial stages, along with Mr. Compton, in establishing the necessary data flow which made our efforts possible.

J. M. Price (AB/SSD) is acknowledged for his continued analyses and development of the Langley Atmospheric Information Retrieval System (LAIRS) files which served as our principal source of atmospheric information. The efforts of Mr. Mel Gelman of the National Weather Service are also acknowledged. His "totem-pole" atmospheres, extracted from the Johnson Space Center Best Estimate Trajectory (BET) files, serve as an alternate source of atmospheric data. Additionally, D. Richardson of the Air Force Shuttle Program Office at Edward's Air Force Base is acknowledged for consultation and delivery of jimsphere measurements for subsonic wind evaluation. This latter activity also utilizes in situ measurements from the Orbiter side probes. Post-flight air data information is obtained from either Rockwell International or the Dryden Flight Research Facility. Specific people involved who should be acknowledged are Messrs. A. Dean and S. Motchak of RI and K. Iliff and R. Maine of DFRF.

Messrs. A. Bond and P. Pixley of the Math Physics Branch of JSC are thanked for early release of their BET input products, to include tracking and telemetry source data for the TRW activity under their guidance, as well as the consultation and coordination they have provided. Many persons at the Goddard Space Flight Center must be acknowledged for delivery of the high-speed playback data we utilize. Included are I. Salzberg and F. Kallmeyer of GSFC as well as their contractors from Bendix Field Engineering Corporation, specifically Mrs. Pat Naugle Matthews.

Consultation and support of many individuals throughout the aerospace community must lastly be acknowledged. At the risk of excluding anybody, we would be remiss not to include in our list such colleagues as G. Walberg, Chief and W. Piland, Assistant Chief - SSD of LaRC; J. Jones, Head AB/SSD; Jim Arrington, Head VAB/SSD; W. I. Scallion, G. Ware, W. P. Phillips, R. Powell, and B. Spencer of the VAB/SSD; P. Siemers and D. Throckmorton of the AB/SSD; R. Barton, D. Cooke, J. Underwood, and J. Gamble of the Flight Analysis Branch of the JSC; the aforementioned D. Richardson, who also provided the theodolite data; J. Weaver and E. Henry of MPB of the JSC and J. West of the Descent Flight Analysis Branch of JSC; and R. Pelley of RI.

The list is deservedly long and it is recognized that the authors might have been remiss in failing to acknowledge some contributors. For such an oversight, apologies are in order and, hopefully, accepted.

TABLE OF CONTENTS

<u>Section</u>	<u>Title</u>	<u>Page</u>
	FOREWORD.	i
	LIST OF FIGURES	v
	LIST OF TABLES.	vii
	ABSTRACT.	viii
I	BACKGROUND.	1
II	SUMMARY OF FLIGHT DATA AND PRODUCTS	11
III	SUMMARY OF SHUTTLE CONFIGURATIONS AND LONGITUDINAL PERFORMANCE RESULTS	26
	IIIa. Ensemble results	26
	IIIb. Individual flight results.	29
IV	SUMMARY AND RECOMMENDATIONS	50
	APPENDIX A - Glossary of applicable references of AMA publications of Shuttle data analysis and results.	51
	APPENDIX B - Summary of STS-1 longitudinal results and comparisons.	60
	APPENDIX C - Summary of STS-2 longitudinal results and comparisons.	65
	APPENDIX D - Summary of STS-3 longitudinal results and comparisons.	70
	APPENDIX E - Summary of STS-4 longitudinal results and comparisons.	75
	APPENDIX F - Summary of STS-5 longitudinal results and comparisons.	80
	APPENDIX G - Summary of STS-6 longitudinal results and comparisons.	85
	APPENDIX H - Summary of STS-7 longitudinal results and comparisons.	90
	APPENDIX J - Summary of STS-8 longitudinal results and comparisons.	95

TABLE OF CONTENTS (continued)

<u>Section</u>	<u>Title</u>	<u>Page</u>
	APPENDIX K - Summary of STS-9 longitudinal results and comparisons.	100
	APPENDIX L - Summary of STS-11(41-B) longitudinal results and comparisons.	105
	APPENDIX M - Summary of STS-13(41-C) longitudinal results and comparisons.	110

LIST OF FIGURES

<u>Figure No.</u>	<u>Title</u>	<u>Page</u>
I-1	Shuttle entry data processing for BET products. . . .	7
I-2	Flow chart for Generation of Modified Maximum Likelihood Input Files (GTFILES)	8
I-3	NASA Shuttle Orbiter aerodynamic control surfaces . .	9
I-4	NASA Shuttle Orbiter RCS configuration	10
II-1	Ground tracks and vertical profiles for first eleven Shuttle entries	25
III-1	Range of longitudinal control effectors from the first eleven Shuttle flights	36
III-2	Angle-of-attack and c.g. ranges from the first eleven Shuttle entries	37
III-3	Ensemble lift comparisons from the first eleven Shuttle entries.	38
III-4	Ensemble drag comparisons from the first eleven Shuttle entries.	39
III-5	Ensemble L/D comparisons from the first eleven flights.	40
III-6	Ensemble axial force comparisons from the first eleven Shuttle entries	41
III-7	Ensemble normal force comparisons from the first eleven Shuttle entries	42
III-8	Ensemble pitching moment comparisons from the first eleven Shuttle entires	43
III-9	Ensemble flight/data base lift comparisons below Mach 2 using alternate (remote and in situ) air data sources from the first eleven Shuttle flights	44
III-10	Ensemble flight/data base drag comparisons below Mach 2 using alternate (remote and in situ) air data sources from the first eleven Shuttle flights	45
III-11	Ensemble flight/data base L/D comparisons below Mach 2 using alternate (remote and in situ) air data sources from the first eleven Shuttle flights	46

LIST OF FIGURES (continued)

<u>Figure No.</u>	<u>Title</u>	<u>Page</u>
III-12	Ensemble flight/data base C_A comparisons below Mach 2 using alternate (remote and in situ) air data sources from the first eleven Shuttle flights.	47
III-13	Ensemble flight/data base C_N comparisons below Mach 2 using alternate (remote and in situ) air data sources from the first eleven Shuttle flights.	48
III-14	Ensemble flight/data base pitching moment comparisons below Mach 2 using alternate (remote and in situ) air data sources from the first eleven Shuttle flights.	49

LIST OF TABLES

<u>Table No.</u>	<u>Title</u>	<u>Page</u>
I	NASA Space Shuttle entry flights and data sources for LaRC BETs and aerodynamic investigations. . .	17
II	Summary of NASA Space Shuttle entry flights and LaRC BET products	18
III	Summary of Shuttle trajectory reconstruction results	19
IV	Summary of Shuttle Extended BETs developed	20
V	AEROBET summary, flight profile and event date . . .	21
VI	Summary of Shuttle MMLE input files generated. . . .	22
VII	NASA Space Shuttle mass properties	23

ABSTRACT

NASA Space Shuttle aerodynamic and aerothermodynamic research is but one part of the most comprehensive end-to-end flight test program ever undertaken considering: the extensive pre-flight experimental data base development; the multitude of spacecraft and remote measurements taken during entry flight; the complexity of the Orbiter aerodynamic configuration; the variety of flight conditions available across the entire speed regime; and the efforts devoted to flight data reduction throughout the aerospace community. Shuttle entry flights provide a wealth of research quality data, in essence a veritable "flying wind tunnel", for use by researchers to verify and improve the operational capability of the Orbiter and provide data for evaluations of experimental facilities as well as computational methods.

This final report merely summarizes the major activities conducted by the AMA, Inc. under NASA Contract NAS1-16087 as part of that interesting research. Consequently, some familiarity with AMA's participation in the ongoing Shuttle research is presumed. Investigators desiring more detailed information can refer to the glossary of AMA publications attached herein as Appendix A.

Section I provides a background discussion of software and methodology development to enable Best Estimate Trajectory (BET) generation. This evolutionary discussion describes the increased level-of-effort required to enable more sophisticated LaRC product development, ultimately leading to incorporation of atmospheric information, Shuttle Orbiter wind tunnel results, and alternate measurements of vehicle dynamics. Developed were the so-called Extended and Aerodynamic BETs as well as high frequency input files for performance, control surface, and stability derivative extraction and comparisons with predicted aerodynamic parameters.

Actual products generated are summarized in Section II as tables which completely describe the post-flight products available from the first three-year Shuttle flight history. Data from a total of eleven(11) flights have been reduced, starting with the first historic Columbia flight, STS-1, and culminating with the April 13, 1984 landing of her sister ship, Challenger (STS-13). Two flights, STS-10 and STS-12, were cancelled. Summary results are presented in Section III, with

longitudinal performance comparisons included as Appendices for each of the flights. Configuration comparisons are also presented which reflect graphically those regions of the Orbiter data base sampled during the eleven Shuttle flights.

I. Background

This section presents an historical synopsis of the activities conducted under Contract NAS1-16087, from initial award in January, 1980 through the various modifications necessary to satisfy LaRC requirements. Though not referred to specifically herein, Appendix A contains a glossary of reports published under the Contract defining file contents, software descriptions and user's guides, and analysis of flight results. These references are separated as to journal articles, conference papers, NASA Contractor Reports, and company reports. The latter two categories are sub-divided as to those containing flight results and those documenting software and analysis methodology. Some of the references are actually results of studies done under separate NASA Purchase Orders but are included since these activities were so closely related to or involved extensions of the work performed under the subject Contract.

Early efforts were directed toward simulation and error analysis studies using a representative baseline Shuttle entry trajectory (OFT-1) to determine entry reconstruction accuracies. Effects of instrument errors for both the Inertial Measurement Unit (IMU) and Aerodynamic Coefficient Identification Package (ACIP) were evaluated as well as the effects due to observable model errors such as C-band range, azimuth, and elevation; S-band Doppler, and TACAN. Both Kalman-Schmidt and least squares algorithms were utilized. Further, data pre-processing requirements and software were developed for flight readiness. As part of the initial activity, continued development and validation of the then recently developed LaRC ENTREE⁽¹⁾ program were required. This activity resulted in 1) development of more rigorous S-band and TACAN modelling, to include refraction modelling as appropriate for all tracking observables, and 2) extensive filter modifications. Subsequently, Microwave Scanning Beam Landing System data (MSBLS) were added to ENTREE under separate NASA Purchase Order and altimeter and cine-theodolite tracking capability added under the subject Contract. It is noted that due to measurement accuracy and/or timing problems, neither altimeter, MSBLS

⁽¹⁾Waligora, S. R. et al., "Entry Trajectory Estimation (ENTREE) Program System Description and Users Guide," by Computer Sciences Corporation, Silver Spring, Md., NASA CR-159373, prepared under Contract NAS1-15663, Nov. 1979.

nor TACAN data have ever been utilized in the trajectory reconstruction process, except pseudo altimeter data during roll-out on the runway.

The initial activity was principally oriented toward software development and flight readiness to permit post-flight inertial trajectory determinations. The expected source for spacecraft dynamic measurements required in the prediction algorithm was the strapped down ~170 Hz ACIP data. Error analyses conducted by Bendix Aerospace⁽²⁾ showed that the as-built instrument performance, though within the 1 percent full-scale accuracy requirement, was not sufficient to permit accurate deterministic integration. A major activity was undertaken to utilize the IMU measurements, summed velocity increments in the inertial Mean of 1950 System and quaternion (platform to outer-roll gimbal) attitude information, in the strapped-down formulation. In parallel, the integration algorithm was modified to integrate the $\Sigma\Delta V$ accelerometer measurements in the inertial frame directly, an attitude independent formulation. Given that the "equivalent" strapped-down data could be derived the original prediction algorithm was commonly used.

The only remaining (potential) concern with the IMU data was the relatively limited (~1 Hz) availability of time-homogeneous measurements. For entry reconstruction purposes, this frequency was shown to be sufficient. Later, under separate NASA Purchase Order, the AMA was asked to develop high frequency (25 Hz) Modified Maximum Likelihood Estimation (MMLE) files, the so-called GTFILES. For this purpose, ACIP was to be the primary source for spacecraft dynamics in view of the MMLE input frequency requirements for RCS, stability derivative, and control surface effectiveness studies. Considerable use of the equivalent strapped-down IMU data was required herein. First, IMU data were employed directly to create files. Secondly, the more accurate measurements afforded by the IMUs enabled calibration/rectification of both the ACIP and, when utilized, the Rate Gyro Assembly/Accelerometer Assembly (RGA/AA) data. Methods were developed to rectify these measurements by removal of time interval biases in each channel to eliminate the major signal discrepancies. Later, more rigorous software was developed to calibrate

(2) "ACIP Error Correction Models," Final Report, Oct. 1980; BSR4426; Bendix Corporation, Communications Division; submitted to NASA JSC under Contract NAS9-15588.

the ACIP data versus the tri-redundant IMU measurements. A slightly modified version of the Bendix error correction model was utilized. Actual calibration coefficients were determined for STS-1, 3, 4, 5, 6, 7, 8 and 9 under funding via the JSC, either factored into the subject Contract or directly under Lockheed Engineering Management Services Corporation (EMSCO) Purchase Orders. No ACIP data were available for STS-2 due to a recorder failure. In fact, for this flight, IMU derived axial accelerations were provided by LaRC/AMA for use throughout the Shuttle community since this channel does not exist in the AA package. Generation of GTFILES, as well as the activities associated with evaluating the various dynamic data sources, resulted in a major effort under the Contract to provide LaRC researchers with the best source data available for MMLE extraction on a continuing basis.

After the first flight, AMA, Inc. became involved with development of the so-called Extended BET. This required merging of the (inertial) reconstructed trajectory data with the Langley Atmospheric Information Retrieval System (LAIRS) data. Methods were developed to do the considerable atmospheric analysis required, to include 1) analysis of expected atmospheres from the various soundings, 2) evaluation of the National Weather Service (NOAA "totem-poles") extracted from the Johnson Space Center BET files generated by TRW, 3) comparisons between the two sources (LAIRS and NOAA), 4) investigation of various available models, 5) derivation of expected atmospheres based on accelerometer measurements (requiring use of the Orbiter aerodynamic data base as discussed later), and 6) subsonic horizontal wind evaluations. Models considered were the 1962 and 1976 Standard Atmospheres as well as an Air Force reference model which, as discussed in Section II, was actually utilized for STS-9.

The subsonic wind evaluation activity involved: 1) direct comparisons between measured (from the Orbiter side-probes) and computed air data parameters given the remotely sensed balloon data; 2) comparisons with alternate measurements available from jimsphere balloons; and 3) actual estimation of winds based on the inertial trajectory information and in situ side probe measured parameters. Both deterministic and batch estimation algorithms were developed to fit the measured angle-of-attack (α), sideslip angle (β), and true air speed (V_T). In the batch

mode, a break-point model was developed to allow for a realistic variation of winds with altitude.

The Extended BET development provided LaRC Aerodynamic Coefficient Measurement Experiment (ACME) investigators with the best available post-flight data to extract flight coefficients. A major remaining task was to enable comparisons between flight data and pre-flight wind tunnel results. AMA, Inc. developed software to automate this process and provide aerodynamic comparisons (flight versus predicts) for LaRC investigators. This product, the Aerodynamic BET (AEROBET), incorporates the best available inertial trajectory and atmospheric information, and utilizes the Operational Instrumentation (OI) recorded data to define spacecraft configuration, namely control surface deflections and Reaction Control System (RCS) activity. Incorporated therein are the best available mass properties and, of course, Orbiter aerodynamic predictions. The predictions (and comparisons generated) are based on a version of the Orbiter data base made available by the LaRC which was vintage 1978. As mentioned previously, with the availability of the Orbiter aerodynamic data base, these data could be utilized with the in situ acceleration measurements and reconstructed trajectory data to compute expected atmospheres as part of the overall atmospheric evaluation process. Such Shuttle derived atmospheres resulted in some interesting spin-off meteorological research as discussed in Section II herein.

To summarize, Figure I-1 and I-2 are presented to show the various activities previously discussed. Figure I-1 shows schematically the processes involved from entry reconstruction through development of the AEROBET. Figure I-2 shows functionally the MMLE file development. For completeness, Figure I-3 and I-4 are presented which show the Orbiter control surface and RCS configurations, respectively. The two flow charts depict, in essence, the efforts required to satisfy the contractual obligation that ultimately evolved. Requirements for and software to enable trajectory reconstruction, Extended BETs, GTFILES, and AEROBETs, were developed in the order listed over the first two years of the Contract. These activities were in place by early 1982. All flights preceding this time were re-worked as required and the requirement continued for all ensuing flights up through and including STS-13.

ACIP calibration activities were only performed through STS-9 as alluded to earlier. This activity began in September 1982 requiring analysis of the previous four(4) flights at that time. Alternate funding permitted completion of the remainder of the flights involved. ACIP calibration was no longer supported after STS-9 but these data still needed to be rectified versus IMU measurements for GTFILE development.

Other tasks completed during the contractual period were 1) an analysis of Dryden Flight Research Facility (DFRF) Spin Research Vehicle (SRV) flight data using the software and methodology developed for Shuttle entry reconstruction, dynamic data pre-processing, and wind evaluation, 2) development of Extended AEROBET files to incorporate Shuttle Development Flight Instrumentation (DFI) wing surface and base pressure measurements for the five(5) flights for which DFI data were available, and 3) development of Shuttle derived atmospheres for STS-2, 4 and 6 for use in LaRC Aero-Assisted Orbital Transfer Vehicle (AOTV) trajectory analysis software. The latter two were done under separate NASA Purchase Orders but are included herein since they represent extensions of the data generated under NAS1-16087.

Finally, in support of the major activities discussed and/or to enhance researcher publication requirements, considerable software development was necessary. Some of this ancillary software are published in the form of Interoffice Memoranda and are not included in the glossary of Appendix A but can be made available upon request. Some typical functions performed were: reformatting of the on/board navigation state to obtain BETs and Extended BETs consistent with the LaRC file contents; reformatting of the JSC BETs and atmospheric information to conform to LaRC Extended BETs, AEROBETs and equivalent LAIRS files; provide graphical comparisons between these various trajectory data and the LaRC BET products; generate graphical comparisons between alternate spacecraft dynamic measurement sources as part of the overall evaluation and editing function; provide IMU derived rate and acceleration data to the JSC for Orbiter Maneuvering System (OMS) investigations during the de-orbit burn; generate stand-alone AEROBETs between Mach 2.5 and landing using the side-probe measured air data (from the Rockwell International

(RI) calibrated files) in conjunction with the LaRC BETs and OI data; modifications to the AEROBET plot utility (AROBPLT); and, development of composite statistics on the flight/prediction accuracy versus Mach number based on a selected number of flights. The latter results are more relevant to expect rather than the pre-flight variations since they are based on actual flight results, which includes the actual (perhaps dominant) contribution due to atmospheric uncertainties. To that extent, many aerodynamic investigators throughout the Shuttle community are essentially utilizing STS-3 and 5 DFI derived density to rectify the predicted normal force coefficient, C_{Np} , and, consequently, obtain atmospheres from the accelerometry measurements on other flights. In fact, this was done for Mach>12 in the development of the Flight Assessment Deltas (FADS) to date. AROBPLT modifications alluded to are the added features to display the flight/prediction statistics, including strip-charting and multiple, user selected, flight comparisons (programs STRPLOT and FLTSTRP). Graphics from these programs have been included in many publications and generated in support of LaRC researcher requirements and FADS development.

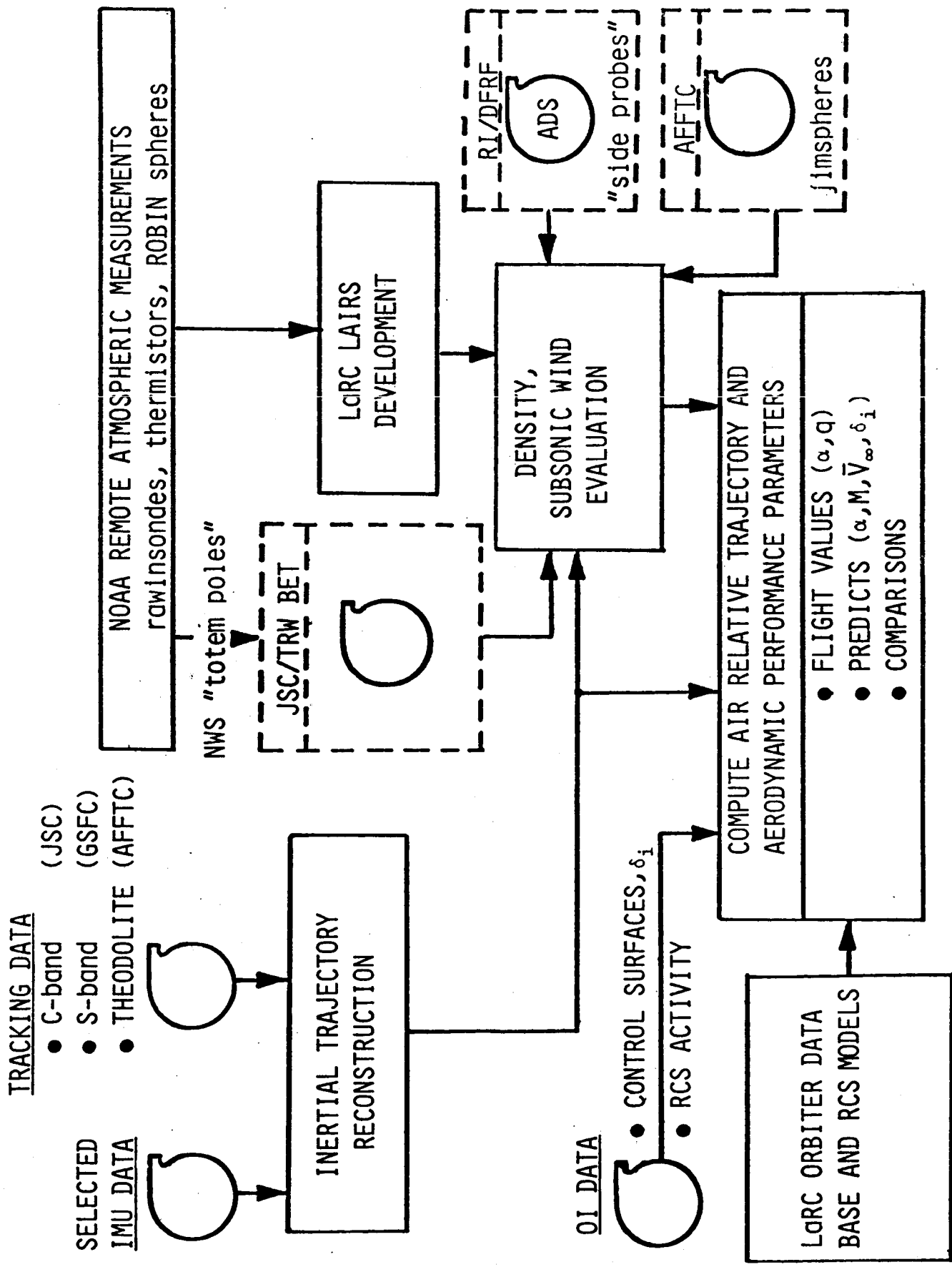
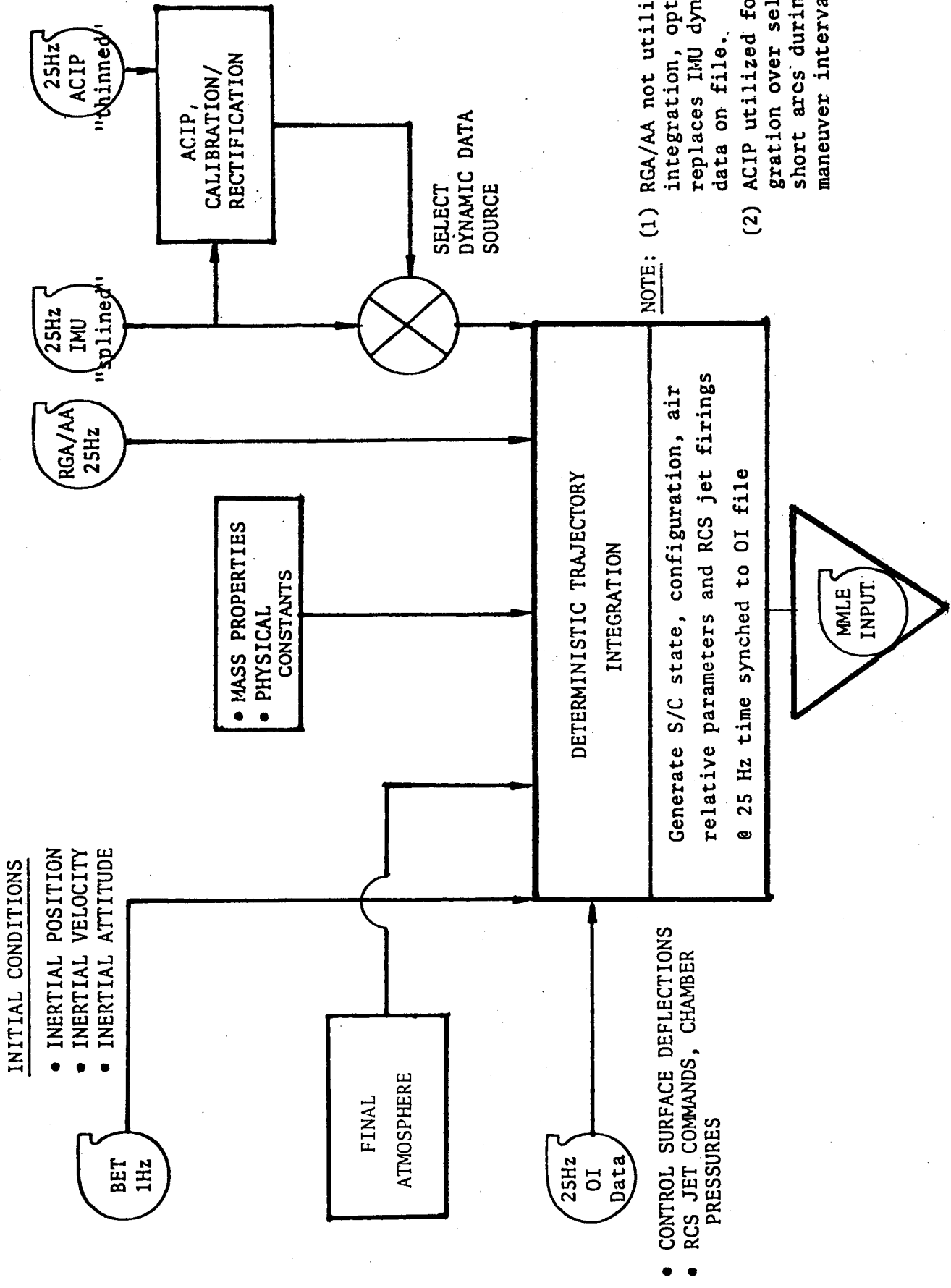


Figure I-1. Shuttle entry data processing for BET products.



NOTE: (1) RGA/AA not utilized for integration, optionally replaces IMU dynamic data on file.
(2) ACIP utilized for integration over selected short arcs during specified maneuver intervals.

Figure I-2. Flow chart for Generation of Modified Maximum Likelihood Input Files (GTFILES).

ORIGINAL PAGE IS
OF POOR QUALITY

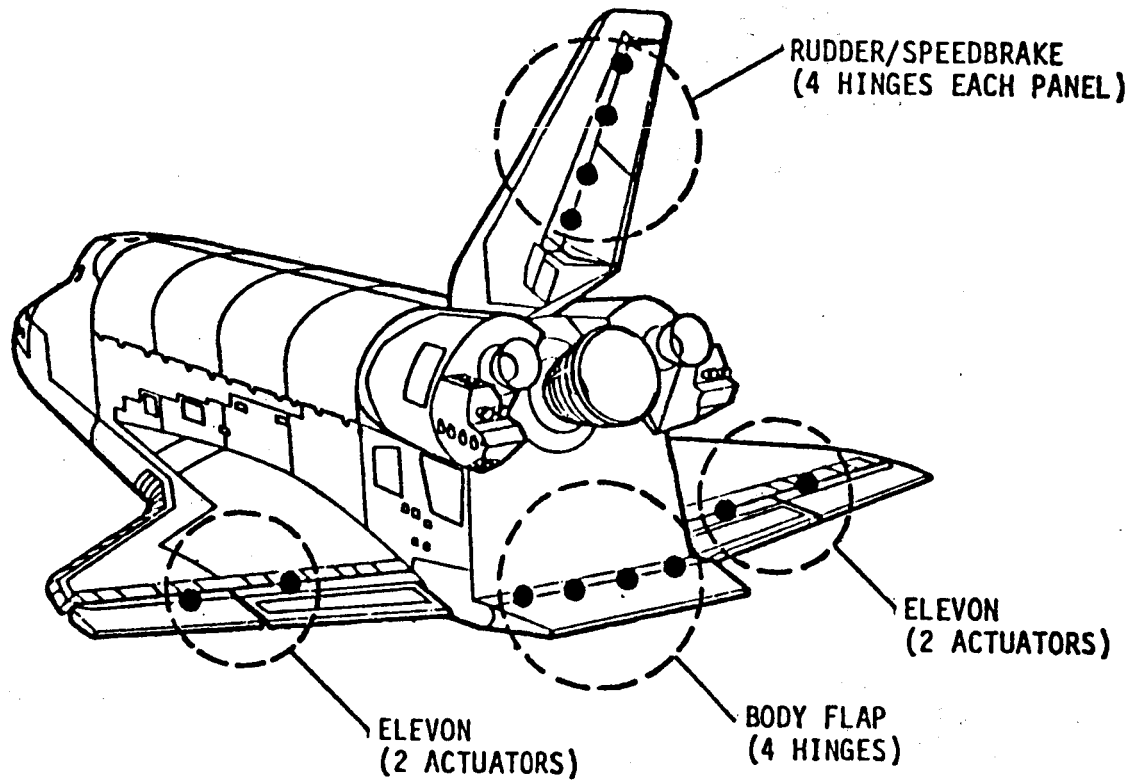


Figure I-3. NASA Shuttle Orbiter aerodynamic control surfaces.

ORIGINAL PAGE IS
OF POOR QUALITY,

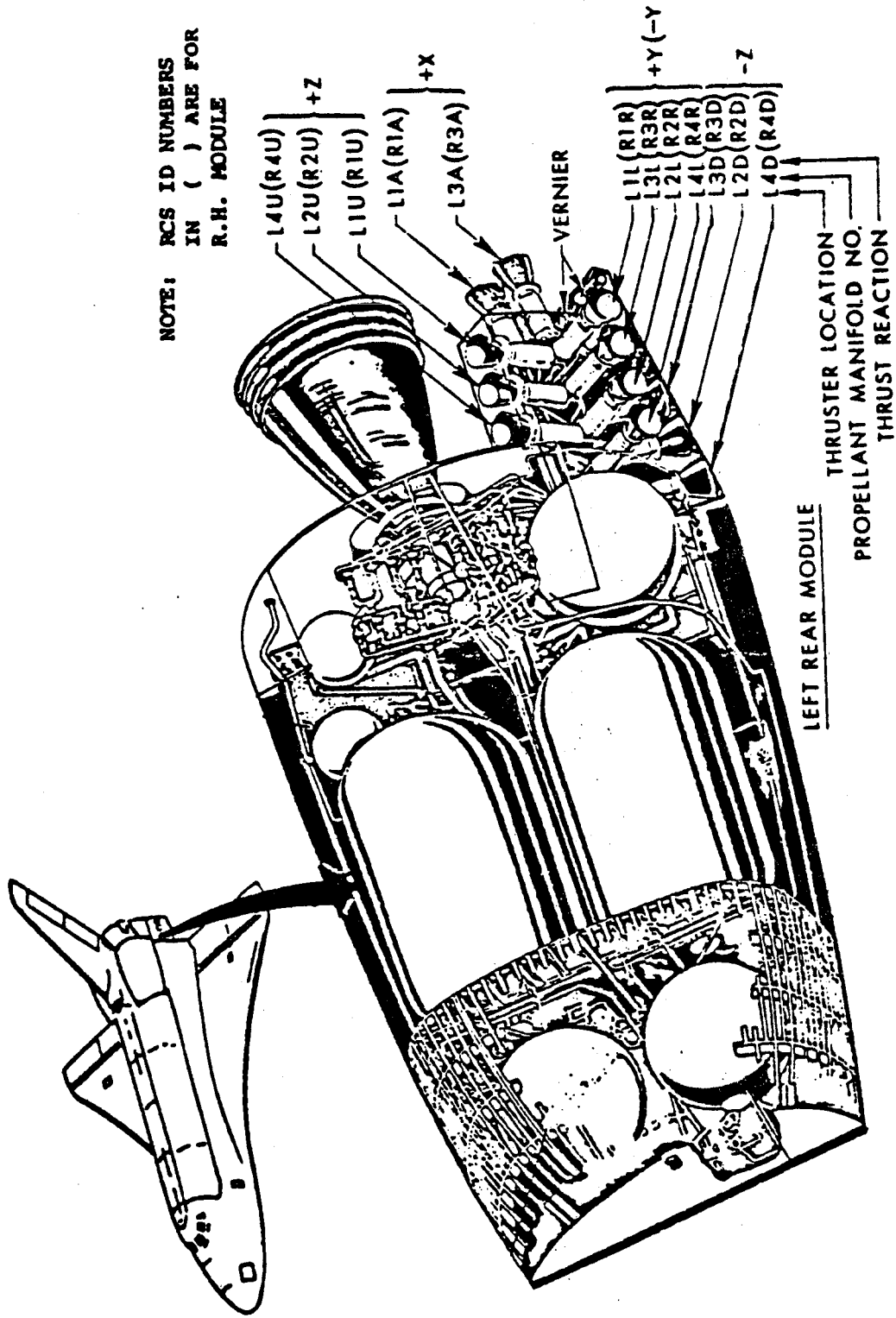


Figure I-4. NASA Shuttle Orbiter RCS configuration.

II. Summary of Flight Data and Products

Tabular summaries are presented herein which define flight data availability, post-flight products generated, and additional pertinent data utilized for the eleven flights reduced under the subject Contract. References and footnotes are included on some of the tables for researcher convenience. Each reference shown is included in Appendix A if more detail is required.

Tables I and II present a summary of the available flight data and products generated, respectively. More detailed information is presented in subsequent tables. Table I is simply an overview of the available data. Each particular flight is presented using the original STS numbering system with alternate flight designation included as relevant, e.g., for STS-11 (41-B) and STS-13 (41-C). The vehicle flown on each mission is indicated as either Columbia or Challenger. Anchor epoch (and corresponding altitude) utilized for each entry trajectory reconstruction is as shown. Dynamic and tracking data utilized are also shown. In this instance, the particular IMU selected from the tri-redundant set is indicated, with ACIP data utilized to fill an approximate two(2) minute gap on STS-7. Tracking data thereon are summarized as to the specific S-band stations, the number of C-band and cine-theodolite trackers and, where camera data were not available, the use of pseudo data during rollout and post-stop.

Atmospheric source information is indicated in the last two columns of Table I. The source for the ambient atmospheric information is seen, for the most part, to have been remote soundings. Here, ROBIN sphere, thermistor, and rawinsonde balloon data were employed. These data were processed by both the LaRC (LAIRS file) and the National Weather Service (NOAA). Density determinations based on in situ DFI pressure measurements are indicated for STS-3 and STS-5. Also, on STS-9, model data were incorporated above 140 kft. Here the Air Force 1978 Model⁽³⁾ was employed to provide for latitudinal and seasonal effects. This flight had the highest orbital inclination ($i \sim 59^\circ$) and, as such, the usual remote sites for atmospheric soundings (Barking Sands, Hawaii and

⁽³⁾ Cole, A. E., and Kantor, A. J., Air Force Reference Atmospheres, AFGL-TR-78-0051, Air Force Surveys in Geophysics, No. 382, 28 February 1978.

ORIGINAL PAGE IS
OF POOR QUALITY

Pt. Mugu, California) were not optimally located with respect to the entry ground-track. Finally, subsonic wind evaluations resulted in the choices as shown.

Table II presents a summary of the major products generated for each of the eleven flights. Footnoted are the AMA reports which define the file contents for user application.

Subsequent to publishing the AEROBET file description report (AMA Report No. 82-9), the five "spare" words, words 32-36, have been allocated to incorporate atmospheric parameters frequently used in the atmospheric evaluation process and subsequent research. The AEROBET files and plot utility are now modified as follows:

Word	Alphanumeric	Units	Symbol	Description
32	RHO RAT	NONE	ρ/ρ_{76}	Ratio of LAIRS density to 1976 Standard
33	CN RHO RAT	NONE	$\rho C_N/\rho_{76}$	Ratio of C_N derived density to 1976 Standard, utilizes predicted normal force coefficient (C_{Np}) and IMU measured normal acceleration.
34	CA RHO RAT	NONE	$\rho C_A/\rho_{76}$	Ratio of C_A derived density to 1976 Standard, utilizes predicted axial force coefficient (C_{Ap}) and IMU measured axial acceleration.
35	T RAT	NONE	T/T_{76}	Ratio of LAIRS temperature to 1976 Standard
36	PINF RAT	NONE	P_∞/P_{76}	Ratio of LAIRS pressure to 1976 Standard

No other changes have been incorporated

Included in Table II are permanent file names for the inertial trajectory information as well as the Extended BET files and Aerodynamic BET reels. MMLE input files generated are not shown thereon but are presented later. All inertial BETs are available under the Technical Monitor's user catalog, UN=169750N. Extended BETs are available under user catalog, UN=274885C. Included in the last column for information are references. These reports and papers provide potential users with the details relative to trajectory reconstruction, atmospheric evaluations which were required, details of the spacecraft configurations flown,

and aerodynamic performance comparisons. Referenced are AMA Reports, NASA CRs, and papers authored or co-authored by AMA personnel. Not included are the many publications by the Technical Monitor and other colleagues at NASA which are readily available to researchers. It is observed that results, at least through STS-8, have been published at various conferences, the last formal paper being presented at the 22nd Aerospace Sciences Meeting in January of this year.

More details relative to the inertial, Extended, and Aerodynamic BETs as well as the high frequency MMLE input files generated are next presented. Table III summarizes the trajectory reconstruction results. Here, additional information is presented relative to the actual tracking stations utilized. Solution sets employed during the weighted-least-squares fitting process are as shown for the particular flights. References are included which are specifically relevant to the trajectory reconstruction. Detailed tracking coverages, IMU selection, goodness of fit, and trajectory comparisons are each discussed in the references. As noted on Table III, the forty(40) word file contents are defined in AMA Report No. 81-1. The journal article noted discusses the IMU treatment to emulate strapped-down measurements, required in the prediction scheme utilized in ENTREE as discussed in Section I. Again, the use of the ACIP data during a gap interval on STS-7 is noted.

Table IV summarizes the Extended BETs developed. Appropriate references are as indicated thereon. Final LAIRS/or equivalent files utilized are shown. Subsonic wind evaluations resulted either in the acceptance of rawinsonde winds, the adoption of jimsphere measurements, or the incorporation of batch estimates as indicated. For the latter, post flight files based on side-probe pressure measurements were obtained from either RI or DFRF as noted. Readers are urged to peruse the two journal articles and the AIAA paper footnoted for more details as to the LAIRS file development (based on remote soundings), the subsonic wind estimation/evaluation techniques employed, and the DFI pressure data analysis. Where NOAA is indicated as the subsonic wind source, these data appeared (in some instances) to be a combination of rawinsonde and jimsphere data. References included pertain to the actual Extended BET development to include atmospheric evaluations and, in some instances, the interesting meteorological research implied in the Shuttle derived

atmospheres. Use of the in situ acceleration measurements and the Orbiter data base to derive atmospheric information suggests significant density shears and or "potholes in the sky" which seemingly conform to (potentially) unstable air masses encountered. Currently, researchers are using Shuttle derived atmospheres for trajectory analysis for future NASA AOTV missions.

Table V presents a summary of the AEROBETs generated. As indicated previously, Orbiter aerodynamic predictions were obtained from a LaRC version of the data base which is vintage 1978. Shown on this table, in addition to the flight, vehicle, epoch utilized and physical reels available, are flight profile and event data to facilitate researcher analyses. Flight profile data shown are columnar lists of time, Mach number, altitude, dynamic pressure, and Reynold's number (based on the Orbiter reference length of 107.5 ft). Eight rows are presented for each flight conforming to: 1) initial flight extraction ($h \sim 320$ kft, $q < 1$); 2) maximum Mach number encountered (altitudes below which assure a monotonically decreasing Mach variation except for very narrow intervals in the subsonic regime due principally to speed-brake sweeps); and 3)-8) six specific Mach occurrences (20, 15, 10, 5, 2, and 1). Investigators are cautioned that the initial altitude selected for flight extraction is marginal due to the ~ 1 mg quantization in the IMU accelerometry. Typically, signal-to-noise (SNR) at these altitudes is ~ 10 in the normal force direction, i.e., the predominant lift and drag producing force during hypersonic flight given the nominal 40 deg entry angle-of-attack. An SNR of ~ 10 in the axial component does not occur until $h \sim 270$ kft. Reasonable signal in both channels ($SNR > 25$) occurs by $h \sim 250$ kft, apart from STS-6 for which the selected IMU had an apparent additional 3-5 mg random noise component.

Events (times) noted are occurrence of Entry Interface (EI/ $h=400$ kft), main gear deployment (GEAR), weight on wheels (WOW), weight on nose gear (WONG), and stop time, to include the particular runway. All times are given to the nearest second relative to epoch. It is noted that, in two instances, the anchor epoch utilized for the BET was post-EI. Also, readers are reminded that the AEROBETs terminate at WOW and thus the remaining events are only included for completeness.

Table VI presents a summary of the high frequency MMLE input files generated for the first eleven Shuttle flights. The number of maneuvers shown for each flight are approximate counts to include bank maneuvers (entry and exit together are considered as one), Programmed Test Inputs, etc. as defined more completely in the identified references based on LaRC/JSC investigator's inputs. The principal source for control surface, RCS, and stability derivative extraction is the ~170 Hz ACIP data. Due to a recorder failure on STS-2, and, as shown, continued for two flights thereafter, alternate files were generated based on the RGA/AA 25 Hz data. For each flight, IMU GTFILes were generated. Here the ~1 Hz IMU data availability is perhaps a limitation even though 25 Hz spline derived dynamics are utilized. The IMU files were generated by integration of the equations of motion, utilizing the best available atmospheric data, and outputting data at 25 Hz time synchronous with the OI data. RGA/AA files were generated by simply replacing the dynamic data (P , Q , R , A_y , and A_z) on the IMU files to serve as MMLE input values. ACIP files were typically generated as a series of short arc trajectory integrations, the number of same selected to encompass each of the identified maneuvers. Thus the ACIP files are multi-file reels which can be accessed as CDC system records on the LaRC machines. Exceptions are the STS-1 files (which were developed as permanent files under user catalog 274885C), and STS-11 and 13. The latter two flights, due to loss of ACIP yaw gyro data, were developed by inclusion of RGA yaw rate information with the remaining ACIP channels to replace the spacecraft dynamic data on the 25 Hz IMU integrated files. In each instance where RGA/AA and ACIP data were incorporated, the major biases in each channel were removed by comparison versus IMU data. Alternate use of ACIP measured angular accelerations on some of the files is as noted on Table VI. In some instances, rigorous calibrations were applied to the ACIP data based on coefficients determined using the tri-redundant IMU data as the fiducial reference. This activity was performed only for those flights for which funding was available. ACIP calibration results are documented in the appropriate references as indicated in Appendix A.

Table VII presents the final mass properties utilized for the various products previously presented, namely, moments and products of

inertia, weight, and center-of-gravity (c.g.) location during entry, the latter in the Orbital Structural Reference system. This table reflects the most recent data available, requiring reworks of the AEROBET files in some instances to incorporate any updates that occurred.

Lastly, to summarize the Shuttle flights of record, Figure II-1 is presented to show the various ground tracks and vertical profiles during entry. Standard NASA symbols (see Table below) are utilized hereon for each specific flight.

FLIGHT	SYMBOL
STS-1	○
STS-2	□
STS-3	◇
STS-4	△
STS-5	▵
STS-6	▷
STS-7	◻
STS-8	◊
STS-9	◇
STS-11	⊕
STS-13	⊕

Data are plotted from epoch thru rollout. Visible by inspection are the unique ground track for the high inclination STS-9 flight, the STS-3 White Sands landing, and the first (STS-11) landing of the Shuttle at Kennedy Space Center. Though there are longitudinal differences for these latter two flights, similarities in the vertical profiles are graphically illustrated. One can infer same from the flight profile data presented in Table V herein, particularly below Mach 20. Spacecraft configuration and longitudinal performance comparisons are presented in the next Section to complete the final summary.

FLIGHT	VEHICLE	DATE	ANCHOR EPOCH / ALTITUDE	DYNAMIC / TRACKING DATA	LAIRS ATMOSPHERE	SUBSONIC WIND
STS-1	Columbia	April 14, 1981	17 ^h 42 ^m 30 ^s .0 GMT / 600kft	IMU 2 S-band : GWMS C-band : (8) stations pseudo Doppler, altimeter	remote measurements	rawheats
STS-2	Columbia	November 14, 1981	20 ^h 44 ^m 00 ^s .0 GMT / 600kft	IMU 2 S-band : GWMS, GDSS C-band : (8) stations pseudo Doppler, altimeter	remote measurements	rawheats
STS-3	Columbia	March 30, 1982	15 ^h 34 ^m 40 ^s .0 GMT / 300kft	IMU 1 S-band : HAWS C-band : (10) stations pseudo Doppler, altimeter	remote measurements DFI p 185kft-ch-240kft	batch estimates
STS-4	Columbia	July 4, 1982	15 ^h 30 ^m 21 ^s .0 GMT / 700kft	IMU 2 S-band : GWMS, GDSS C-band : (5) stations cine-theodolite : (5) cameras	remote measurements	batch estimates
STS-5	Columbia	November 10, 1982	13 ^h 54 ^m 20 ^s .0 GMT / 603kft	IMU 2 S-band : GWMS C-band : (7) stations cine-theodolite : (5) cameras	remote measurements DFI p 136kft-ch-240kft	rawheats
STS-6	Challenger	April 8, 1983	18 ^h 23 ^m 20 ^s .0 GMT / 404kft	IMU 3 S-band : none C-band : (7) stations cine-theodolite : (4) cameras	remote measurements	Imphere
STS-7	Challenger	June 24, 1983	13 ^h 17 ^m 20 ^s .0 GMT / 603kft	IMU 2, ACP in gap S-band : GWMS C-band : (8) stations cine-theodolite : (7) cameras	remote measurements	rawheats batch estimates h<8kft
STS-8	Challenger	September 5, 1983	7 ^h 1 ^m 50 ^s .0 GMT / 617kft	IMU 2 S-band : GWMS C-band : (7) stations pseudo Doppler, altimeter	remote measurements	Imphere
STS-9	Columbia	December 8, 1983	23 ^h 17 ^m 23 ^s .0 GMT / 350kft	IMU 2 S-band : GDSS C-band : (8) stations cine-theodolite : (8) cameras	remote measurements AF78 Model h>140kft	NOAA
STS-10		---	----- C A N C E L L E D -----			
STS-11 (41-B)	Challenger	February 11, 1984	11 ^h 29 ^m 40 ^s .0 GMT / 827kft	IMU 2 S-band : GWMS, HAWS, MLS, MLXS C-band : (8) stations pseudo Doppler, altimeter	remote measurements	NOAA
STS-12		---	----- C A N C E L L E D -----			
STS-13 (41-C)	Challenger	April 13, 1984	13 ^h 1 ^m 30 ^s .0 GMT / 700kft	IMU 2 S-band : GDSS C-band : (8) stations cine-theodolite : (8) cameras	remote measurements	NOAA

Table I. NASA Space Shuttle entry flights and data sources for LaRC BETs and aerodynamic investigations

FLIGHT	VEHICLE	DATE	ANCHOR EPOCH / ALTITUDE	INERTIAL BET ⁽¹⁾	EXTENDED BET ⁽²⁾	AERODYNAMIC BET ⁽³⁾ (primary/duplicate)	REFERENCES
STS-1	Columbia	April 14, 1981	17°42'30".0 (83750°.0 GMT) / 800kft	AMABETH	STS1BET	NL1020/NL1021	NASA CR- 3581 Compton, et al AIAA 81-2424 AMA Report No. 82-16 AMA Report No. 82-24 AIAA 83-0115 AMA Report No. 83-5 NASA CP-2283 Part 2 AIAA 84-0485
STS-2	Columbia	November 14, 1981	20°44'00".0 (74840°.0 GMT) / 598kft	BET2D18	STS2BET	NL1022/NL1023	AMA Report No. 82-8 AMA Report No. 82-16 AMA Report No. 82-21 AMA Report No. 82-24 AIAA 83-0115 AMA Report No. 83-5 NASA CP-2283 Part 2 AIAA 84-0485
STS-3	Columbia	March 30, 1982	15°34'40".0 (56080°.0 GMT) / 399kft	BET3M05	STS3BET	NY1003/NE1235	AMA Report No. 82-32 AMA Report No. 82-24 AIAA 83-0115 AMA Report No. 83-5 NASA CP-2283 Part 2 AIAA 84-0485
STS-4	Columbia	July 4, 1982	15°30'21".0 (55820°.0 GMT) / 788kft	BET4A31	STS4BET	NX0605/NU1165	AMA Report No. 82-33 AIAA 83-0115 AMA Report No. 83-5 NASA CP-2283 Part 2 AIAA 84-0485
STS-5	Columbia	November 16, 1982	13°54'20".0 (50060°.0 GMT) / 683kft	BET5J03	STS5BET	NK0807/NK0816	AMA Report No. 83-2 AMA Report No. 83-5 AMA Report No. 83-11 NASA CP-2283 Part 2 AIAA 84-0485
STS-6	Challenger	April 9, 1983	18°23'20".0 (86200°.0 GMT) / 404kft	BET6M26	STS6BET	NJ0417/NK0917	AMA Report No. 83-9 AIAA 84-0485
STS-7	Challenger	June 24, 1983	13°17'20".0 (47840°.0 GMT) / 683kft	BET7A12	STS7BET	NY1037/NA0810	AMA Report No. 83-17 AIAA 84-0485
STS-8	Challenger	September 5, 1983	7° 1'50".0 (25310°.0 GMT) / 617kft	BET8T06	STS8BET	NX0483/NX0484	NASA CR- 172257 AIAA 84-0485
STS-9	Columbia	December 8, 1983	23°17'23".0 (83843°.0 GMT) / 356kft	BET9J13	STS9BET	NL0624/NL0701	NASA CR- 172314
STS-10			----- C A N C E L L E D -----				
STS-11 (41-B)	Challenger	February 11, 1984	11°29'40".0 (41380°.0 GMT) / 827kft	BT11A12	ST11BET	NL0429/NF0349	NASA CR- 172349
STS-12			----- C A N C E L L E D -----				
STS-13 (41-C)	Challenger	April 13, 1984	13° 1'30".0 (46890°.0 GMT) / 700kft	BT13M23	ST13BET	NC0728/NC0740	NASA CR- 172350

(1) see AMA Report No. 81-1 for description of file
(2) see AMA Report No. 81-11 for description of file
(3) see AMA Report No. 82-9 for description of file

Table II. Summary of NASA Space Shuttle entry flights and LaRC BET products

FLIGHT	INERTIAL BET ⁽¹⁾	IMU ⁽²⁾	TRACKING COVERAGE	SOLUTION SET	REFERENCES
STS-1	AMABETH	2	S-band : GWMS C-band : (8) PTPC,PPTC,SNFC,VDBC,VDSC,VDFC,FRCC,EAFC pseudo Doppler,altimeter	state gyro drifts accelerometer scale factors	NASA CR- 3561 Compton ,et al AIAA 81-2450
STS-2	BET2D18	2	S-band : GWMS,GDSS C-band : (8) PTPC,PPTC,VDBC,VDSC,FRCC,EAFC pseudo Doppler,altimeter	state accelerometer scale factors	AMA Report No. 82-8
STS-3	BET3M05	1	S-band : HAWS C-band : (10) VDBC,VDFC,VDSC,FRCC,EAFC,WHSC,SPKC,MTLC,WSSC,HOLC pseudo Doppler,altimeter	state gyro drifts accelerometer scale factors	AMA Report No. 82-32
STS-4	BET4A31	2	S-band : GWMS,GDSS C-band : (5) PTPC,VDBC,VDFC,FRCC,EAFC dine-theodolite : (5) cameras	state accelerometer scale factors	AMA Report No. 82-33
STS-5	BET5J03	2	S-band : GWMS C-band : (7) PTPC,PPTC,HAWC,VDBC,VDSC,FRCC,EAFC dine-theodolite : (5) cameras	state only	AMA Report No. 83-2
STS-6	BET6M26	3	S-band : none C-band : (7) PTPC,SNFC,KPTC,VDBC,VDSC,FRCC,EAFC dine-theodolite : (4) cameras	state accelerometer scale factors	AMA Report No. 83-9
STS-7	BET7A12	2 ⁽²⁾	S-band : GWMS C-band : (8) SNFC,VDBC,VDFC,VDSC,FRCC,EFFC dine-theodolite : (7) cameras	state gyro drifts	AMA Report No. 83-17
STS-8	BET8T06	2	S-band : GWMS C-band : (7) PTPC,SNFC,VDBC,VDSC,FRCC,EFFC,EAFC pseudo Doppler,altimeter	state accelerometer scale factors	NASA CR- 172257
STS-9	BET9J13	2	S-band : GDSS C-band : (8) PTPC,PPTC,VDBC,VDSC,FRCC,EAFC dine-theodolite : (8) cameras	state accelerometer scale factors	NASA CR- 172314
STS-10	--	--	C A N C E L L E D	--	--
STS-11 (41-B)	BT11A12	2	S-band : GWMS,HAWS,MILS,MLXS C-band : (8) KMTC,KPTC,MLMC,MLAC,PATC,ONVC pseudo Doppler,altimeter	state gyro drifts accelerometer scale factors	NASA CR- 172349
STS-12	--	--	C A N C E L L E D	--	--
STS-13 (41-C)	BT13M23	2	S-band : GDSS C-band : (8) KMTC,KPTC,SNFC,VDBC,VDSC,EFFC,EAFC,FRCC dine-theodolite : (5) cameras	state accelerometer scale factors	NASA CR- 172350

(1) see AMA Report No. 81-1 for description of file
(2) see Heck ,et al JGCD Vol.7, No.1 pp.15-19 Jan.-Feb.,1984
(3) ACIP data used during OI gap , approximately two minutes

Table III. Summary of Shuttle trajectory reconstruction results

ORIGINAL PAGE IS
OF POOR QUALITY

FLIGHT	EXTENDED BET ⁽¹⁾	LAIRS ⁽²⁾ ATMOSPHERE	SUBSONIC WIND SOURCE ⁽³⁾	REFERENCES
STS-1	STS1BET	USE8	rawinsonde	NASA CR- 3561 Compton ,et al AIAA 81-2459
STS-2	STS2BET	USE7698	rawinsonde	AMA Report No. 82-8
STS-3	STS3BET	FLAIR3X ⁽⁴⁾ DFI ρ 185kft<h<246kft ⁽⁵⁾	batch estimate , RI ADS	AMA Report No. 82-32
STS-4	STS4BET	STS42B3	batch estimate , RI ADS	AMA Report No. 82-33
STS-5	STS5BET	STS5MET (LRS5MOD) DFI ρ 139kft<h<248kft ⁽⁵⁾	rawinsonde	AMA Report No. 83-2 AMA Report No. 83-11
STS-6	STS6BET	LAIRJ8	limsphere	AMA Report no. 83-9
STS-7	STS7BET	LAIR7B3	rawinsonde/batch h<8kft,DFRF ADS	AMA Report No. 83-17
STS-8	STS8BET	STS8MET	limsphere	NASA CR- 172257
STS-9	STS9BET	FLAIR9 AF'78 Model h>140kft	NOAA	NASA CR- 172314
STS-10	-----	C A N C E L L E D	-----	-----
STS-11 (41-B)	ST11BET	FLAIR11	NOAA	NASA CR- 172349
STS-12	-----	C A N C E L L E D	-----	-----
STS-13 (41-C)	ST13BET	NOAA13	NOAA	NASA CR- 172350

- (1) see AMA Report No. 81-11 for description of file
- (2) see Price , JSR Vol. 20,No. 2, pp. 133-140 , Mar.-Apr. 1983
- (3) see Kelly ,et al JSR Vol. 20,No. 4, pp. 390-393 , Jy.-Aug. 1983
- (4) this atmosphere was extrapolated above 246 kft
- (5) see Siemers , et al AIAA 83-0118 for DFI density derivation

Table IV. Summary of Shuttle Extended BETs developed

FLIGHT	VEHICLE	ANCHOR EPOCH	AERODYNAMIC BET ⁽¹⁾ (primary/duplicate)	FLIGHT PROFILE DATA				EVENT TIMES (secs. from epoch)							
				Time(sec)	Mach	h(ft)	q(psf)	R _{st}	EI	GEAR	WOW	WONG	STOP	RUNWAY	
STS-1	Columbia	Apr. 14, 1981 (83750° 0 GMT) @ 600kft	NL1020/NL1021	560	26.8	320	<1	1.5E4	397	2284	2308	2317	2368	23	EAFB
				641	27.4	283	4	1.2E5							
				1242	20.0	219	51	1.9E6							
				1405	15.0	194	85	3.4E6							
				1559	10.0	167	107	6.0E6							
				1770	5.0	118	193	2.4E7							
				1946	2.0	78	200	7.2E7							
2035	1.0	52	156	1.1E8											
STS-2	Columbia	Nov. 14, 1981 (74840° 0 GMT) @ 596kft	NL1022/NL1023	584	27.5	320	<1	1.6E4	398	2334	2351	2367	2408	23	EAFB
				617	28.0	295	2	6.6E4							
				1228	20.0	220	48	1.8E6							
				1422	15.0	194	76	3.0E6							
				1585	10.0	164	110	6.2E6							
				1804	5.0	115	200	2.6E7							
				1983	2.0	78	193	7.2E7							
2078	1.0	50	180	1.4E8											
STS-3	Columbia	Mar. 30, 1982 (86080° 0 GMT) @ 396kft	NY1003/NE1235	161	26.4	320	<1	1.8E4	<0	1798	1805	1820	1882	17	WHITE SANDS
				289	27.1	270	8	2.7E5							
				741	20.0	220	48	1.5E6							
				830	15.0	197	75	2.8E6							
				1094	10.0	167	108	5.8E6							
				1312	5.0	117	194	2.5E7							
				1492	2.0	77	188	6.9E7							
1580	1.0	54	148	1.1E8											
STS-4	Columbia	Jy. 4, 1982 (88820° 0 GMT) @ 768kft	N00808/NU1165	743	27.0	320	<1	1.4E4	808	2339	2359	2370	2424	22	EAFB
				787	27.3	298	2	5.7E4							
				1314	20.0	218	58	2.0E6							
				1485	15.0	194	86	3.5E6							
				1648	10.0	169	107	6.1E6							
				1842	5.0	117	209	2.6E7							
				2013	2.0	78	209	7.5E7							
2108	1.0	50	178	1.3E8											
STS-5	Columbia	Nov. 16, 1982 (80080° 0 GMT) @ 683kft	NK0807/NK0818	682	26.0	320	<1	1.6E4	530	2325	2344	2354	2411	22	EAFB
				816	26.6	280	11	3.5E5							
				1233	20.0	223	40	1.3E6							
				1454	15.0	192	84	3.3E6							
				1620	10.0	165	103	6.1E6							
				1831	5.0	117	190	2.5E7							
				2006	2.0	78	193	7.0E7							
2103	1.0	51	163	1.2E8											
STS-6	Challenger	Apr. 8, 1983 (88200° 0 GMT) @ 404kft	NJ0417/NK0917	158	26.5	320	<1	1.6E4	7	1803	1821	1834	1873	22	EAFB
				247	27.3	277	5	1.7E5							
				786	20.0	221	47	1.7E6							
				932	15.0	195	82	3.3E6							
				1087	10.0	172	92	5.3E6							
				1289	5.0	128	140	1.7E7							
				1472	2.0	78	177	6.2E7							
1571	1.0	51	157	1.2E8											
STS-7	Challenger	Ja. 24, 1983 (47840° 0 GMT) @ 683kft	NY1037/NA0810	673	26.6	320	<1	1.2E4	522	2368	2386	2400	2463	15	EAFB
				744	29.2	285	3	1.2E5							
				1297	20.0	220	51	1.8E6							
				1485	15.0	194	87	3.6E6							
				1639	10.0	167	115	6.5E6							
				1850	5.0	118	200	2.5E7							
				2025	2.0	77	199	7.1E7							
2120	1.0	53	158	1.2E8											
STS-8	Challenger	Sept. 5, 1983 (25310° 0 GMT) @ 617kft	N00483/N00484	679	27.3	320	<1	1.4E4	518	2309	2330	2339	2386	22	EAFB
				736	27.8	292	2	7.4E4							
				1264	20.0	219	50	1.7E6							
				1450	15.0	191	92	3.8E6							
				1602	10.0	171	92	5.3E6							
				1810	5.0	122	160	2.0E7							
				1987	2.0	77	191	6.9E7							
2085	1.0	50	180	1.4E8											
STS-9	Columbia	Dec. 8, 1983, (83843° 0 GMT) @ 356kft	NL0624/NL0701	86	24.7	316	<1	1.5E4	<0	1780	1800	1814	1852	17	EAFB
				180	25.9	272	5	1.6E5							
				688	20.0	215	48	1.6E6							
				897	15.0	184	108	4.3E6							
				1047	10.0	160	124	6.9E6							
				1282	5.0	113	223	3.2E7							
				1453	2.0	75	208	7.6E7							
1538	1.0	52	159	1.2E8											
STS-11 (41-B)	Challenger	Feb. 11, 1984 (41380° 0 GMT) @ 827kft	NLD429/NF0348	1092	26.7	320	<1	1.4E4	936	2757	2774	2787	2842	15	KSC
				1140	27.1	296	2	5.0E4							
				1706	20.0	215	50	1.8E6							
				1894	15.0	187	96	4.1E6							
				2042	10.0	168	93	5.4E6							
				2252	5.0	119	171	2.2E7							
				2424	2.0	78	200	7.4E7							
2514	1.0	51	167	1.2E8											
STS-13 (41-C)	Challenger	Apr. 13, 1984 (46880° 0 GMT) @ 700kft	NC0728/NC0740	510	26.5	320	<1	1.6E4	382	2178	2196	2212	2246	17	EAFB
				621	26.5	266	9	3.1E5							
				1134	20.0	220	48	1.8E6							
				1313	15.0	194	81	3.3E6							
				1469	10.0	170	93	5.4E6							
				1678	5.0	123	148	1.8E7							
				1857	2.0	77	186	6.7E7							
1954	1.0	51	168	1.3E8											

⁽¹⁾ see AMA Report No. 82-9 for description of file, Table II herein for references

Table V. AEROBET summary, flight profile and event data

ORIGINAL PAGE IS
OF POOR QUALITY

FLIGHT	MANEUVERS ⁽²⁾	IMU ⁽³⁾	IMU MMLE FILE	RGA/AA MMLE FILE	ACIP MMLE FILEs	REFERENCES
STS-1	5	2	NW0818	none	ROLL1A , (ROLL1B) BANK1 , BANK2 , BANK3 , BANK4	AMA Report No. 81-26
STS-2	29	2	NA0682	NY1021	none	AMA Report No. 82-4
STS-3	9	1	NL1016	NV0686	9 on NW0460	AMA Report No. 82-25
STS-4	11	2	NW0461	NU1158	12 on NU1160 , (NU1163) ⁽⁴⁾	AMA Report No. 82-33
STS-5	30	2	NK0819	none	17 on NK0809 , (NF1129) ⁽⁴⁾	AMA Report No. 83-2
STS-6	23	3	NK0867	none	16 on NK0924	AMA Report No. 83-9
STS-7	25	2	NY1022	none	13 on NA0809	AMA Report No. 83-17
STS-8	25	2	NX0844	none	15 on NX0943	NASA CR- 172257
STS-9	26	2	NL0606	none	18 on ND1162	NASA CR- 172314
STS-10	-----	-----	C A N C E L L E D			-----
STS-11 (41-B)	29	2	NF0364	none	1 on NF0422 ⁽⁴⁾	NASA CR- 172349
STS-12	-----	-----	C A N C E L L E D			-----
STS-13 (41-C)	26	2	NC0780	none	1 on NC0757 ⁽⁴⁾	NASA CR- 172350

- (1) MMLE input files (GTFILes) as described in AMA Report No. 81-20
(2) as specified by NASA LaRC/JSC aerodynamic investigators
(3) see Heck ,et al JGCD Vol.7, No.1 pp.15-19 Jan.-Feb.,1984
(4) measured angular accelerations on alternate reel
(5) RGA yaw rate , measured angular accelerations utilized

Table VI. Summary of Shuttle MMLE input files⁽¹⁾ generated

ORIGINAL PAGE IS
OF POOR QUALITY

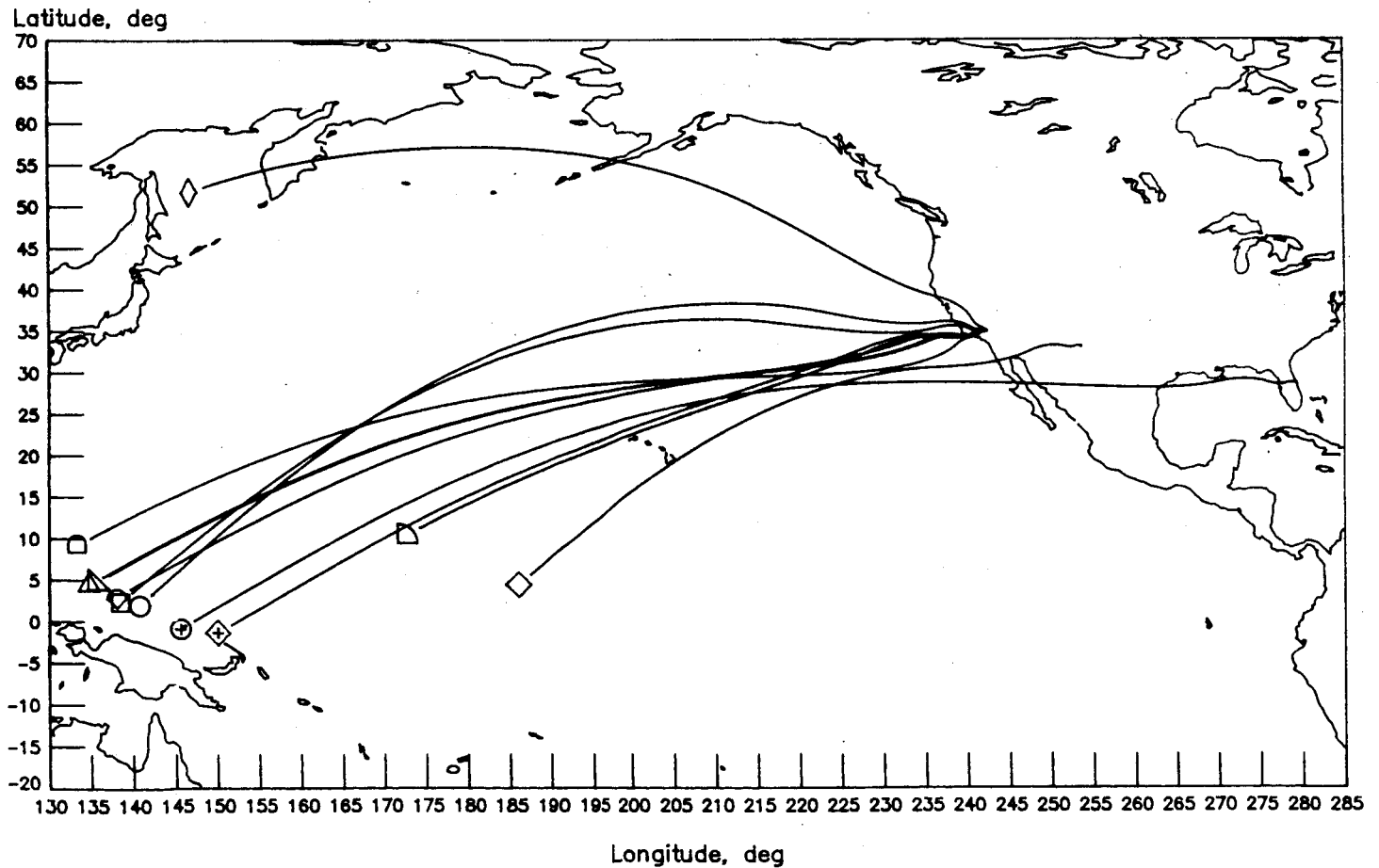
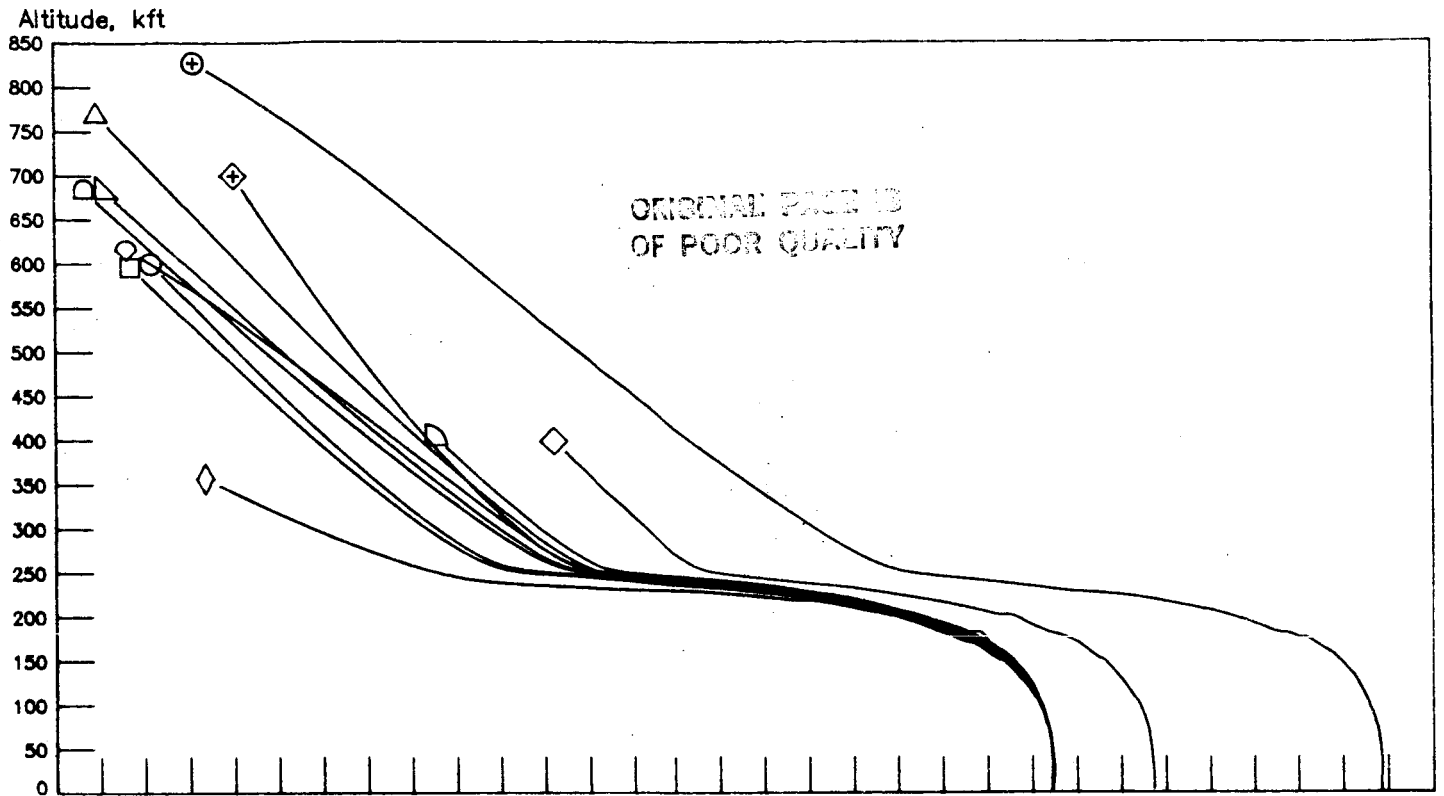
FLIGHT	MOMENTS AND PRODUCTS OF INERTIA (slugs/ft ²)																	
	I _{xx}			I _{yy}			I _{zz}			I _{xz}			I _{xy}			I _{yz}		
	EI	Mach 3	Landing	EI	Mach 3	Landing	EI	Mach 3	Landing	EI	Mach 3	Landing	EI	Mach 3	Landing	EI	Mach 3	Landing
STS- 1	882349	878858	907026	6906543	6890180	6908160	7178963	7162879	7157348	172710	167867	161592	-6587	-6099	-6110	939	1033	1099
STS- 2	930751	924149	951755	6910271	6881500	6895845	7210810	7182678	7173518	169933	160819	153630	-3128	-2975	-2698	737	715	676
STS- 3	929537	925066	953290	6894428	6873712	6891677	7201737	7181394	7175760	158717	152487	146076	-7486	-7213	-7095	-278	-295	-282
STS- 4	944326	934087	963756	6994859	6930248	6949505	7303725	7242412	7236498	159111	153033	152846	-8305	-7924	-7836	-1032	-970	-959
STS- 5	869706	863995	893142	6846693	6806871	6826284	7107288	7089455	7064216	164615	153512	147838	-19670	-19383	-19329	234	279	405
STS- 6	890570	886108	914573	6600285	6567511	6583584	6894870	6863936	6855693	156079	146895	140666	-8104	-7945	-7852	1384	1391	1437
STS- 7	905443	901034	929971	6789100	6752640	6770424	7086601	7052271	7045268	145393	132576	125433	13891	13965	14122	-2572	-2597	-2668
STS- 8	900285	895848	925221	6800431	6761535	6780901	7095637	7059155	7053631	140718	130242	123260	3541	3042	3227	-1375	-1616	-1609
STS- 9	941897	937237	966421	7091395	7056376	7076083	7399084	7365932	7360570	161505	151813	144046	-5696	-5559	-5660	775	746	673
STS-10							- - -	- C A N C	E L L E D									
STS-11 (41-B)	910919	902322	903097	6891002	6834344	6852250	7192289	7139057	7132480	153843	136928	129258	9817	7965	7959	2742	1918	2075
STS-12							- - -	- C A N C	E L L E D									
STS-13 (41-C)	898841	893657	922665	6661185	6626678	6644962	6959391	6926881	6920668	150451	140370	134902	-4673	-4510	-4319	-1588	-1585	-1592

Table VII NASA Space Shuttle mass properties

ORIGINAL PAGE IS
OF POOR QUALITY

FLIGHT	WEIGHT (lbs)			CENTER-OF-GRAVITY (Inches in Orbiter Structural Reference)													
				X _{CG}			Y _{CG}			Z _{CG}							
	El	Mach 3	Landing	El	Mach 3	Landing	El	Mach 3	Landing	El	Mach 3	Landing					
STS- 1	196587	195578	195473	1097.8	1096.4	1098.1	.7	.7	.7	372.8	372.4	369.6					
STS- 2	205879	204050	203732	1098.9	1096.7	1098.0	-.4	-.4	-.4	373.3	372.4	369.7					
STS- 3	208475	207195	207073	1096.9	1095.4	1096.9	0.0	0.0	0.0	373.0	372.4	369.8					
STS- 4	211184	209141	208947	1096.2	1092.9	1094.4	-.5	-.5	-.5	374.5	373.3	370.7					
STS- 5	203776	202643	202480	1096.6	1094.8	1096.3	1.0	1.0	1.0	371.6	371.0	368.3					
STS- 6	191384	190627	190330	1101.2	1099.6	1101.2	.3	.4	.4	371.5	370.9	368.0					
STS- 7	204983	204340	204043	1091.3	1089.8	1091.2	-.8	-.6	-.6	373.3	372.8	370.1					
STS- 8	205020	204468	204272	1091.5	1090.0	1091.6	-.1	-.1	-.1	373.5	373.0	370.3					
STS- 9	221143	220288	220027	1087.3	1085.8	1087.1	-.1	-.1	-.1	373.7	373.2	370.7					
STS-10			-	-	-	-	C	A	N	C	E	L	E	D	-	-	-
STS-11 (41-B)	202967	201529	201239	1090.7	1087.9	1089.3	1.3	1.3	1.3	372.6	371.6	368.8					
STS-12			-	-	-	-	C	A	N	C	E	L	E	D	-	-	-
STS-13 (41-C)	198153	197233	197058	1101.5	1099.7	1101.3	-.1	-.1	-.1	371.6	371.0	368.2					

Table VII (concluded)



STS 1-9,11,13 Entry Ground Tracks

Figure II-1. Ground tracks and vertical profiles for first eleven Shuttle entries.

III. Summary of Shuttle Configuration and Longitudinal Performance Results

This section summarizes the results obtained from the first eleven Shuttle flights. Presented are configuration and longitudinal performance comparisons. Ensemble results are first presented. These results are separated by vehicle with the Columbia flight envelope shaded and the Challenger flights indicated by dashed intervals. Individual flight results are also discussed with figures attached as Appendices. More details relative to actual flight configuration and results can be seen therein. No vehicular distinction is made, rather, actual flight results are presented with (shaded) comparisons included based on the remaining ten(10) flights. Alternative atmospheres and/or air data are discussed as relevant.

IIIa. Ensemble results

Longitudinal control surface deflections are shown in Figure III-1 versus Mach number. Presented are elevator, body flap, and speed brake profiles, the latter with respect to the aerodynamic reference line. As indicated, the results are separated as to the particular vehicle flown. This is simply a matter of interest for presentation since there are no expected aerodynamic differences between the two. The results simply demonstrate the opportunities (and repeated opportunities) for extraction provided by the particular vehicle, in essence, the region of the data base sampled during each vehicle's flights. The total range of longitudinal control surface deflections available would, of course, be represented by the extremes of either boundary, i.e., whichever is maximum or minimum within the interval.

The composite plots of Figure III-1 reflect a somewhat narrow band of elevator deflections (apart from some deflections during major longitudinal maneuver periods) when compared to the full throw positions of -35 deg (up) to 20 deg (down). As shown, the Challenger flights do add some opportunities toward the positive (downward) direction. The range of body flap deflections exercised is far more appreciable when compared to the full range of deflections available, namely, -11.7 deg upward to 22.55 degrees downward. Columbia, principally due to STS-9, offers the most opportunity to investigate negative (upward) body flap effectiveness throughout most of the hypersonic regime, at least for

Mach > 10. Below Mach 10. Challenger flights STS-8 and 11 as well as STS-13 extend the range of body flap deflections to evaluate, the former two governing negative deflections and STS-13 providing the narrow (positive) profile around Mach 2. Speed brake deflections, apart from the various sweeps performed during subsonic flight, are basically two profiles. Columbia flight STS-9 does present a somewhat unique opportunity at Mach ~1.5.

Figure III-2 shows angle-of-attack and center-of-gravity profiles for the Shuttle entries to date, again separated as to the particular vehicle flown. The c.g. data presented thereon, in the Orbiter Structural Reference System, are for information only and are perhaps more relative when compared to the nominal 65 percent value commensurate with the data base, namely, $X_{CG} = 1076.7$ inches and $Z_{CG} = 375$ inches. The most aft c.g. flown was on Challenger (STS-6 and 13) and the most forward value on Columbia (STS-9). Again, the α profiles, apart from maneuvers effected during hypersonic flight, correspond to two separate (nominal) profiles. Challenger typically flew the higher α profile below Mach 12. More variation is seen in α during subsonic flight. Details on these parameters can be seen in the attached Appendices. This concludes the ensemble configuration discussion. Next, longitudinal performance results are presented.

The next six figures, Figures III-3 through III-8, show ensemble comparisons (by vehicle) for lift, drag, L/D, axial, normal, and pitching moment coefficients, respectively. Shown on each figure are percentage differences (flight-data base/flight) as well as actual coefficient differences (flight-data base). Columbia results are represented by the shaded band and Challenger results by the dashed lines. A line drawn through the middle of either interval would reflect the mean difference. The width of either interval is $\pm 1\sigma$ about the mean, i.e., 2σ wide. It is felt that the mean curves would be a good estimate of any data base prediction deficiency. The spread is representative of the flight determination accuracy, in particular, influenced if not dominated by atmospheric uncertainties. It is noted that the Columbia statistics are influenced at the uppermost Mach numbers by: 1) STS-9 results, for which no adequate remote atmospheric data were available; and, 2) STS-2 and STS-4 results, for which severe density structure was

evident in the accelerometry but not indicated in the remote measurements for various reasons and/or limitations. These latter two flights were the first to exhibit significant density shears or "potholes-in-the-sky". From the results, it would appear that a reasonable upper threshold for accurate flight reduction and/or data base comparisons would be Mach~26.

Referring to Figures III-3 through III-8 one can see some differences in the results when separated by vehicle. This result is indicative of the different α profiles between Mach 4 and 12 for the two spacecraft, i.e., configuration dependent and not differing vehicular aerodynamics. Composite statistics for the two vehicles together can be inferred in the figures by inspection. Such results are presented in the Appendices in which, for a particular flight, the sample statistics shown were generated based on the remaining ten flights independent of vehicle.

In the Appendices, Mach number is plotted on a log scale to show greater detail in the subsonic/supersonic regimes. As a consequence, since the data below Mach 2 are more visible, it is worthwhile to present similar expanded results herein. This permits incorporation of the Orbiter air data measurements from the side-probes as an alternative to the measured/evaluated winds. Figure III-9 through III-14 show C_L , C_D , L/D , C_A , C_N , and C_m results below Mach 2. No vehicular distinction is made herein. The shaded region represents the ensemble statistics using the measured winds (from the AEROBETs). The dashed interval utilizes the measured air data (α and q). Both percentage differences and coefficient deltas are presented on each figure. The most significant differences seen are 1) the noticeable broadening in the uncertainties for lift and drag (and C_N of course) near landing when employing the side probe data, and 2) the systematic differences, though small, above Mach 1.2. For the latter, the AEROBET results are considered less susceptible to systematic flight-to-flight biases since common algorithms are utilized to reduce the in situ side probe pressure measurements. In any event, it might be more reasonable to eyeball some mean curve combining both sources, utilizing whichever boundary represents the extreme within a Mach interval to reflect the current composite accuracy for the first eleven flights.

IIIb. Individual flight results

STS-1 (See Appendix B)

Presented in Appendix B are STS-1 flight results cast versus the remaining ten flights (shaded regions). Control surface deflections are given as Figure B-1. STS-1, of course, provided investigators with the first real opportunity to compare flight data and wind tunnel results over the entire speed regime. Even after eleven flights, STS-1 still provides some of the better opportunities for negative elevon, positive body-flap, over much of the hypersonic regime.

Figure B-2 presents the α profile for STS-1 as well as the c.g. flown with comparisons versus the other flights. The α profile shows, as one might expect, that the first historic flight was virtually devoid of aerodynamic extraction maneuvers per se. Performance comparisons for STS-1 are presented as Figure B-3. Here lift, drag, L/D, C_A , C_N , and C_m are presented as percentage differences. In Figure B-5, a significant shift in ΔC_A is observed at Mach ~14 conforming to boundary layer transition ostensibly initiated by a gouged tile.

It is observed that there are some regions where STS-1 results appear as outliers from the remaining ensemble of flights. To that extent, results are shown (as the dashed line) based on the NOAA "totem-pole" atmospheres. The alternative atmosphere for this flight, at least within the major regions of disagreement, does yield more consistent results. Though this has not generally been the rule, in retrospect it might have been prudent to adopt the NOAA atmosphere for this flight. In any event, though hindsight is often valuable, the STS-1 flight, independent of atmosphere, was the first to show investigators the small increased performance (L/D) during hypersonic flight and the large pitching moment discrepancy, attributable for the most part to real gas effects on the basic pitching moment.

STS-2 (See Appendix C)

Figures C-1 through C-3 present control surface, α , c.g. profiles, and longitudinal performance comparisons for STS-2. For this flight, the first real indication of significant density structure was encountered. A "pothole-in-the-sky" is suggested in Figure C-3 between Mach 22.5 and 26 in which, abruptly, less density was suggested in the

accelerometry than that sensed by the remote soundings. Alternate atmospheres for this flight yielded virtually the same results. This structure, possibly a gravity wave, was centered around an altitude of 240 kft and was some 20 kft deep. Another possible explanation of this phenomenon is that a convectively unstable air mass was encountered. Most aerodynamic investigators have ruled out flow field arguments since the phenomenon was not repeatable from flight to flight. Some indication of the aerodynamic extraction maneuvers performed during this flight can be seen in the α and control surface profiles. The ACIP data were lost due to a recorder failure so MMLE investigators were required to utilize the RGA/AA measurements (supplemented by IMU derived axial acceleration) for this flight.

STS-3 (See Appendix D)

Similar results for STS-3 are given in Appendix D as Figures D-1 through D-3, respectively. For this flight, in situ DFI fuselage pressure measurements were utilized to derive q in the high Mach environment ($13.4 < M < 25.6$). Above this Mach range, the remote sounding data were rectified to remove the considerable shift in density (~25 percent) and scaled upward accordingly. An error analysis of the DFI derived density suggested these data to be accurate to ~5 percent. STS-3 was the first and only mission that landed at White Sands and the subsonic winds encountered were the most significant to date.

STS-4 (See Appendix E)

Longitudinal control deflections (Figure E-1), α and c.g. profiles (Figure E-2), and longitudinal performance comparisons (Figure E-3) are presented for STS-4 in Appendix E. The atmosphere encountered on this flight, at least as suggested in the accelerometry data, showed the most significant structure to date. Large, abrupt, density shears can be seen above Mach ~23 in the performance comparison curves. This structure, as was the case for STS-2, was also suggested in the 230 kft to 250 kft altitude region and was not substantiated by any of the remote sounding data available. Two significant longitudinal extraction opportunities are seen in the α profile for this flight, specifically at Mach 7.5 and 12.

STS-5 (See Appendix F)

STS-5 longitudinal comparisons, presented in Appendix F as Figure F-3, were also based on DFI q. For this flight, the derivation was done for an altitude range of 139 kft <math>< 248</math> kft, i.e., conforming to essentially the same uppermost Mach number as STS-3 (M~26) but extended down to M~7. It is stated that for this flight excellent remote data were available and the resultant flight/data base comparisons from either source were excellent, with some differences observed locally in the region of Mach 17. From Figure F-1 one can observe that STS-5 was the first flight to fly the lower speed brake profile in the (approximate) Mach range, 3 to 10.

At this time in the Shuttle Program the Columbia was taken off line and reconfigured for the European Space Agency Spacelab 1 mission (STS-9). What is not apparent from the figures in the Appendices is the more consistent hypersonic pitching moment difference curves which result based only on the first five Shuttle flights. In contrast, the largest C_m discrepancy was for STS-9, also, a Columbia flight, which had the most forward c.g. and negative body flap profile. However, over the first five flights a somewhat less range of elevon deflections was flown but, more importantly, significantly less were the ranges of body flap and X_{CG} profiles associated with these flights. Typically, the hypersonic pitching moment difference through STS-5 was -65 percent (± 10 percent) based on the data base reference length ($.65 X/\ell$), due principally to the fact that the LaRC data base does not provide for the (expected) nose up moment due to real gas effects.⁽⁴⁾ More discussion on the hypersonic pitching moment differences are presented at the end of this Section.

STS-6 (See Appendix G)

Results of STS-6, the first Challenger flight, are given in Appendix G. This flight was the first to fly the higher α profile ($3 < M < 10$) as shown in Figure G-2. Within that interval, the data base comparisons suggested an even larger overprediction (see Figure G-3) with

⁽⁴⁾ for example, refer to Griffith, B. J., Maus, J. R., and Best, J. T., "Explanation of the Hypersonic Longitudinal Stability Problem - Lessons Learned," NASA CP 2283, Part 1, March 1983.

the adopted LAIRS atmosphere. Since the L/D difference in part of the interval, and pitching moment discrepancy throughout, was quite different than the first five flights this was felt to be a possible α effect, awaiting STS-8 results for substantiation. Now, again in retrospect, it does appear more likely that the data base differences are merely atmospheric in nature. This can be seen by referring to the alternate NOAA results of Figure G-3 which are more consistent with the sample statistics. Additionally, referring to the ΔC_A figure, the increased noise (3-5 mg random component) on the selected IMU for this flight is quite noticeable (e.g., above Mach 6). As a consequence, boundary layer transition, if it occurred at all, is not as noticeable on this flight as with most other Challenger flights.

STS-7 (See Appendix H)

The STS-7 results in Appendix H suggest no major differences though the hypersonic pitching moment difference curve (Figure G-3) is noticeably different. Again, boundary layer transition is quite noticeable in the ΔC_A curve at Mach ~13. It is observed that the pitching moment between Mach ~2 to Mach ~10 is almost exactly as predicted.

STS-8 (See Appendix J)

Longitudinal control effectors presented as Figures J-1 show STS-8 does provide some unique body flap possibilities between Mach 2.5 and 9. On average, the body flap is some 7 degrees more negative in most of this interval when compared to the STS-7 profile. Since the pitching moment therein was almost perfectly predicted during STS-7, one could look at the reasonably solid (on average) -15 percent STS-8 ΔC_m to obtain a first order effect. Again, the α profiles for these two flights were different, by as much as 5 degrees at Mach 10. As with STS-6, this flight flew the (nominally) higher α profile below Mach ~10. The effect alluded to in the STS-6 discussion (principally in terms of force difference) was thus unsubstantiated. Boundary layer transition on STS-8, as with most of the Challenger flights, occurred quite early, viz. M~15.

STS-9 (See Appendix K)

This Columbia flight establishes many boundaries of opportunity considering the flights of record. Near Mach 1, a higher α was flown. Hypersonically (and again during transonic flight) the most

negative body flap was flown. Also, some different (though not significant) elevator deflections were flown, viz, $M \sim 1.5$. In this interval, a unique speed brake opportunity is available for investigators. Finally, this flight represents the most forward c.g. flown (see Figure K-2). As alluded to earlier, considering the entry ground track in relation to the remote rocket sites, not surprisingly the remote atmospheres were unuseable. Thus, the AF'78 Reference Model was necessarily adopted and, again not surprisingly, hypersonic flight/data base comparisons are of questionable accuracy. The atmosphere notwithstanding, the hypersonic pitching moment difference curve (Figure K-3) is quite unique.

STS-11 (See Appendix L)

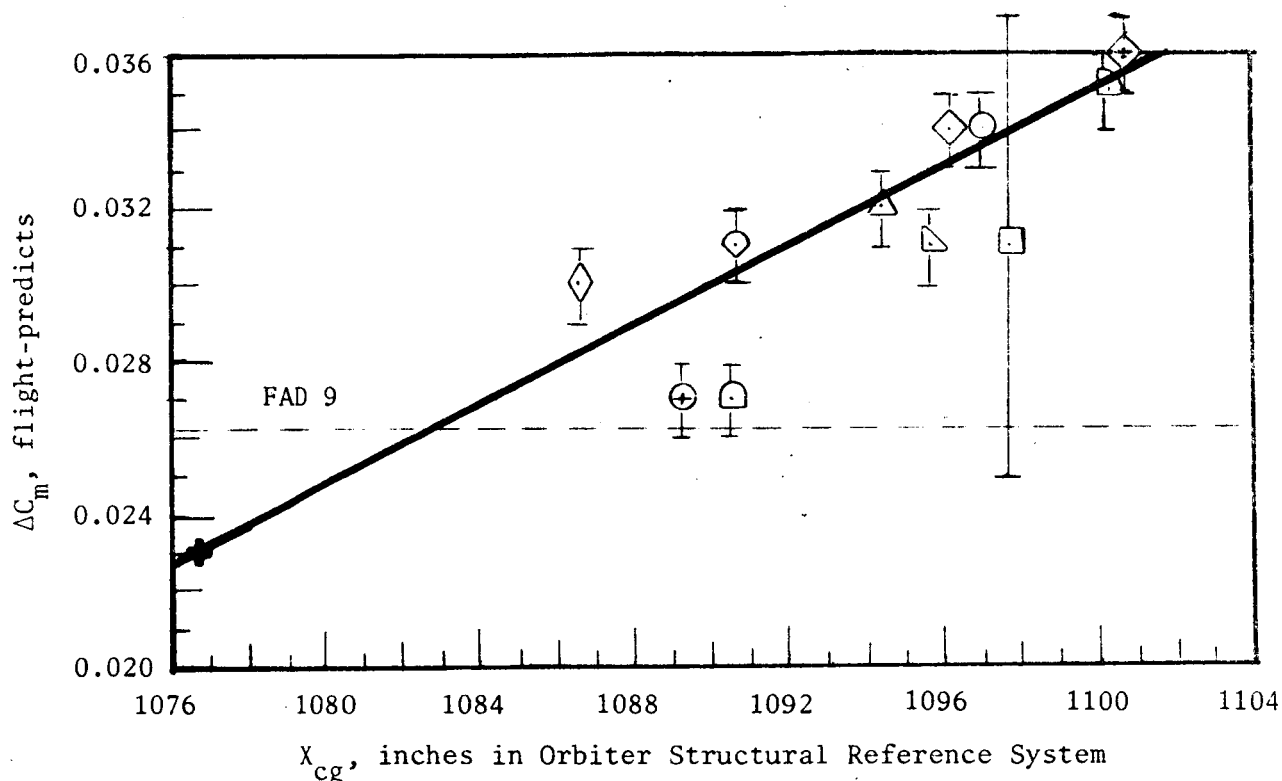
STS-11 results are summarized in Appendix L. The longitudinal control surface plots (Figure L-1) show only narrow regions wherein unique opportunities are provided. The performance comparisons for the adopted LAIRS atmosphere (Figure L-3) do show significant curvature in the vicinity of Mach 10 where, perhaps coincidentally, the body flap is moved from its uppermost position. The alternate NOAA "totem-pole" atmosphere results are superimposed on the performance curves for comparison, however, throughout most of this interval the LAIRS data yield much better results. Though the difference between atmospheres above Mach ~ 7 is not readily explainable, each (including the AF'78 model) suggest the ~ 13 percent overprediction at this Mach number.

STS-13 (See Appendix M)

Results from the final flight analyzed under the Contract are presented in Appendix M. The control surface profiles show more positive (downward) δ_E opportunities exist in the hypersonic regime than the preceding 10 flights. Also, in the Mach 1 to 2 range, the body flap boundaries are extended downward to as much as 5 degrees. Flight/data base differences (Figure M-3) show no major regions wherein this flight's results would appear as outliers from the remaining ensemble. A possible exception is ΔC_m wherein hypersonic results are less negative in general and supersonic results are trending to the opposite side of the statistical band. This flight, along with STS-6, represents the most aft c.g. profile flown and, not coincidentally, the STS-6 pitching moment difference curve is virtually identical as indicated. In contrast, STS-7,

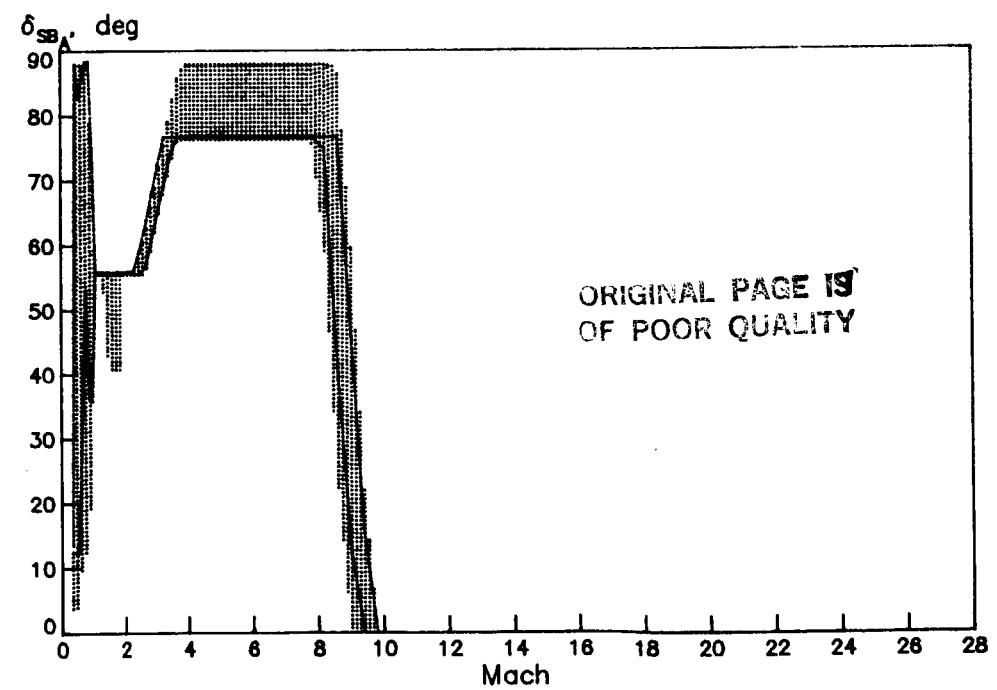
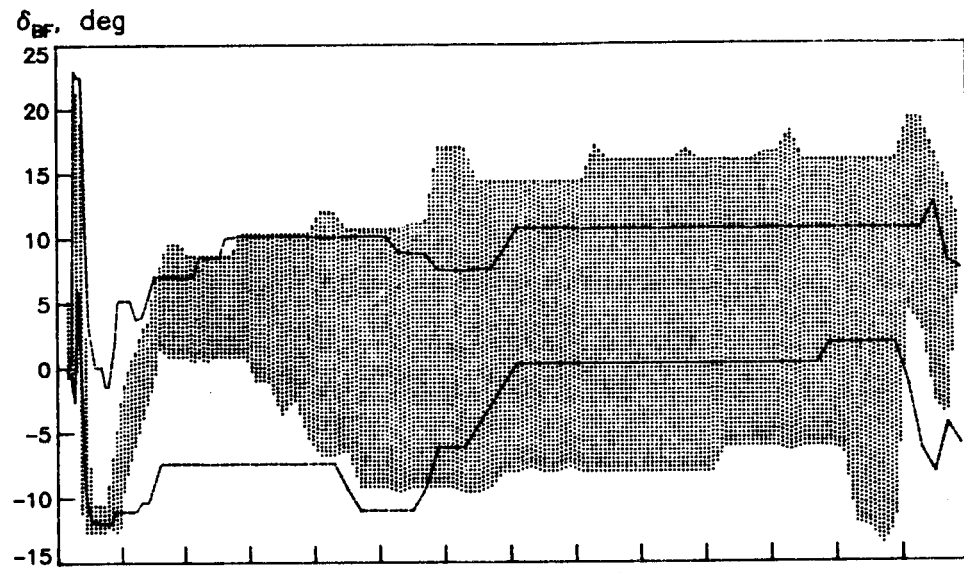
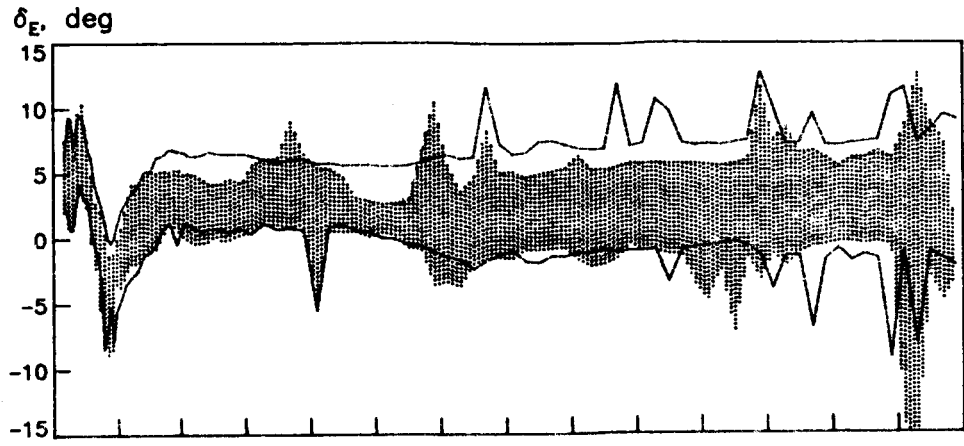
ORIGINAL PAGE IS
OF POOR QUALITY

8,9, and 11 results showed similar correlations. These flights were the most forward c.g. flights. Typically, the most aft c.g. flights show the smallest C_m percentage error, the more forward indicate larger percentage discrepancies. In terms of the actual coefficient delta, the reverse is true. The following figure shows plots of the delta C_m (flight-predicts) versus X_{CG} at Mach 20 as a typical example.



Shown thereon are the mean results for each flight (using the previously established symbols) and a measure of the uncertainty about each point. The broad range shown for STS-2 results from the fact that a maneuver was performed during this Mach interval. Also shown on this figure is the FAD 9 pitch up incremental (0.0261) and a (reasonable) fairing through the flight data. The fairing drawn passes through ~ 0.023 at the data base reference c.g., comparing with the published results of Griffith, et al. footnoted earlier. Admittedly, honoring the current FAD would have yielded a reasonable fairing except for STS-5, 7, and 11. Applying the FAD 9 correction to the LaRC data base would make the percentage error in C_m actually less for the more forward flights. Certainly the hypersonic discrepancy is not entirely due to real gas

effects though resolution at this time is difficult. The previous FAD (STS-6 Deltas) had a C_{m_0} correction of 0.0296, more in line with the earlier more aft c.g. flights which also had the more positive body flap profiles. Currently investigators are considering less body flap effectiveness for the positive (downward) deflections. Many factors must be addressed, e.g., c.g. uncertainty (an inch is very significant); control effectiveness for the two contra-opposing pitch control effectors (body flap and elevons); and the contribution due to the basic body (apart from the real gas effect). Correlations with both body flap and elevon are not as readily seen in the flight data. Nor is there any apparent correlation with Z_{CG} which might lead one to determination of a viscous contribution. Certainly, additional flights will provide the necessary data to resolve this highly coupled problem. For the moment there is (hopefully) sufficient data in the attached Appendices to facilitate researchers in their aerodynamic investigations.

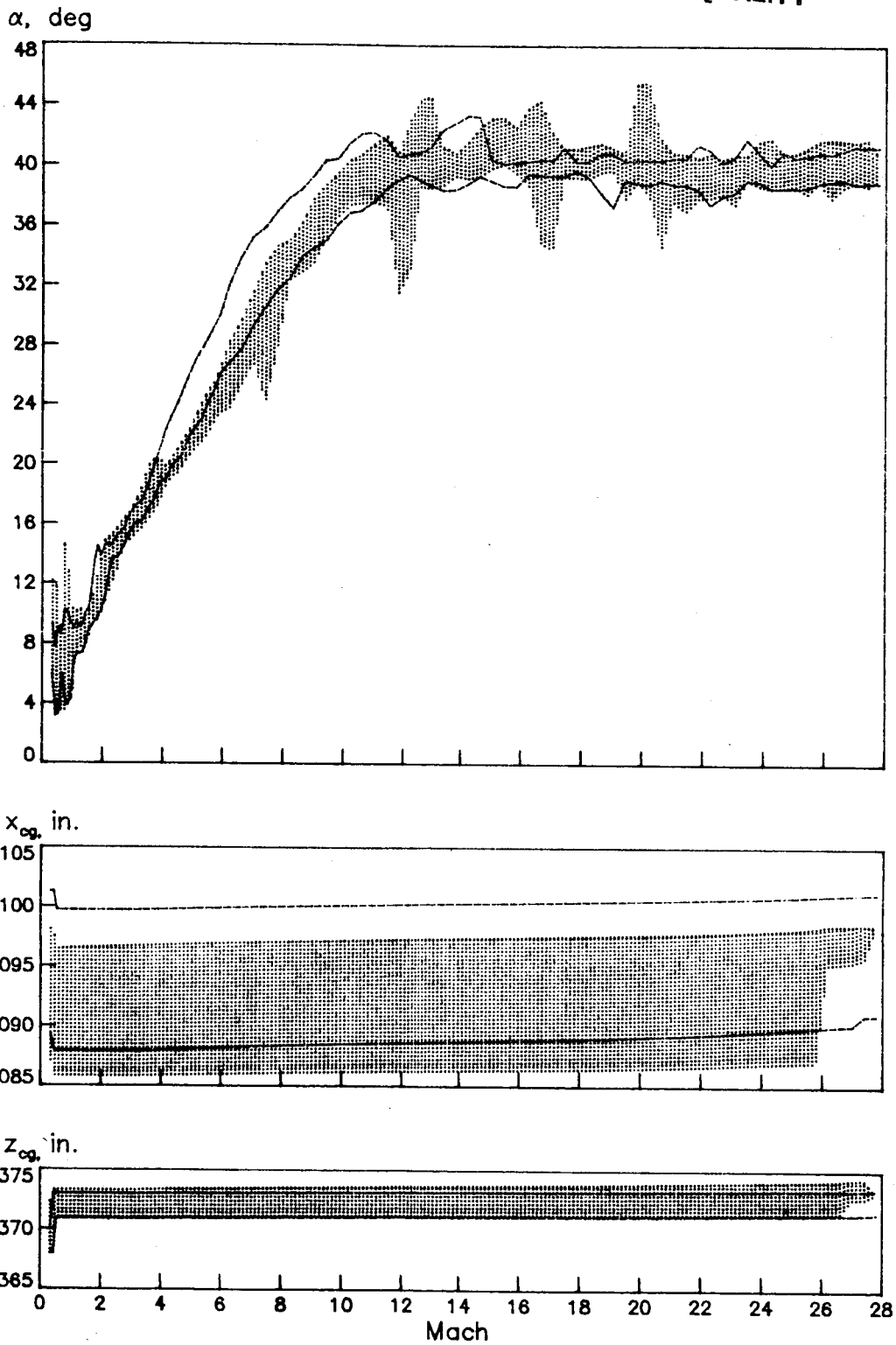


ORIGINAL PAGE IS
OF POOR QUALITY

NOTE : Columbia (shade) ; Challenger (dash)

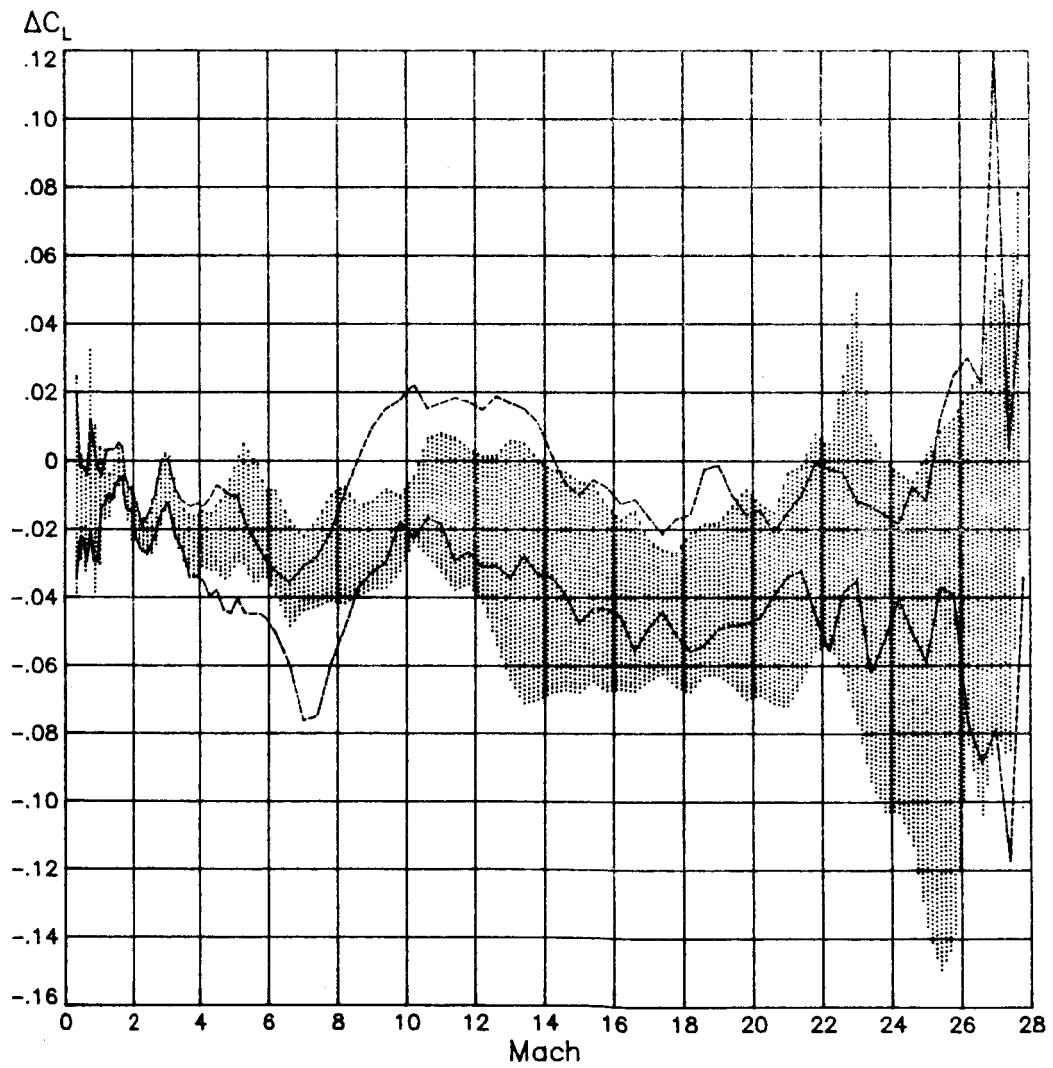
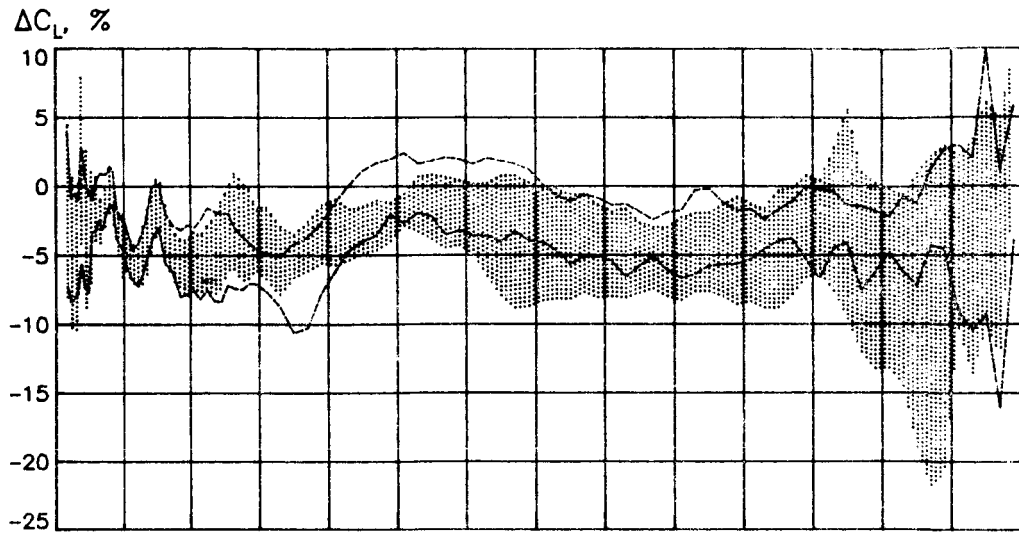
Figure III-1. Range of longitudinal control effectors from the first eleven Shuttle flights.

ORIGINAL PAGE IS
OF POOR QUALITY



NOTE : Columbia (shade) ; Challenger (dash)

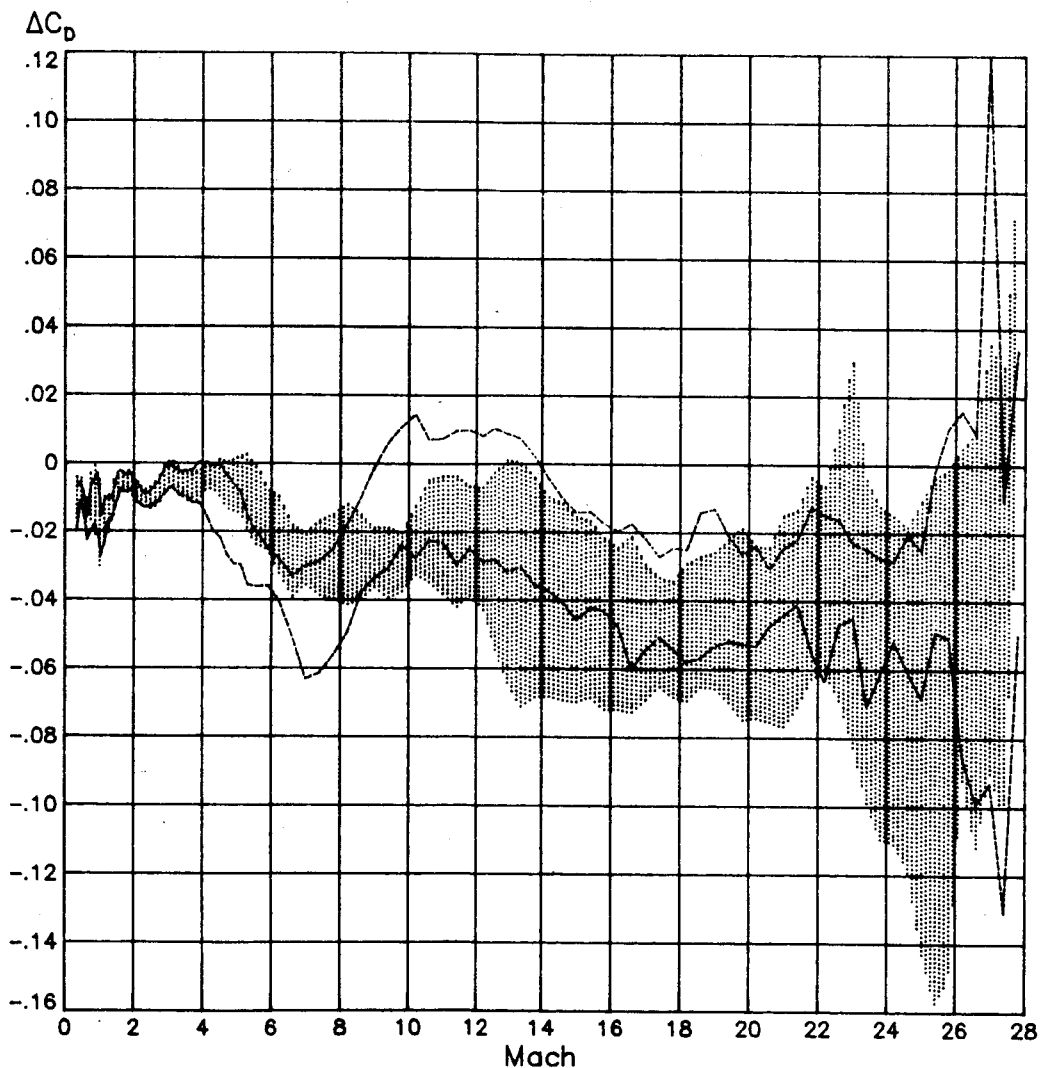
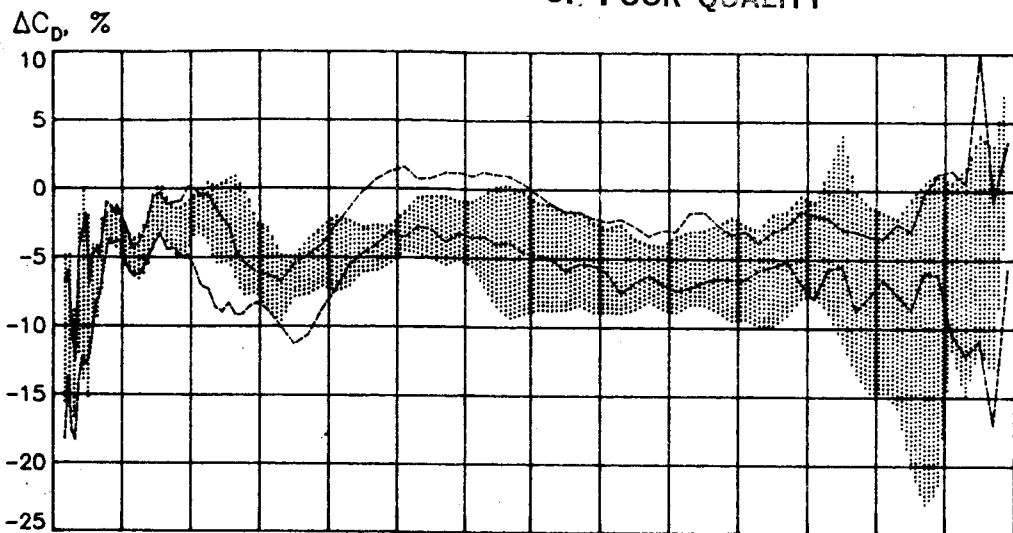
Figure III-2. Angle-of-attack and c.g. ranges from the first eleven Shuttle entries.



NOTE : Columbia (shade) ; Challenger (dash)

Figure III-3. Ensemble lift comparisons from the first eleven Shuttle entries.

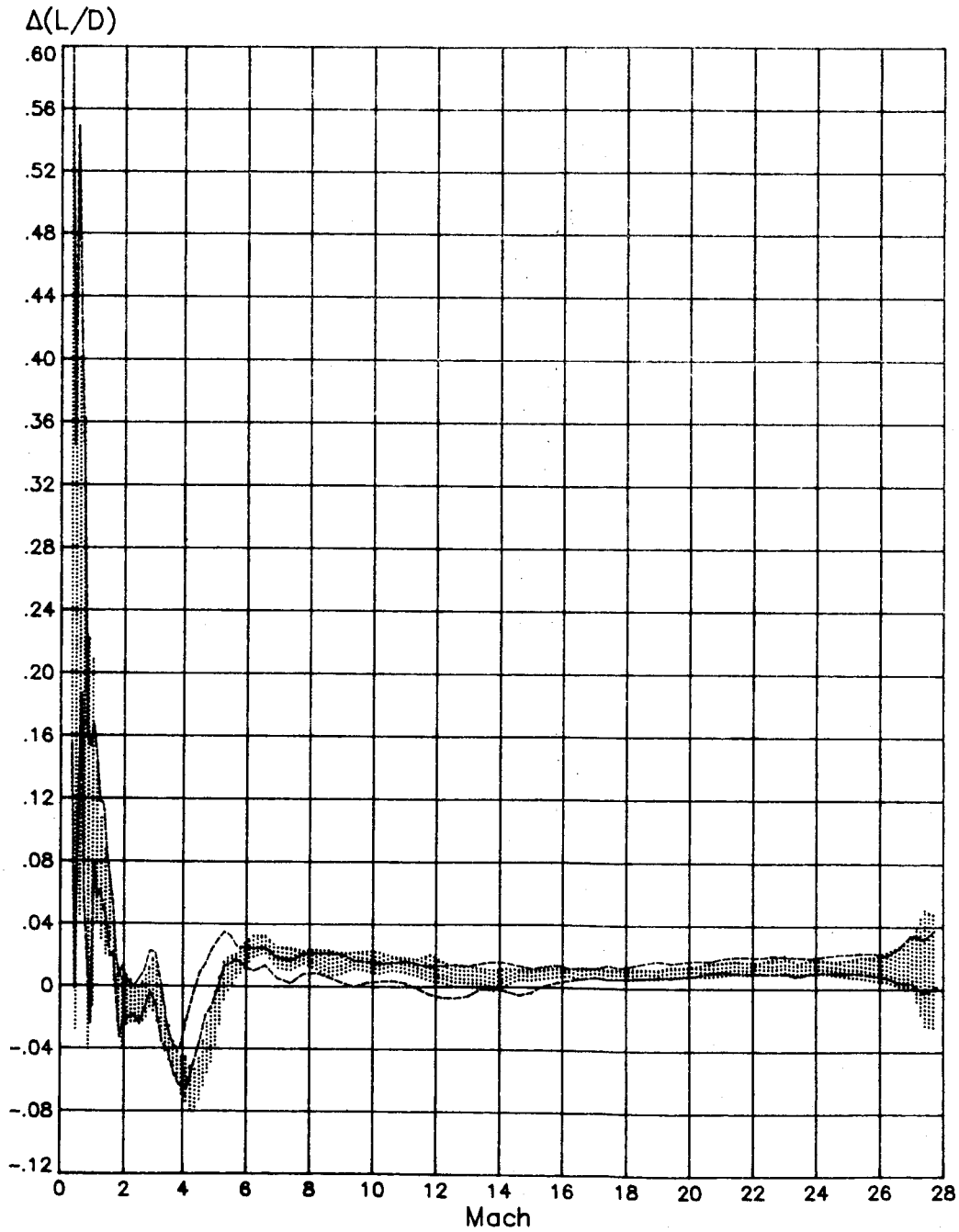
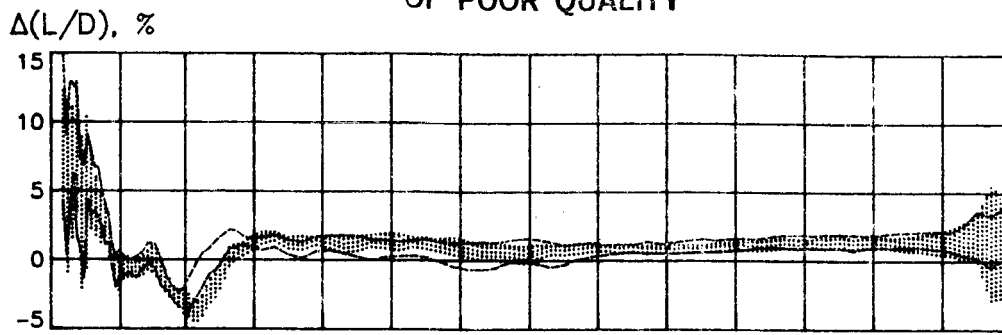
ORIGINAL PAGE IS
OF POOR QUALITY



NOTE: Columbia (shade) ; Challenger (dash)

Figure III-4. Ensemble drag comparisons from the first eleven Shuttle entries.

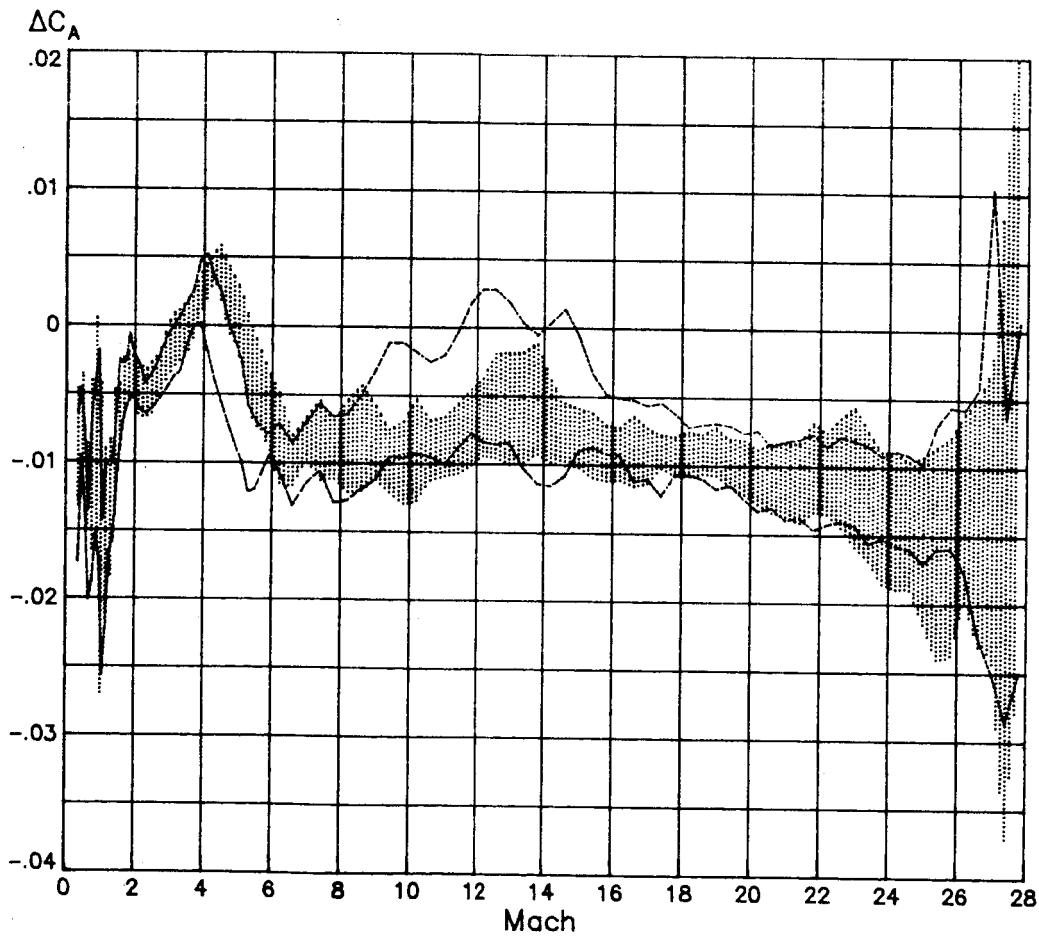
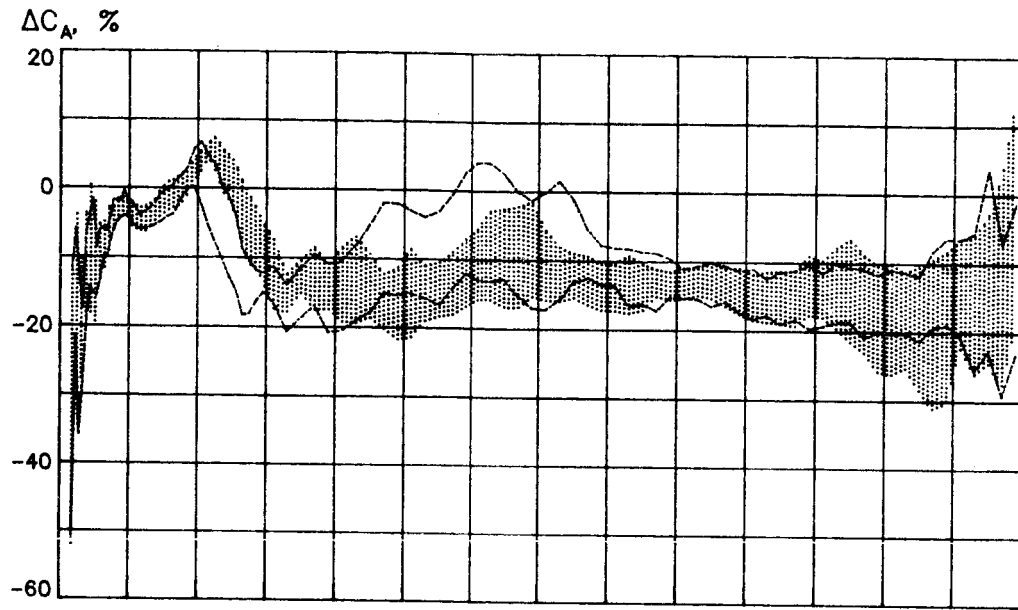
ORIGINAL PAGE IS
OF POOR QUALITY



NOTE: Columbia (shade) ; Challenger (dash)

Figure III-5. Ensemble L/D comparisons from the first eleven flights.

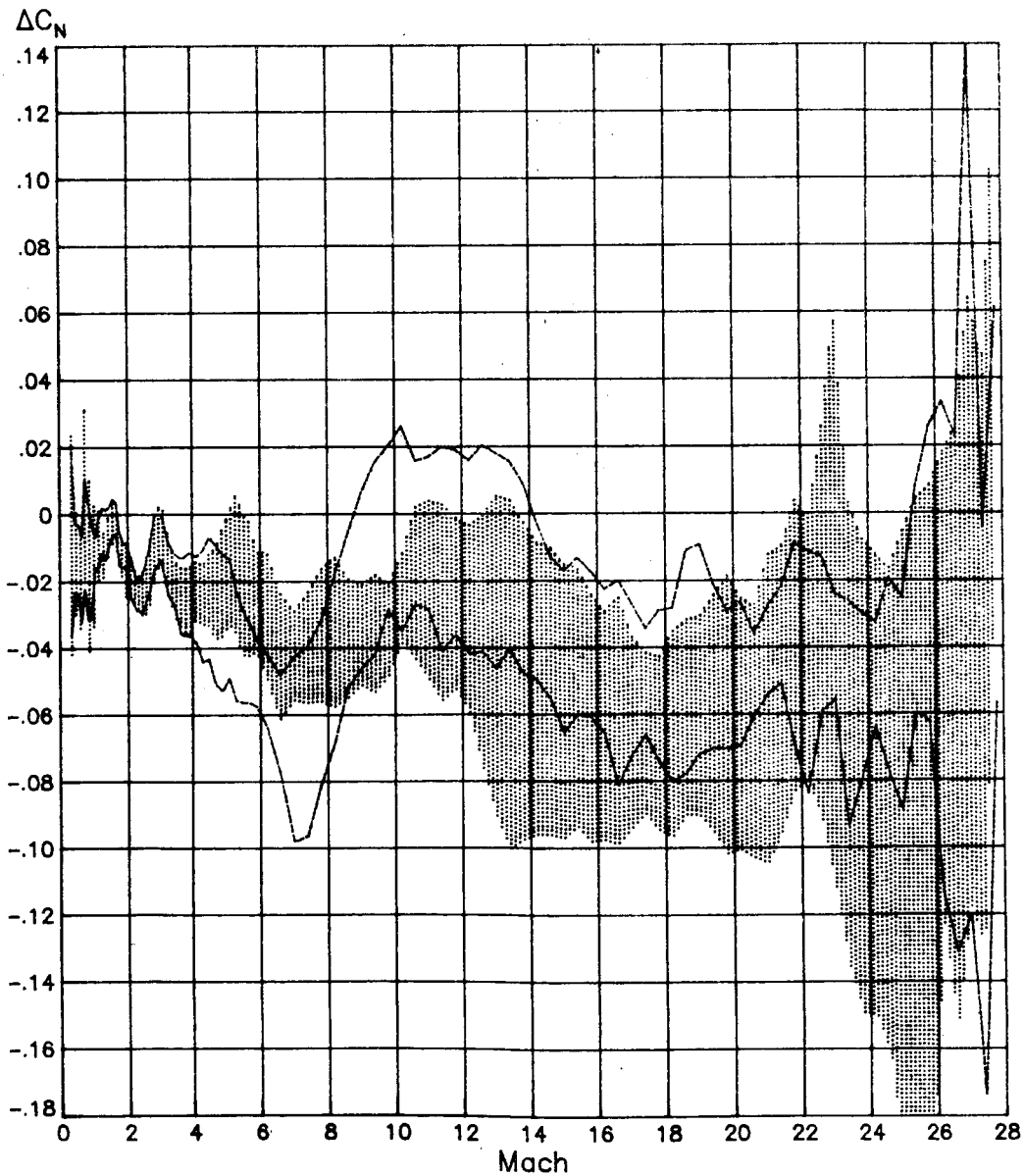
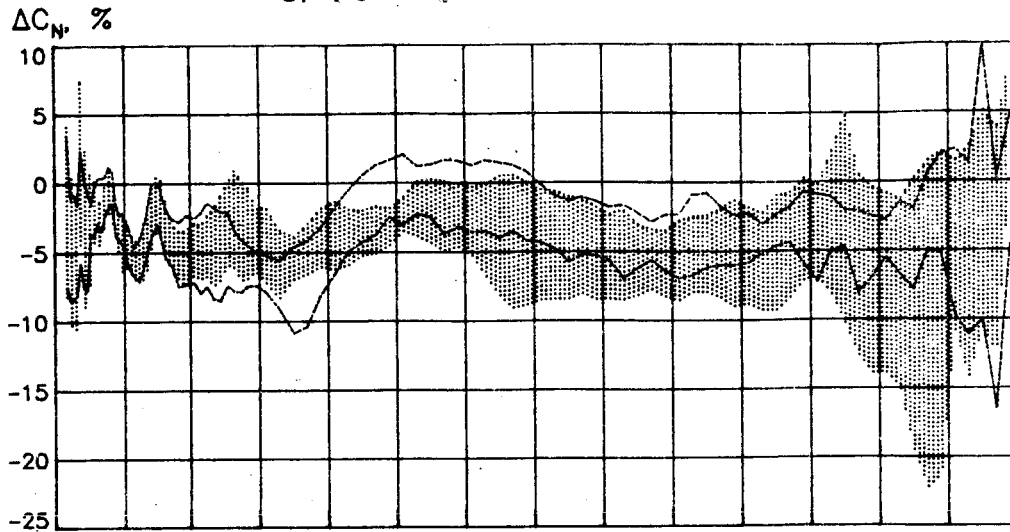
ORIGINAL PAGE IS
OF POOR QUALITY



NOTE : Columbia (shade) ; Challenger (dash)

Figure III-6. Ensemble axial force comparisons from the first eleven Shuttle entries.

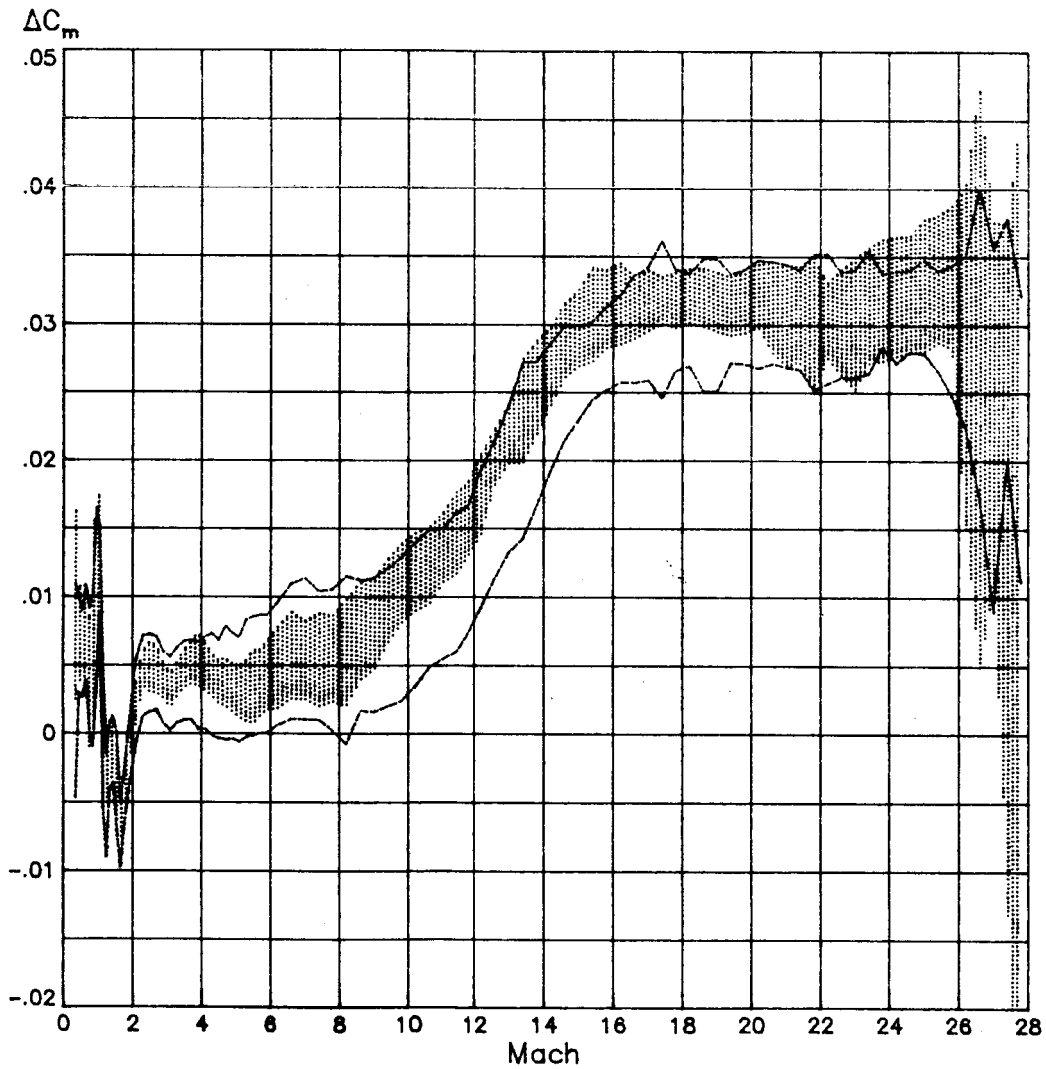
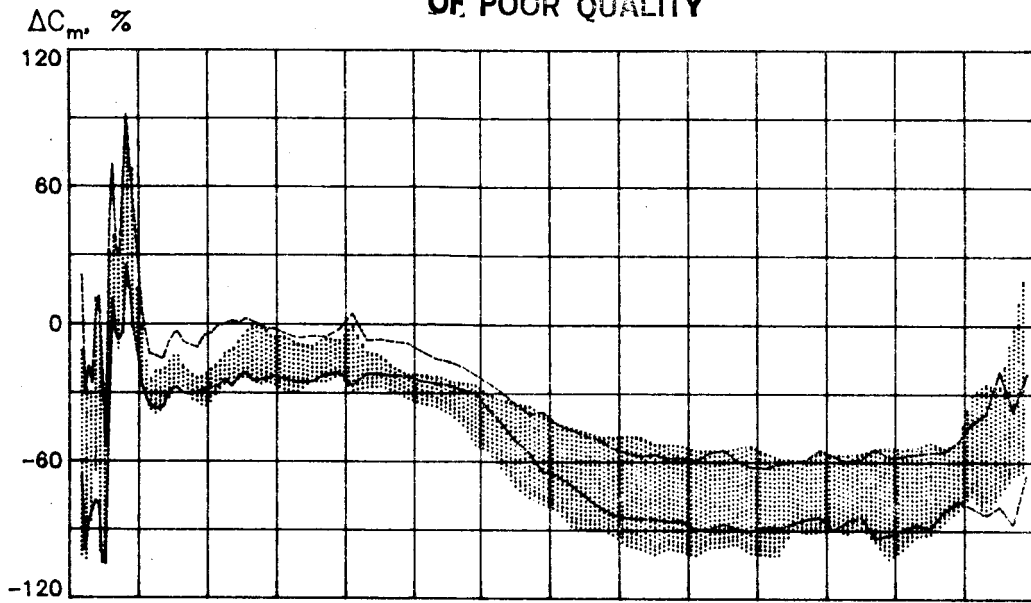
ORIGINAL PAGE IS
OF POOR QUALITY



NOTE : Columbia (shade) ; Challenger (dash)

Figure III-7. Ensemble normal force comparisons from the first eleven Shuttle entries.

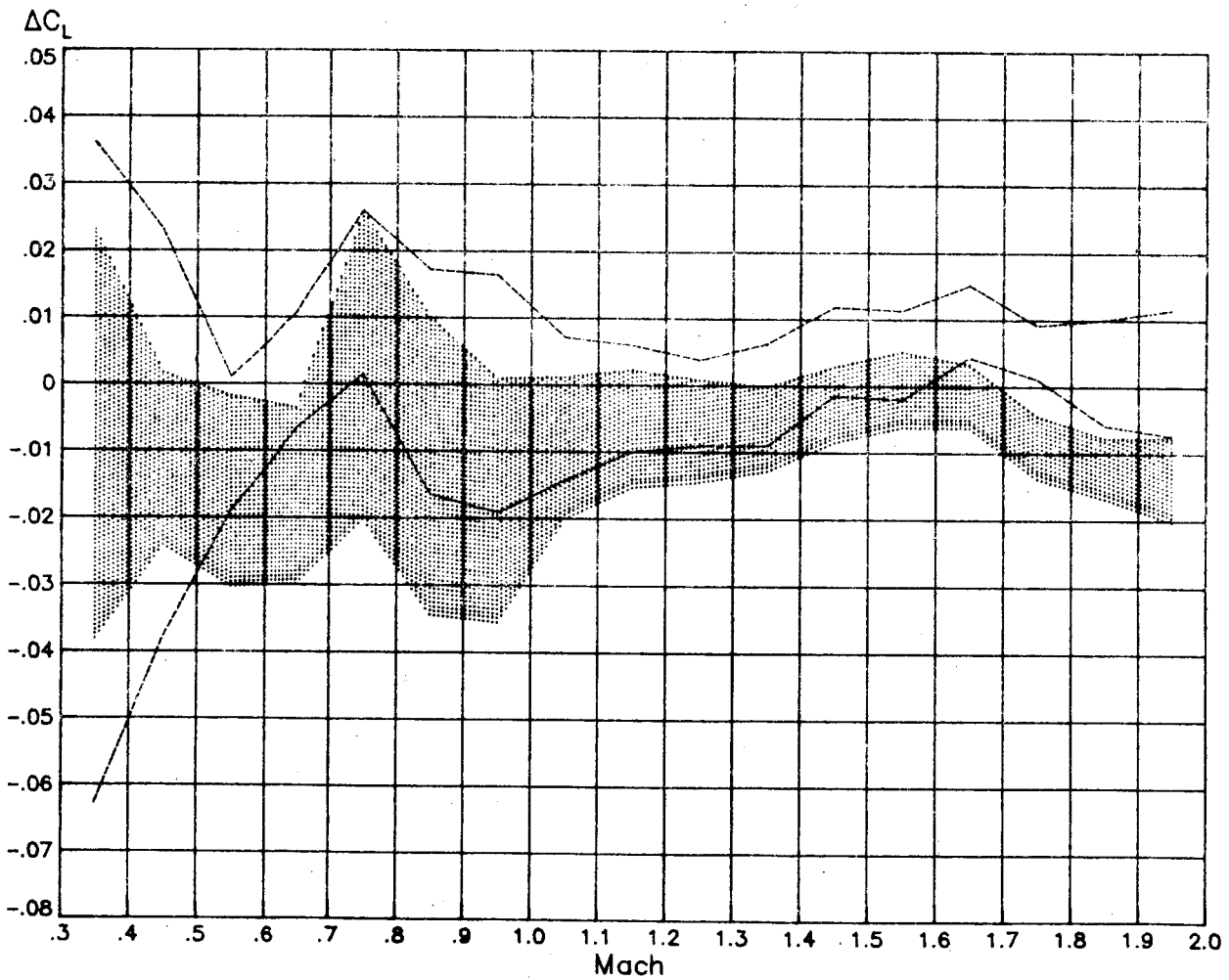
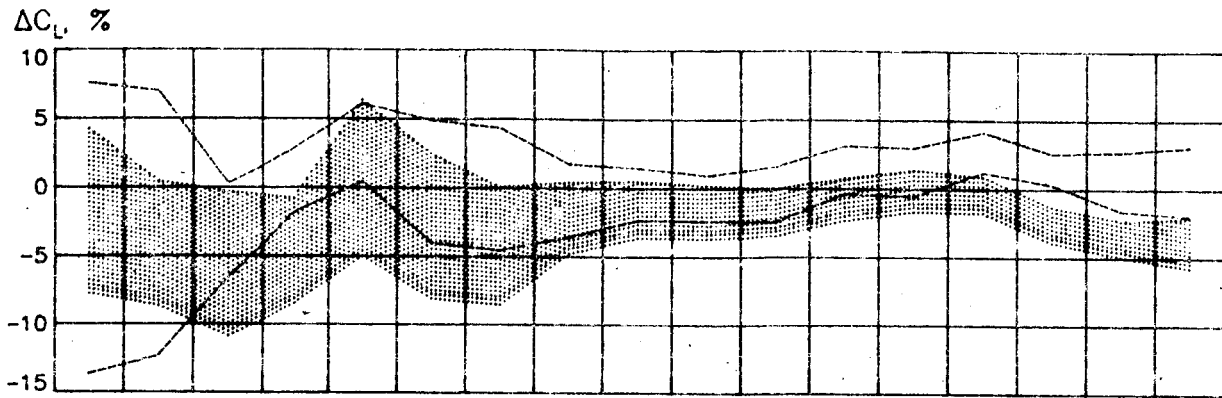
ORIGINAL PAGE IS
OF POOR QUALITY



NOTE : Columbia (shade) ; Challenger (dash)

Figure III-8. Ensemble pitching moment comparisons from the first eleven Shuttle entries.

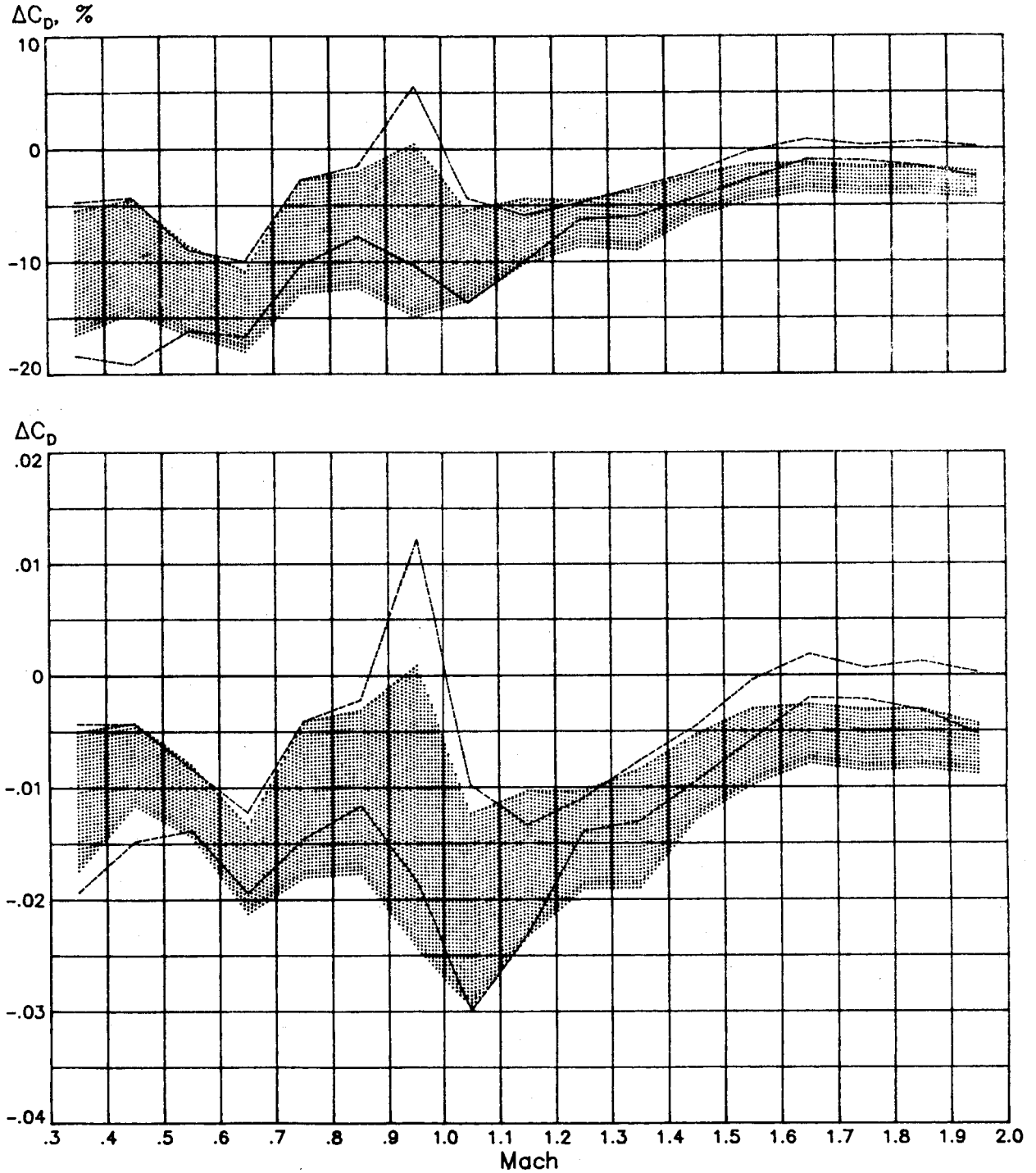
ORIGINAL SOURCE
OF POOR QUALITY



NOTE : LARC (shade) ; ADS (dash)

Figure III-9. Ensemble flight/data base lift comparisons below Mach 2 using alternate (remote and in situ) air data sources from the first eleven Shuttle flights.

ORIGINAL FILE IS
OF POOR QUALITY

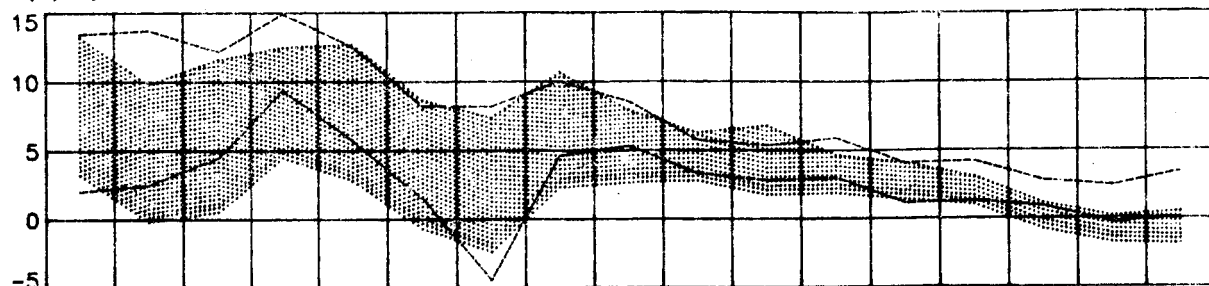


NOTE : LARC (shade) ; ADS (dash)

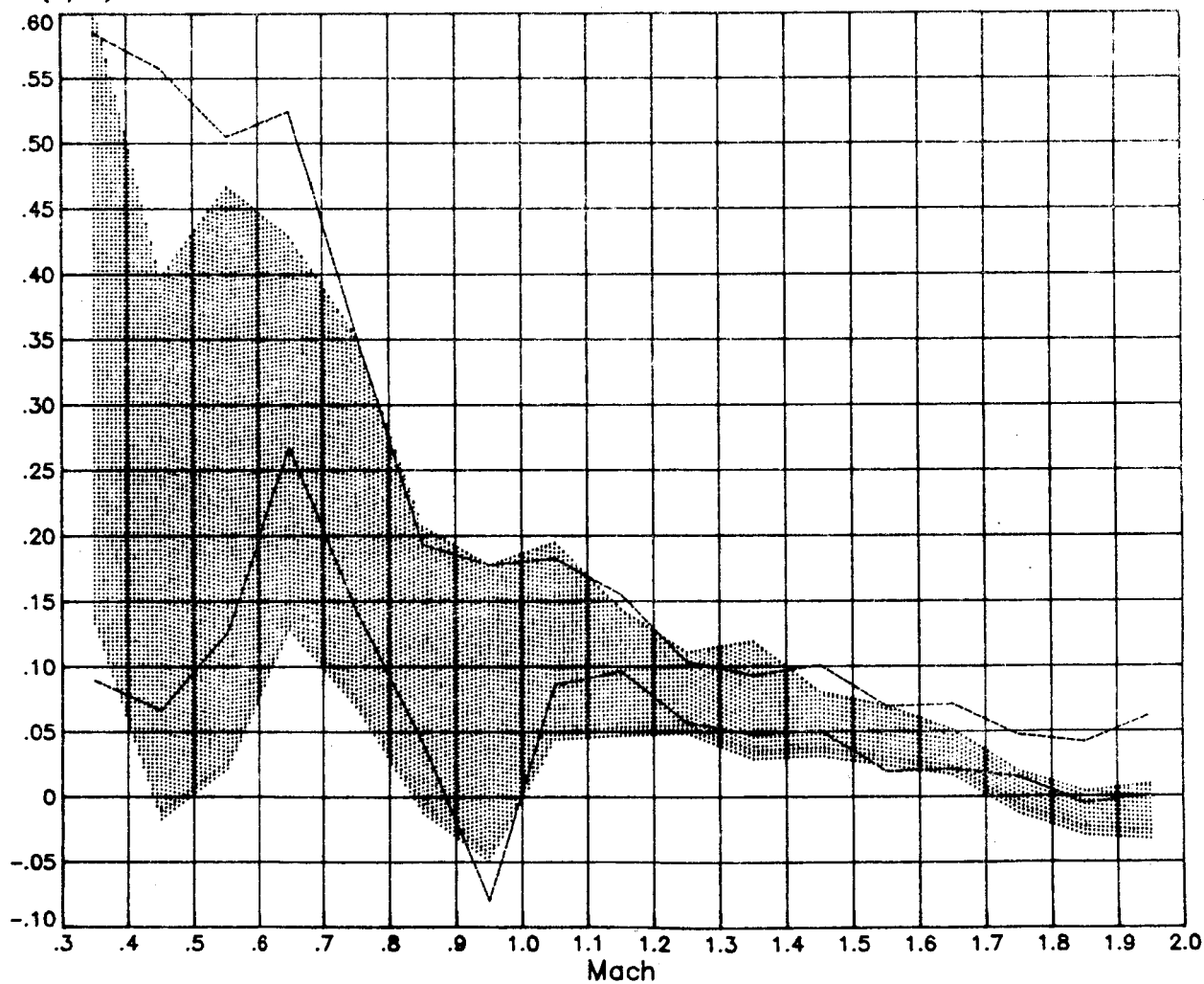
Figure III-10. Ensemble flight/data base drag comparisons below Mach 2 using alternate (remote and in situ) air data sources from the first eleven Shuttle flights.

ORIGINAL PAGES
OF POOR QUALITY

$\Delta(L/D), \%$



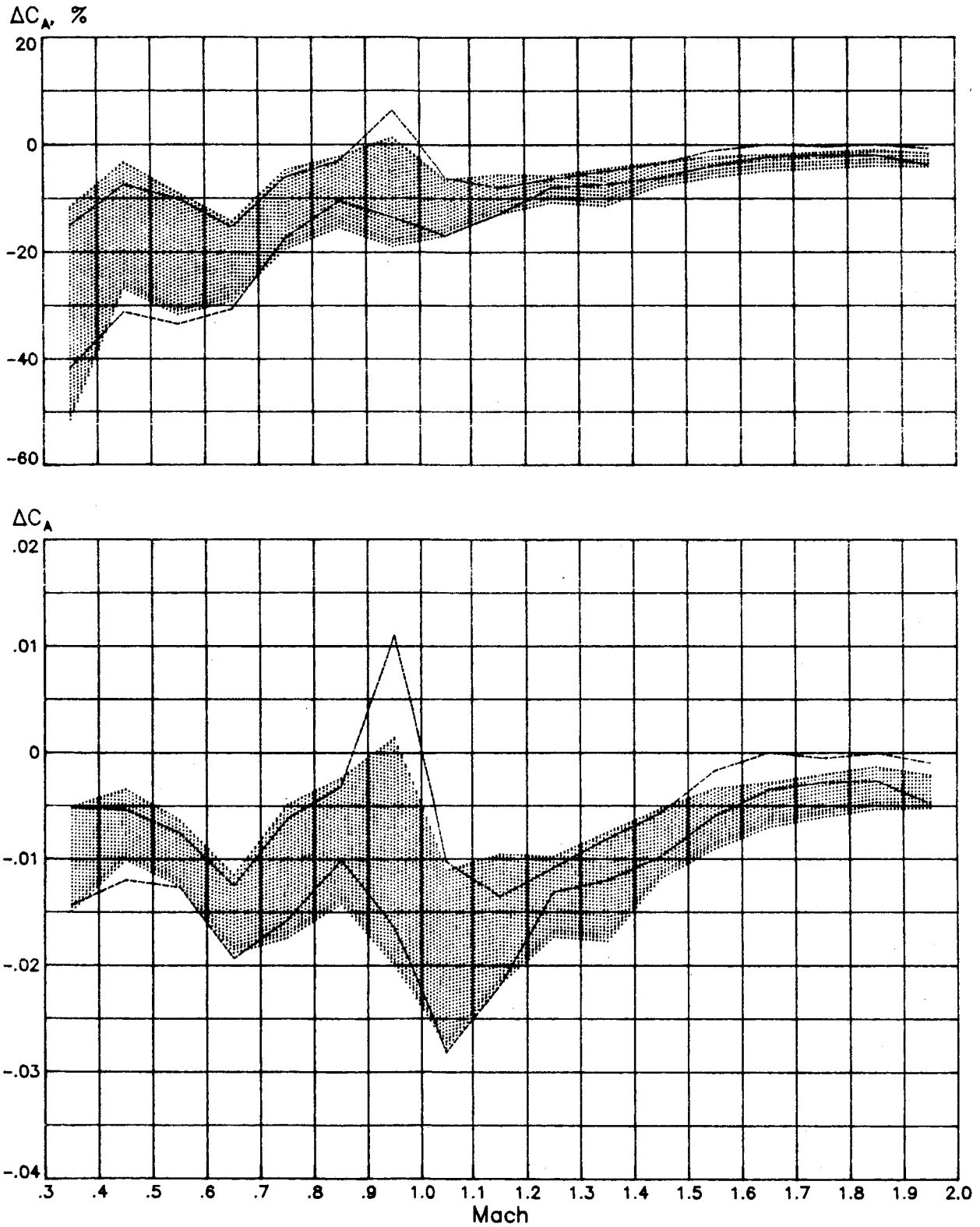
$\Delta(L/D)$



NOTE : LARC (shade) ; ADS (dash)

Figure III-11. Ensemble flight/data base L/D comparisons below Mach 2 using alternate (remote and in situ) air data sources from the first eleven Shuttle flights.

ORIGINAL PAGE IS
OF POOR QUALITY



NOTE : LARC (shade) ; ADS (dash)

Figure III-12. Ensemble flight/data base C_A comparisons below Mach 2 using alternate (remote and in situ) air data sources from the first eleven Shuttle flights.

ORIGINAL PAGE IS
OF POOR QUALITY

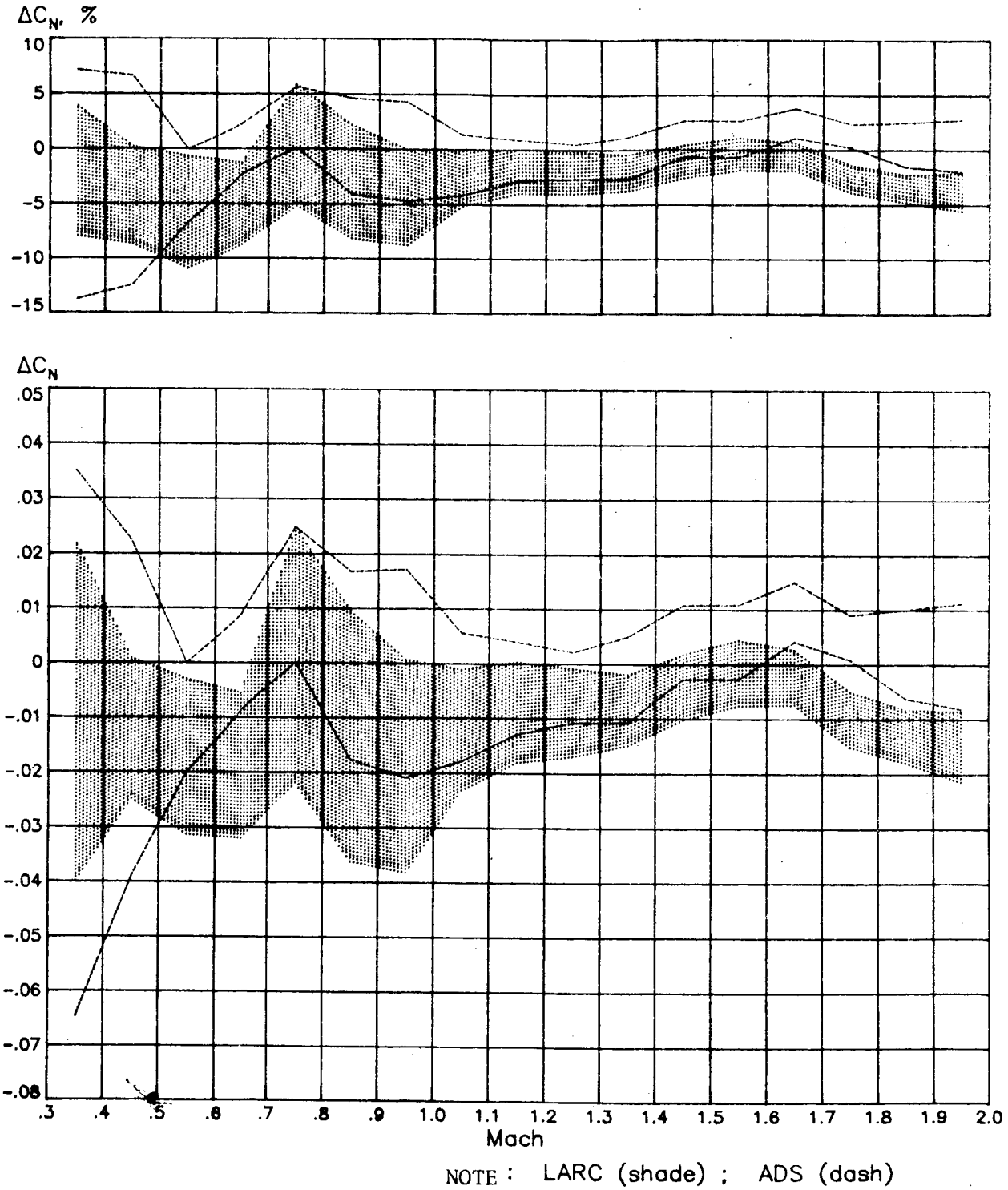
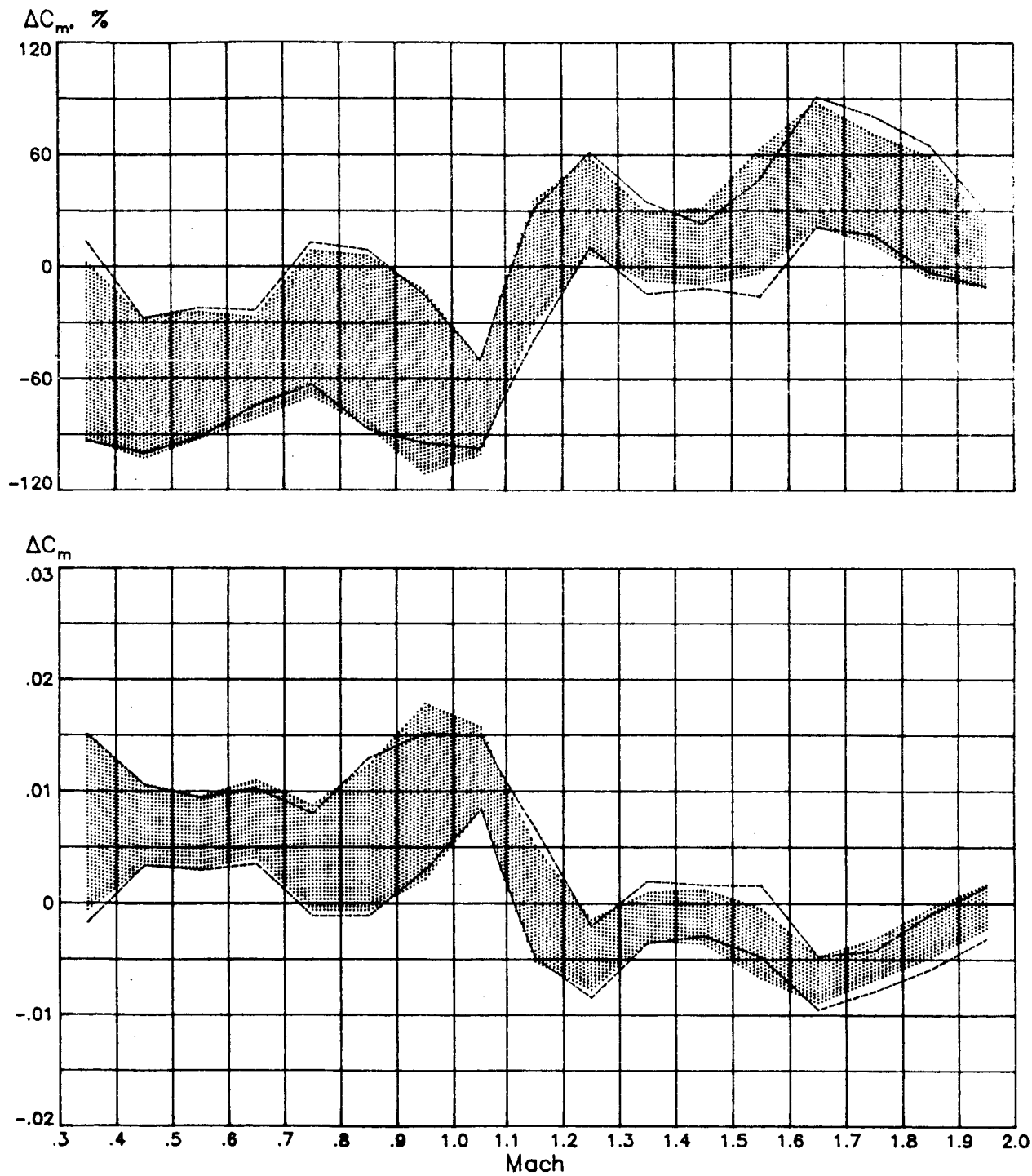


Figure III-13. Ensemble flight/data base C_N comparisons below Mach 2 using alternate (remote and in situ) air data sources from the first eleven Shuttle flights.

ORIGINAL PAGE IS
OF POOR QUALITY



NOTE : LARC (shade) ; ADS (dash)

Figure III-14. Ensemble flight/data base pitching moment comparisons below Mach 2 using alternate (remote and in situ) air data sources from the first eleven Shuttle flights.

IV. Summary and Recommendations

An extensive flight data base for aerodynamic investigation has been developed based on the first eleven Shuttle entries using the software and methods developed under the subject Contract. Combining these results with similar results from future flights can only enhance researcher opportunities to compare flight results with experimental and theoretical predictions. Though few discrepancies have been observed there still are many interesting areas of concentration. Many tools have been developed to enable analysis of flight data. In the future, considering the large volume of data and the latent accuracy of same (some of which was addressed herein), more rigorous methods need be developed. Software is required to implement the flight data in some data base structure to facilitate user access, enable direct comparisons with alternate data bases and/or actual wind tunnel results, and provide additional analysis capability. The results of this Shuttle research will be most helpful in design of future NASA space vehicles.

APPENDIX A

Glossary of Applicable References of
AMA Publications of Shuttle Data Analysis
and Results

I. JOURNAL ARTICLES

1. Kelly, G. M., Findlay, J. T., and Compton, H. R., "Shuttle Subsonic Horizontal Wind Estimation," Journal of Spacecraft and Rockets, Vol. 20, Number 4, July-August 1983, pp. 390-393.
2. Heck, M. L., Findlay, J. T., Kelly, G. M., and Compton, H. R., "The Adaptation of a Strap Down Formulation for Processing Inertial Platform Data," Journal of Guidance, Control, and Dynamics, Vol. 7, Number 1, January-February 1984, pp. 15-19.

II. LANGLEY CONFERENCE - Shuttle Performance: Lessons Learned

1. Findlay, J. T., Kelly, G. M., McConnell, J. G., and Compton, H. R., "Subsonic Longitudinal Performance Coefficient Extraction from Shuttle Flight Data--An Accuracy Assessment for Determination of Data Base Updates," NASA CP-2283, Part 2, March 1983.
2. Heck, M. L., Findlay, J. T., and Compton, H. R., "Aerodynamic Coefficient Identification Package Dynamic Data Accuracy Determination," NASA CP-2283, Part 1, March 1983.

III. AIAA CONFERENCE PAPERS

1. Compton, H., Findlay, J., Kelly, G., and Heck, M., "Shuttle (STS-1) Entry Trajectory Reconstruction," AIAA Paper No. 81-2459, Nov. 1981.
2. Heck, M. L., Findlay, J. T., Kelly, G. M., and Compton, H. R., "The Adaptation of a Strap-Down Formulation for Processing Inertial Platform Data," AIAA Paper No. 82-1332, August 1982.
3. Kelly, G. M., Findlay, J. T., and Compton, H. R., "Wind Estimation Using Air Data Probe Measurements to Evaluate Meteorological Measurements Made During Space Shuttle Entries," AIAA Paper No. 82-1333, August 1982.
4. Findlay, J. T. and Compton, H. R., "On the Flight Derived/ Aerodynamic Data Base Performance Comparisons for the NASA Space Shuttle Entries During the Hypersonic Regime," AIAA Paper No. 83-0115, Jan. 1983.
5. Heck, M. L., Findlay, J. T., and Compton, H. R., "Calibration of the Aerodynamic Coefficient Identification Package Measurements from the Shuttle Entry Flights Using Inertial Measurement Unit Data," AIAA 83-2100, August 1983.
6. Phillips, W. P., Findlay, J. T., and Compton, H. R., "Base Drag Determination for STS Flights 1-5," AIAA Paper No. 83-2719, Nov. 1983.
7. Findlay, J. T., Kelly, G. M., McConnell, J. G., and Compton, H. R., "Shuttle 'Challenger' Aerodynamic Performance From Flight Data - Comparisons with Predicted Values and 'Columbia' Experience," AIAA Paper No. 84-0485, January 1984.

IV.a. NASA CONTRACTOR REPORTS (with flight results)

1. Findlay, J. T., Kelly, G. M., and Heck, M. L., "Reconstruction of the 1st Space Shuttle (STS-1) Entry Trajectory," NASA CR-3561, June 1982.
2. Findlay, J. T., and McConnell, J. G., "Inertial Measurement Unit Pre-Processors and Post-Flight STS-1 Comparisons," NASA CR-165883, April 1982.
3. Kelly, G. M., and Findlay, J. T., "Horizontal Wind Estimates Deterministically Derived from the STS-1 Entry Flight Data-- a Comparison With Available Meteorology Data," NASA CR-165881, April 1982.
4. Findlay, J. T., Kelly, G. M., Heck, M. L., and McConnell, J. G., "STS-8 BET Results," NASA CR-172257, November 1983.
5. Findlay, J. T., Kelly, G. M., Heck, M. L., McConnell, J.G., Henry, M. W., "STS-9 BET Products," NASA CR-172314, February 1984.
6. Kelly, G. M., McConnell, J. G., Findlay, J. T., Heck, M. L., and Henry, M. W., "Final STS-11 (41-B) Best Estimate Trajectory Products: Development and Results from the First Cape Landing Mission," NASA CR-172349, April 1984.
7. Findlay, J. T., Kelly, G. M., McConnell, J. G., and Heck, M. L., "STS-13 (41-C) BET Products," NASA CR-172350, July 1984.

IV.b. NASA CONTRACTOR REPORTS (analysis and software)

1. Kelly, G. M., "Recommended ENTREE S-band Range and Doppler Models," NASA CR-165884, April 1982.
2. Findlay, J. T., and Heck, M. L., "Formulation of Additional Observables for ENTREE," NASA CR-165880, April 1982.
3. Heck, M. L., "The Processing of IMU Data in ENTREE-Implementation and Preliminary Results," NASA CR-165879, April 1982.
4. Findlay, J. T., Kelly, G. M., and Henry, M. W., "An Extended BET Format for LaRC Shuttle Experimenters: Definition and Development," NASA CR-165882, April 1982.

V.a. COMPANY REPORTS (with flight results)

1. Findlay, J. T., "ACIP Performance Assessment During STS-1 Reentry - Comparisons with IMU Measurements and Trajectory Prediction Considerations," AMA Report 81-26, Contract NAS1-16087, September 1981.
2. Findlay, J. T., Kelly, G. M., Heck, M. L., and McConnell, J.G., "Final IMU Preprocessing Results Based on the Second NASA Space Shuttle 'Columbia' Entry Flight," AMA Report 81-38, Contract NAS1-16087, December 1981.
3. Findlay, J. T., "Comparison of RGA/AA Measurement vs. IMU Data for the Complete Maneuver Schedule During the Second Columbia Entry," AMA Report 82-4, Contract NAS1-16087, January 1982.
4. Findlay, J. T., Kelly, G. M., Heck, M. L., and McConnell, J.G., "Entry Reconstruction of the 2nd Space Shuttle Columbia Flight: Results and Methodology," AMA Report 82-8, Contract NAS1-16087, March 1982.
5. Findlay, J. T., and McConnell, J. G., "A Summary of STS-1 and STS-2 Flight Derived and Aerodynamic Data Base Comparisons - A Data Package for ACME Investigations," AMA Report 82-16, Contract NAS1-16087, April 1982.
6. Findlay, J. T., and McConnell, J. G., "Contributions of the Various Elements of the LaRC Shuttle Aerodynamic Data Base to the Overall STS-2 Predicted Coefficients," AMA Report 82-21, Contract NAS1-16087, May 1982.
7. Heck, M. L., "STS-2 Theodolite Data Evaluation," AMA Report 82-22, Contract NAS1-16087, May 1982.
8. Findlay, J. T., McConnell, J. G., and Kelly, G. M., "Hypersonic Flight/Data Base Comparisons for the First Three STS Entries - A Summary for Review by Aerodynamicists and Meteorologists," AMA Report 82-24, Contract NAS1-16087, July 1982.
9. McConnell, J. G., "GTFILE Generation for the 3rd Space Shuttle (STS-3) Flight," AMA Report 82-25, Contract NAS1-16087, July 1982.
10. Findlay, J. T., "Signal Detection Software for ACIP Data Evaluation and Calibration Versus IMU Derived Body Axis Measurements," AMA Report 82-27, Contract NAS1-16087, July 1982.
11. Kelly, G. M., Heck, M. L., McConnell, J. G., and Findlay, J. T., "A Summary of STS3 Post-Flight Best Estimate Trajectory Results," AMA Report 82-32, Contract NAS1-16087, August 1982.
12. Kelly, G. M., McConnell, J. G., Heck, M. L., and Findlay, J.T., "STS4 Best Estimate Trajectory, AEROBET, and GT File Development and Results," AMA Report 82-33, Contract NAS1-16087, Sept. 1982.

13. Findlay, J. T., Kelly, G. M., and McConnell, J. G., "Final Report - DFI Base Pressure and Wing Surface Pressure Measurements for the First Four Shuttle Entries," AMA Report 82-46, P.O. L-44942B, December 1982.
14. Heck, M. L., "Aerodynamic Coefficient Identification Package Calibration Study Results Using Inertial Measurement Units," AMA Report 83-1, Contract NAS1-16087, January 1983.
15. Kelly, G. M., McConnell, J. G., Heck, M. L., and Findlay, J.T., "Development of and Results from the STS-5 Post-Flight Products for LaRC Aerodynamic and Aerothermodynamic Investigations," AMA Report 83-2, Contract NAS1-16087, February 1983.

(Addendum published as AMA 83-11)

Findlay, J. T., and McConnell, J. G., "Upper Altitude Extension for STS-5 BET (Addendum to AMA Report No. 83-2), AMA Report 83-11, Contract NAS1-16087, July 1983.

16. Findlay, J. T., Kelly, G. M., and McConnell, J. G., "FINAL REPORT STS-5 DFI Base Pressure and Wing Surface Pressure Results," AMA Report 83-3, P.O. L-48076B, February 1983.
17. Findlay, J. T., McConnell, J. G., "Revised AEROBETs for First Five(5) Columbia Entry Flights," AMA Report 83-5, Contract NAS1-16087, March 1983.
18. Findlay, J. T., Kelly, G. M., Heck, M. L., McConnell, J. G., "Results from the First Entry Flight of the NASA Space Shuttle 'Challenger' STS-6," AMA Report 83-9, Contract NAS1-16087, June 1983.
19. Heck, M. L., "Calibration of the STS-6 Aerodynamic Coefficient Identification Package Using Inertial Measurement Unit Data," AMA Report 83-10, Lockheed P.O. 0200101769, July 1983.
20. Kelly, G. M., "Trajectory Reconstruction of the Dryden Flight Research Facility's Spin Research Vehicle Flights 31 and 36," AMA Report 83-13, Contract NAS1-16087, July 1983.
21. Findlay, J. T., Kelly, G. M., Heck, M. L., and McConnell, J.G., "STS-7 Post Flight Best Estimate Trajectory Products," AMA Report 83-17, Contract NAS1-16087, September 1983.
22. Findlay, J. T., and McConnell, J. G., "Atmospheres for Aero-Assisted Orbital Transfer Vehicles Based on Shuttle Flight Experience," AMA Report 83-18, P.O. L-58260B, September 1983.
23. Heck, M. L., "Calibration of the STS-7 Aerodynamic Coefficient Identification Package Using Inertial Measurement Unit Data," AMA Report 83-19, Lockheed P.O. 0200101769, September 1983.

24. Heck, M. L., "Calibration of the STS-8 Aerodynamic Coefficient Identification Package Using Inertial Measurement Unit Data," AMA Report 83-23, Lockheed P.O. 0200103434, November 1983.
25. Heck, M. L., "Calibration of the STS-9 Aerodynamic Coefficient Identification Package Using Inertial Measurement Unit Data," AMA Report 84-2, Lockheed P.O. 0200103434, February 1984.

V.b. COMPANY REPORTS (analysis and software)

1. Findlay, J. T., "RESPLTS: RESidual PLoTting Software for Shuttle Entry Trajectory Reconstruction," AMA Report 80-14, Contract NAS1-16087, September 1980.
2. Findlay, J. T., "SDPLTS: State Difference PLoT Utility for Shuttle Entry Trajectory Reconstruction Analysis," AMA Report 80-17, Contract NAS1-16087, September 1980.
3. Findlay, J. T., "A Compendium of Shuttle Deterministic Trajectory Prediction Errors Resulting from Improper Dynamic Modelling," AMA Report 80-24, Contract NAS1-16087, Nov. 1980.
4. Heck, M. L., "Non-Systematic IMU Error Effects on Deterministic Shuttle Re-entry Trajectory Generation," AMA Report 80-27, Contract NAS1-16087, Nov. 1980.
5. Findlay, J. T., "Best Estimate Trajectory (BET) File for Shuttle Experimenters," AMA Report 81-1, Contract NAS1-16087, January 1981.
6. Henry, M. W., "BET Atmospheric Plotting Program - Program Description and Users' Guide," AMA Report 81-19, Contract NAS1-16087, July 1981.
7. Flanagan, P. F., "Final Report GTFILE Generation - Definition and Development," AMA Report 81-20, P.O. L-23695B, July 1981.
8. Findlay, J. T., "Specialized Dynamic Data Processors, PQRPLTS and DPQRPLT, for Shuttle Post-flight Investigation," AMA Report 81-23, Contract NAS1-16087, August 1981.
9. Heck, M. L., "Tracking Data Preprocessor Modifications Required to Process MSBLS Data," AMA Report 81-28, P. O. L-28197B, October 1981.
10. McConnell, J. G., "Extended BET Difference Plot Utility-- Software to Evaluate State and Atmospheric Differences Between Extended BETs," AMA Report 81-29, Contract NAS1-16087, Oct. 1981.
11. Heck, M. L., "MSBLS Observable Incorporation into ENTREE," AMA Report 81-31, P.O. L-28197B, October 1981.
12. Kelly, G. M., "PRTBET: Utility for Block Printing of LaRC Best Estimated Shuttle Entry Trajectory Parameters," AMA Report 81-32, Contract NAS1-16087, November 1981.
13. Henry, M. W., "Modifications to Programs PQRPLTS and DPQRPLT," AMA Report 81-33, Contract NAS1-16087, November 1981.
14. McConnell, J. G., "RESPLTS: RESidual PLoTting Software for Shuttle Entry Trajectory Reconstruction (Revised)," AMA Report 82-3, Contract NAS1-16087, January 1982.

15. Findlay, J. T., Kelly, G. M., McConnell, J. G., "An AERODynamic Best Estimate Trajectory File (AEROBET) for NASA Langley Research Center Shuttle Investigations," AMA Report 82-9, Contract NAS1-16087, March 1982.
16. Findlay, J. T., "A Users' Guide for the Aerodynamic Best Estimate Trajectory Plot Utility (AROBPLT)," AMA Report 82-12, Contract NAS1-16087, March 1982.
17. Kelly, G. M., "PRTBET Revision 1," AMA Report 82-13, Contract NAS1-16087, March 1982.
18. Henry, M. W., "Extended BET Plot Program (XBETPLT) Program Description and User's Guide," AMA Report 82-20, Contract NAS1-16087, May 1982.
19. Heck, M. L., "Description and User's Guide for the ACIP Calibration Estimation Software," AMA Report 82-34, Contract NAS1-16087, December 1982.
20. Kelly, G. M., "Formatted AEROBET File Description," AMA Report 82-37, Contract NAS1-16087, September 1982.
21. Heck, M. L., "Update to ACIP Calibration Estimation Software," AMA Report 83-24, Contract NAS1-16087, November 1983.

ORIGINAL PAGE IS
OF POOR QUALITY

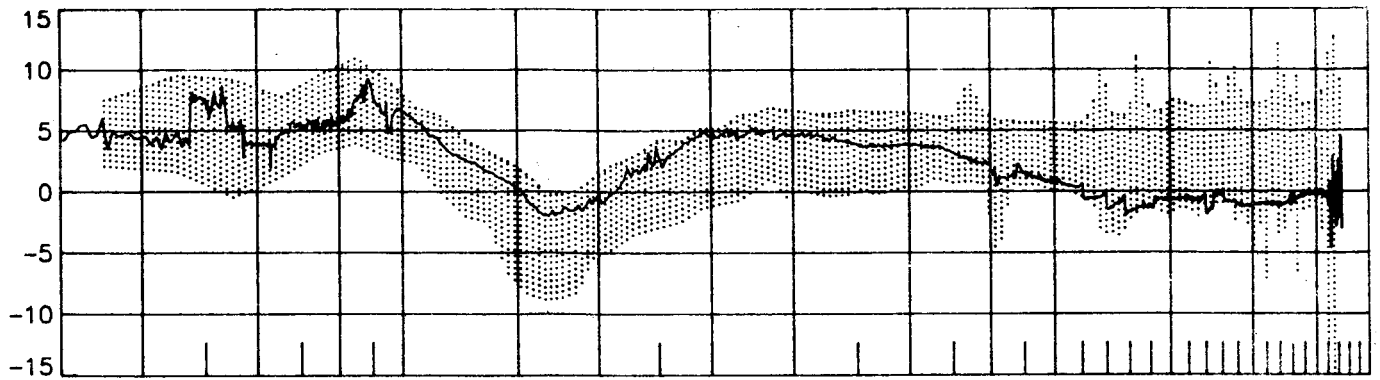


APPENDIX B

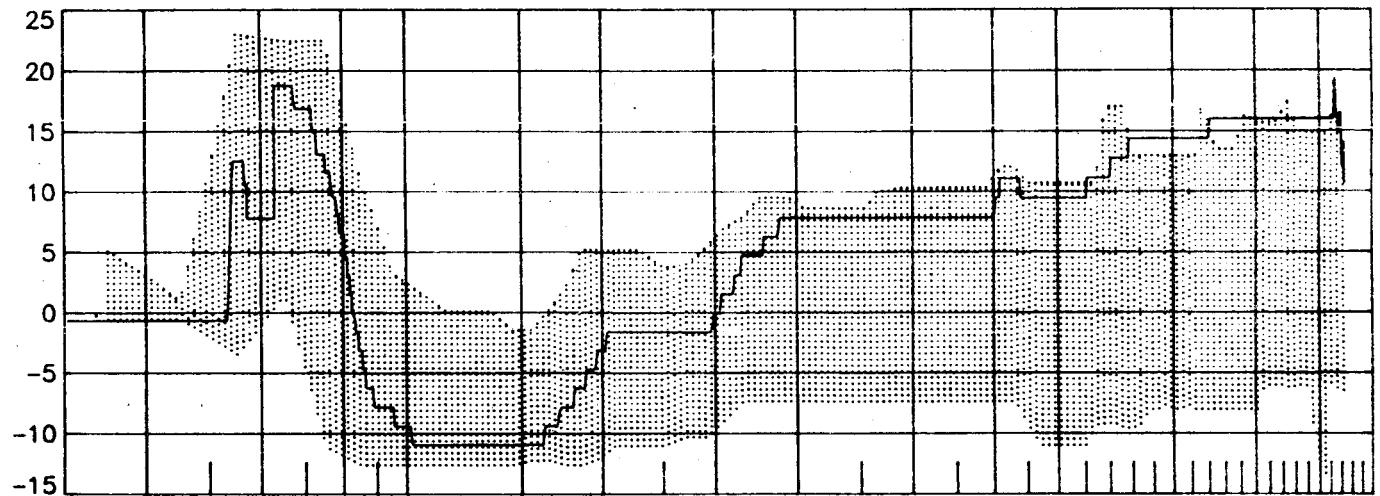
Summary of STS-1 longitudinal results and comparisons.

ORIGINAL PAGE IS
OF POOR QUALITY

δ_E , deg



δ_{BF} , deg



δ_{SBA} , deg

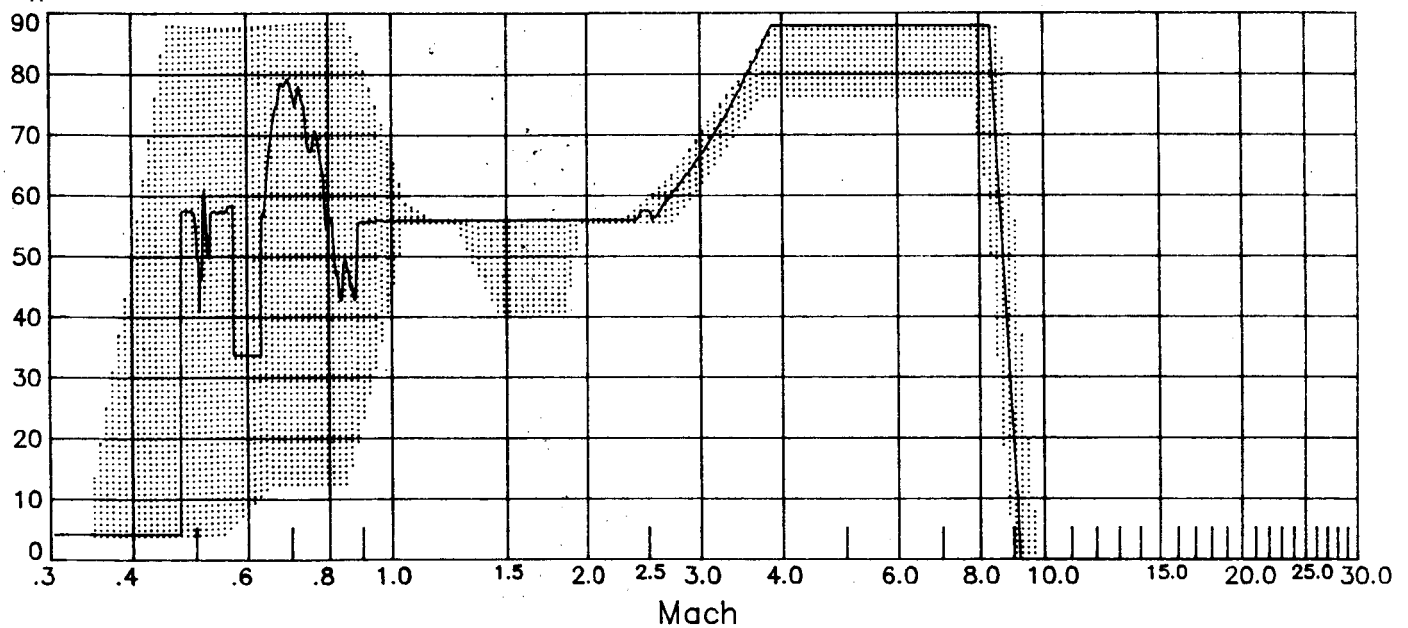
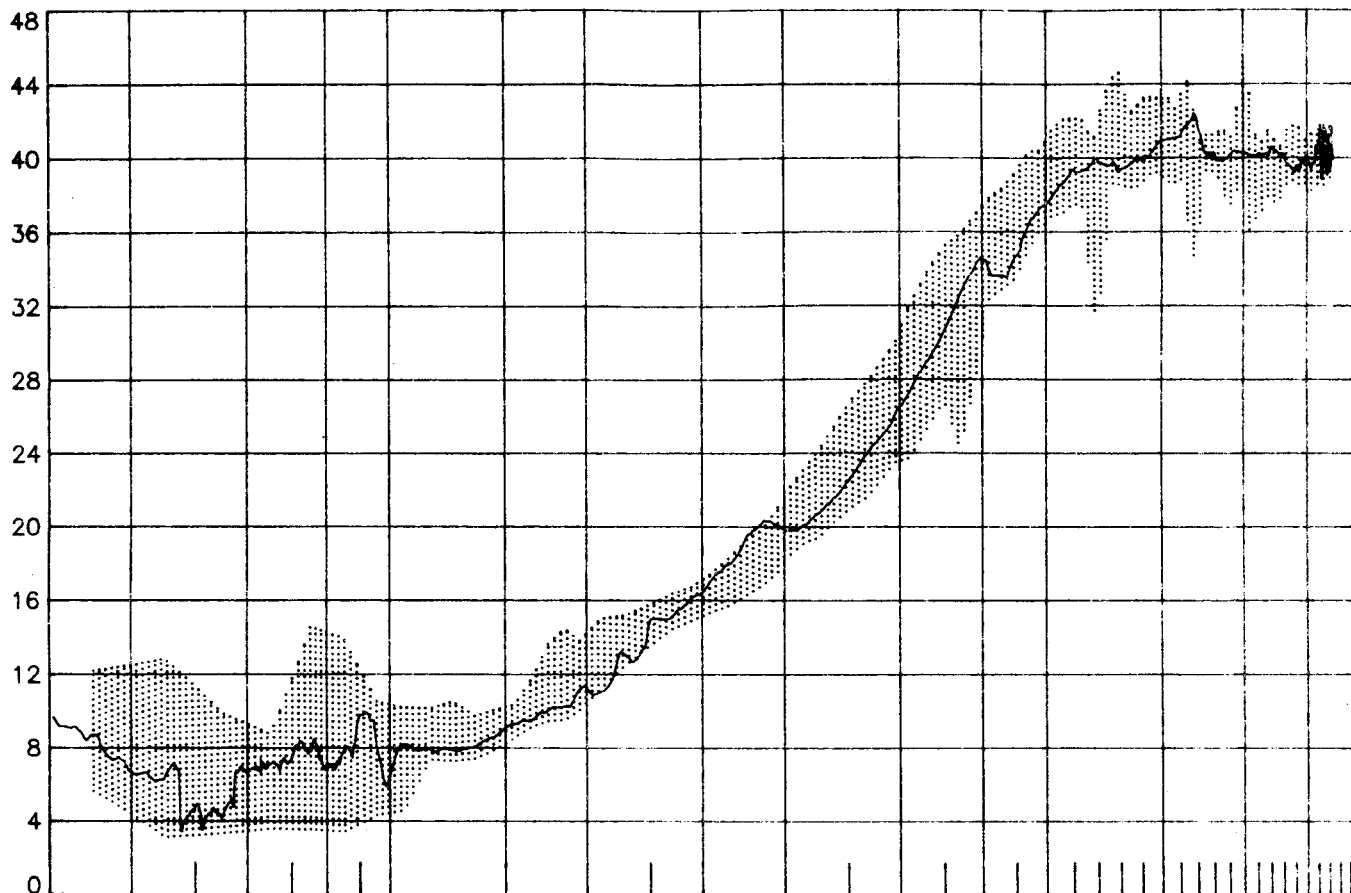


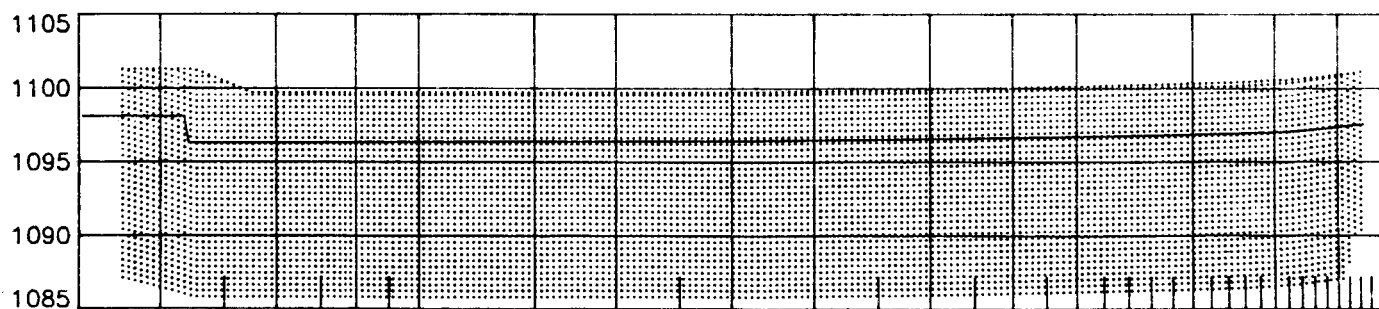
Figure B-1 STS-1 longitudinal control surface deflections
(shaded region defined by remaining ten flights)

ORIGINAL PAGE IS
OF POOR QUALITY

α , deg



x_{cg} , in



z_{cg} , in

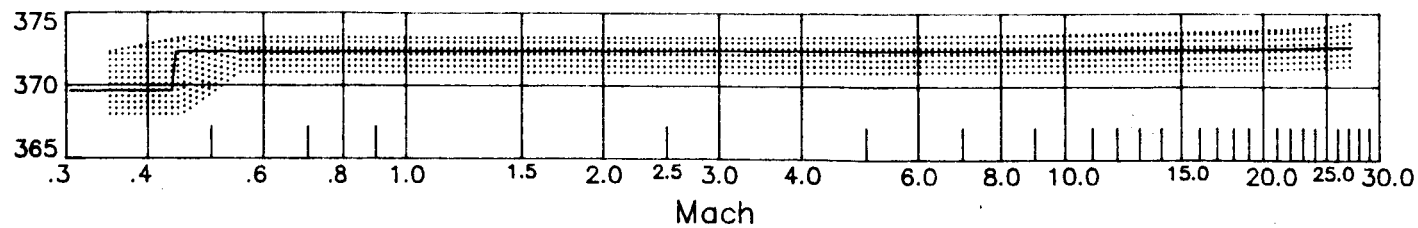
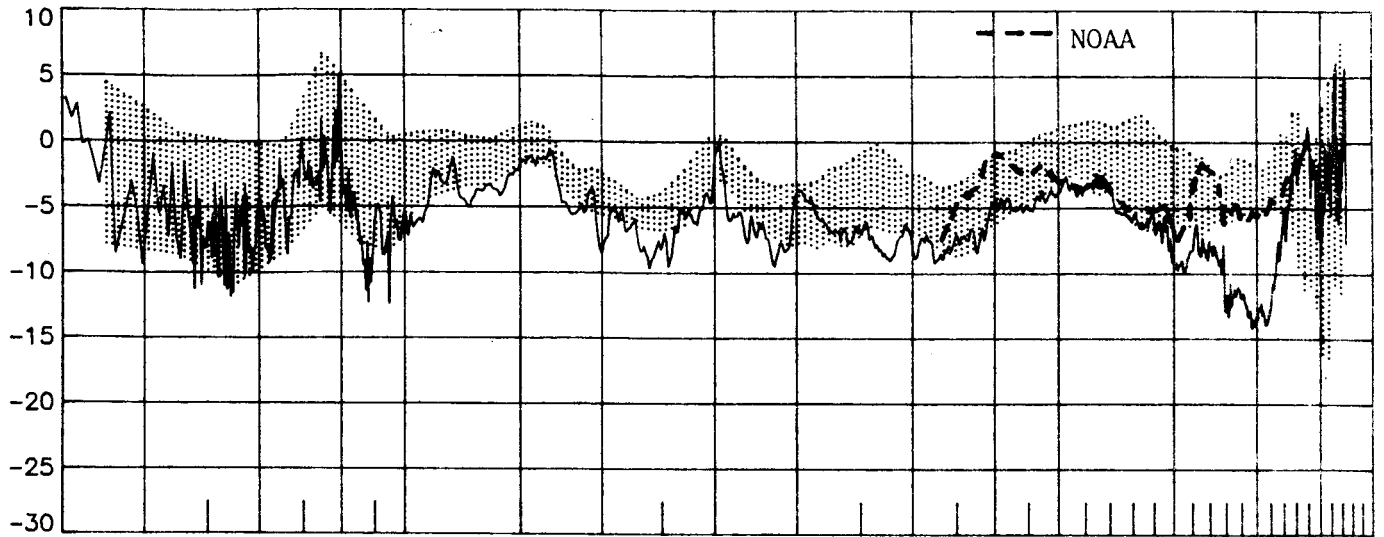
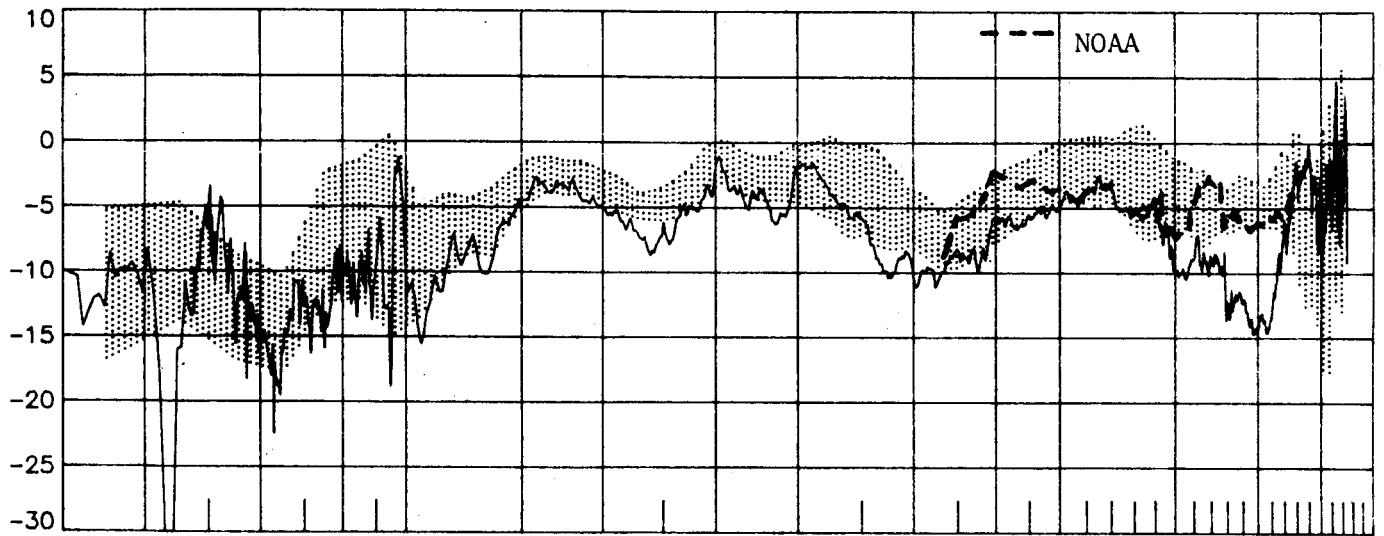


Figure B-2 STS-1 angle-of-attack and c.g. profiles
(shaded region defined by remaining ten flights)

ΔC_L , percent



ΔC_D , percent



$\Delta(L/D)$, percent

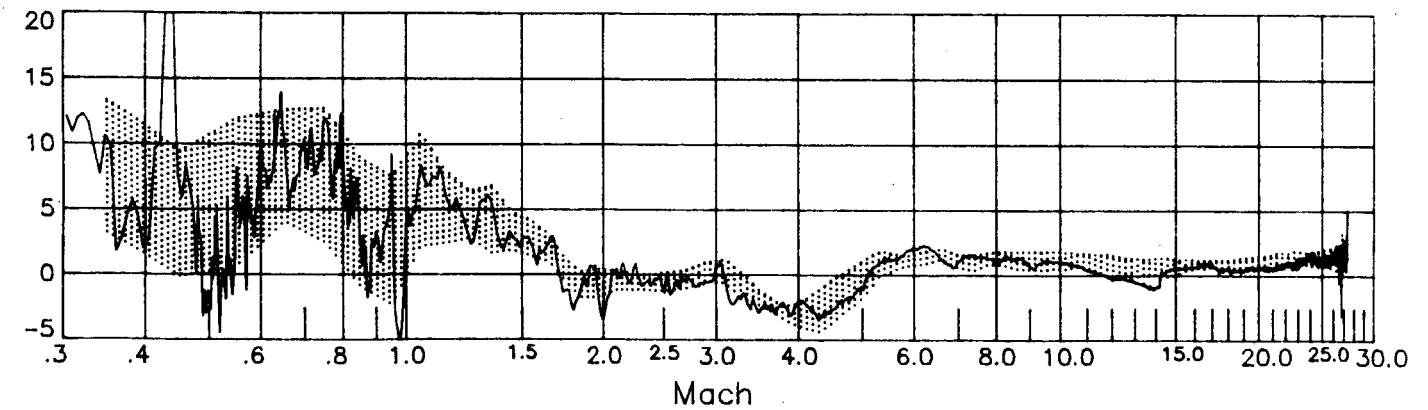
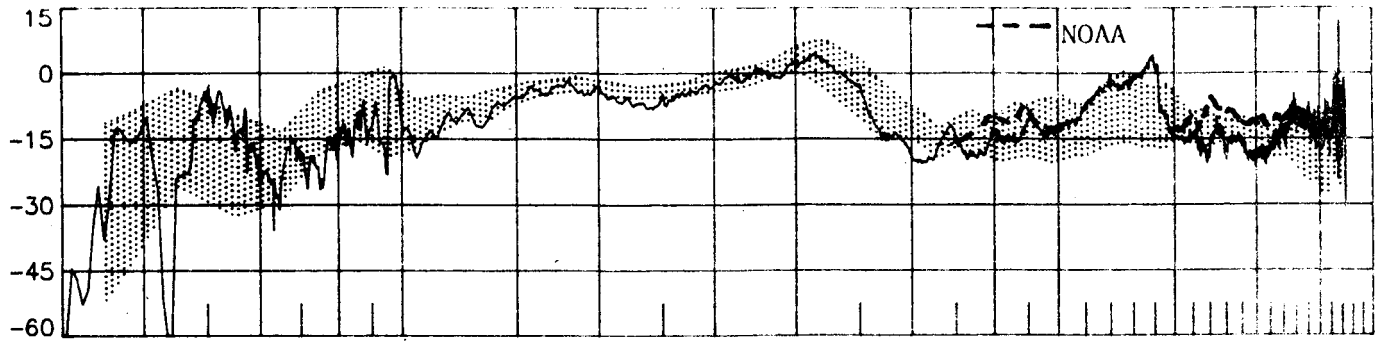


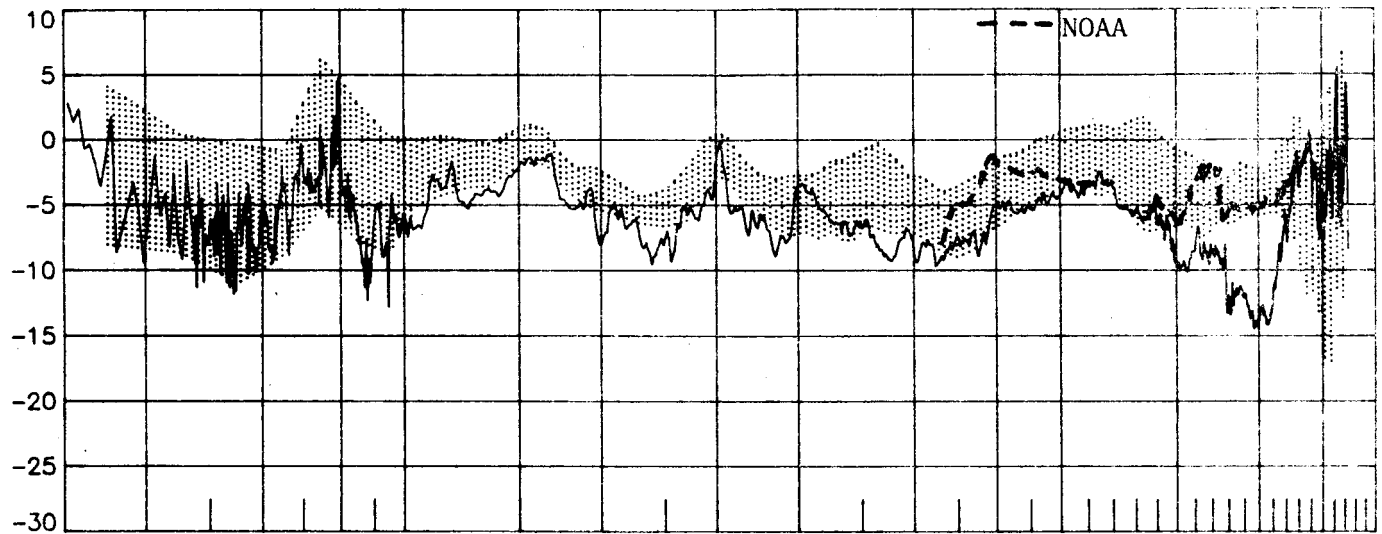
Figure B-3 STS-1 longitudinal performance comparisons
(shaded region defined by remaining ten flights)

ORIGINAL PAGE IS
OF POOR QUALITY

ΔC_A , percent



ΔC_N , percent



ΔC_m , percent

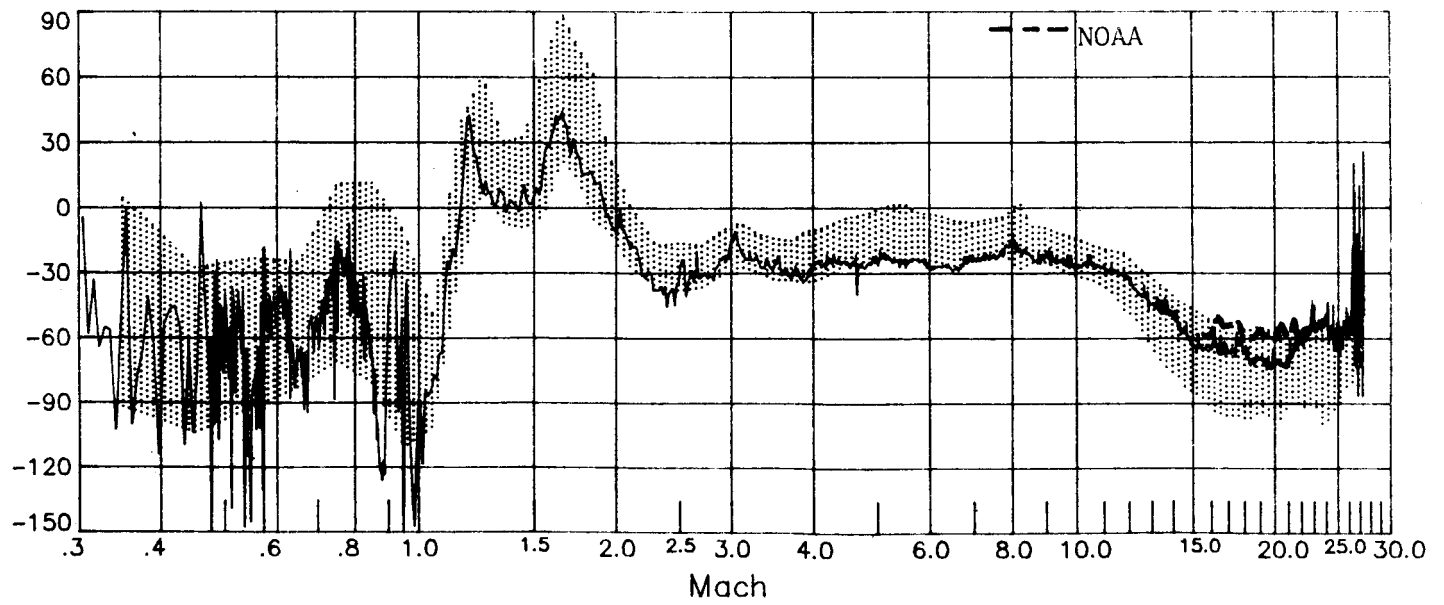


Figure B-3 (concluded)

(shaded region defined by remaining ten flights)

ORIGINAL FILED TO
OF POOR QUALITY

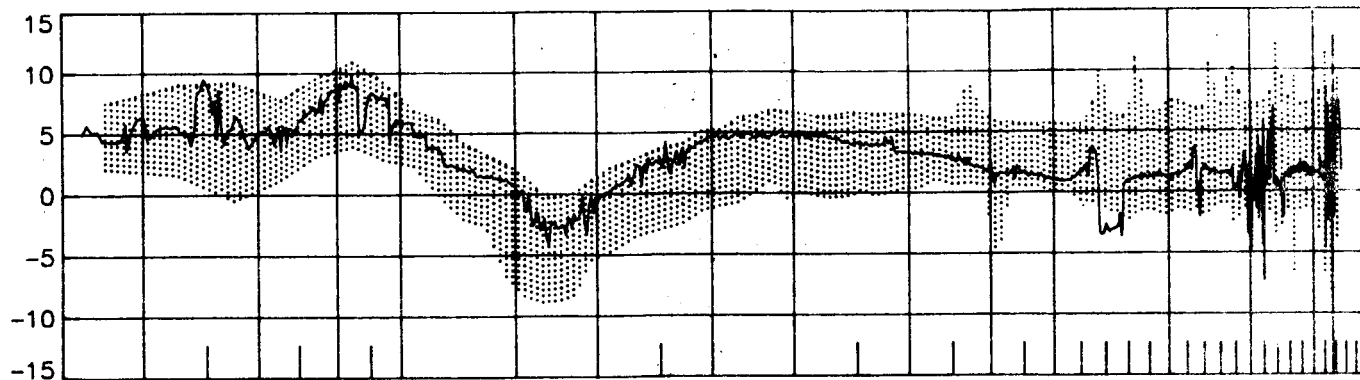


APPENDIX C

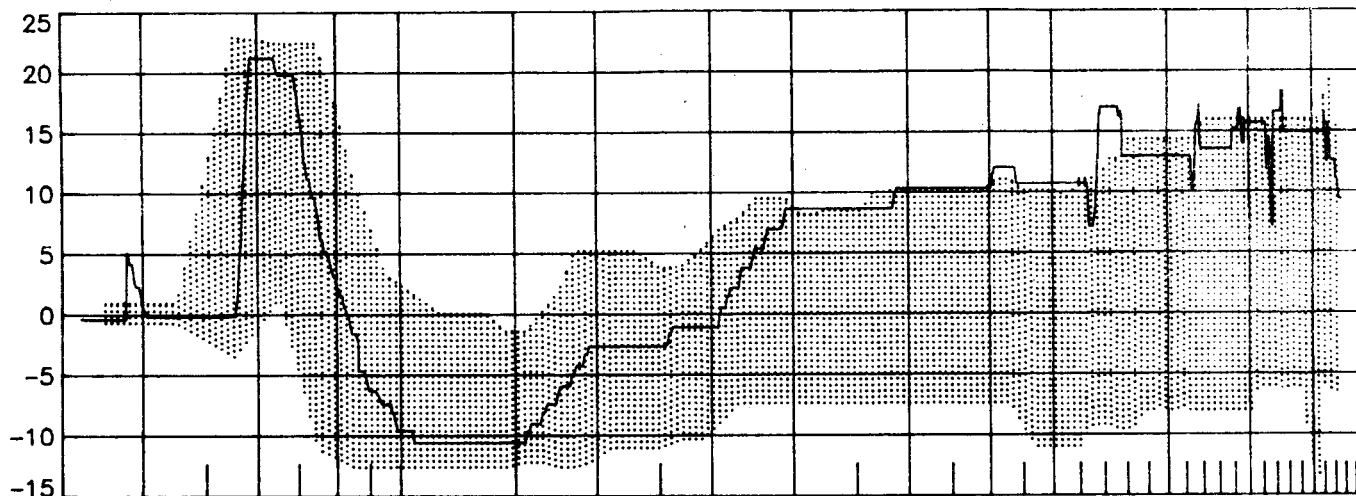
Summary of STS-2 longitudinal results and comparisons.

ORIGINAL PAGE IS
OF POOR QUALITY

δ_E , deg



δ_{BF} , deg



δ_{SBA} , deg

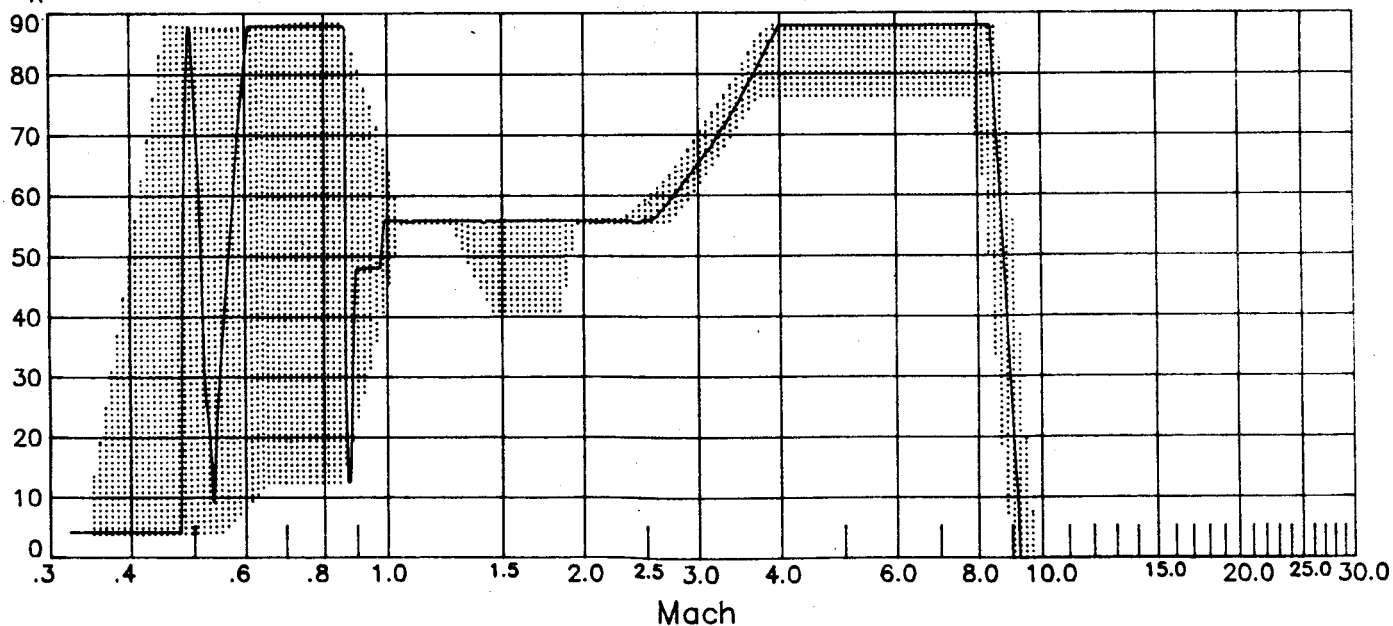
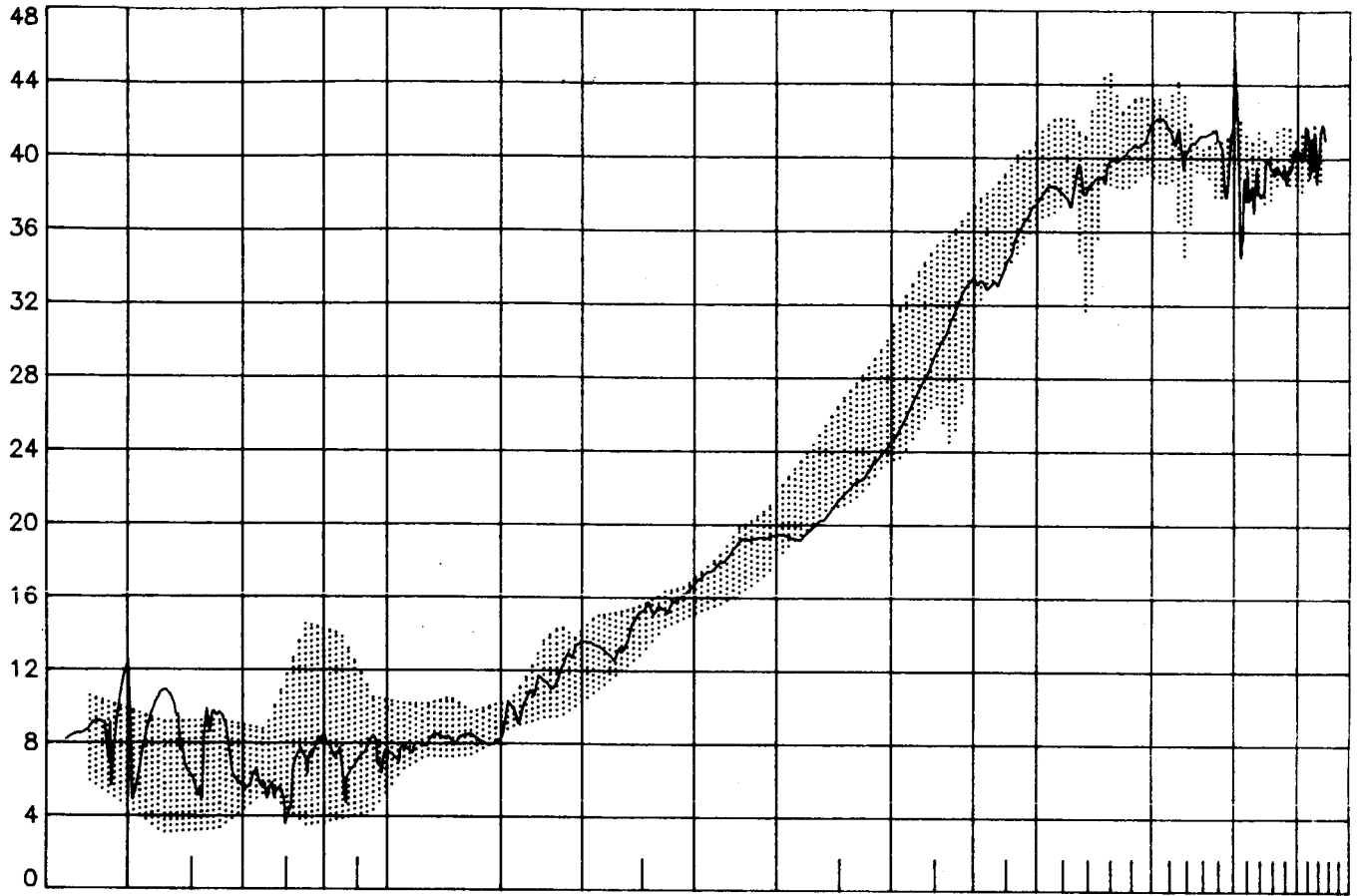


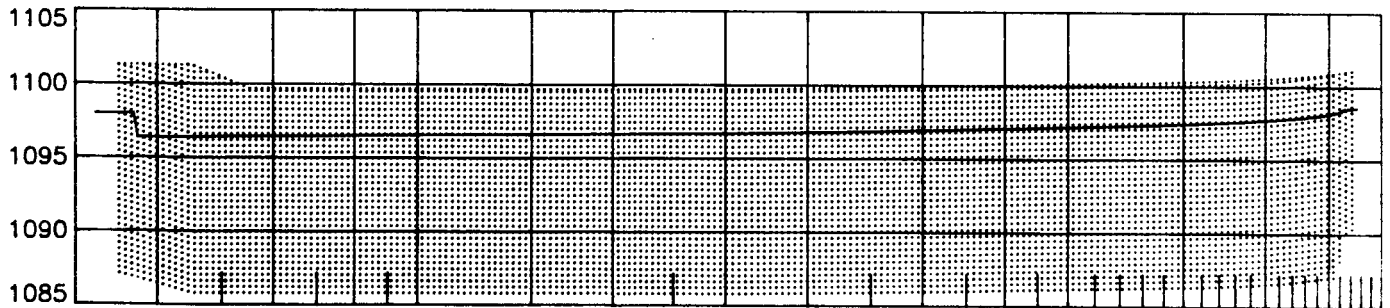
Figure C-1 STS-2 longitudinal control surface deflections
(shaded region defined by remaining ten flights)

ORIGINAL PAGE IS
OF POOR QUALITY

α , deg



x_{cg} , in



z_{cg} , in

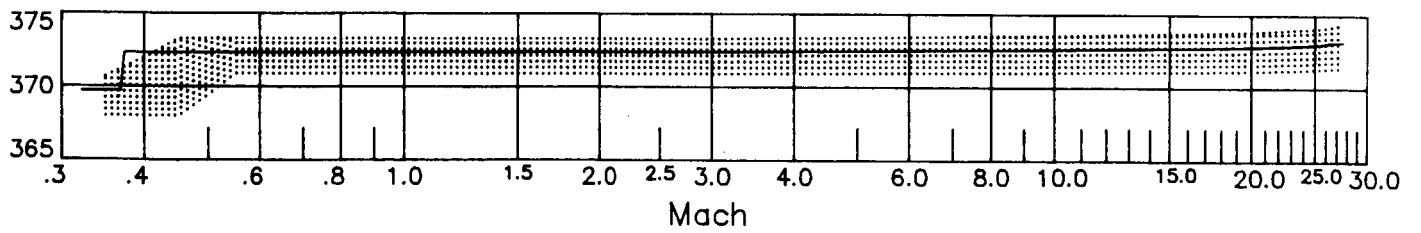
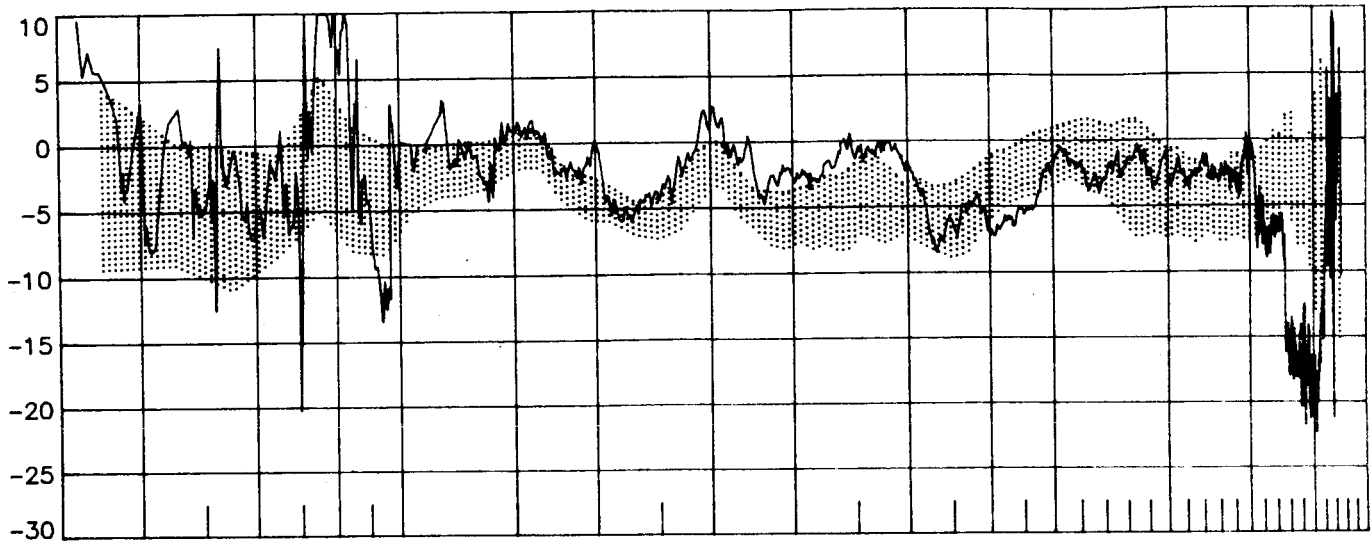


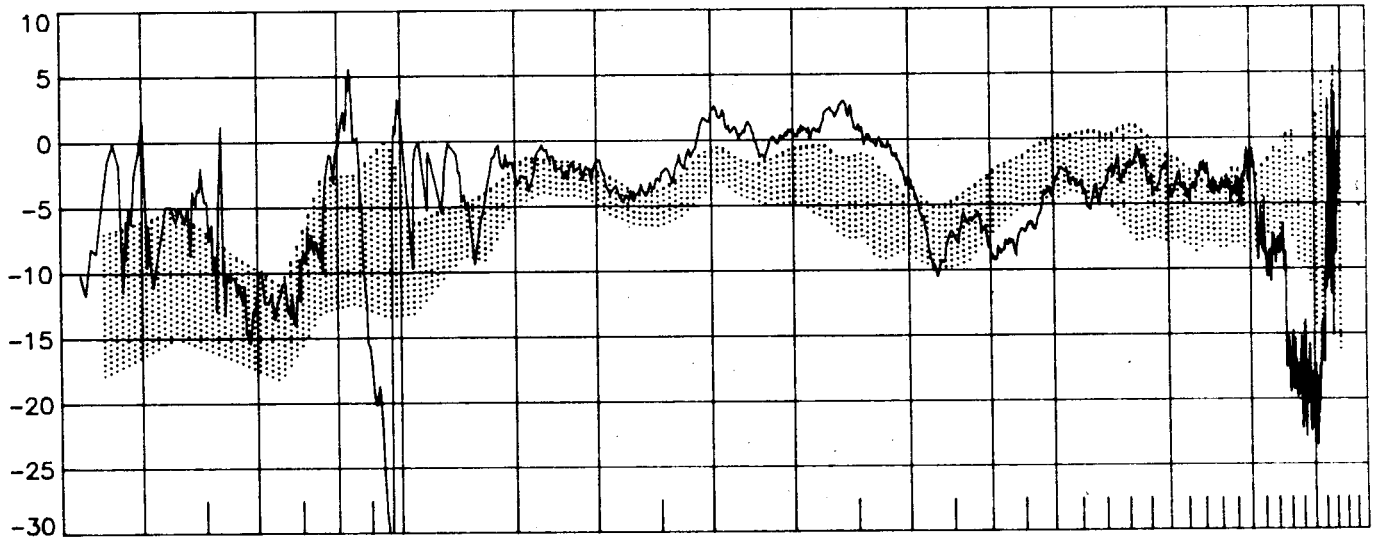
Figure C-2 STS-2 angle-of-attack and c.g. profiles
(shaded region defined by remaining ten flights)

ORIGINAL PAGE IS
OF POOR QUALITY

ΔC_L , percent



ΔC_D , percent



$\Delta(L/D)$, percent

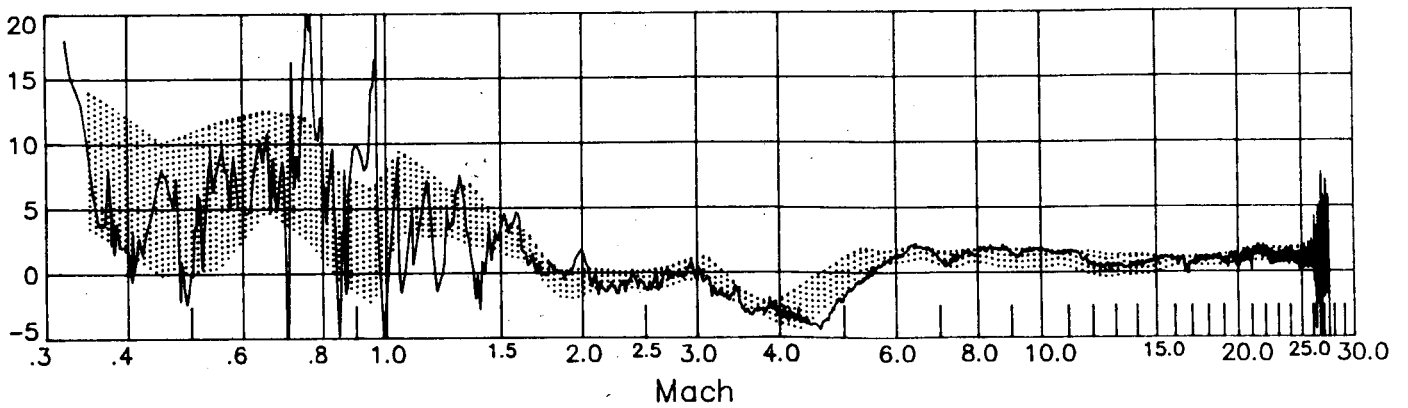
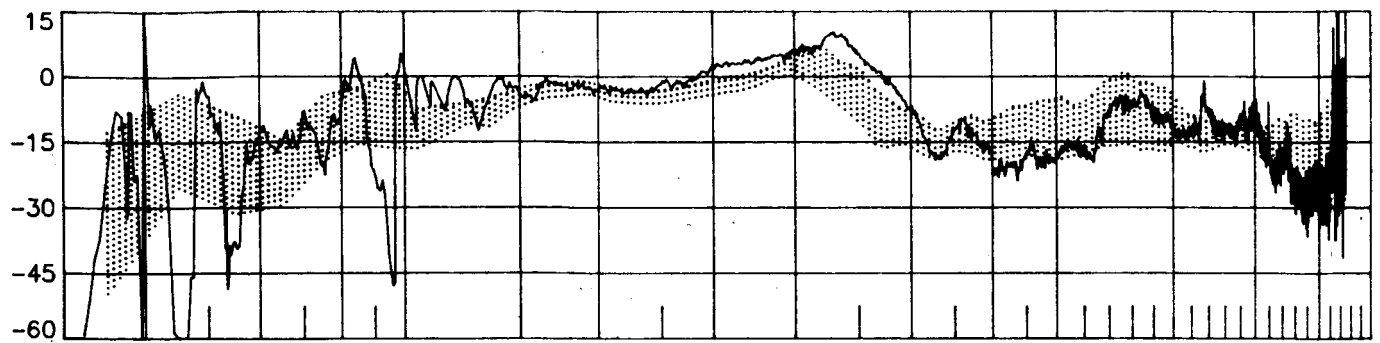


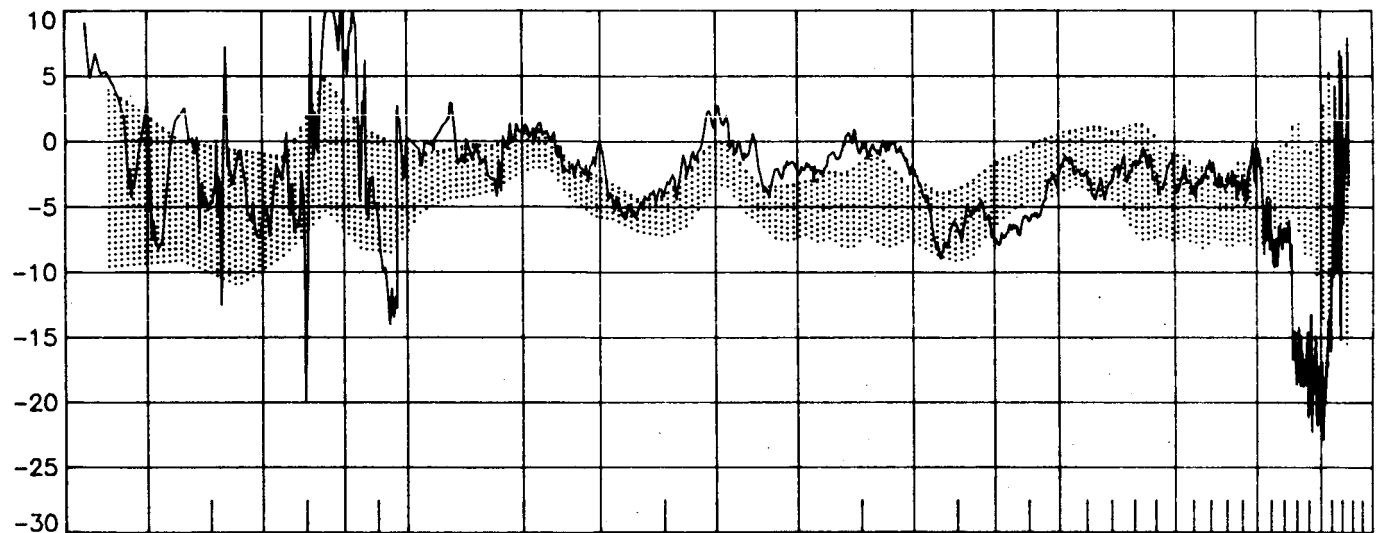
Figure C-3 STS-2 longitudinal performance comparisons
(shaded region defined by remaining ten flights)

ORIGINAL PAGE IS
OF POOR QUALITY

ΔC_A , percent



ΔC_N , percent



ΔC_m , percent

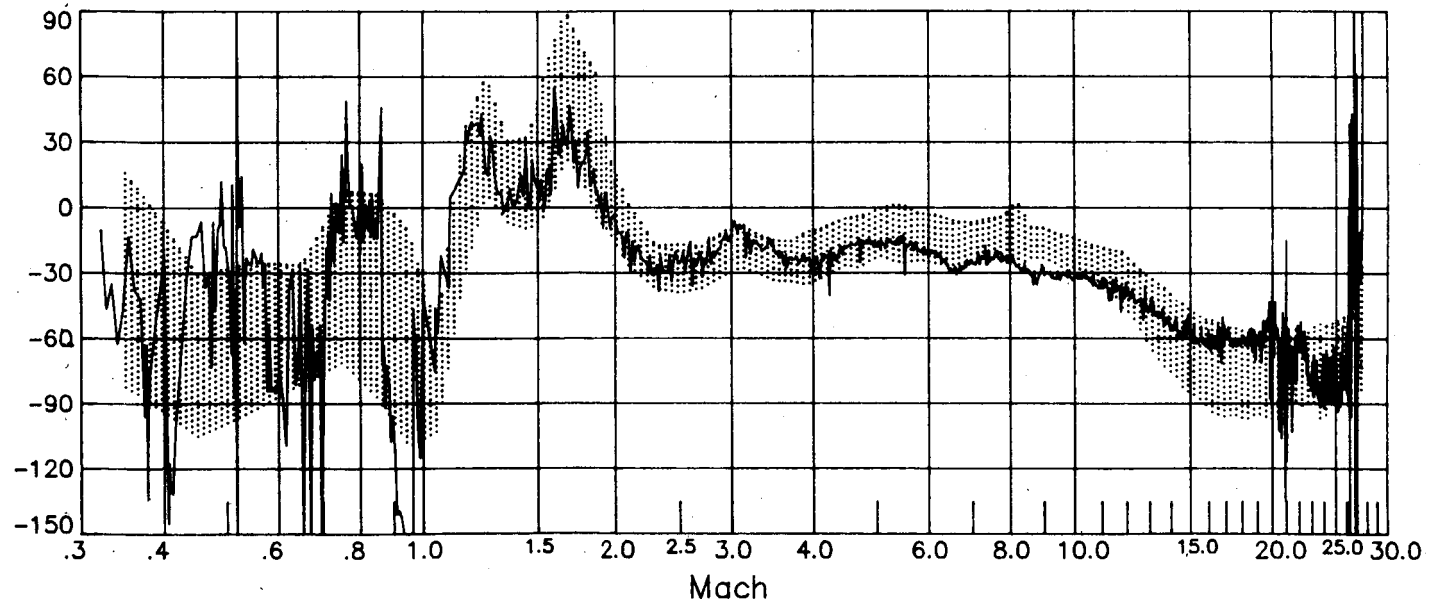


Figure C-3 (concluded)

(shaded region defined by remaining ten flights)

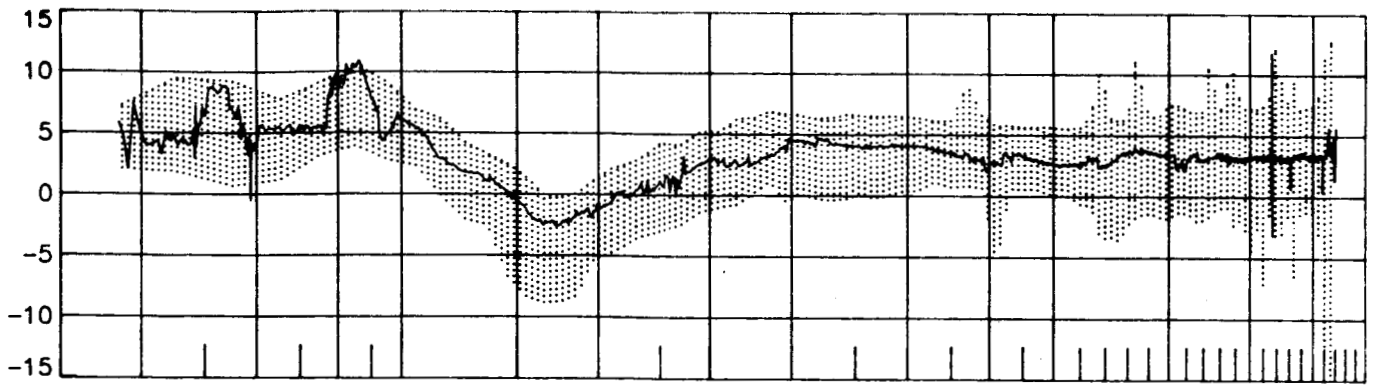
ORIGINAL PAGE IS
OF FOUR QUALITY



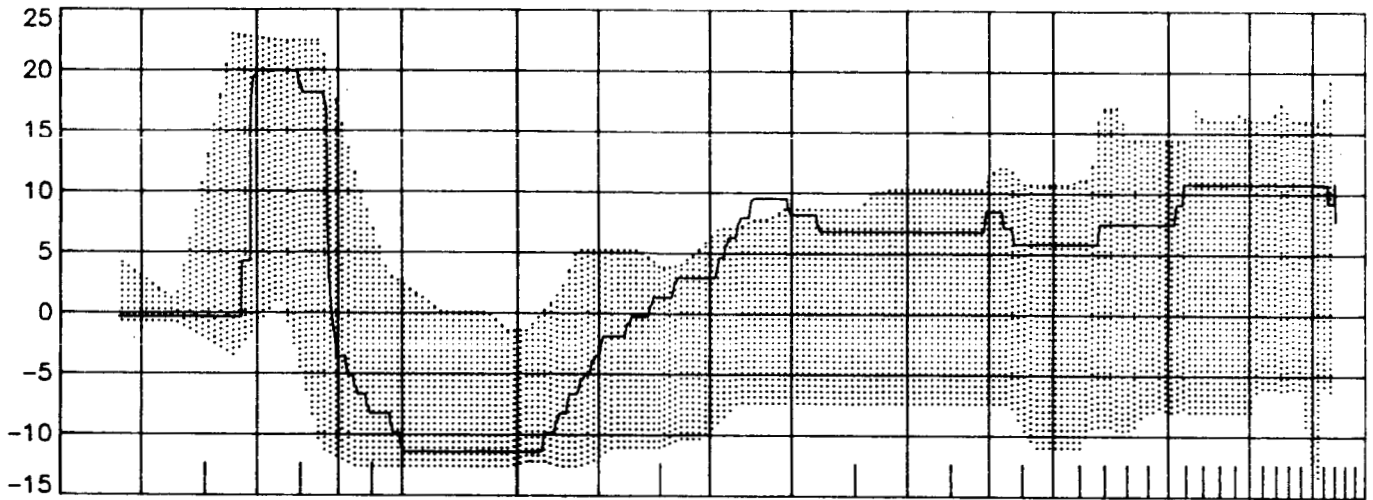
APPENDIX D

Summary of STS-3 longitudinal results and comparisons.

δ_E , deg



δ_{BF} , deg



δ_{SBA} , deg

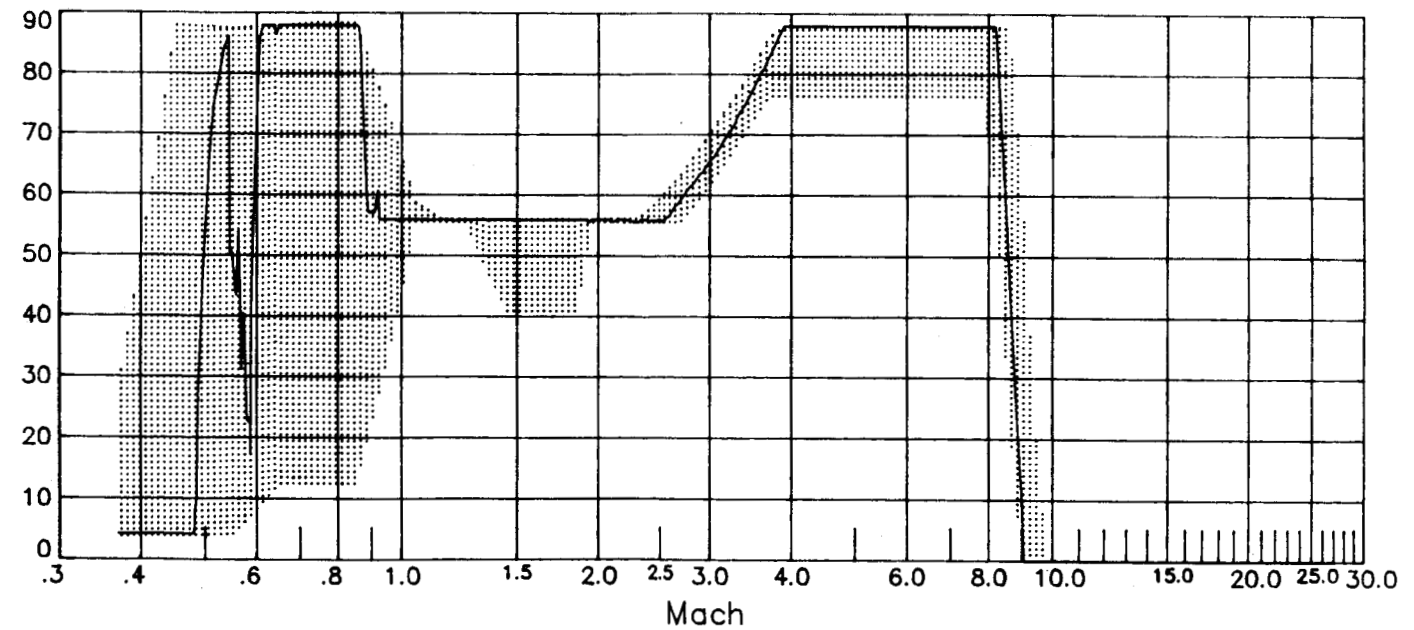
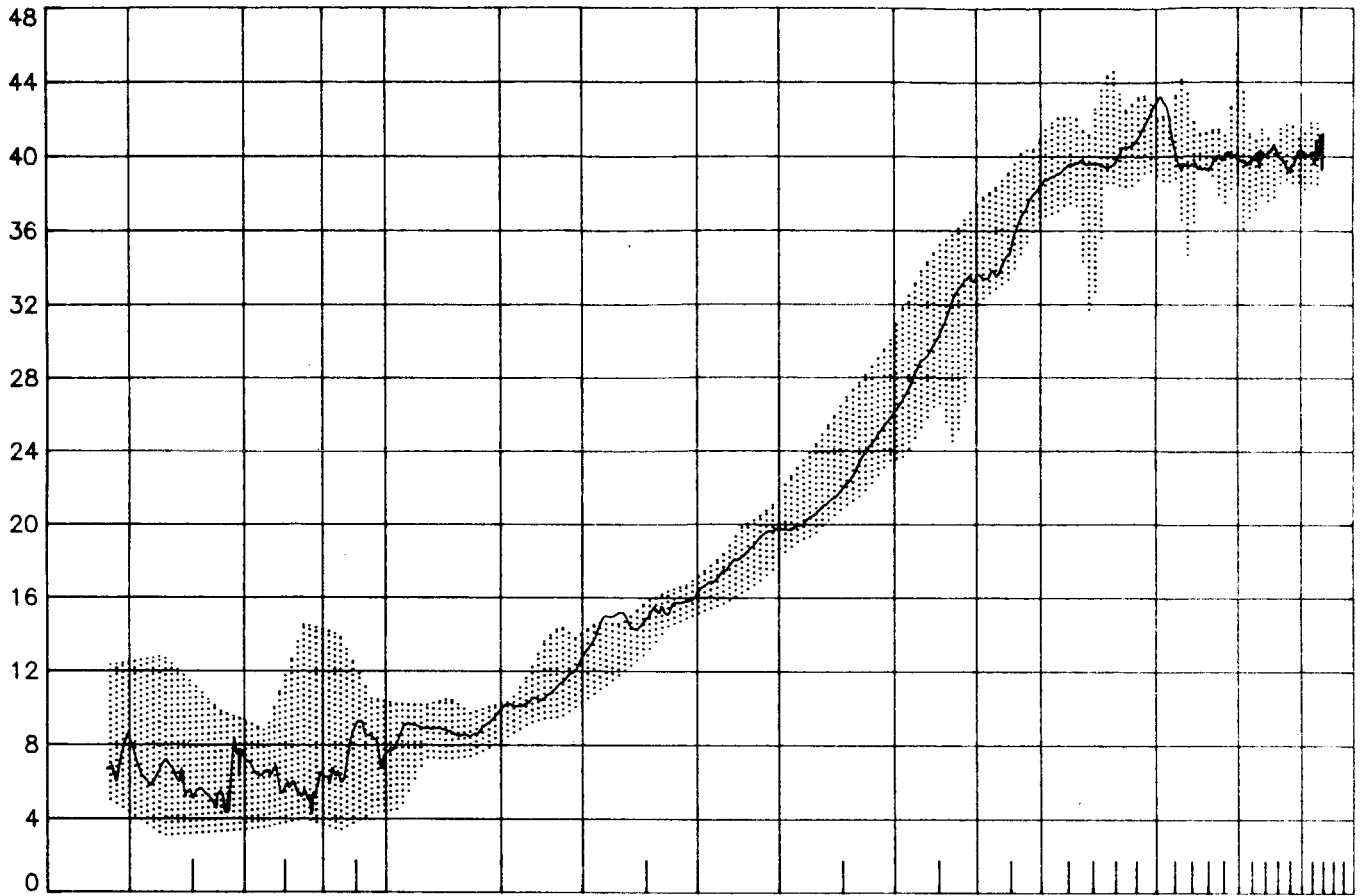
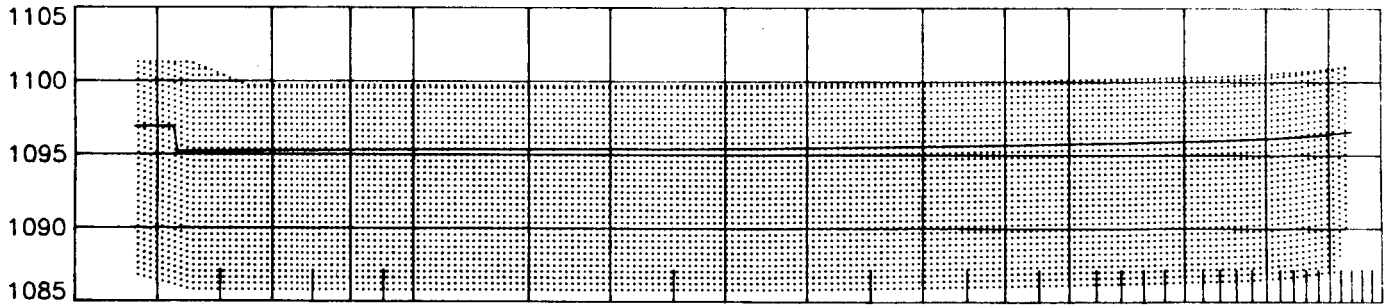


Figure D-1 STS-3 longitudinal control surface deflections
(shaded region defined by remaining ten flights)

α , deg



x_{cg} , in



z_{cg} , in

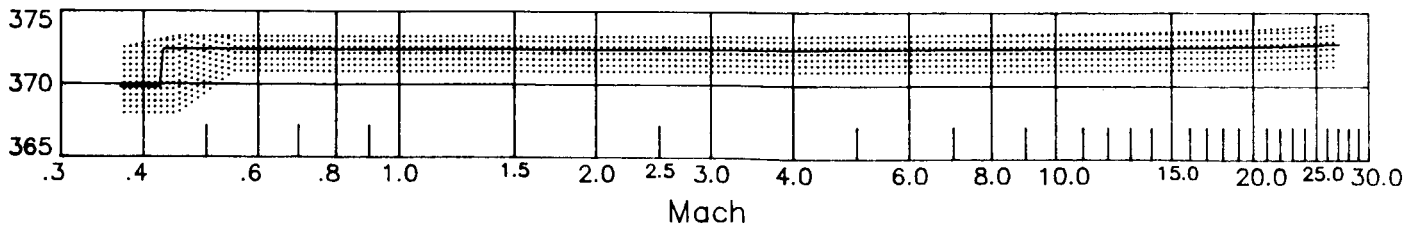
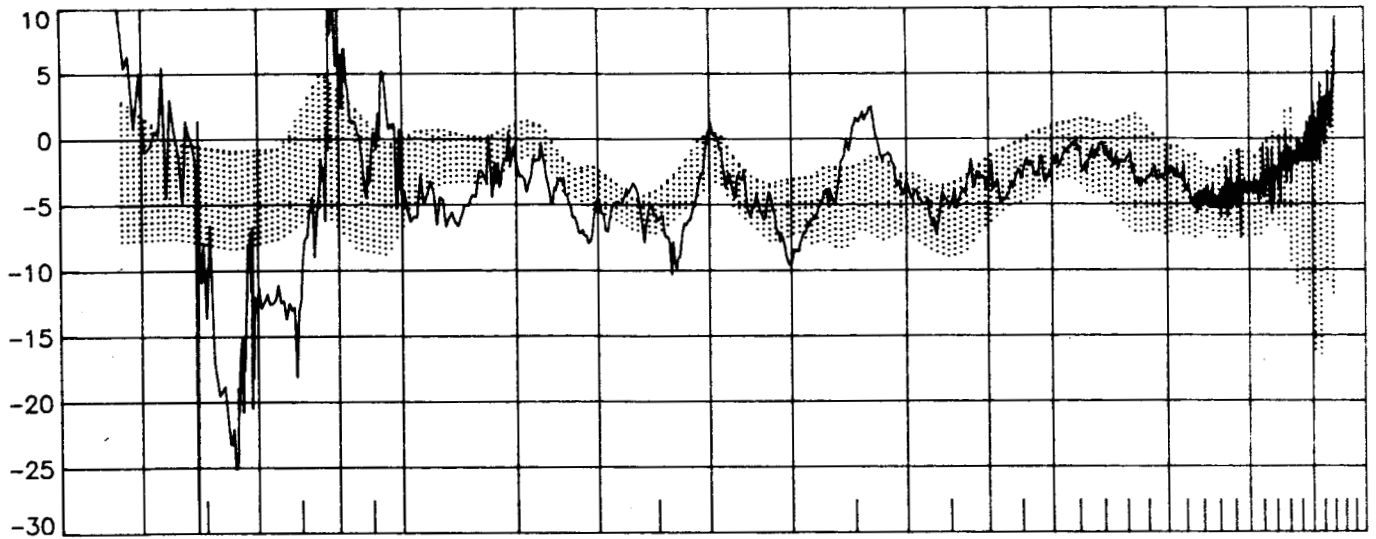


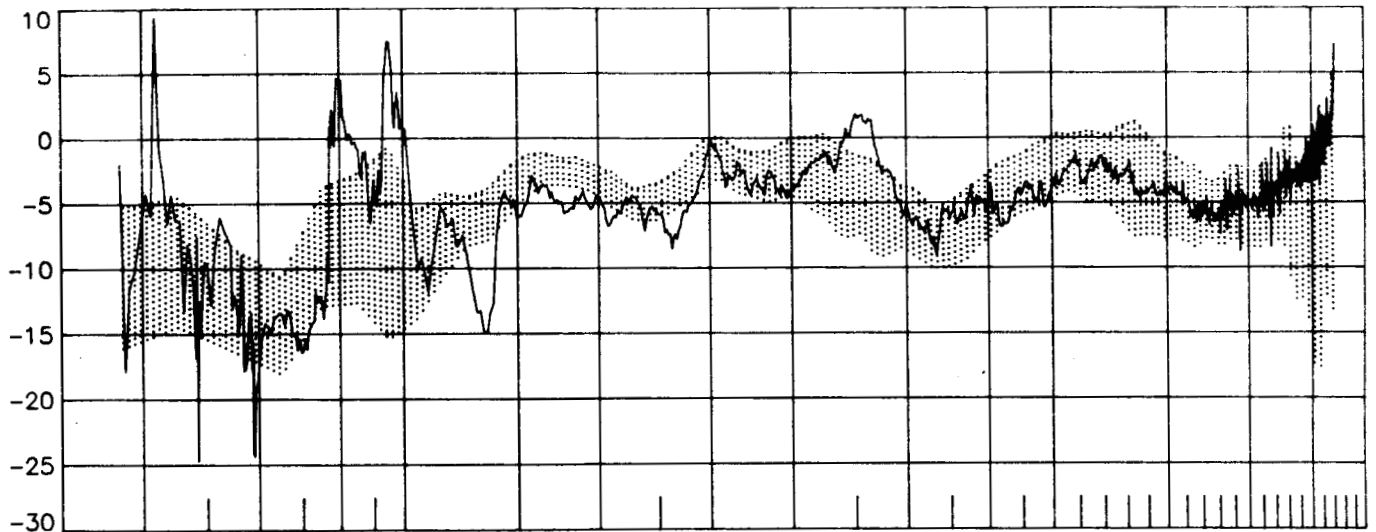
Figure D-2 STS-3 angle-of-attack and c.g. profiles
(shaded region defined by remaining ten flights)

ORIGINAL PAGE IS
OF POOR QUALITY

ΔC_L , percent



ΔC_D , percent



$\Delta(L/D)$, percent

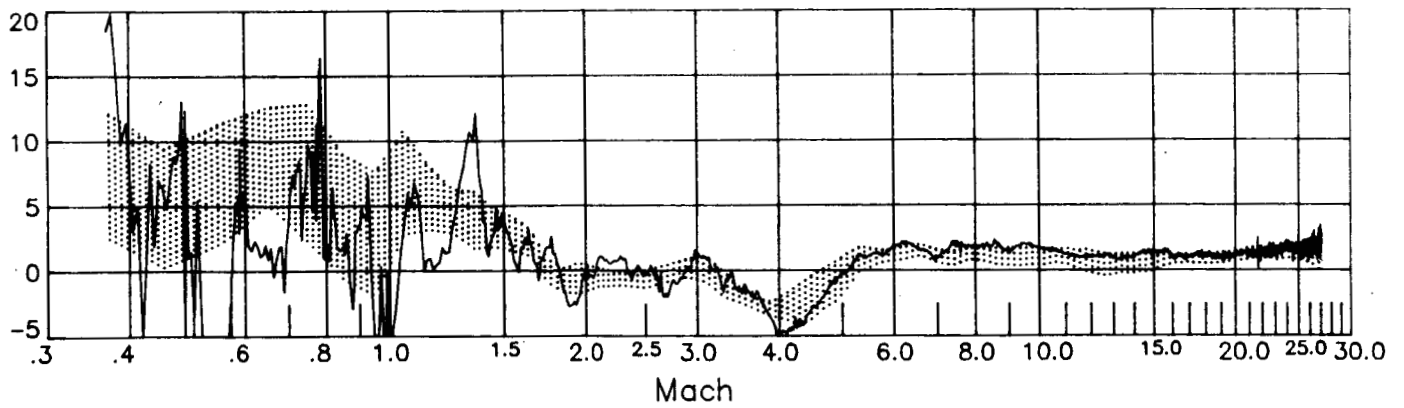
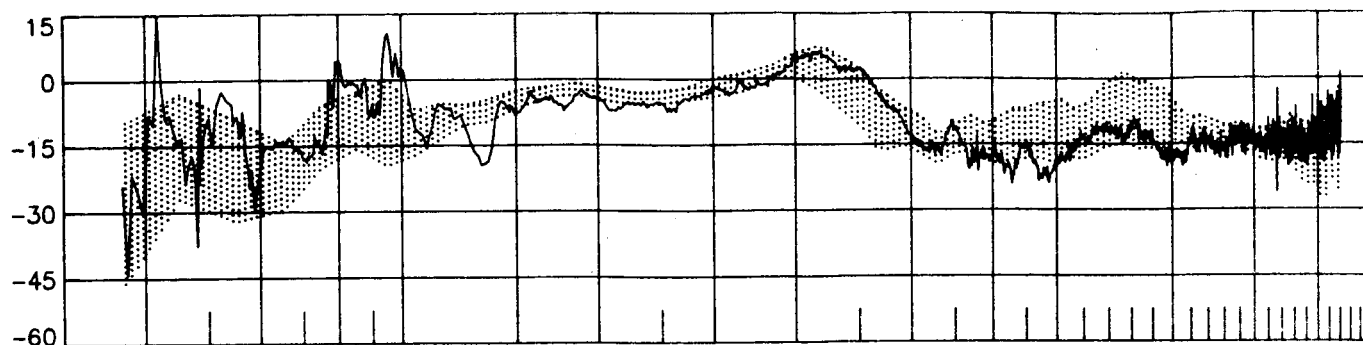


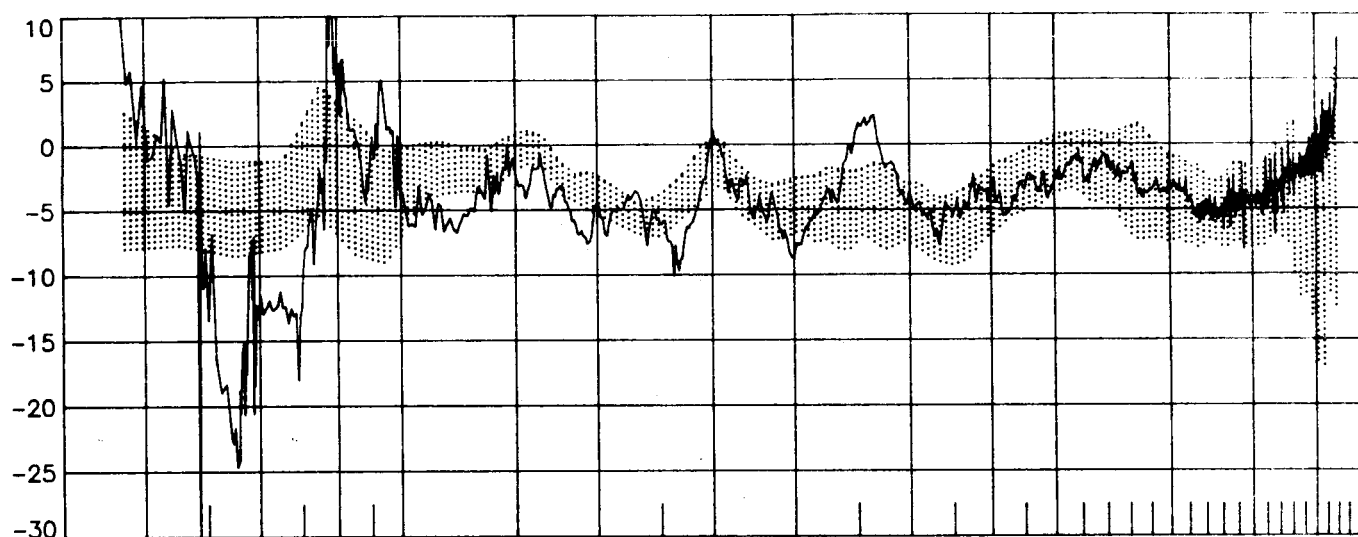
Figure D-3 STS-3 longitudinal performance comparisons
(shaded region defined by remaining ten flights)

ORDER OF, VALUE OF
OF FOUR QUALITY

ΔC_A , percent



ΔC_N , percent



ΔC_m , percent

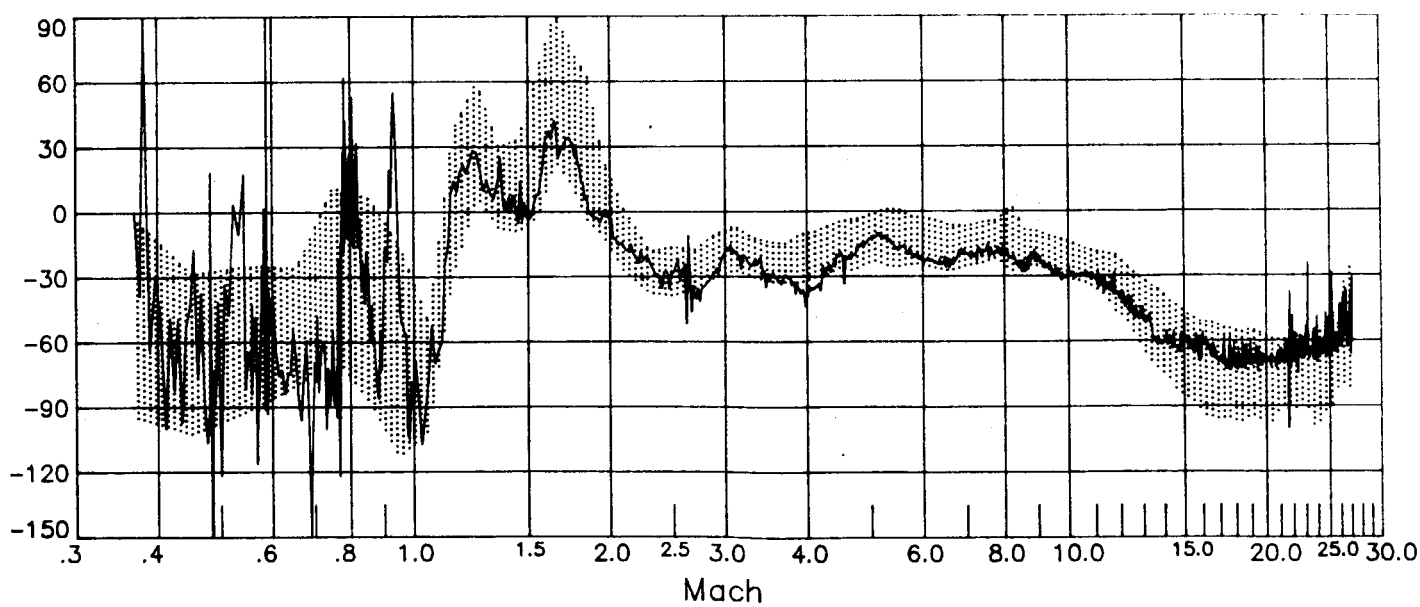


Figure D-3 (concluded)

(shaded region defined by remaining ten flights)

ORIGINAL PAGE IS
OF POOR QUALITY

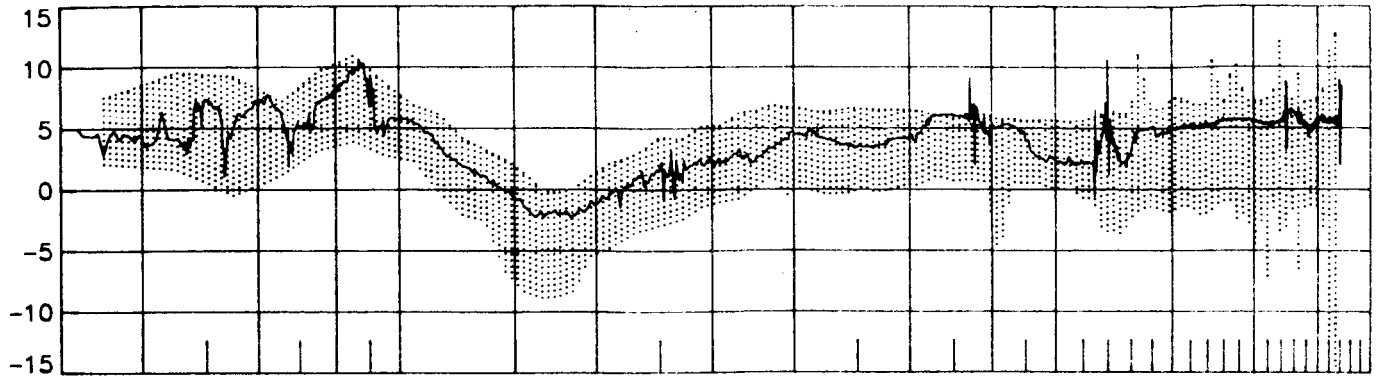


APPENDIX E

Summary of STS-4 longitudinal results and comparisons.

ORIGINAL PAGE IS
OF POOR QUALITY

δ_E , deg



δ_{BF} , deg



δ_{SBA} , deg

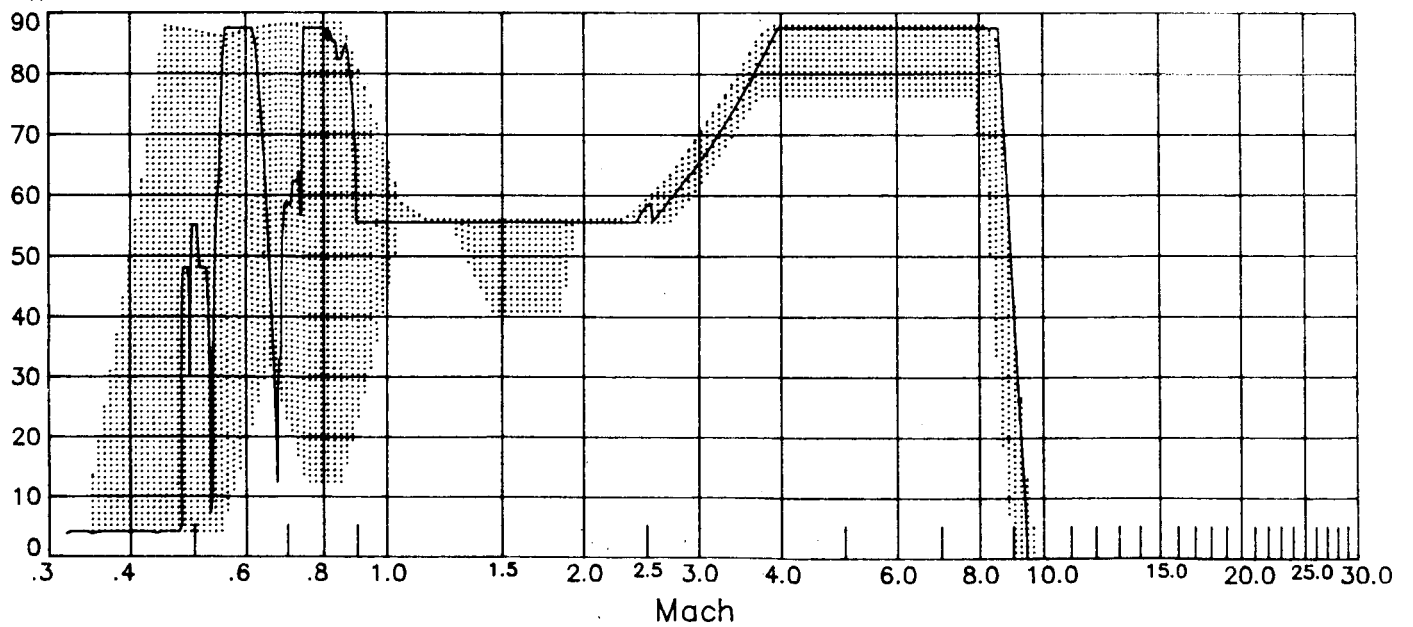
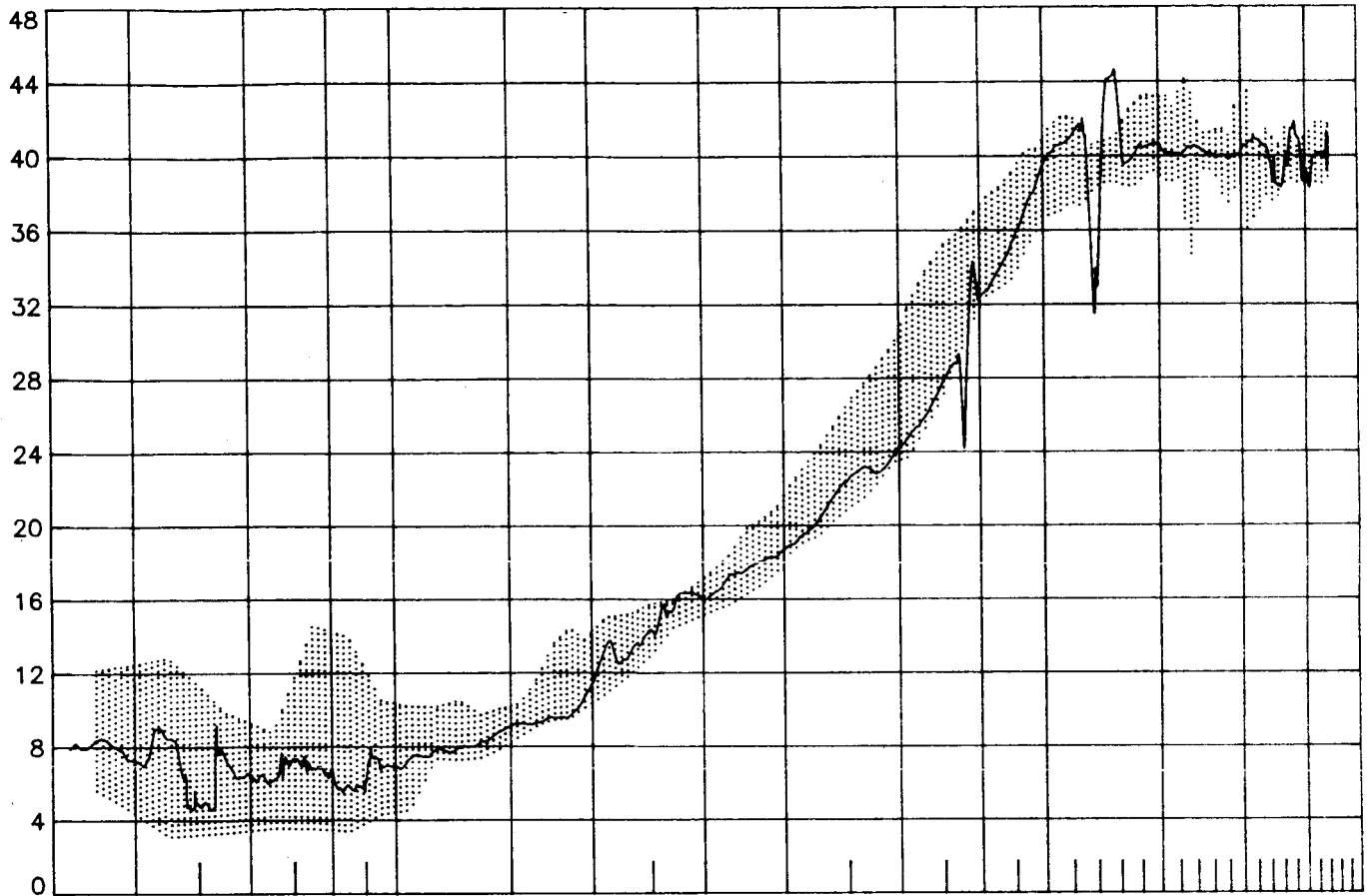


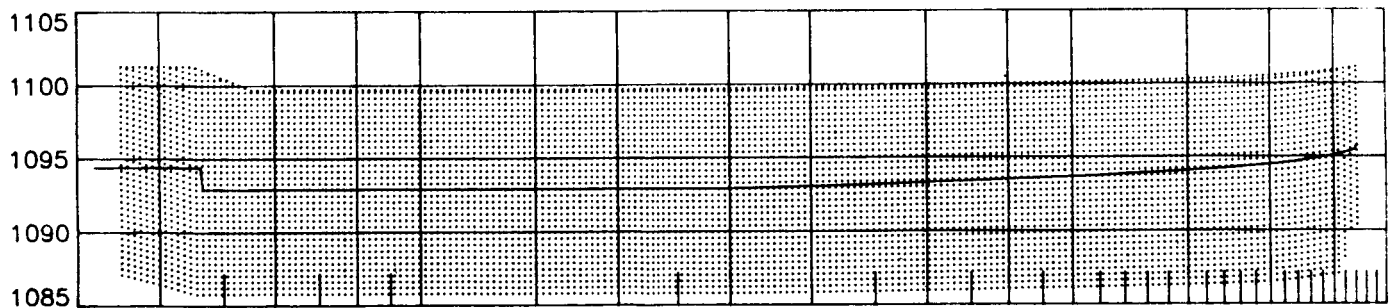
Figure E-1 STS-4 longitudinal control surface deflections
(shaded region defined by remaining ten flights)

ORIGINAL PAGE IS
OF POOR QUALITY

α , deg



x_{cg} , in



z_{cg} , in

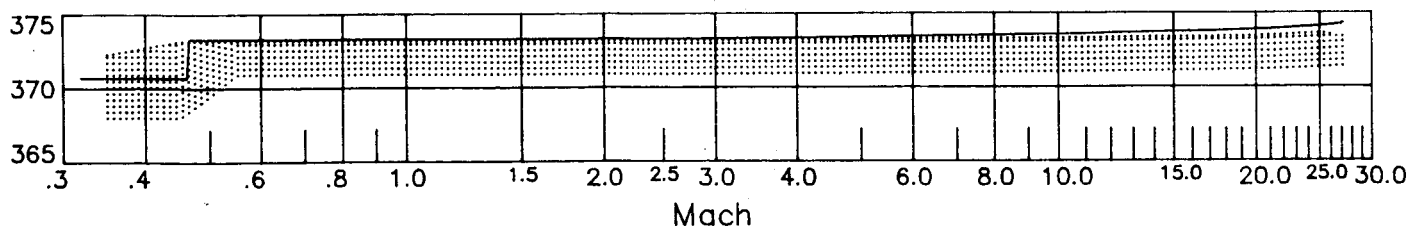
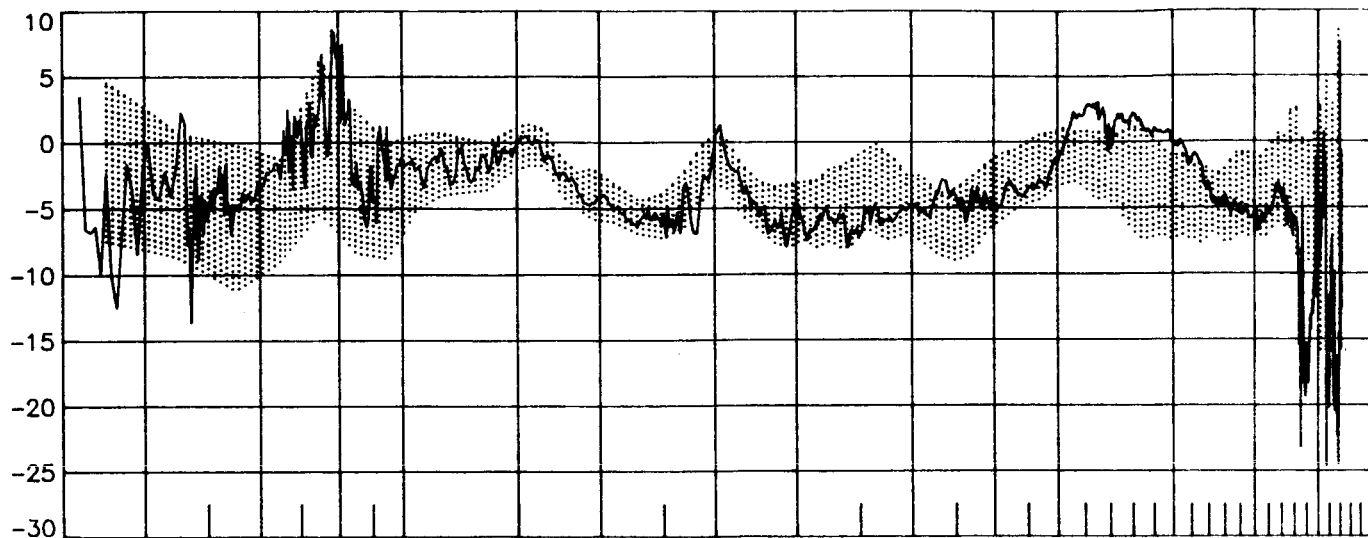


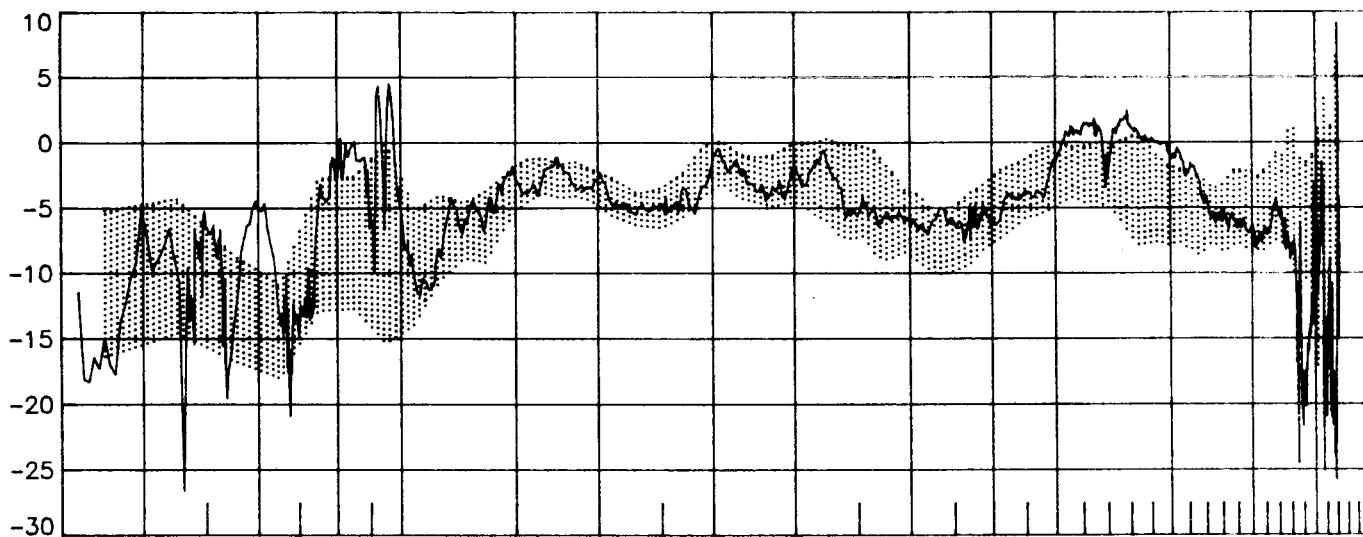
Figure E-2 STS-4 angle-of-attack and c.g. profiles
(shaded region defined by remaining ten flights)

ORIGINAL PAGE IS
OF FOUR QUALITY

ΔC_L , percent



ΔC_D , percent



$\Delta(L/D)$, percent

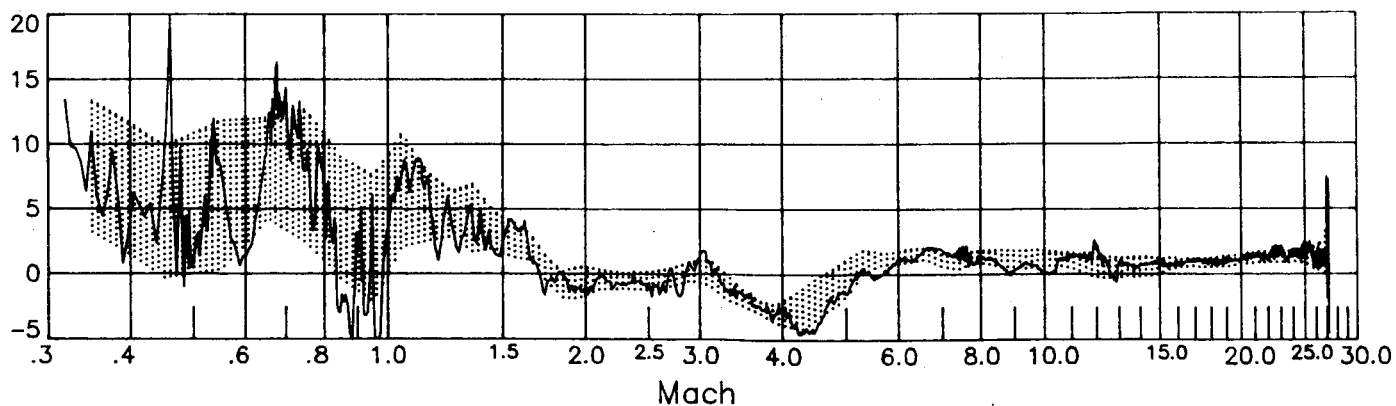
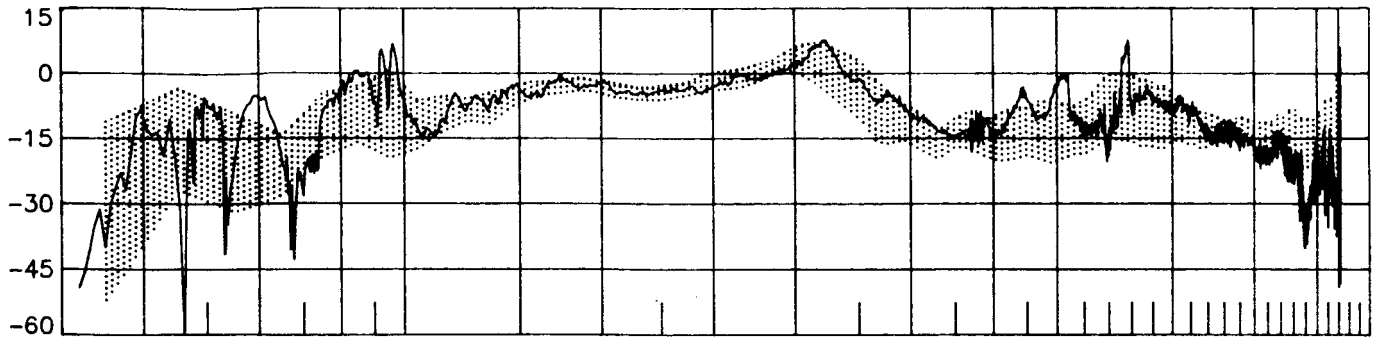


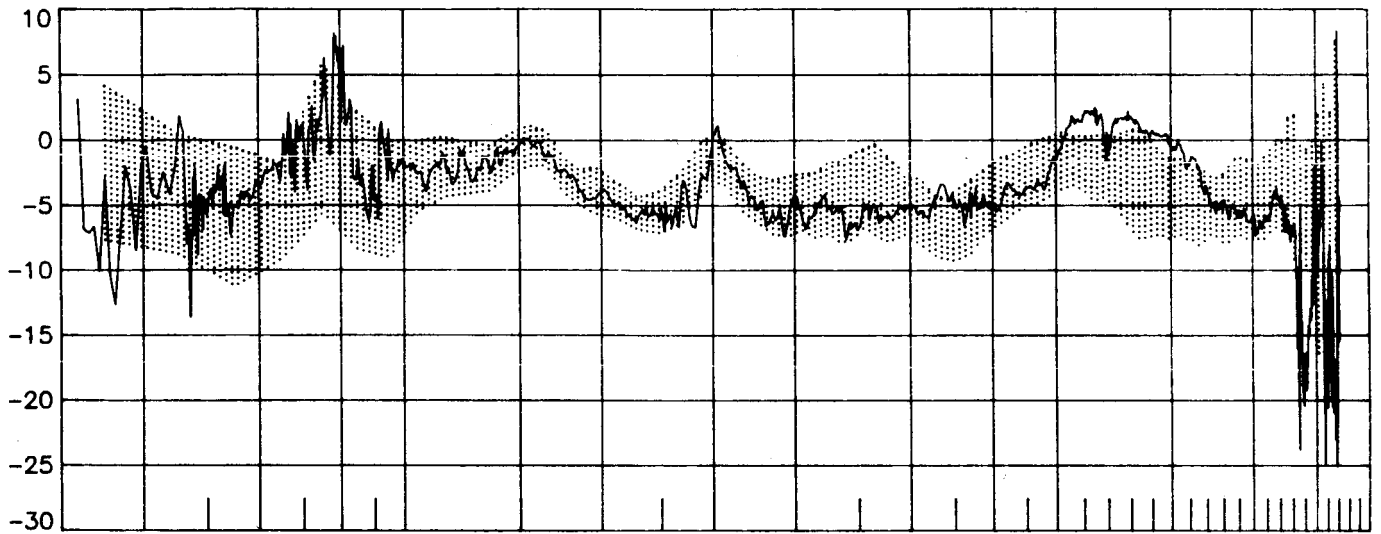
Figure E-3 STS-4 longitudinal performance comparisons
(shaded region defined by remaining ten flights)

ORIGINAL FILE IS
OF POOR QUALITY

ΔC_A , percent



ΔC_N , percent



ΔC_m , percent

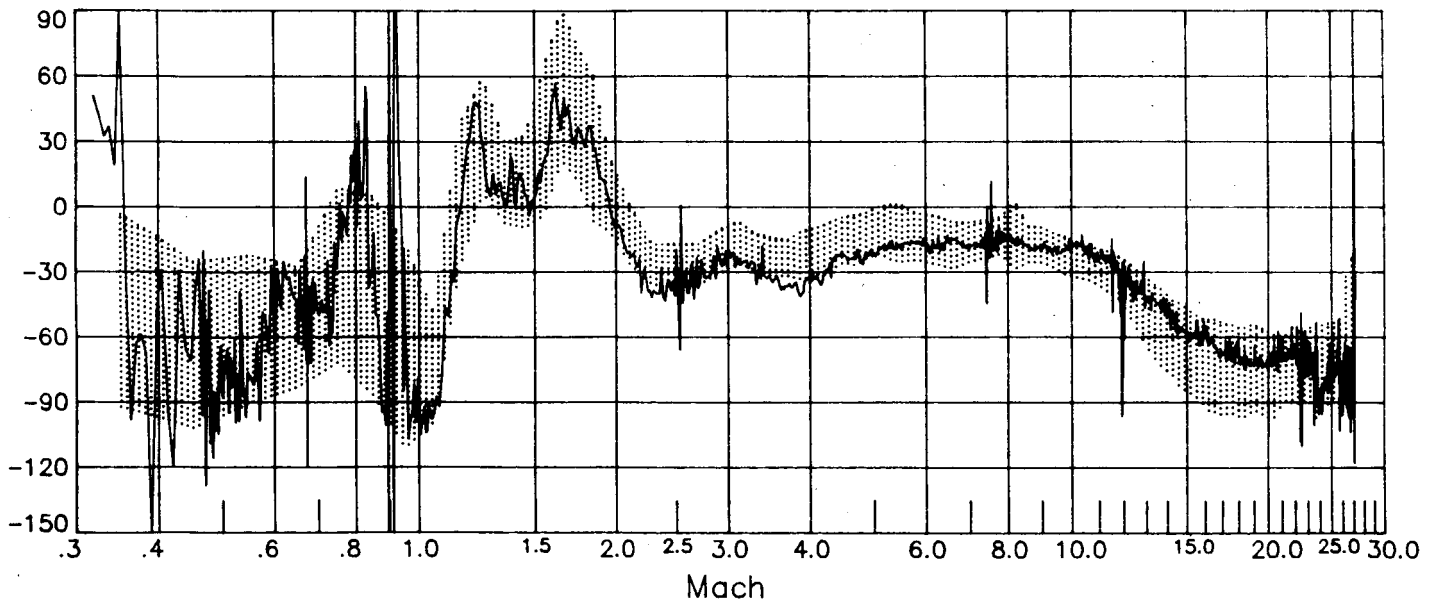


Figure E-3 (concluded)

(shaded region defined by remaining ten flights)

ORIGINAL PAGE IS
OF POOR QUALITY

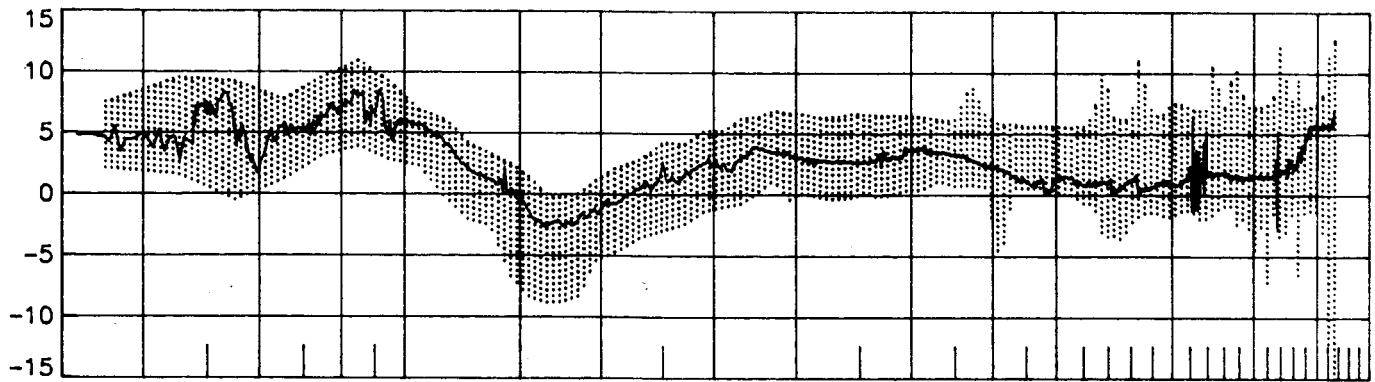


APPENDIX F

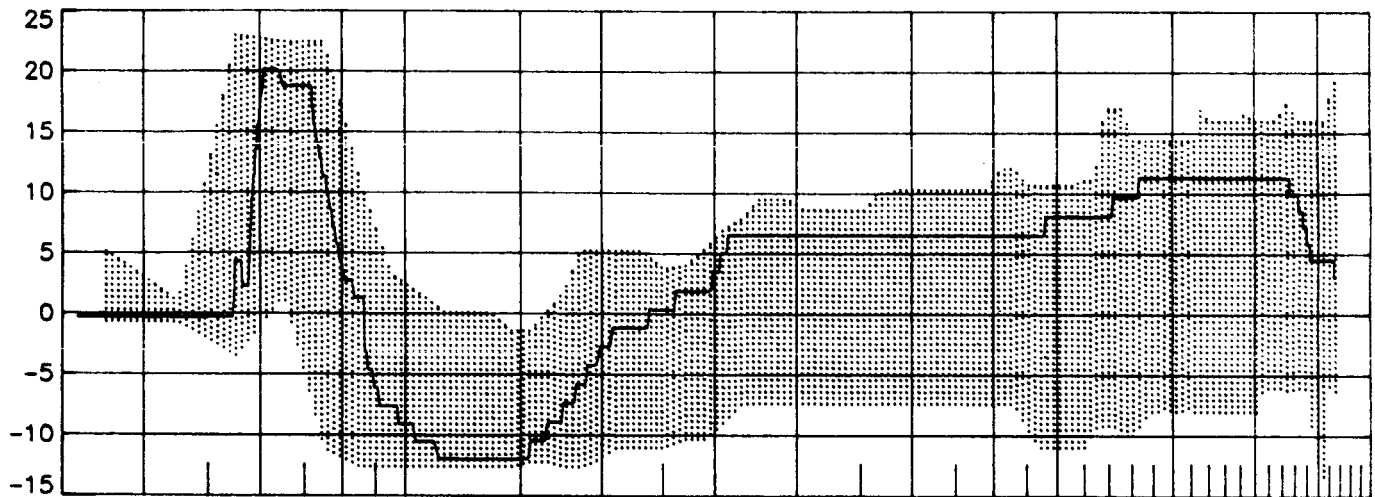
Summary of STS-5 longitudinal results and comparisons.

ORIGINAL PAGE IS
OF POOR QUALITY

δ_E , deg



δ_{BF} , deg



δ_{SBA} , deg

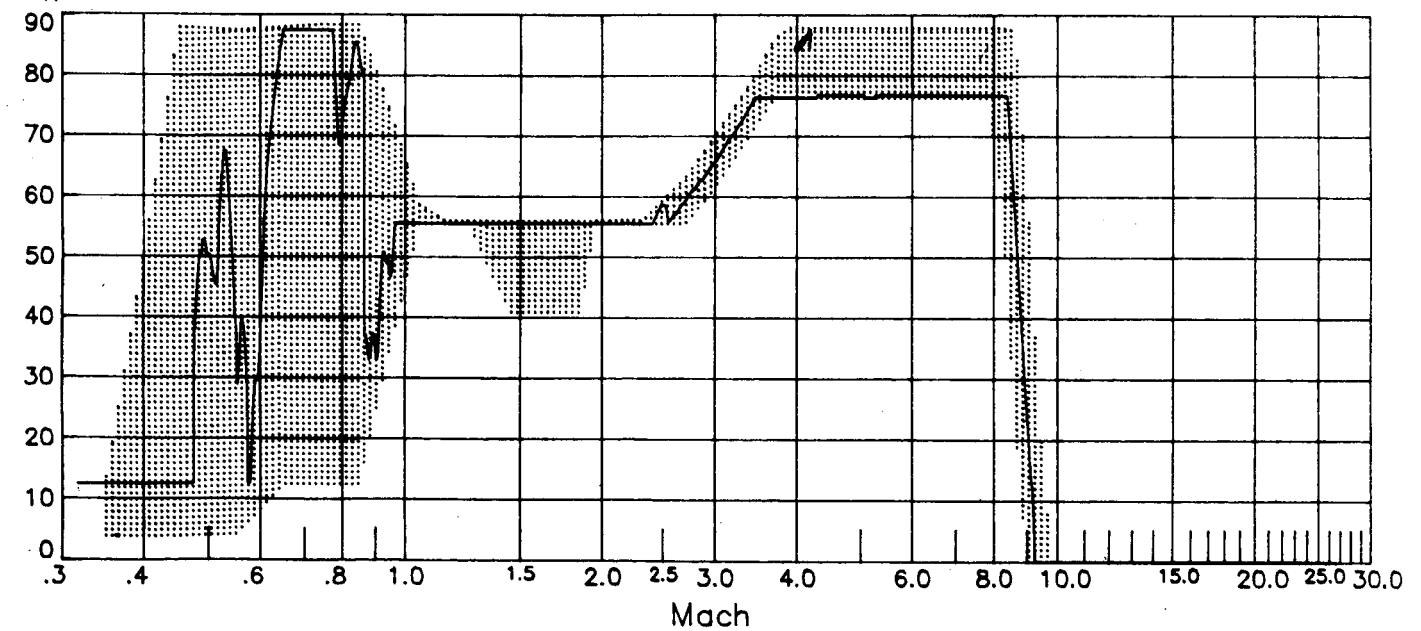
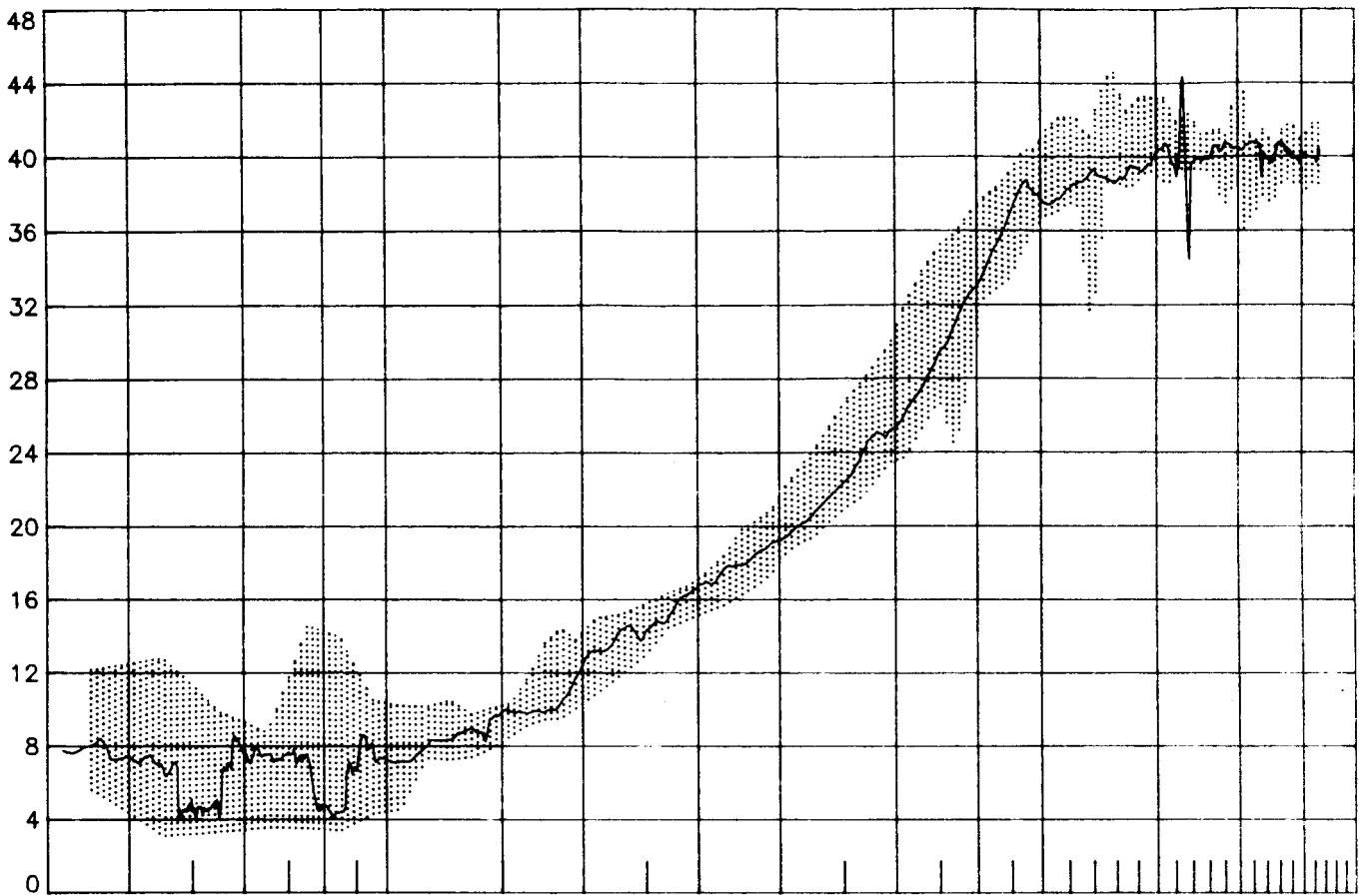
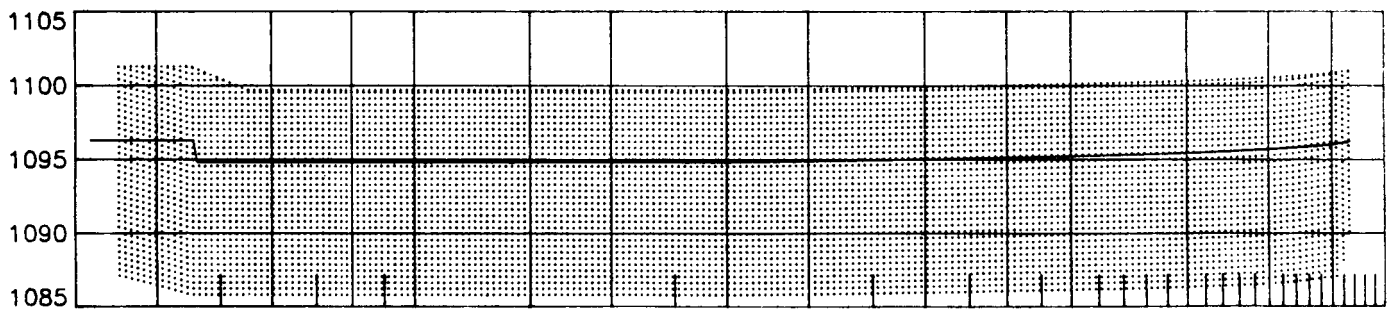


Figure F-1 STS-5 longitudinal control surface deflections
(shaded region defined by remaining ten flights)

α , deg



x_{cg} , in



z_{cg} , in

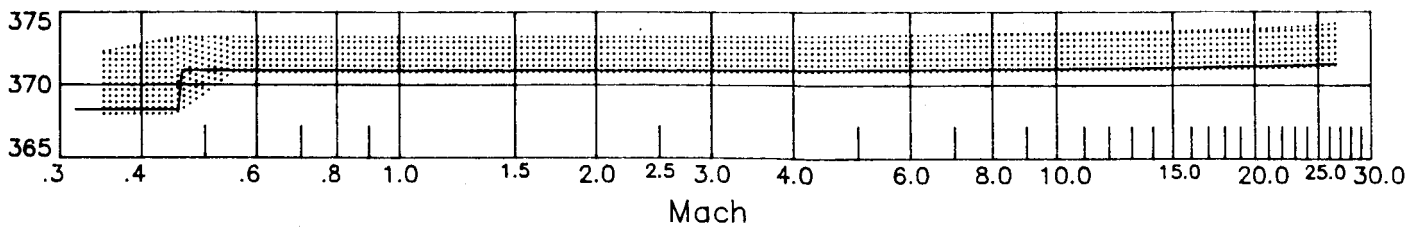
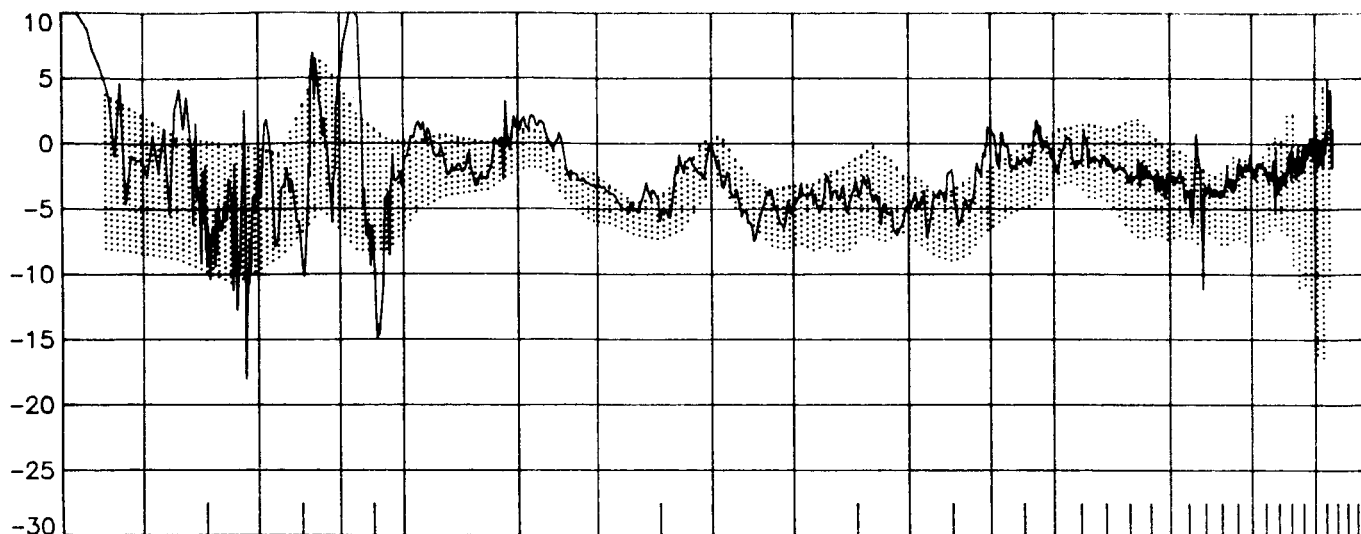
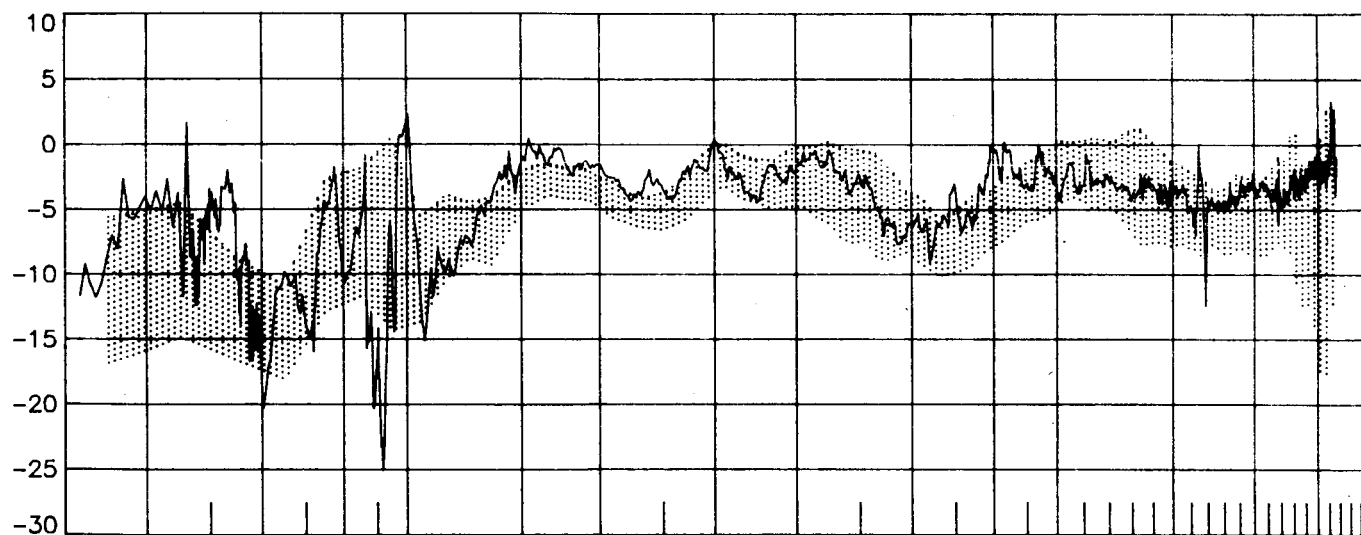


Figure F-2 STS-5 angle-of-attack and c.g. profiles
(shaded region defined by remaining ten flights)

ΔC_L , percent



ΔC_D , percent



$\Delta(L/D)$, percent

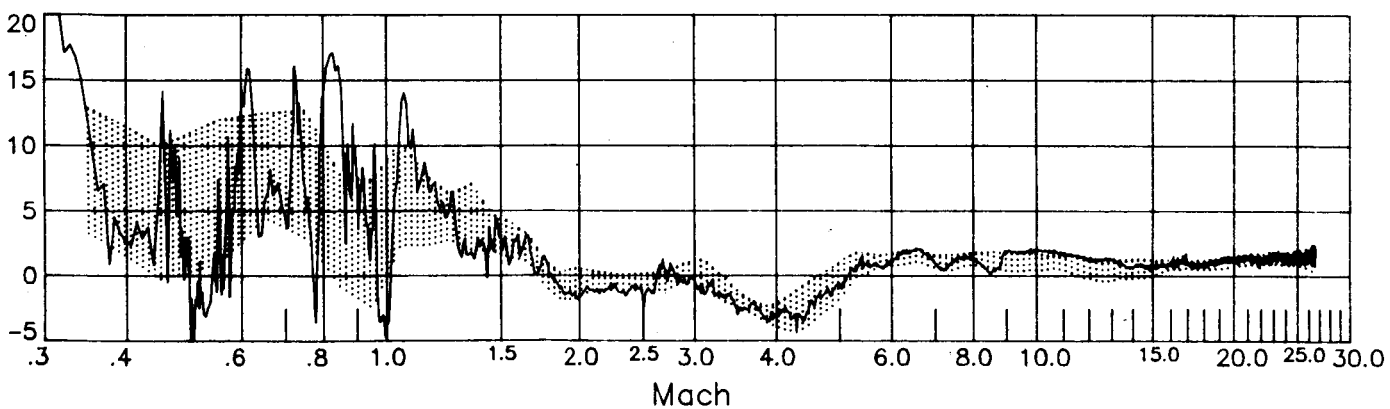
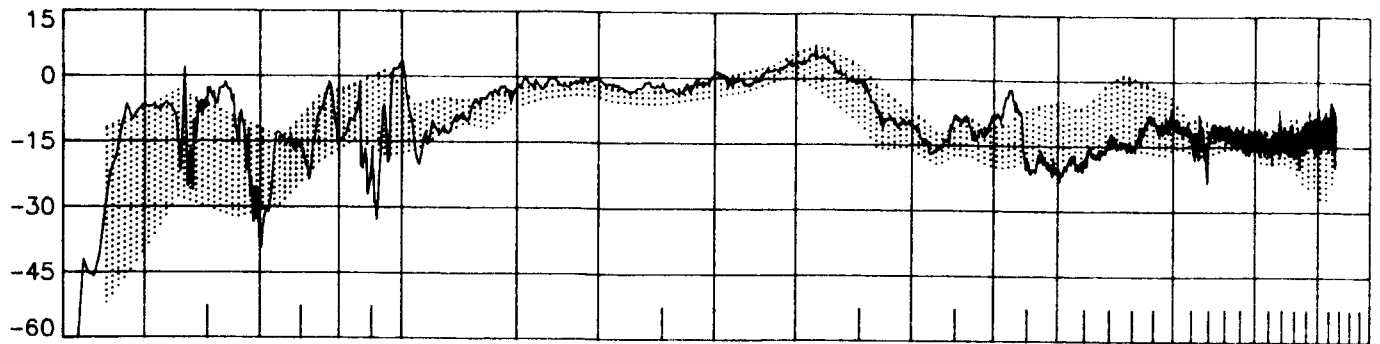


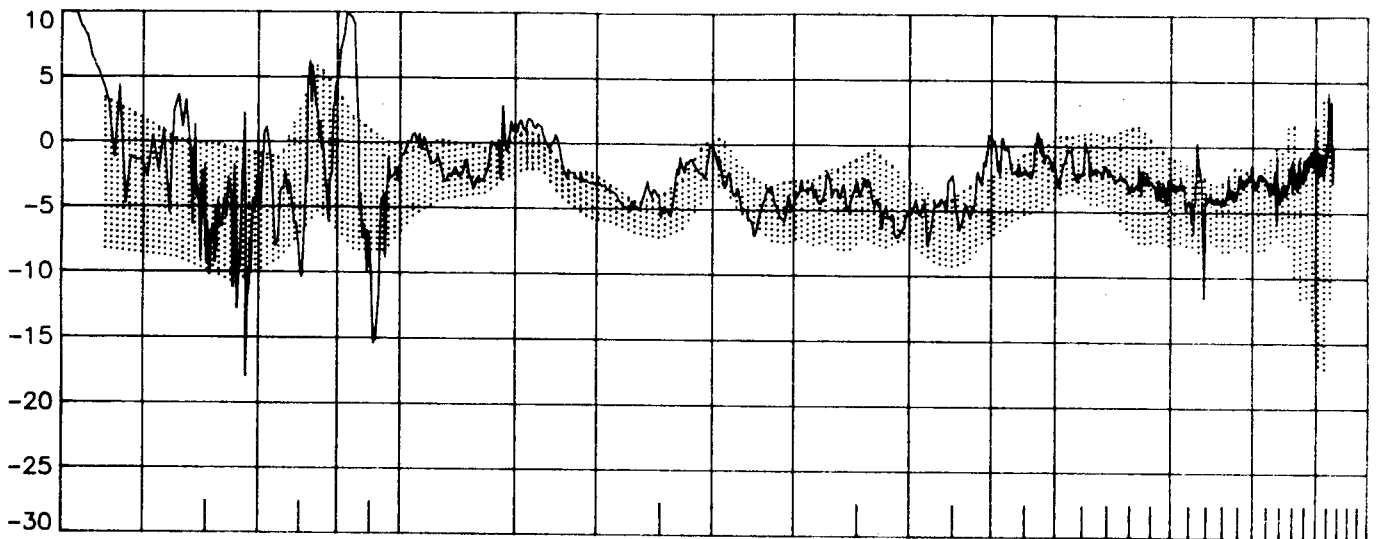
Figure F-3 STS-5 longitudinal performance comparisons
(shaded region defined by remaining ten flights)

ORIGINAL PAPER IS
OF POOR QUALITY

ΔC_A , percent



ΔC_N , percent



ΔC_m , percent

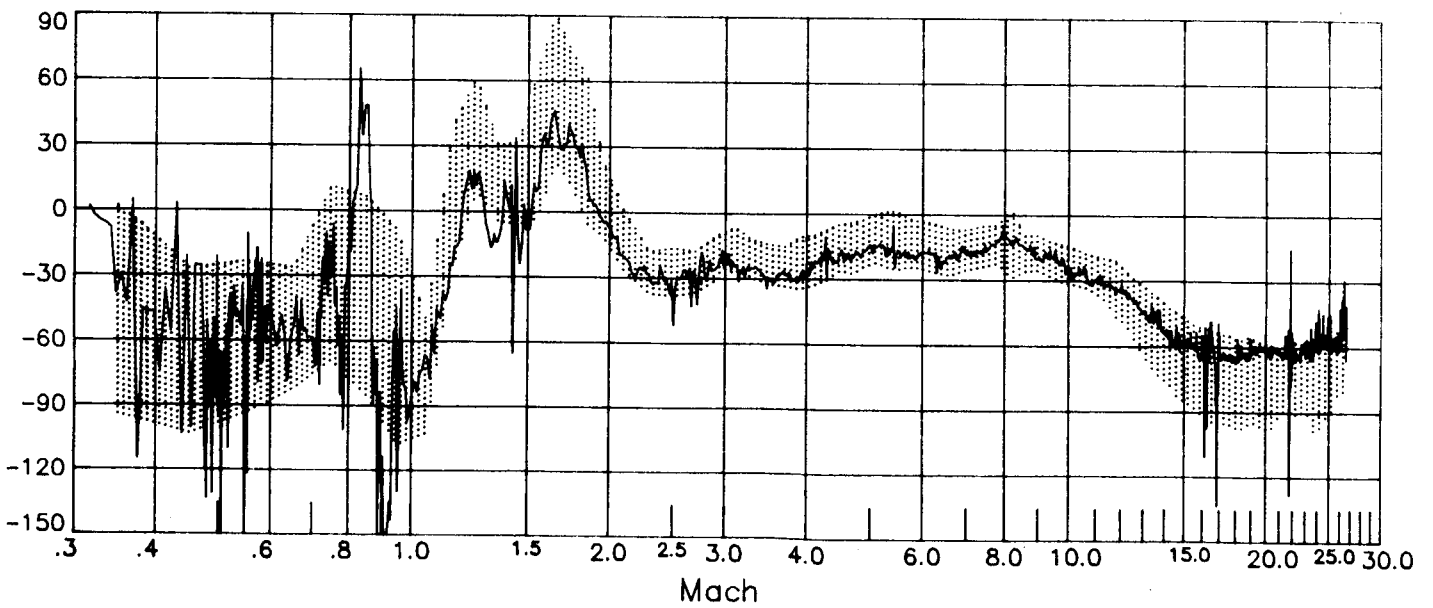


Figure F-3 (concluded)

(shaded region defined by remaining ten flights)

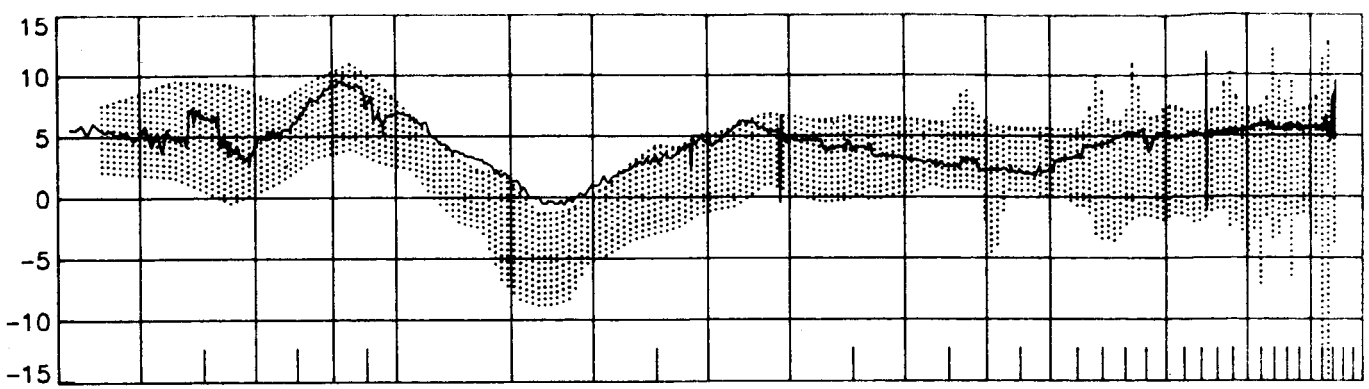
ORIGINAL PAGE 10
OF POOR QUALITY



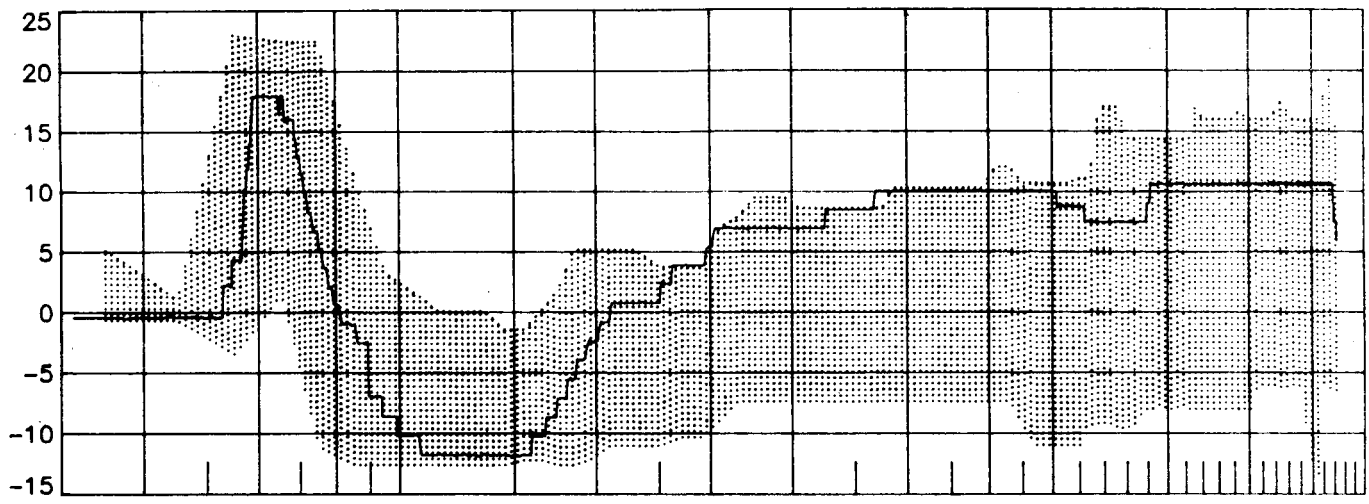
APPENDIX G.

Summary of STS-6 longitudinal results and comparisons.

δ_E , deg



δ_{BF} , deg



δ_{SBA} , deg

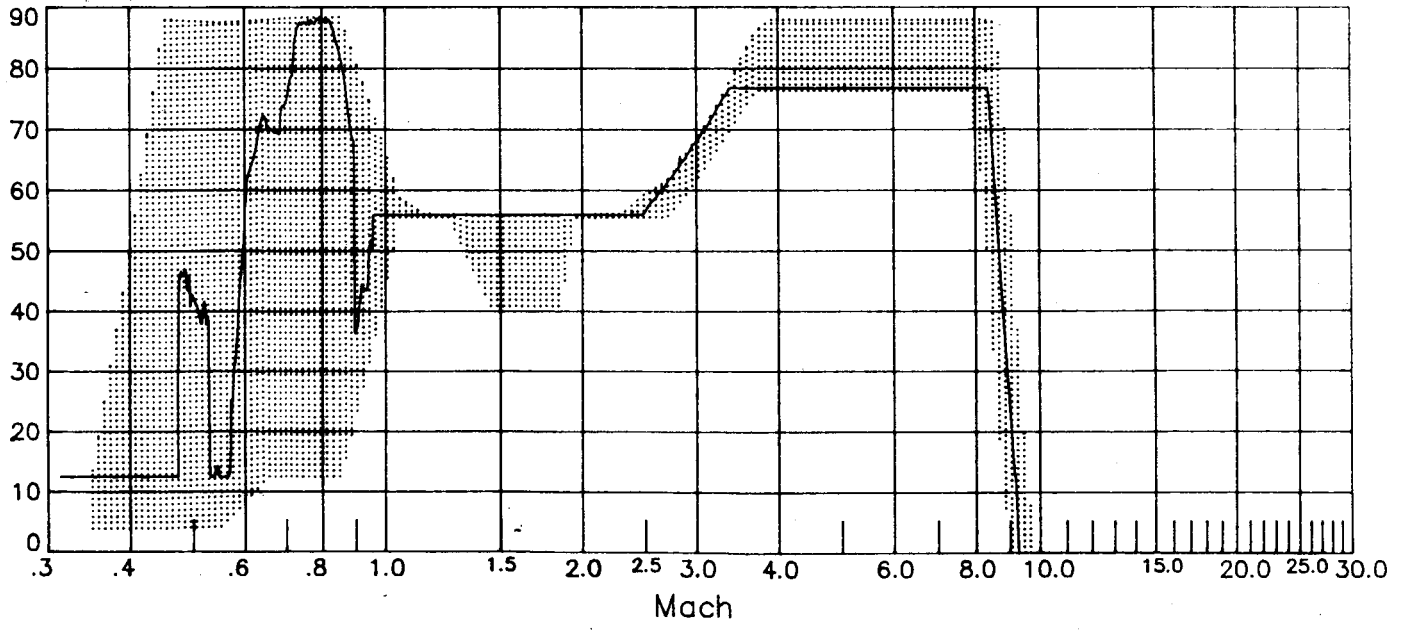
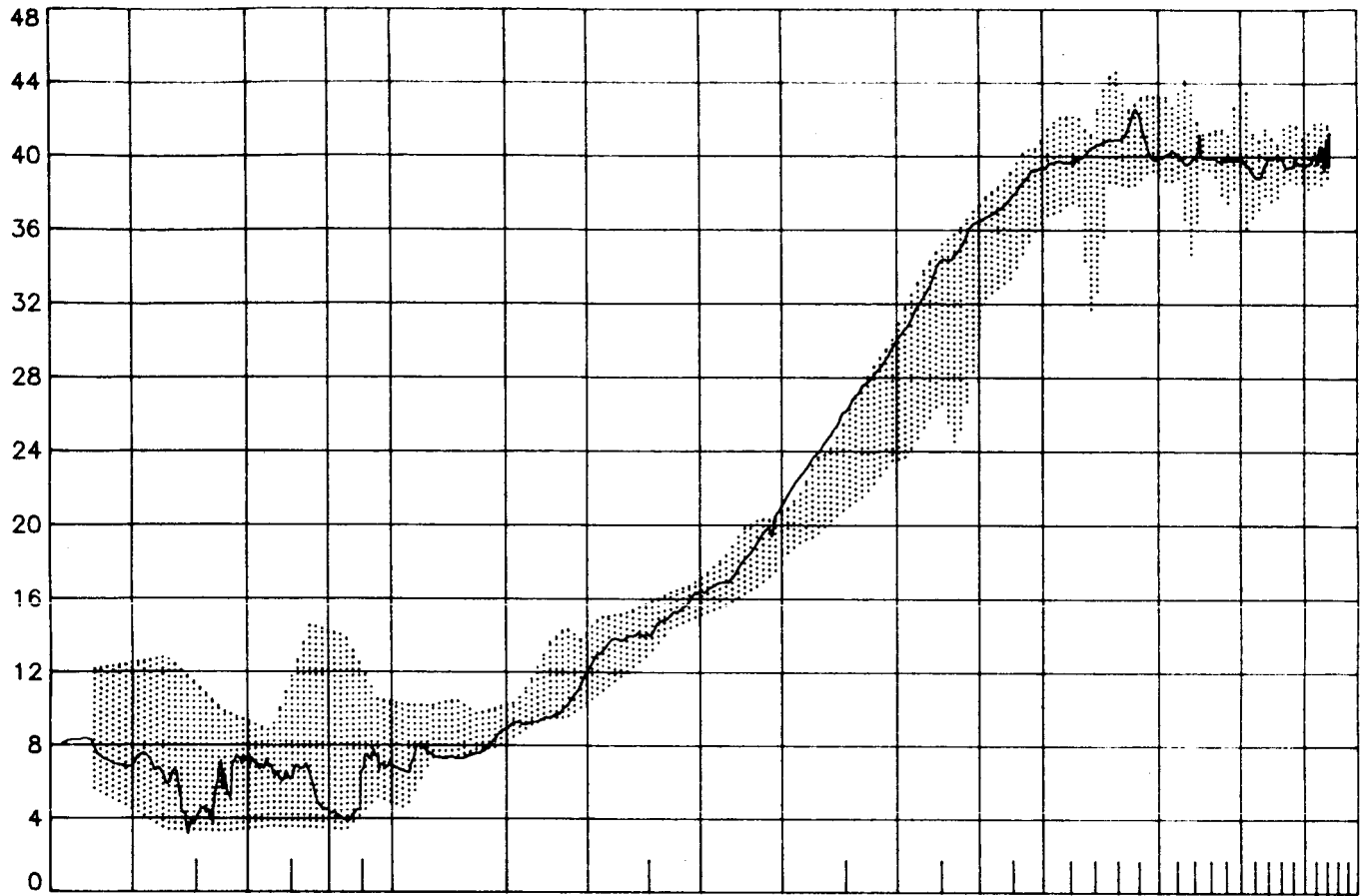


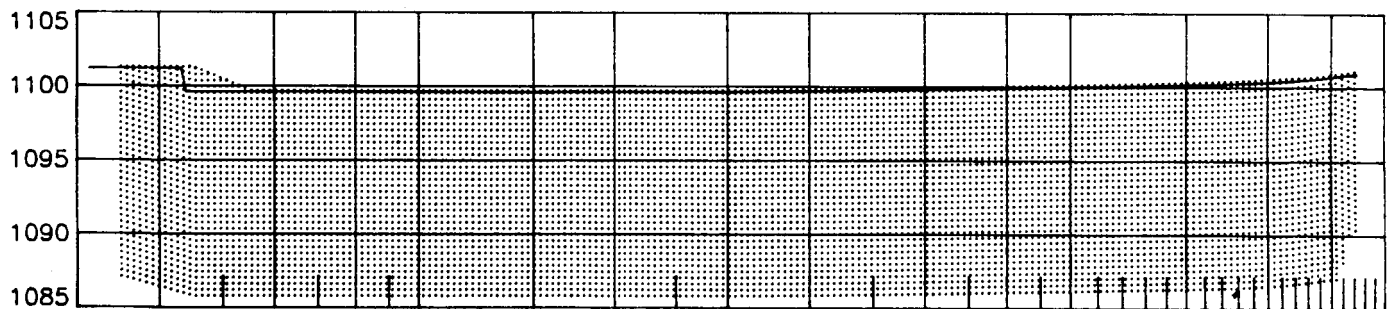
Figure G-1 STS-6 longitudinal control surface deflections
(shaded region defined by remaining ten flights)

ORIGINAL PLOTS
OF POOR QUALITY

α , deg



x_{cg} , in



z_{cg} , in

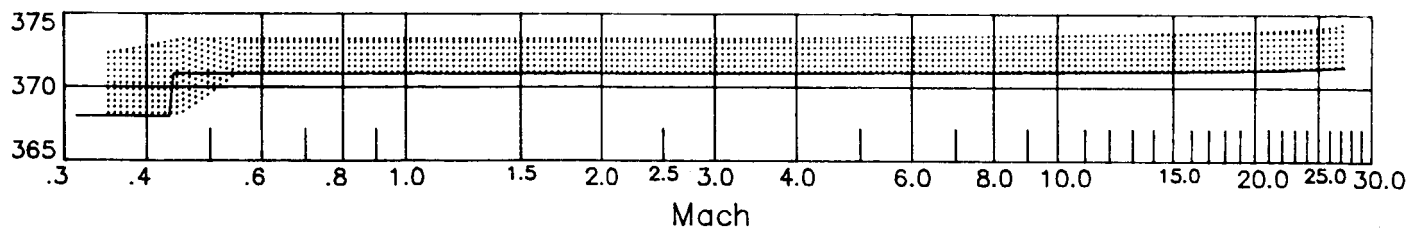
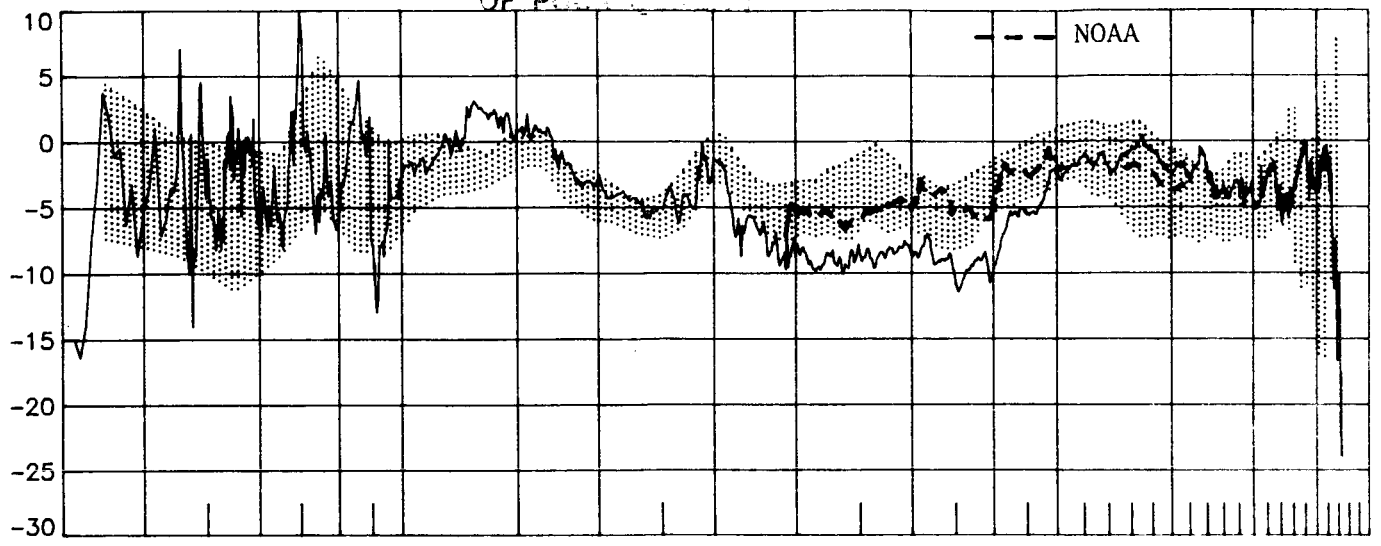


Figure G-2 STS-6 angle-of-attack and c.g. profiles
(shaded region defined by remaining ten flights)

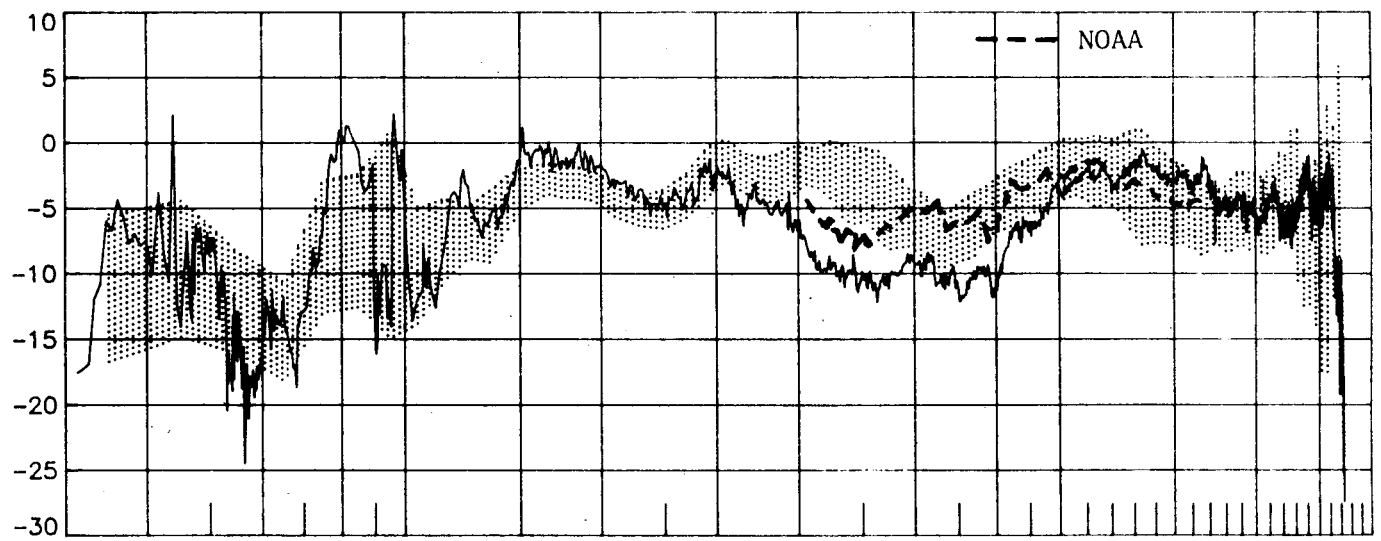
C-2

ΔC_L , percent

ORIGINALLY PUBLISHED
OF ECN-87-000001



ΔC_D , percent



$\Delta(L/D)$, percent

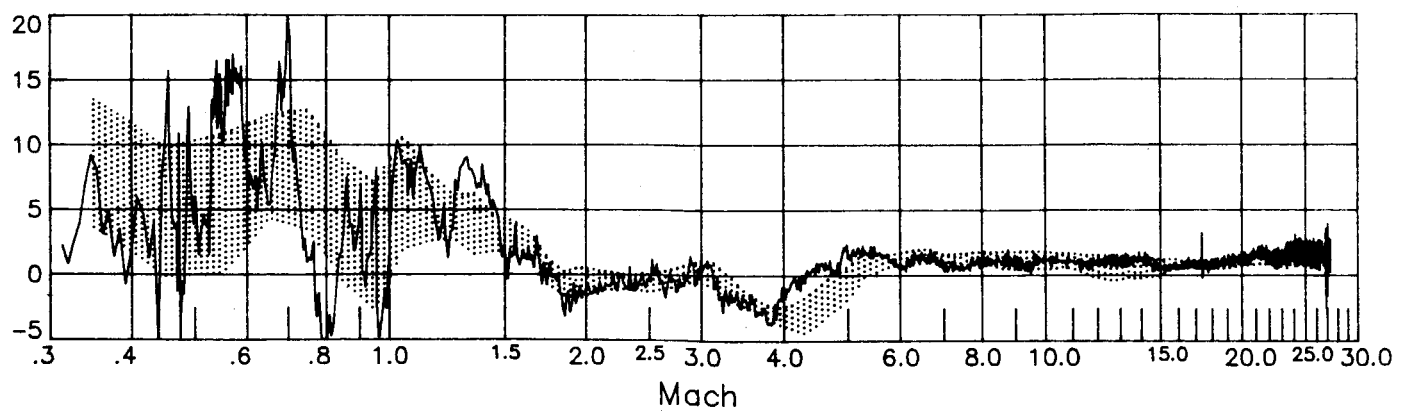
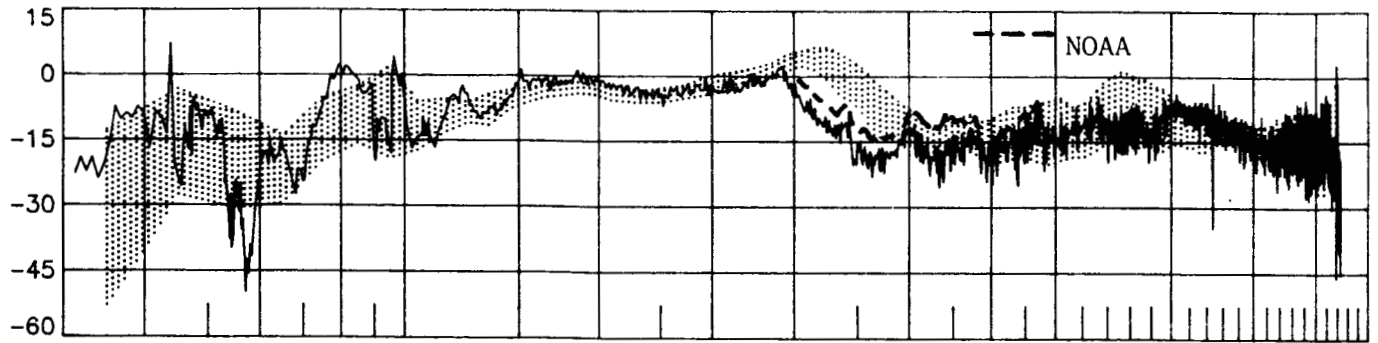


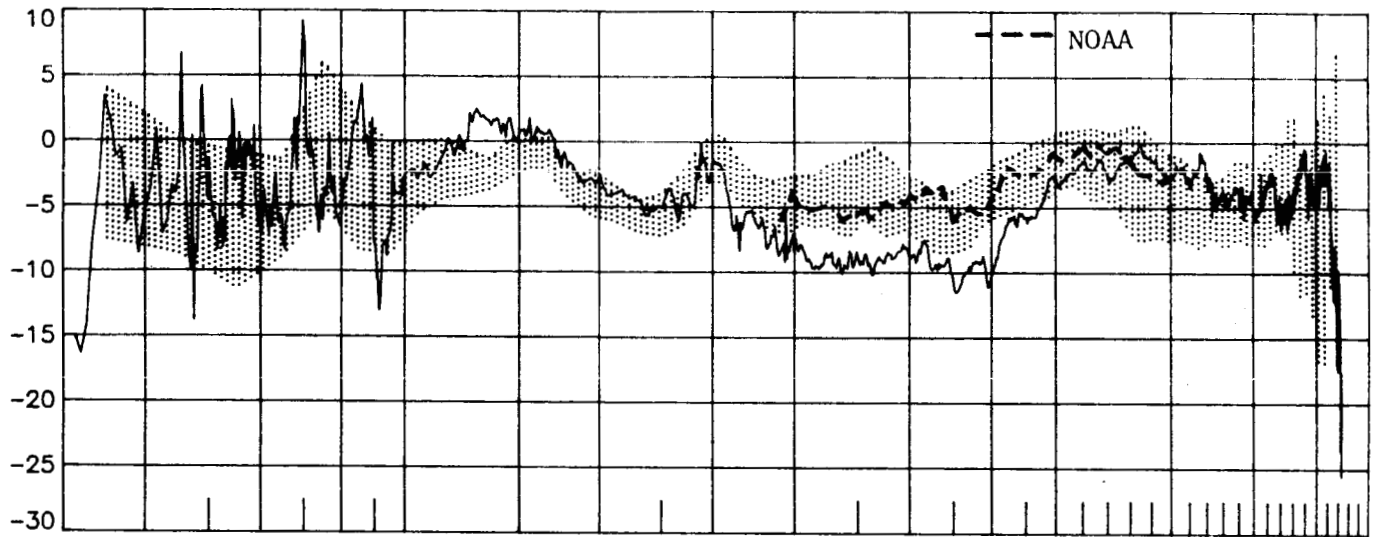
Figure G-3 STS-6 longitudinal performance comparisons
(shaded region defined by remaining ten flights)

ORIGINAL DATA
OF POOR QUALITY

ΔC_A , percent



ΔC_N , percent



ΔC_m , percent

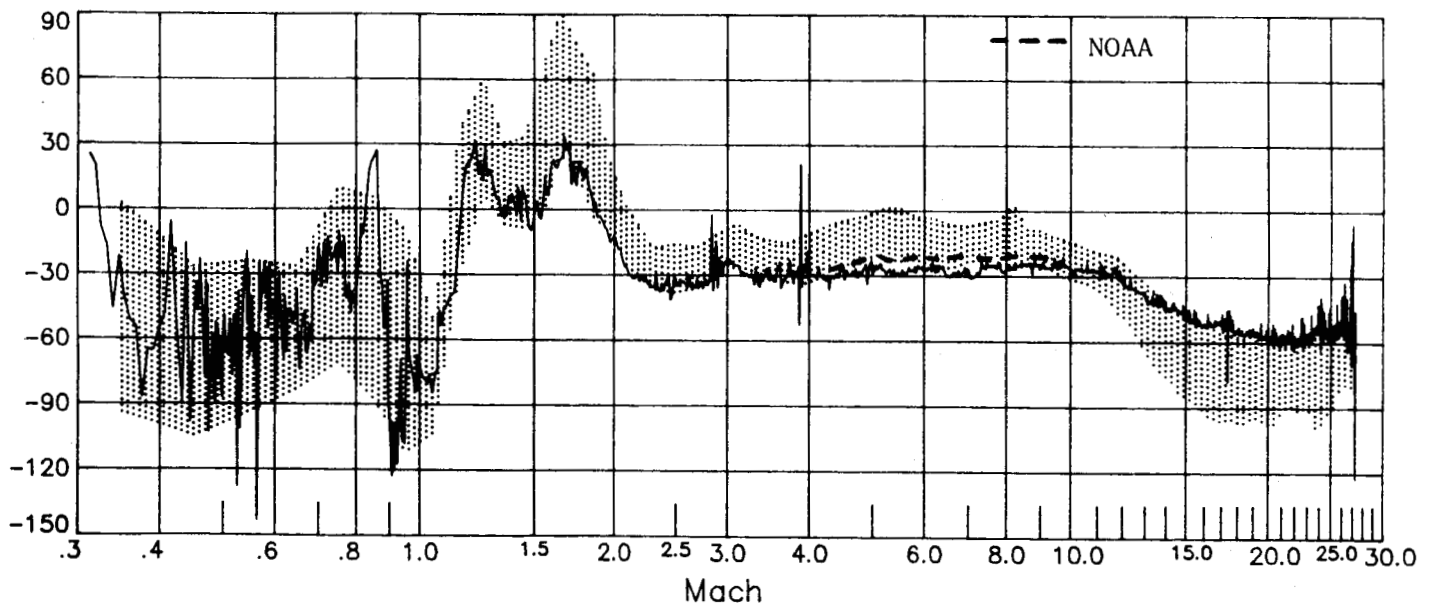
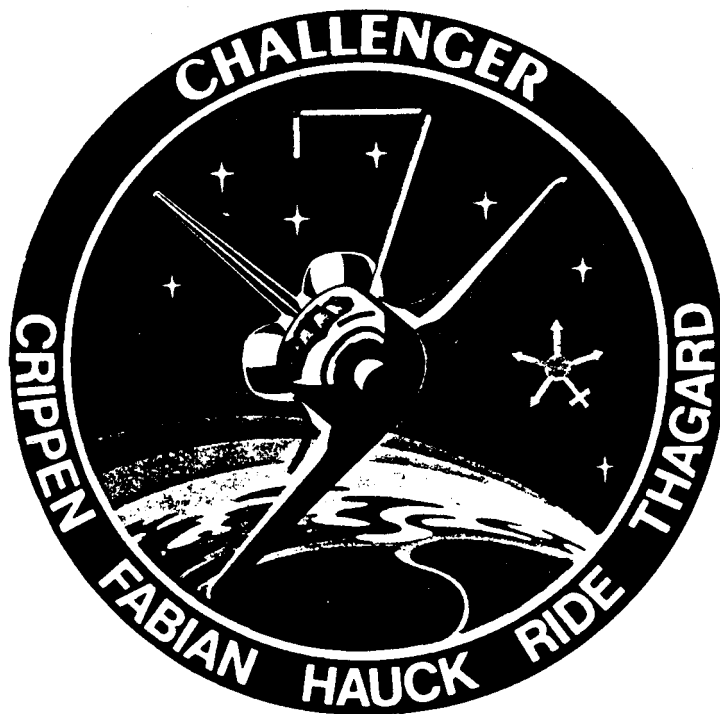


Figure G-3 (concluded)

(shaded region defined by remaining ten flights)

ORIGINAL FILED IN
OF POOR QUALITY

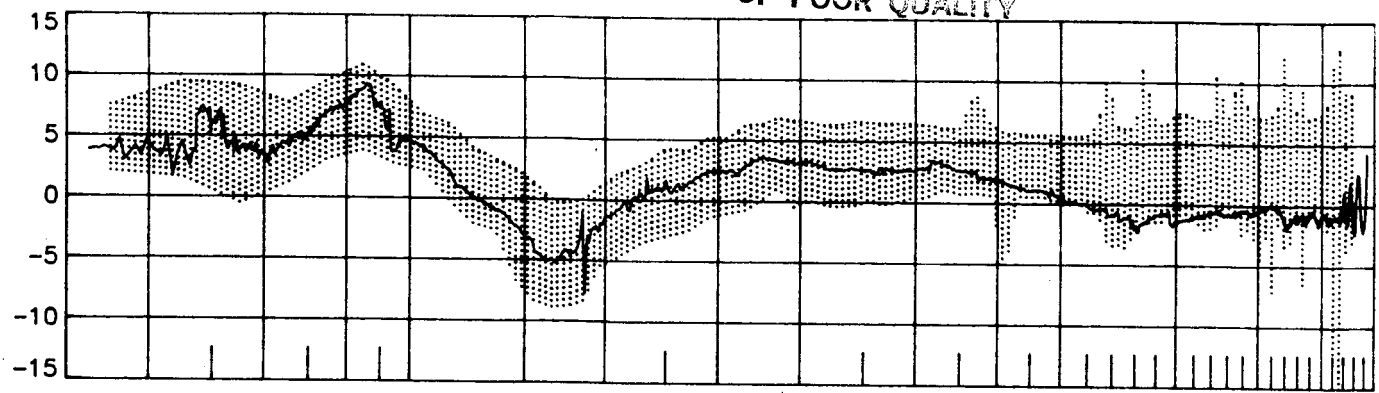


APPENDIX H

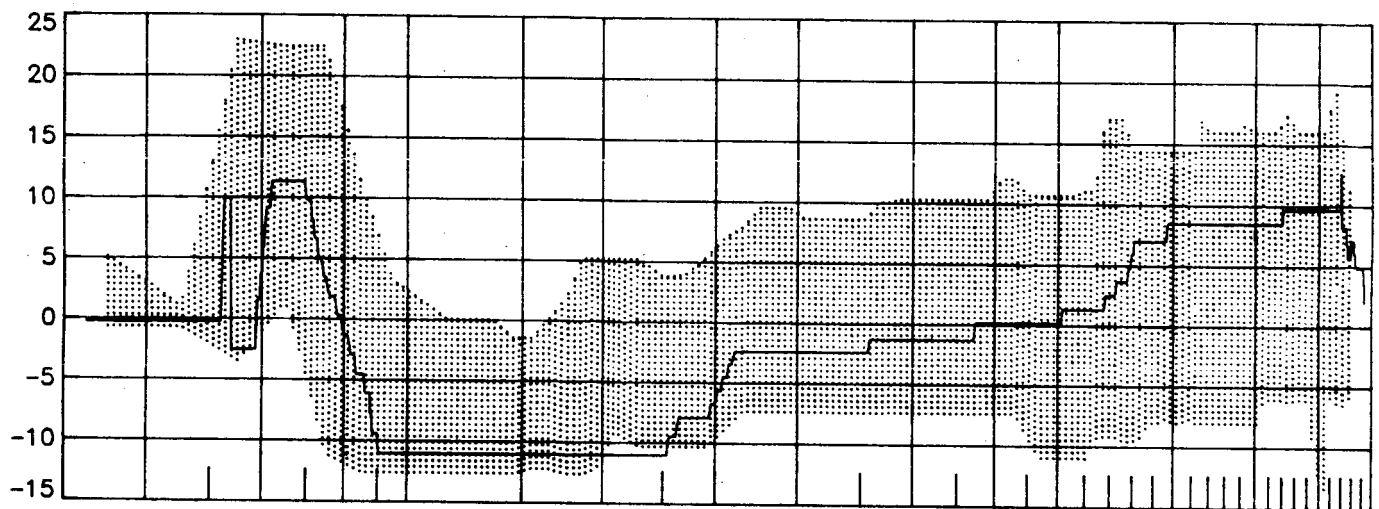
Summary of STS-7 longitudinal results and comparisons.

ORIGINAL PAGE IS
OF POOR QUALITY

δ_E , deg



δ_{BF} , deg



δ_{SB_A} , deg

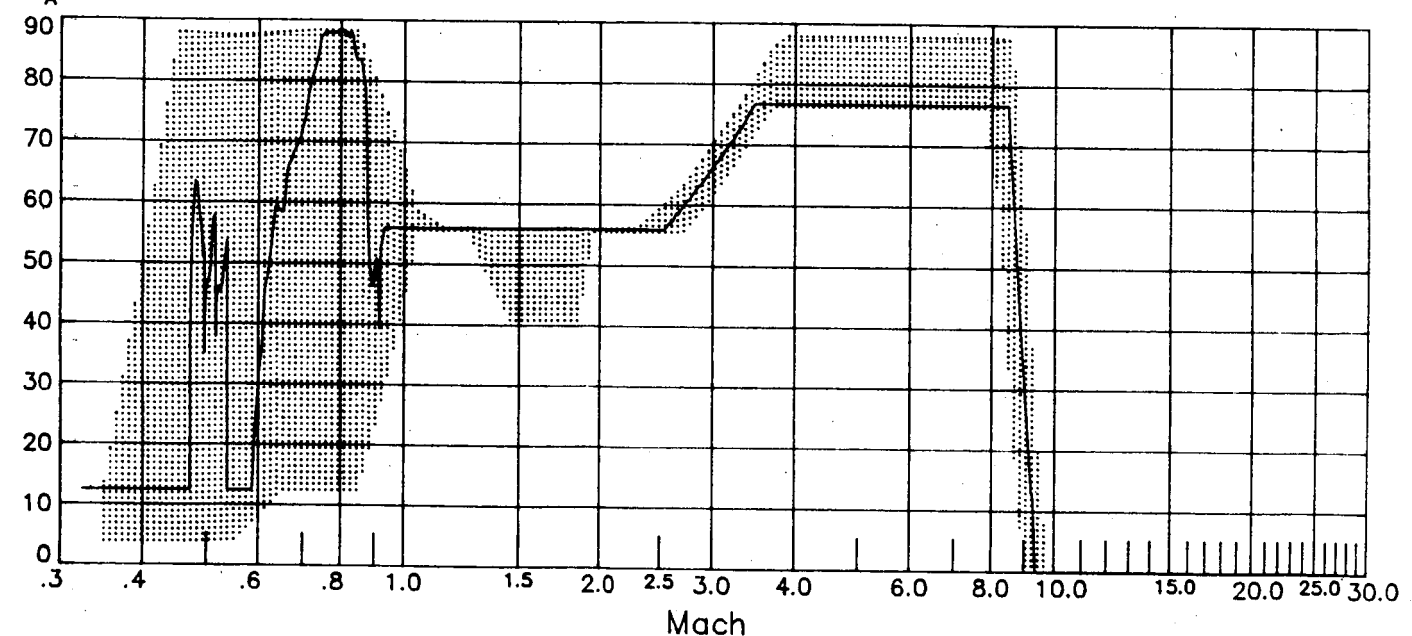
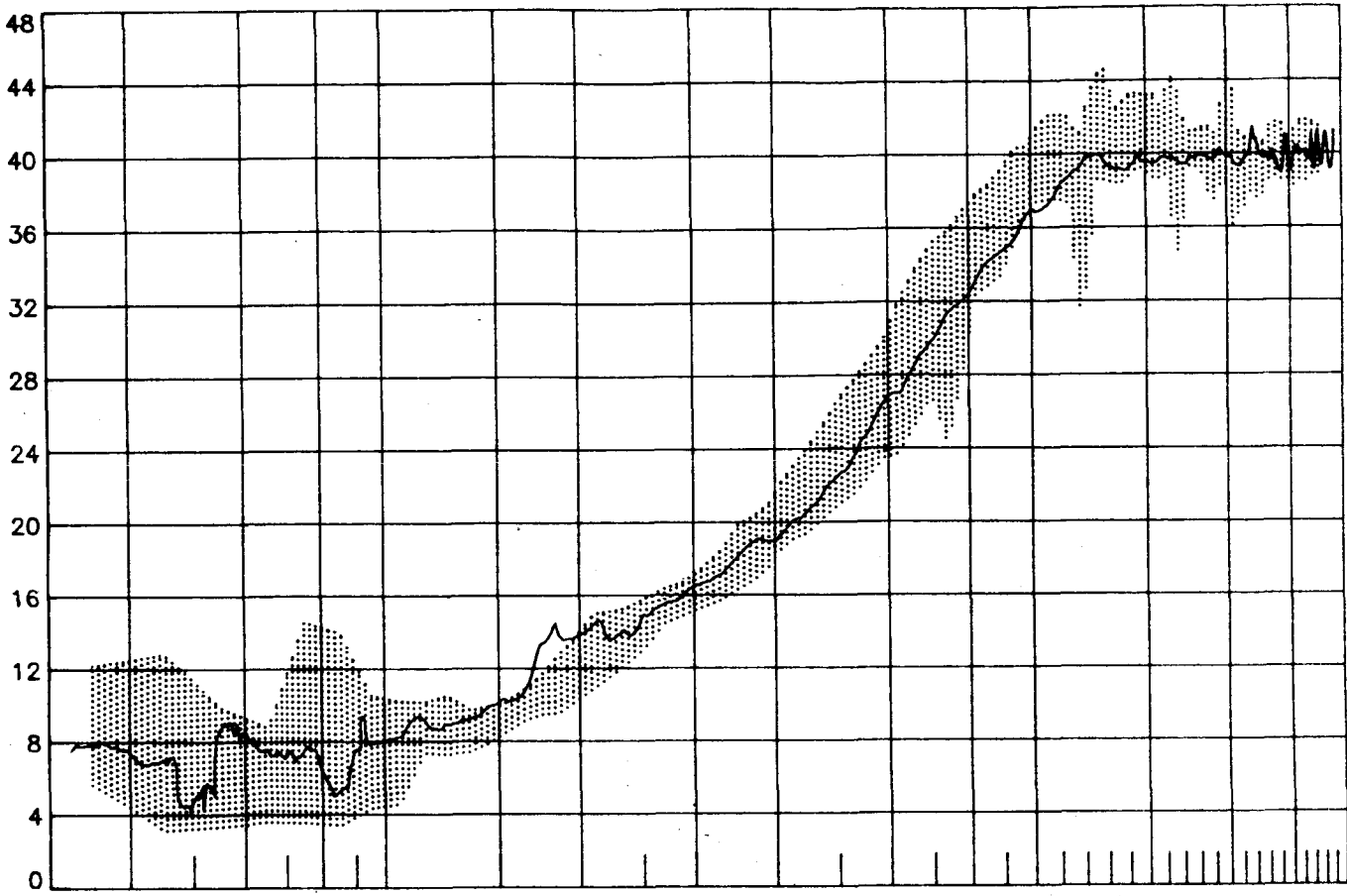


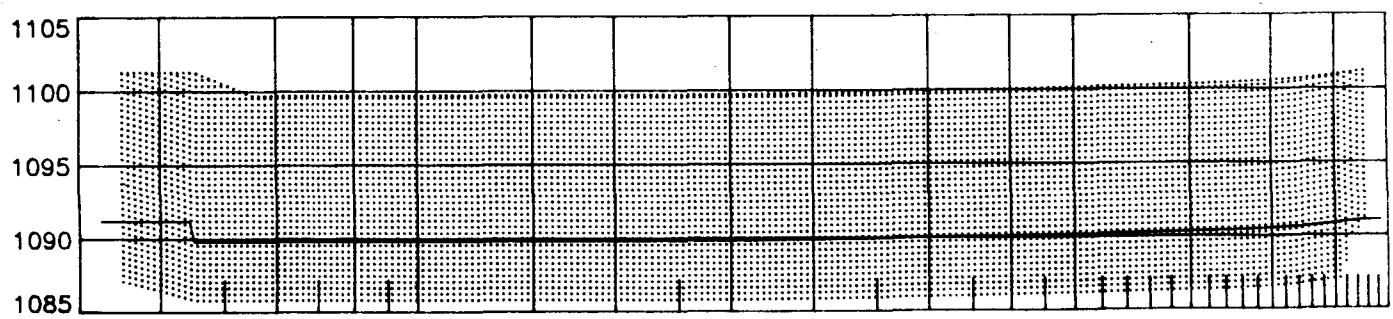
Figure H-1 STS-7 longitudinal control surface deflections
(shaded region defined by remaining ten flights)

ORIGINAL FIGURES
OF POOR QUALITY

α , deg



x_{cg} , in



z_{cg} , in

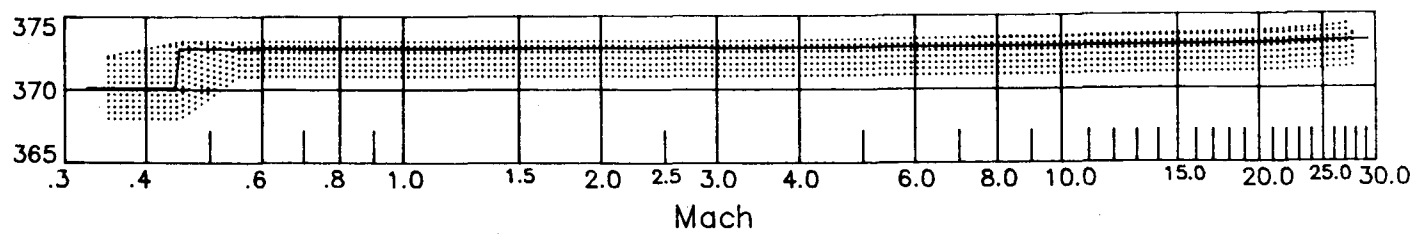
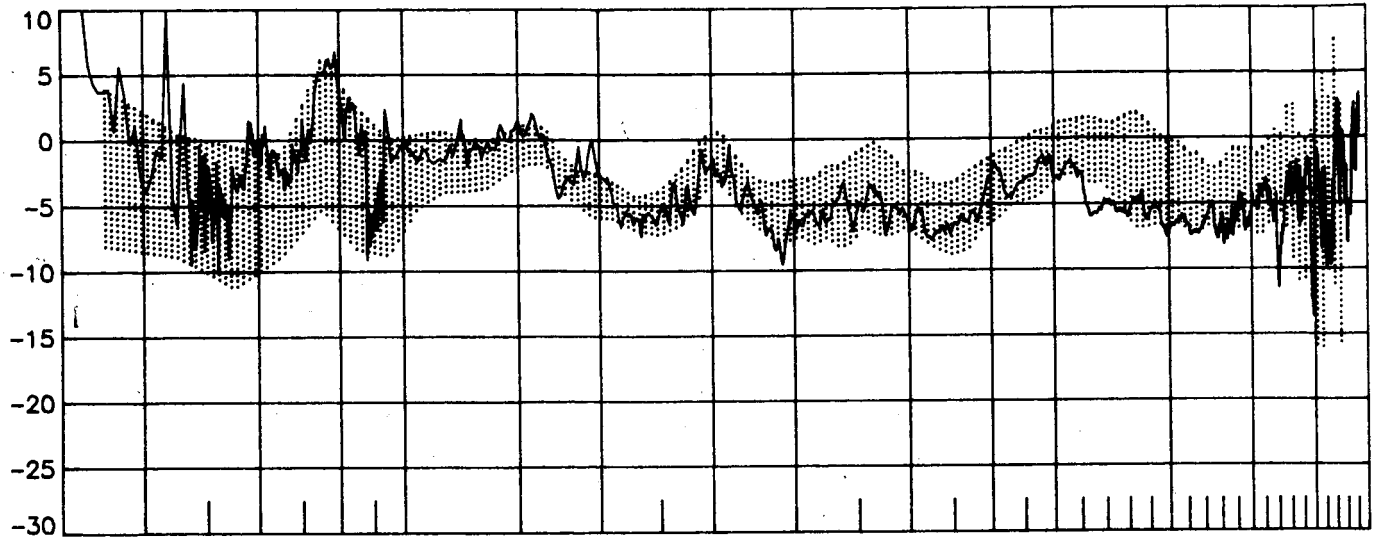


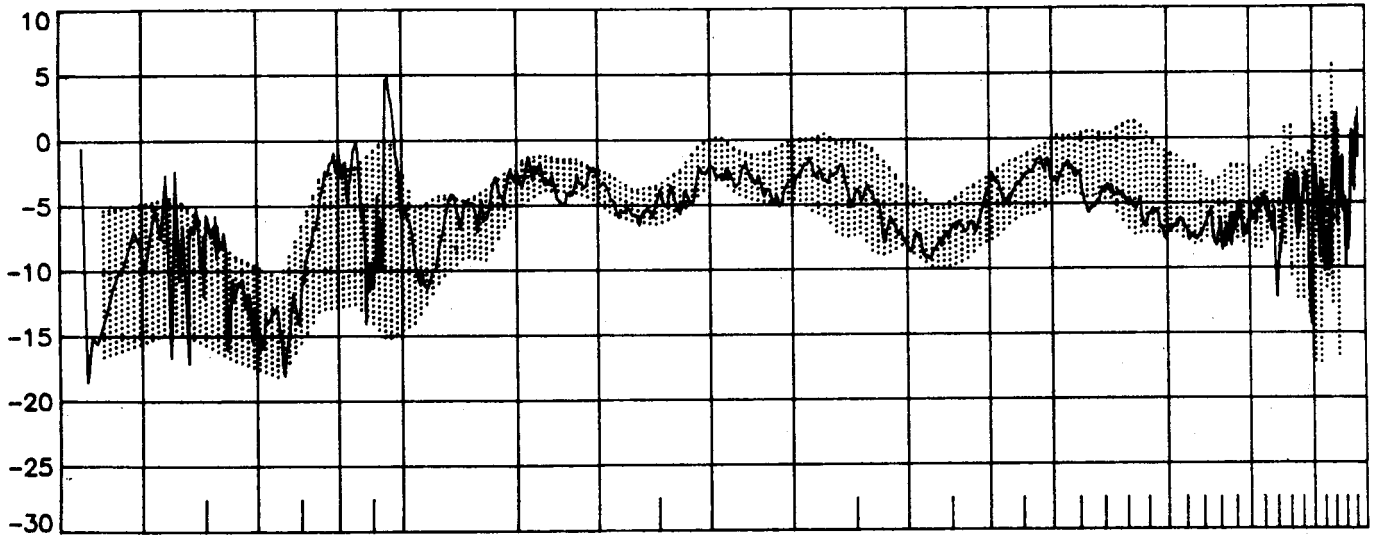
Figure H-2 STS-7 angle-of-attack and c.g. profiles
(shaded region defined by remaining ten flights)

ORIGINAL PAGE IS
OF POOR QUALITY

ΔC_L , percent



ΔC_D , percent



$\Delta(L/D)$, percent

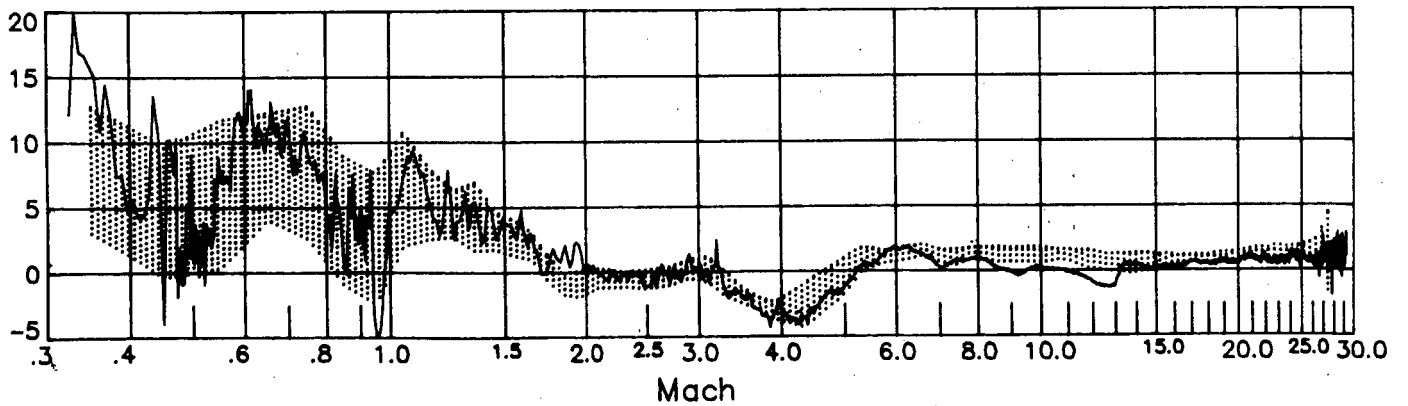
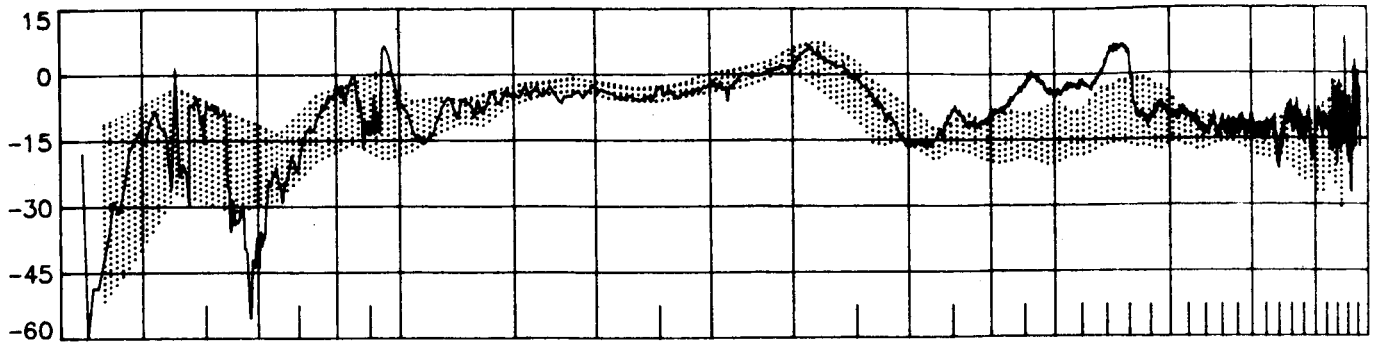


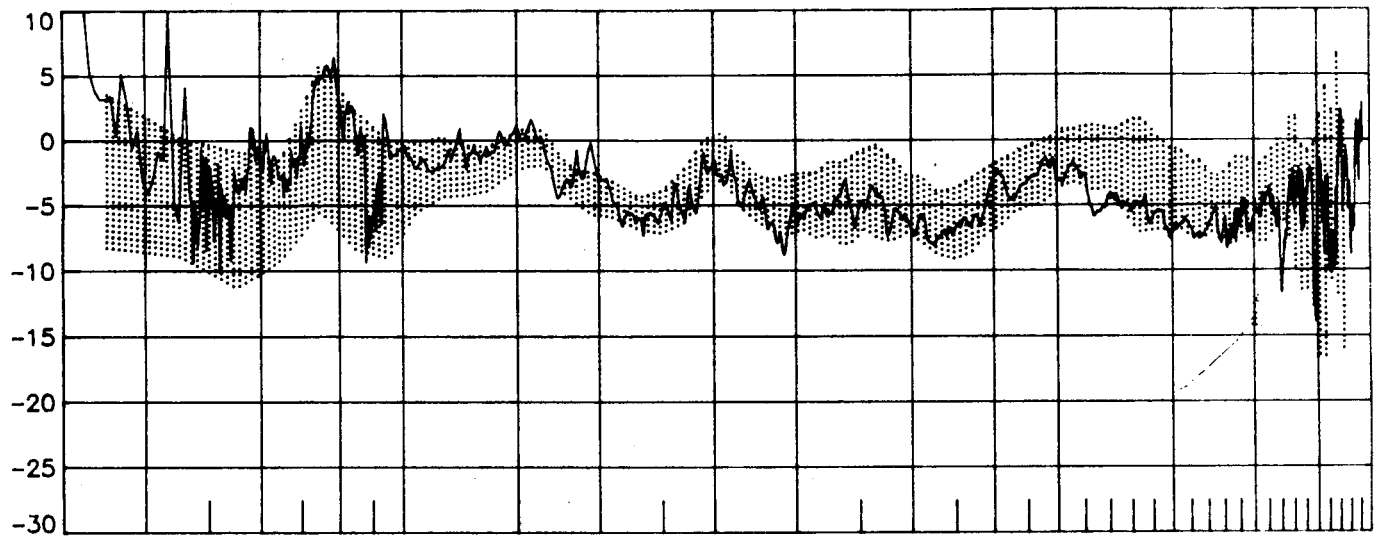
Figure H-3 STS-7 longitudinal performance comparisons
(shaded region defined by remaining ten flights)

ORIGINAL PLANS E.
OF FOUR QUALITY

ΔC_A , percent



ΔC_N , percent



ΔC_m , percent

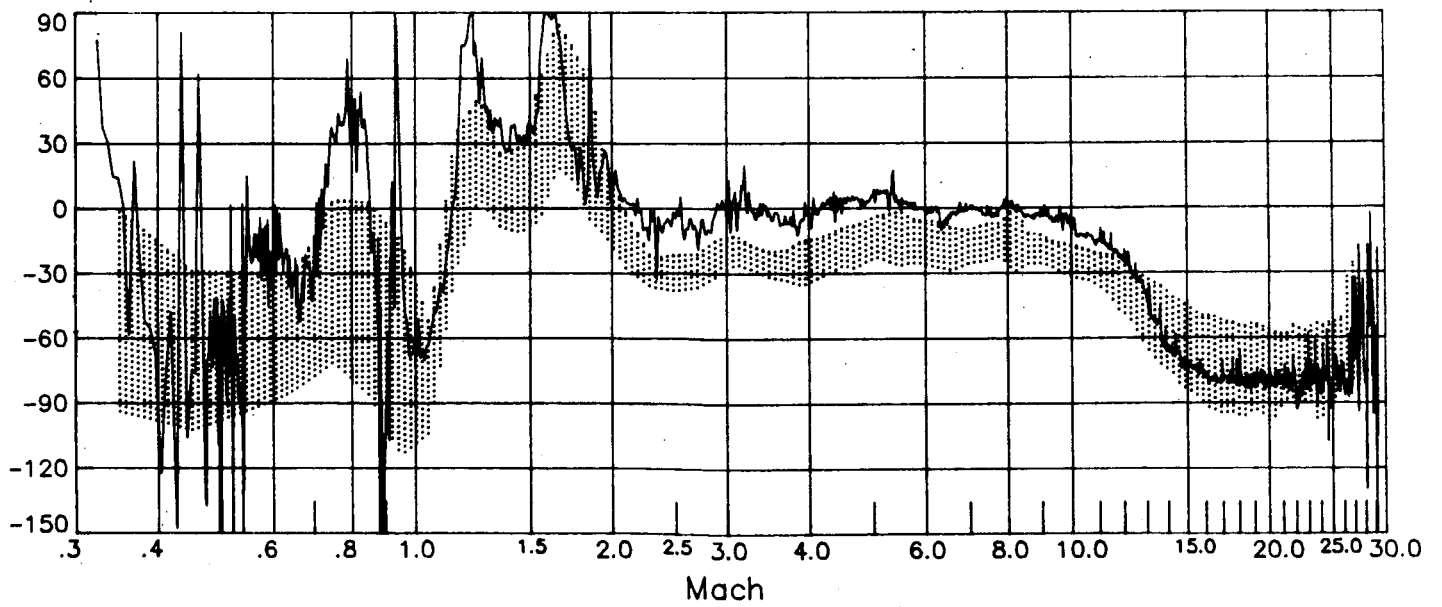


Figure H-3 (concluded)

(shaded region defined by remaining ten flights)

ORIGINAL PAGE IS
OF POOR QUALITY

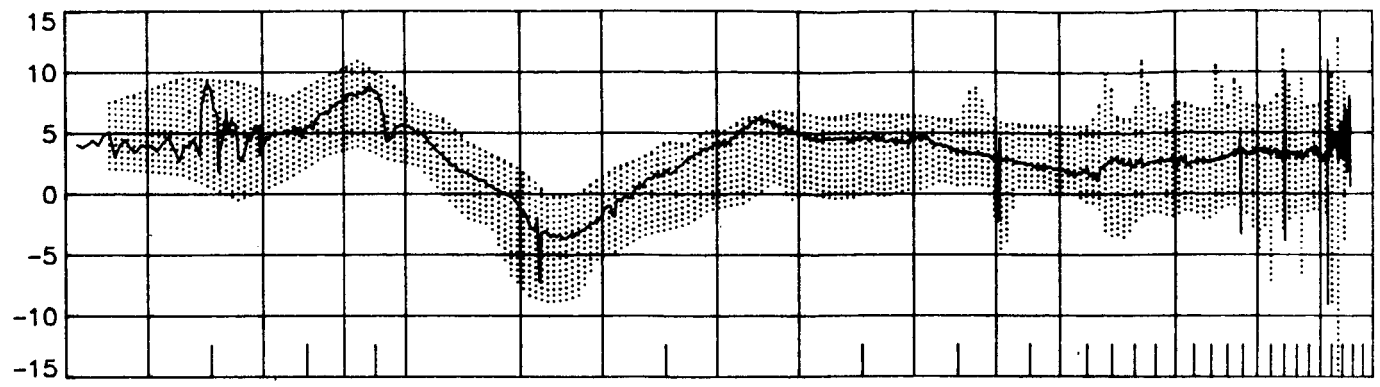


APPENDIX J

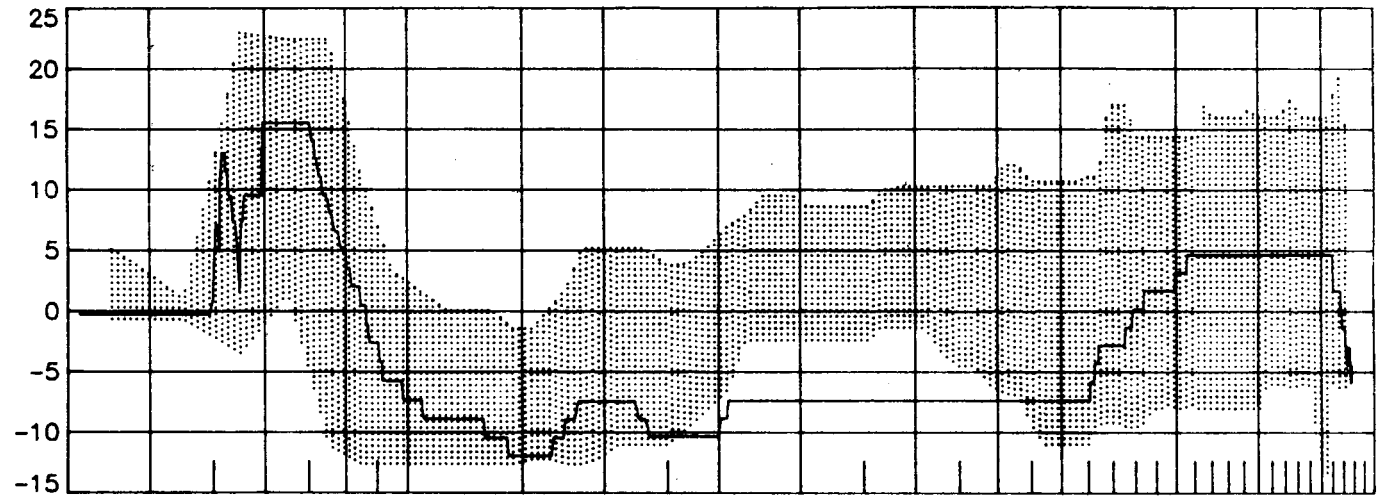
Summary of STS-8 longitudinal results and comparisons.

ORIGINAL COPY
OF PDR CONTROL

δ_E , deg



δ_{BF} , deg



δ_{SBA} , deg

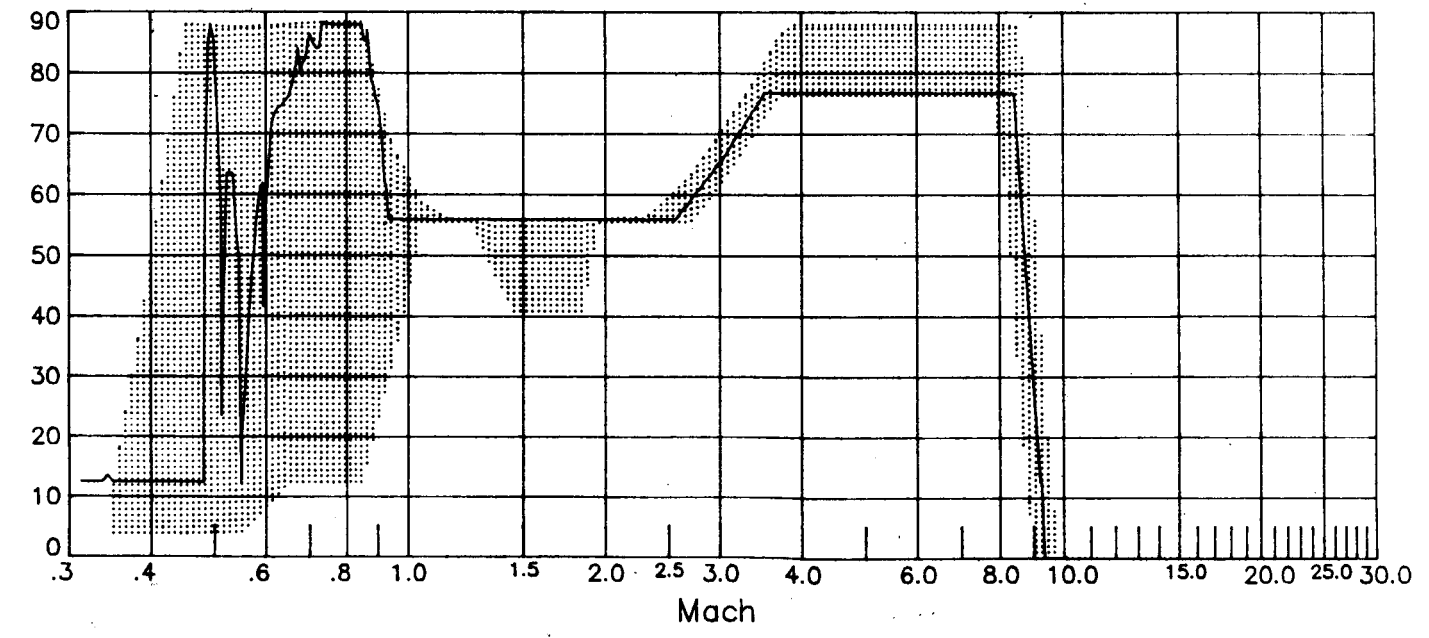
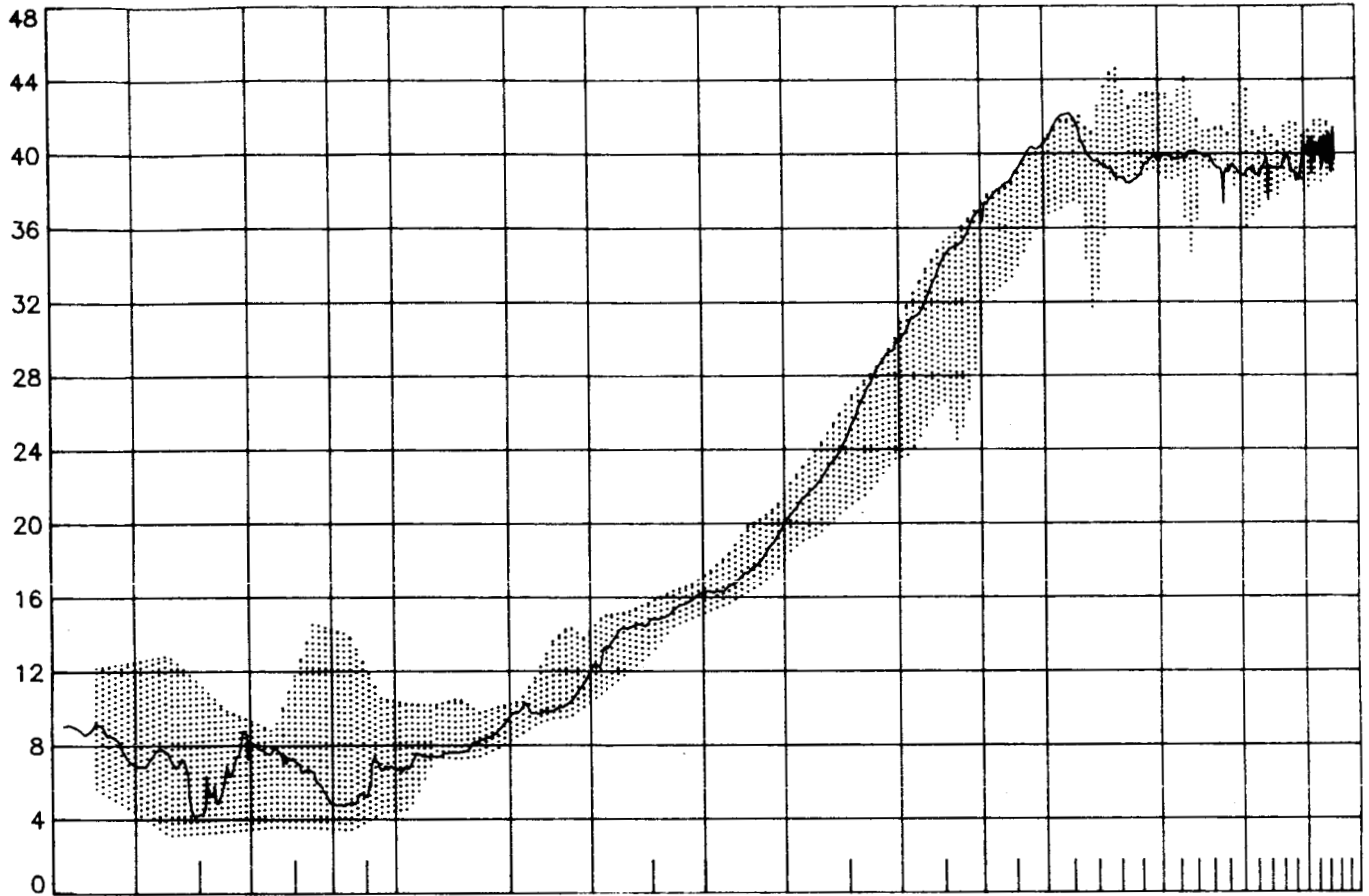


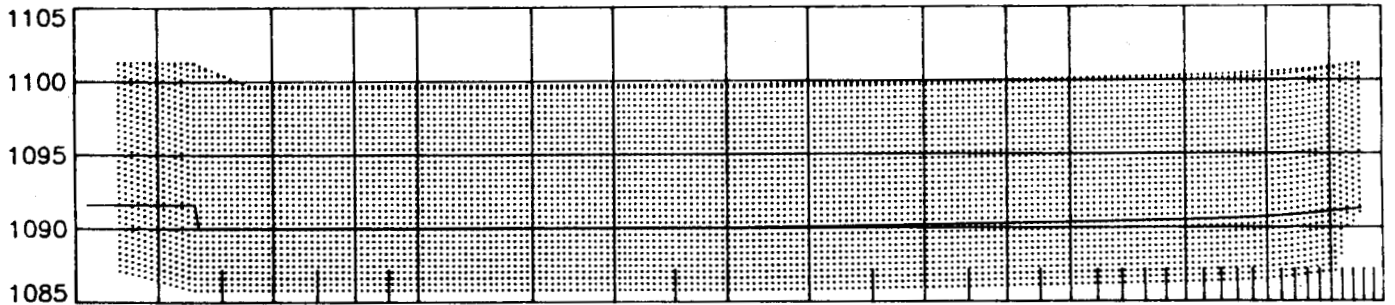
Figure J-1 STS-8 longitudinal control surface deflections
(shaded region defined by remaining ten flights)

ORIGINAL SOURCE OF POOR QUALITY

α , deg



x_{cg} , in



z_{cg} , in

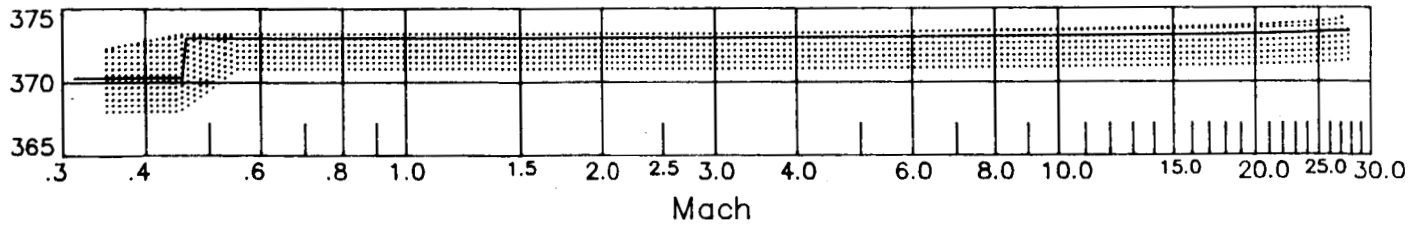
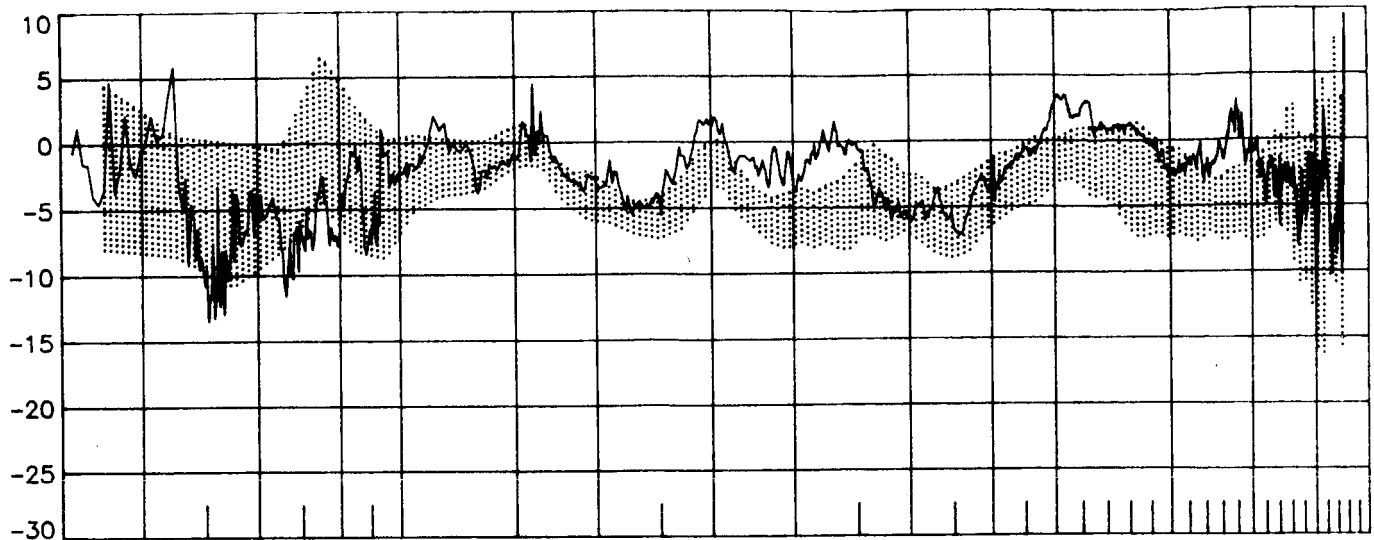


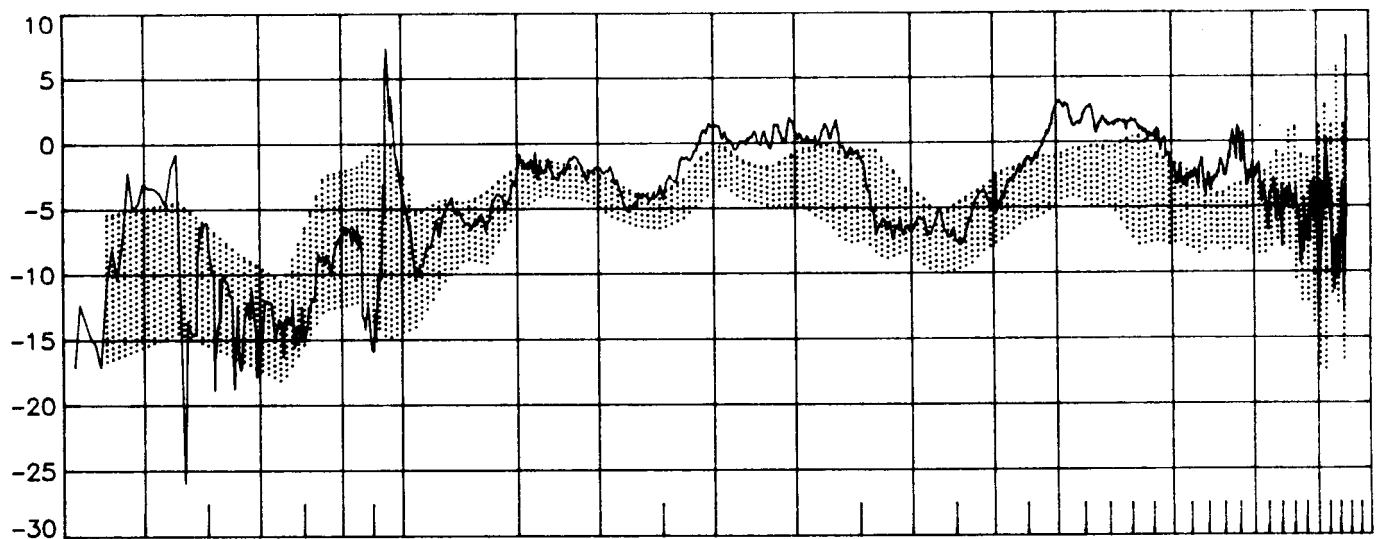
Figure J-2 STS-8 angle-of-attack and c.g. profiles
(shaded region defined by remaining ten flights)

ORIGINAL PERFORMANCE
OF POOR QUALITY

ΔC_L , percent



ΔC_D , percent



$\Delta(L/D)$, percent

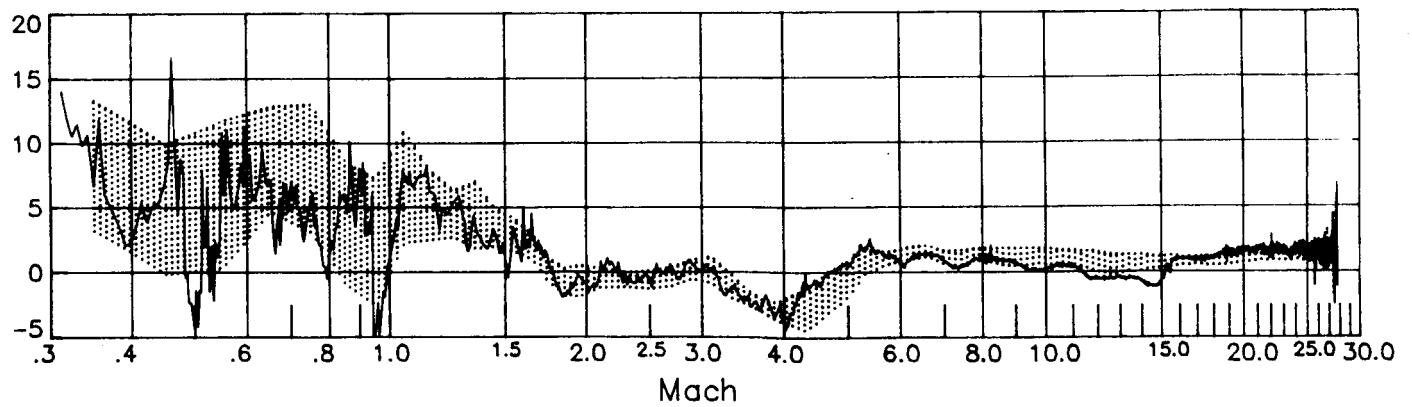
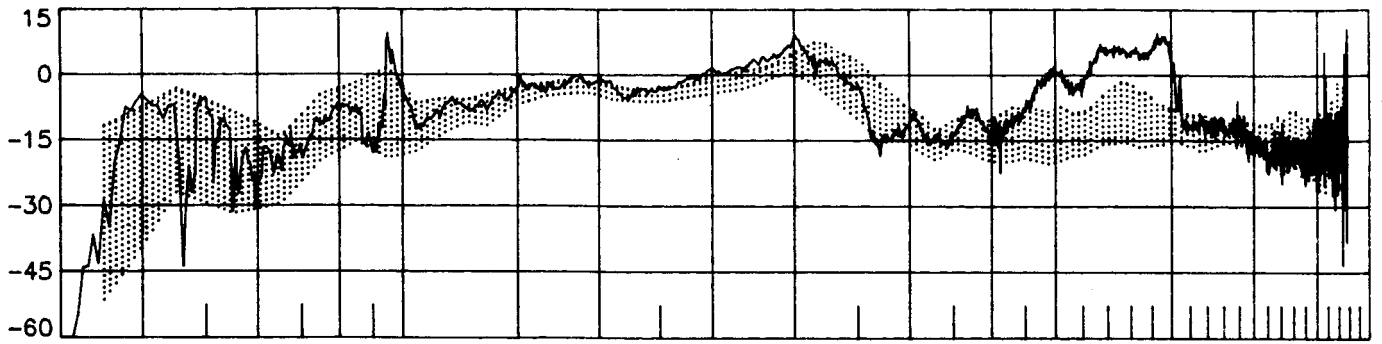


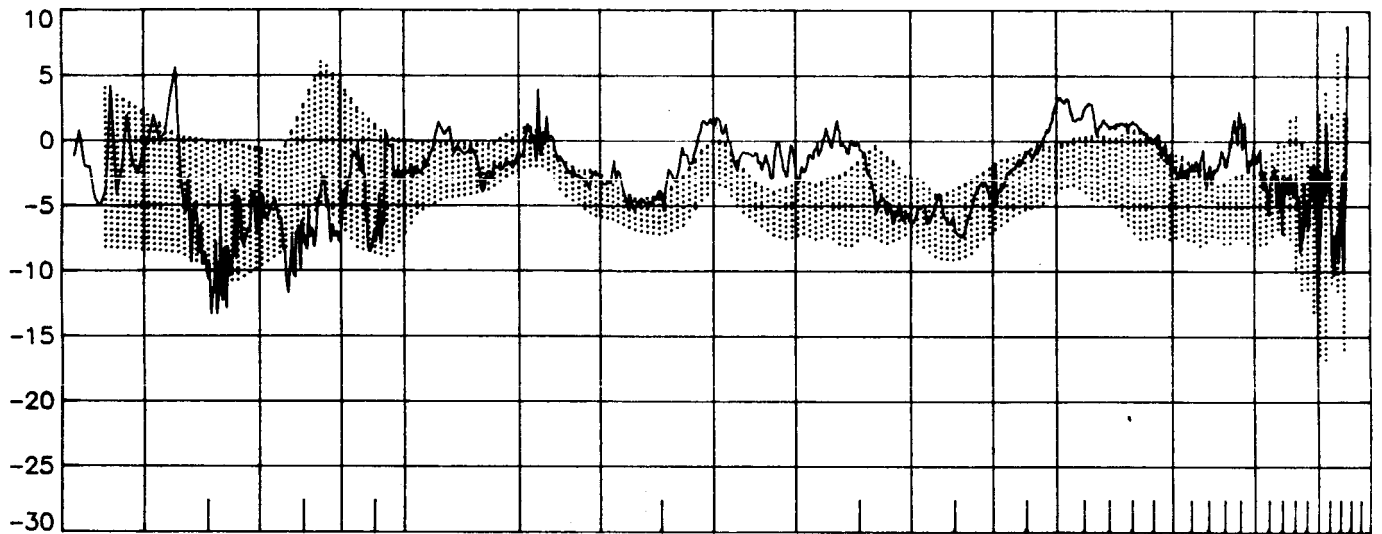
Figure J-3 STS-8 longitudinal performance comparisons
(shaded region defined by remaining ten flights)

ORIGINAL DATA
OF FOUR FLIGHTS

ΔC_A , percent



ΔC_N , percent



ΔC_m , percent

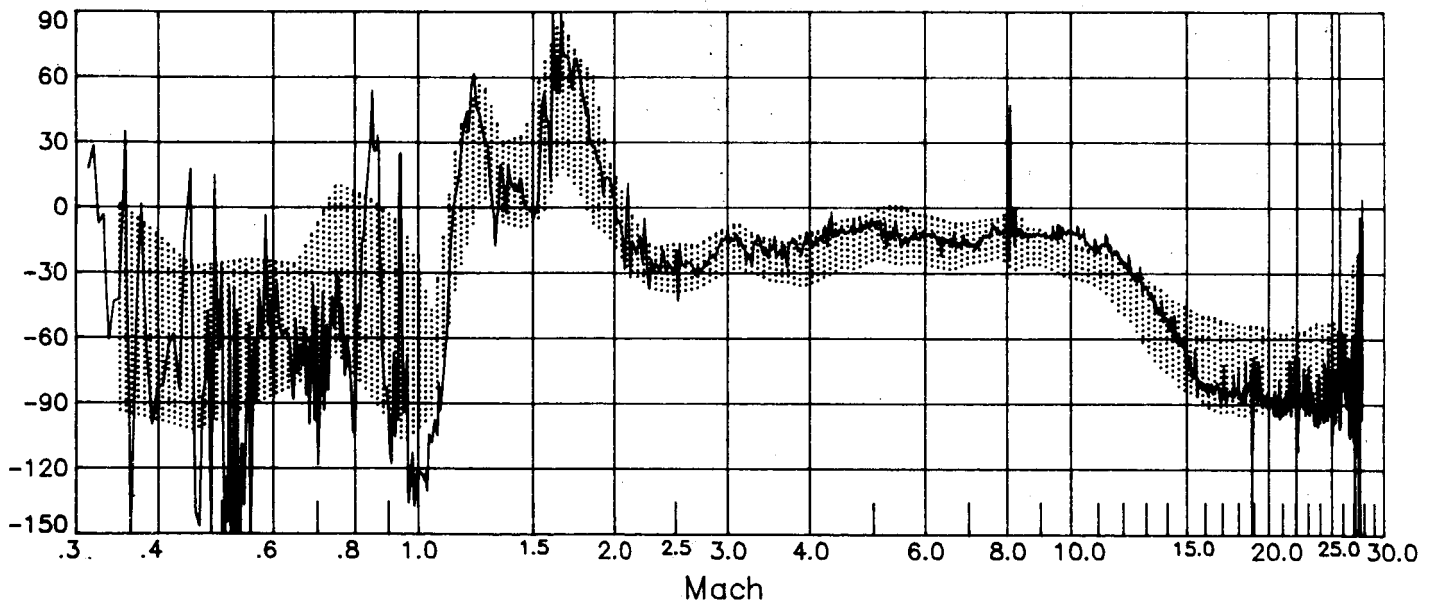


Figure J-3 (concluded)

(shaded region defined by remaining ten flights)

ORIGINAL SOURCE
OF PCR DATA

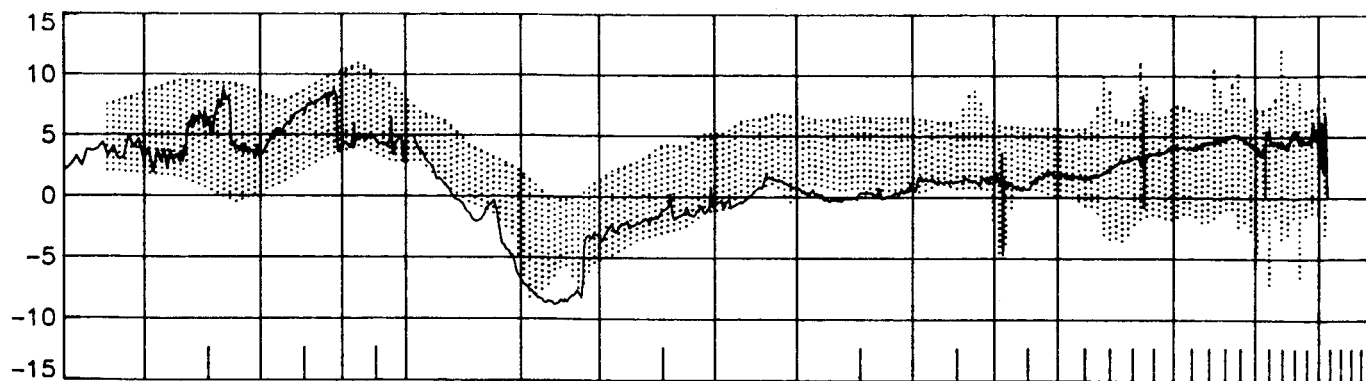


APPENDIX K

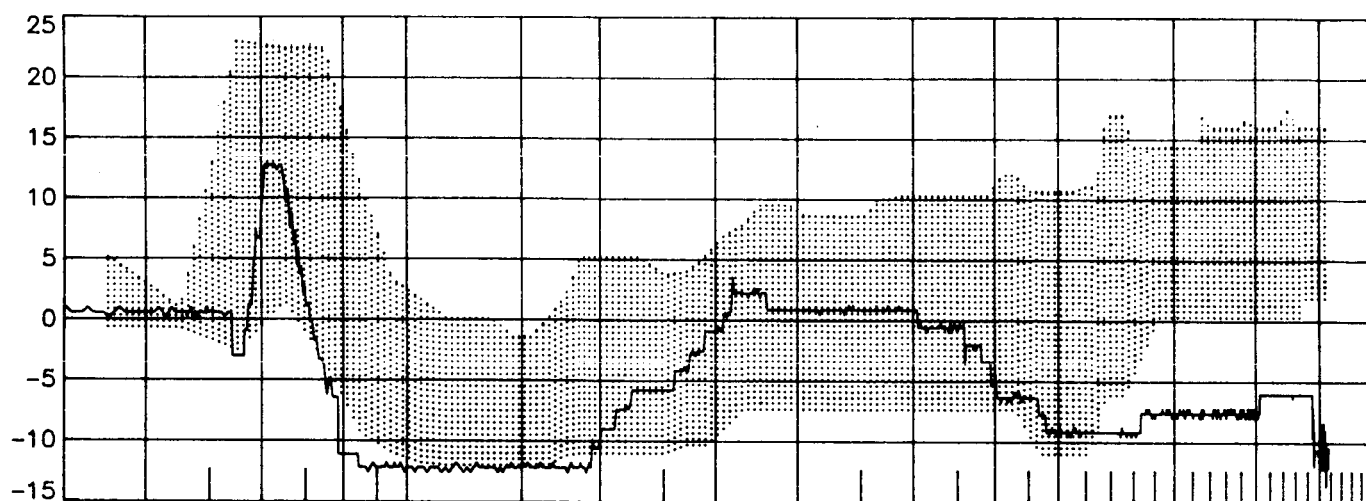
Summary of STS-9 longitudinal results and comparisons.

ORIGINAL POSITION
OF POOR QUALITY

δ_E , deg



δ_{BF} , deg



δ_{SBA} , deg

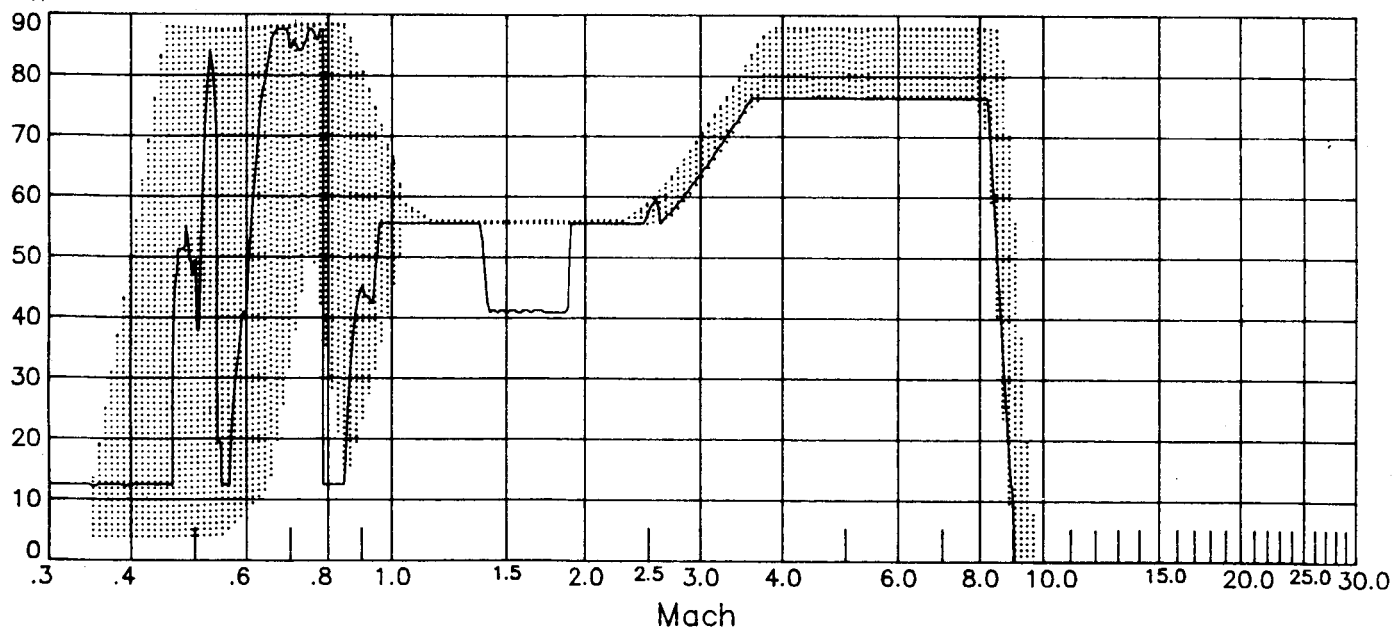
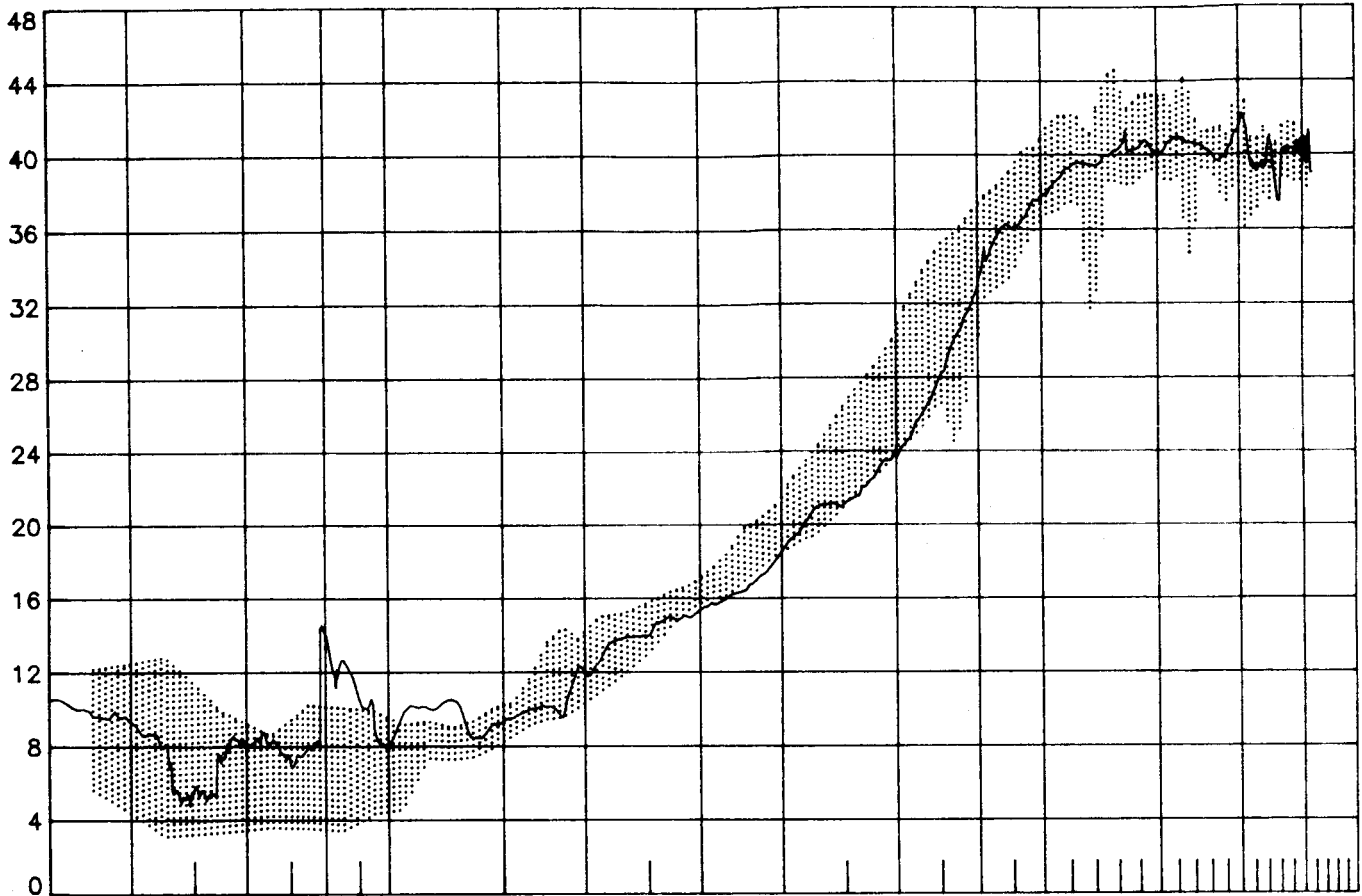


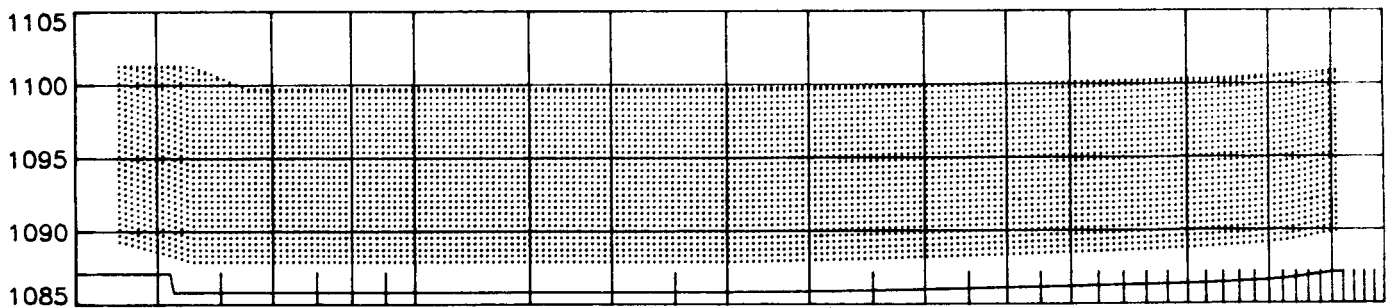
Figure K-1 STS-9 longitudinal control surface deflections
(shaded region defined by remaining ten flights)

ORIGINAL PROFILE
OF POOR (LINE)

α , deg



x_{cg} , in



z_{cg} , in

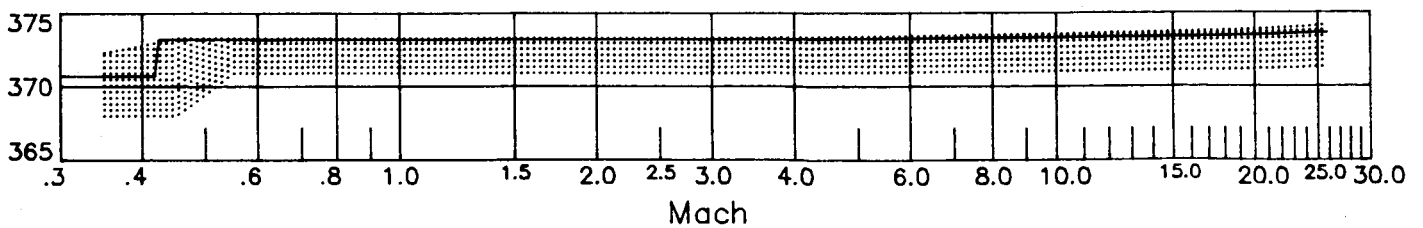
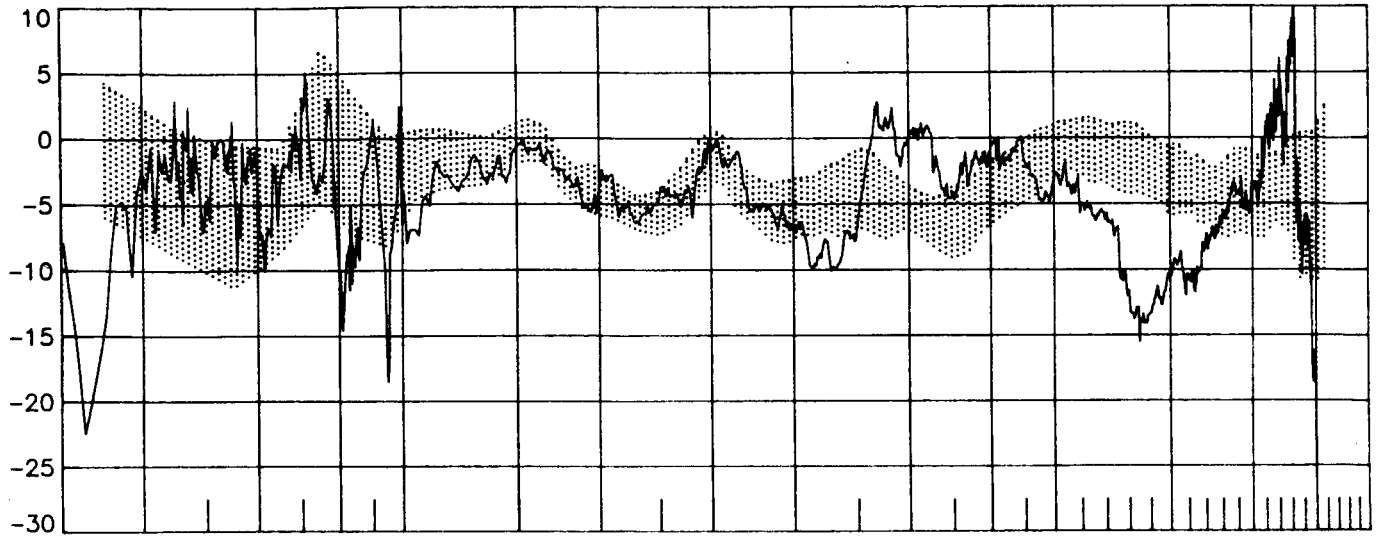


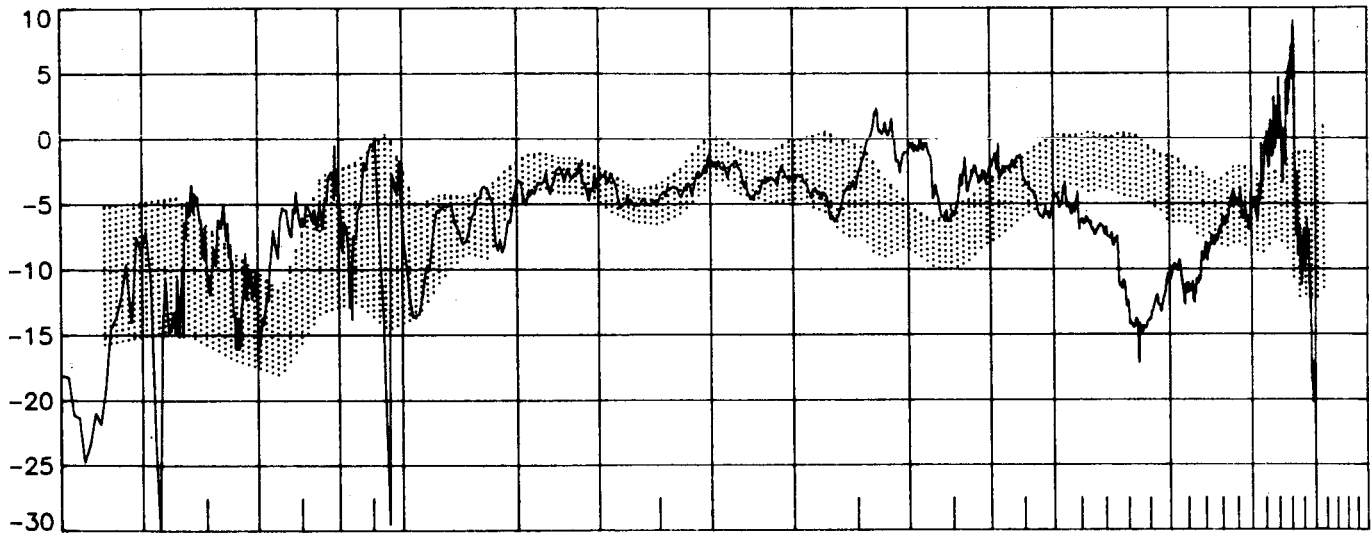
Figure K-2 STS-9 angle-of-attack and c.g. profiles
(shaded region defined by remaining ten flights)

ORIGINAL PAGE IS
OF POOR QUALITY

ΔC_L , percent



ΔC_D , percent



$\Delta(L/D)$, percent

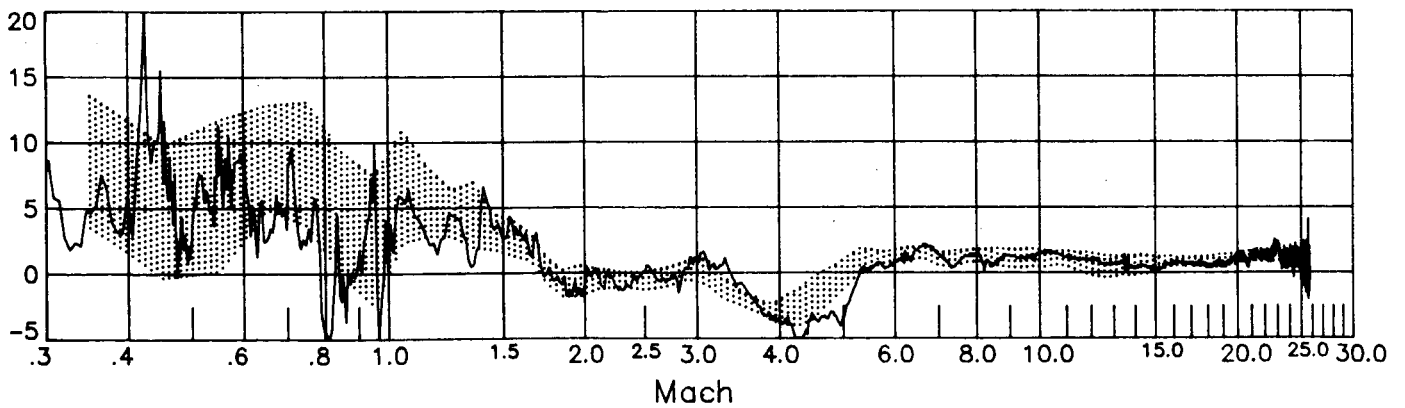


Figure K-3 STS-9 longitudinal performance comparisons
(shaded region defined by remaining ten flights)

ORIGINAL RECORD
OF POOR QUALITY

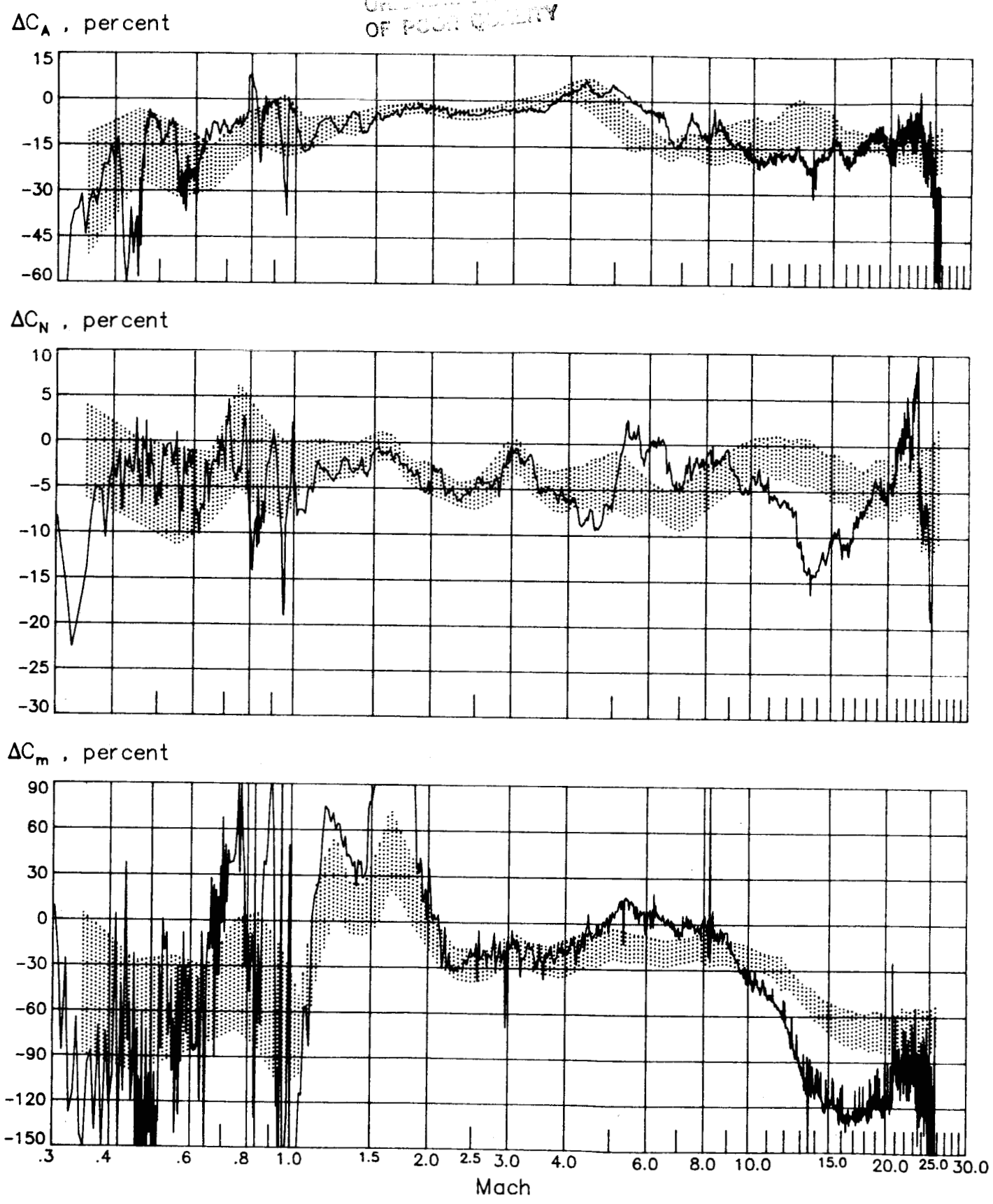


Figure K-3 (concluded)

(shaded region defined by remaining ten flights)

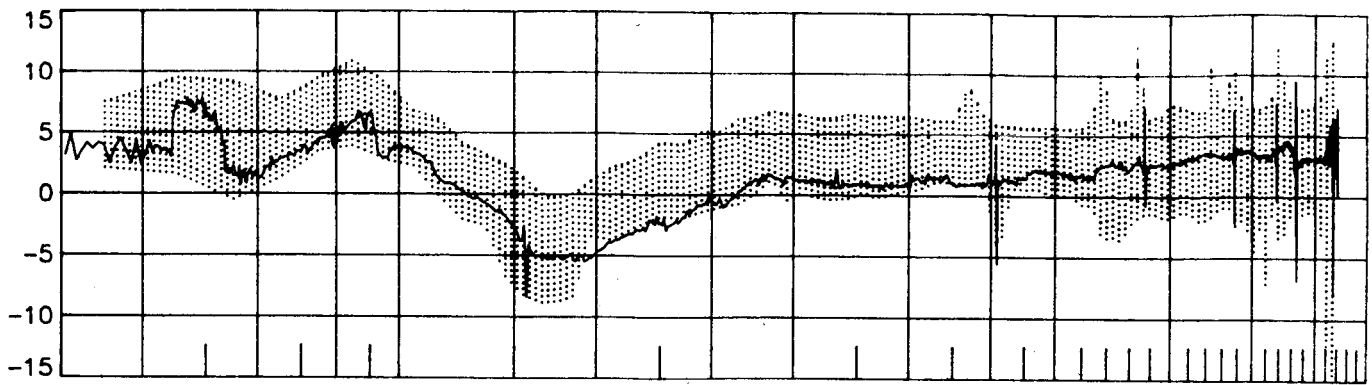
ORIGINAL PAGE IS
OF POOR QUALITY



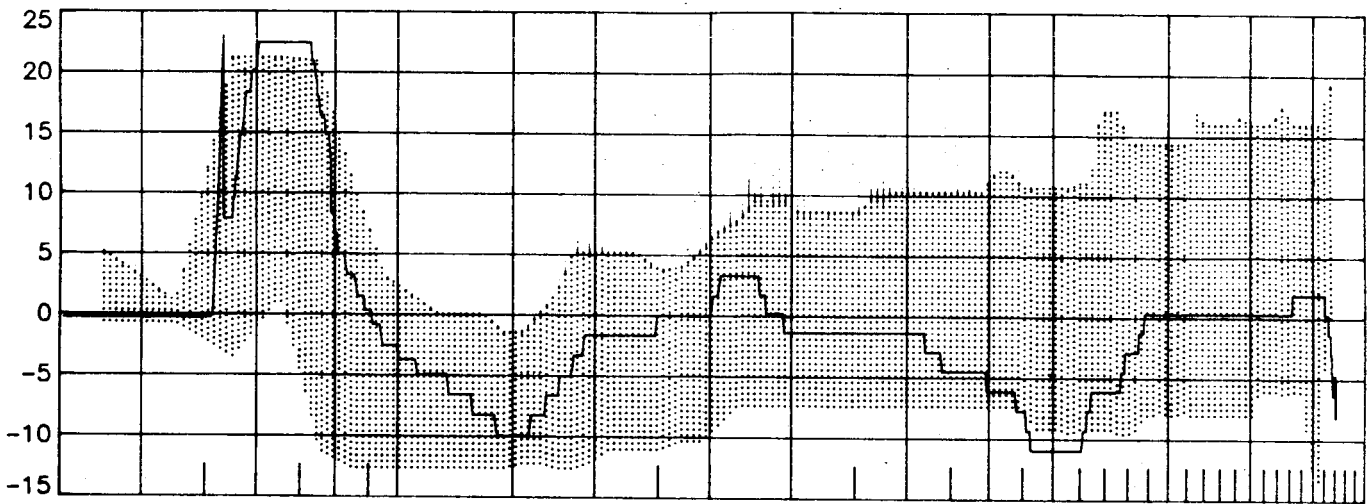
APPENDIX L

Summary of STS-11 (41-B) longitudinal results and comparisons.

δ_E , deg



δ_{BF} , deg



δ_{SBA} , deg

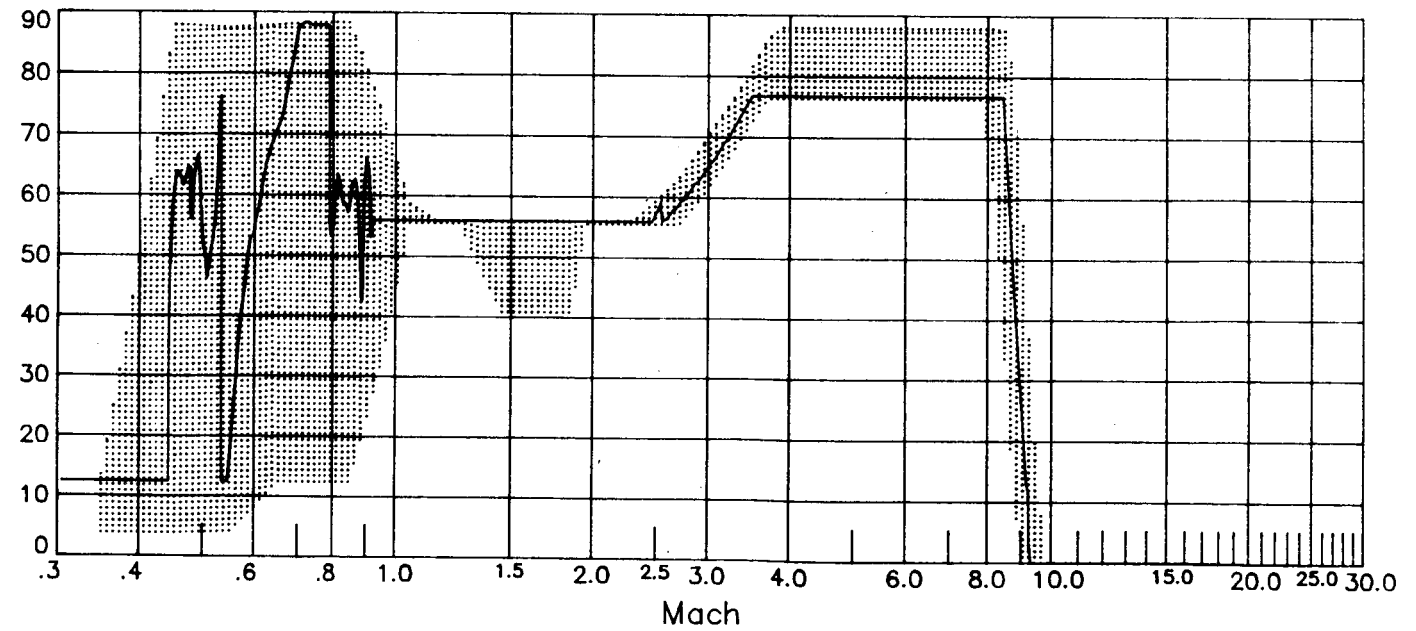
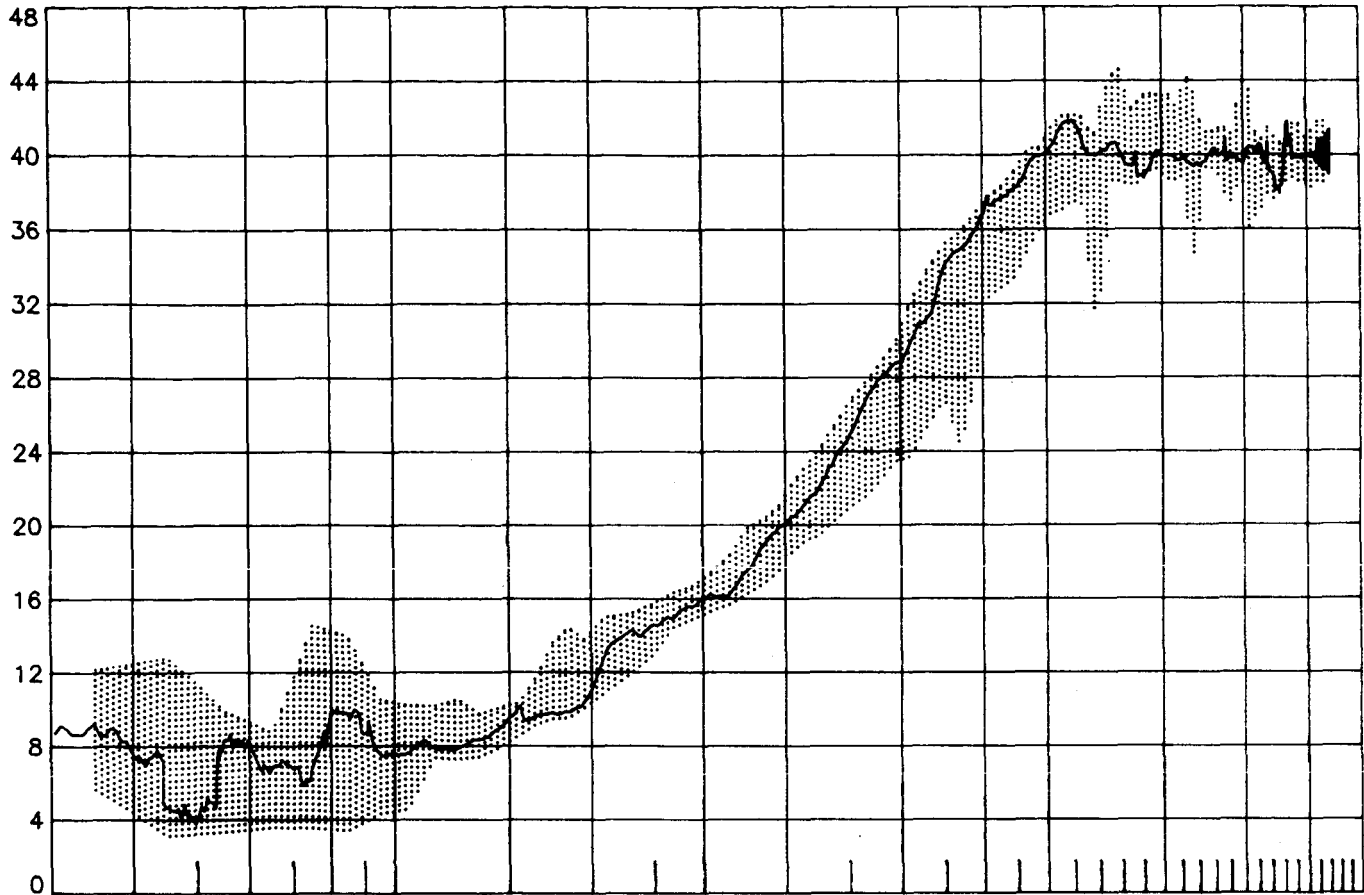


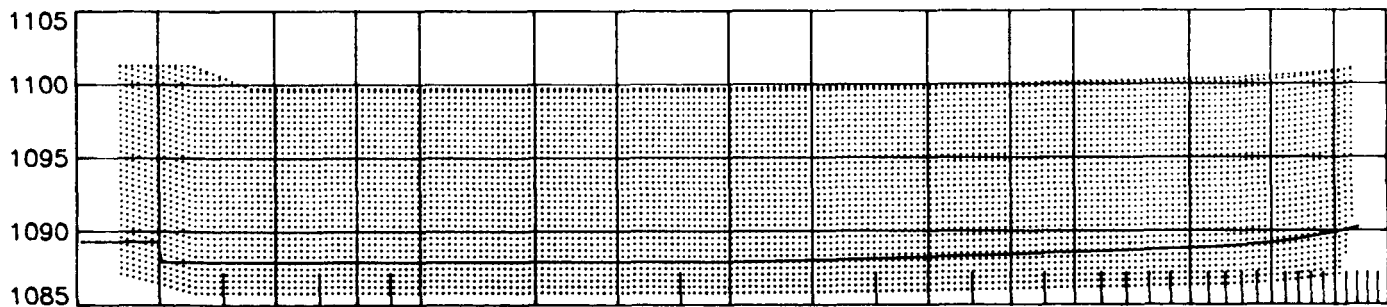
Figure L-1 STS-11 longitudinal control surface deflections
(shaded region defined by remaining ten flights)

ORIGINAL FIGURE
OF POOR QUALITY

α , deg



x_{cg} , in



z_{cg} , in

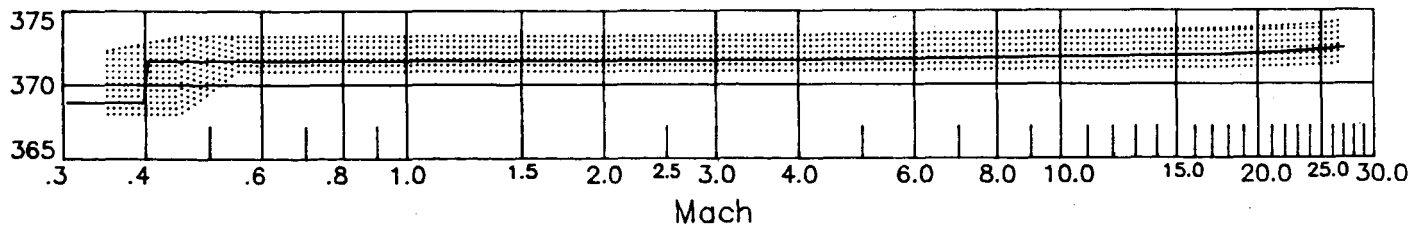
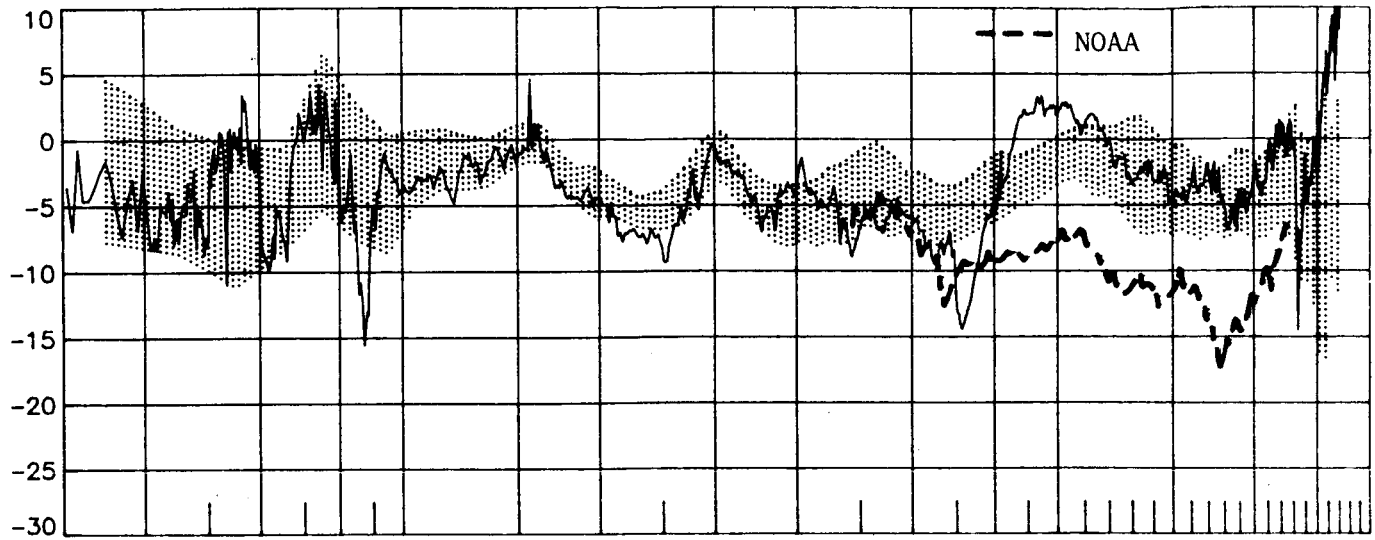


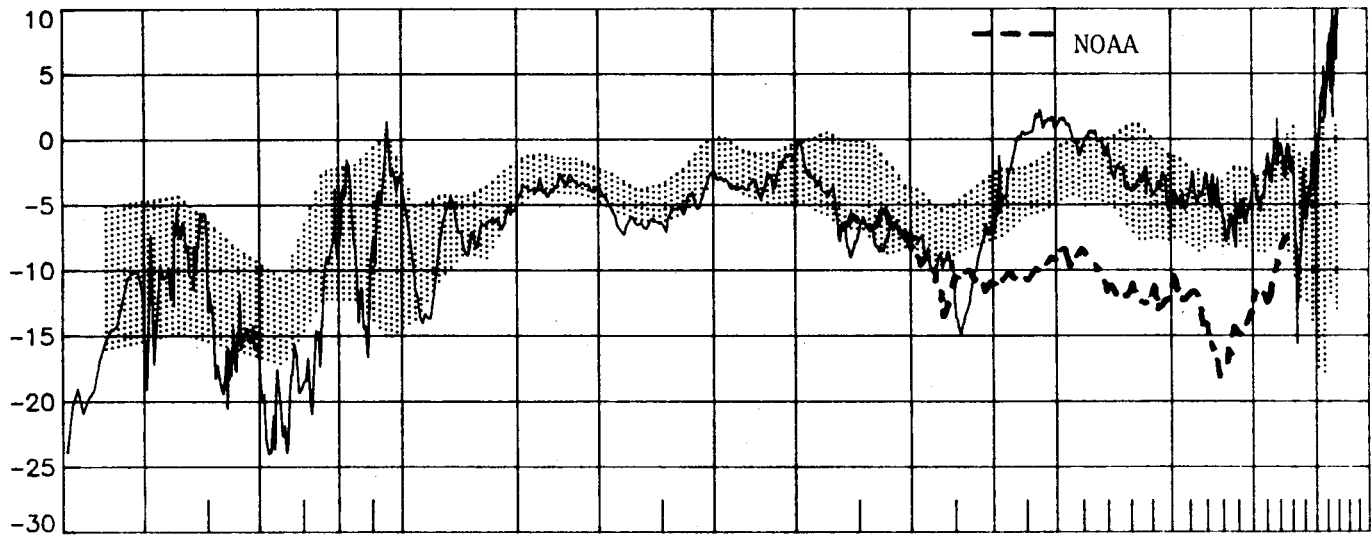
Figure L-2 STS-11 angle-of-attack and c.g. profiles
(shaded region defined by remaining ten flights)

ORIGINAL DATA
OF POOR QUALITY

ΔC_L , percent



ΔC_D , percent



$\Delta(L/D)$, percent

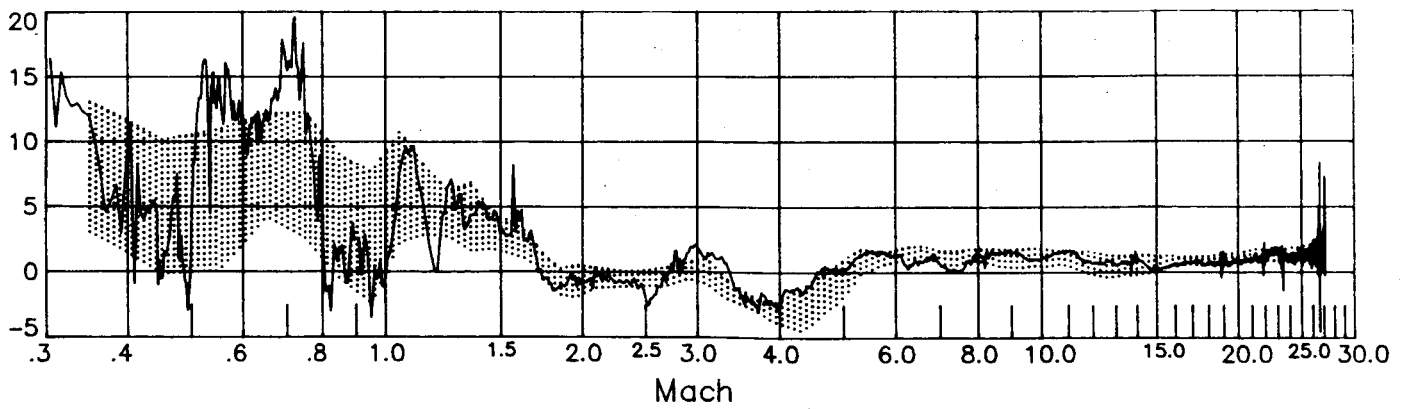
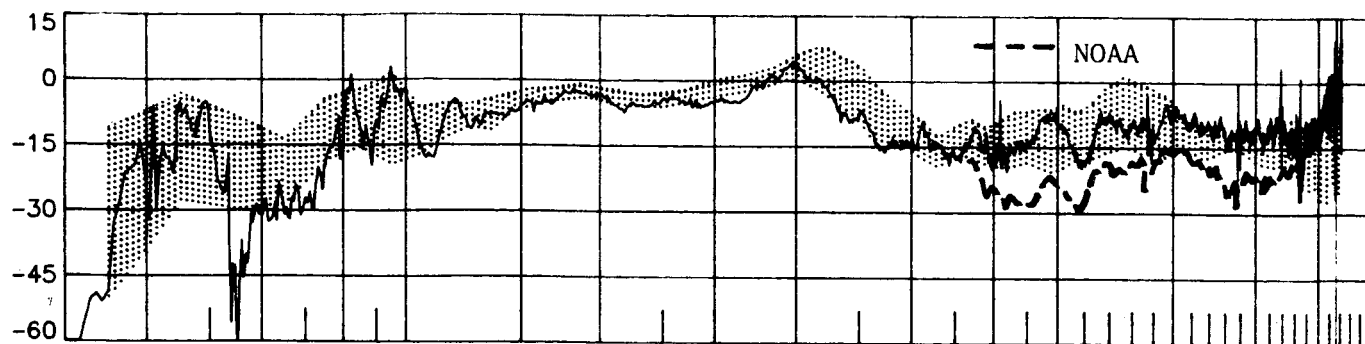
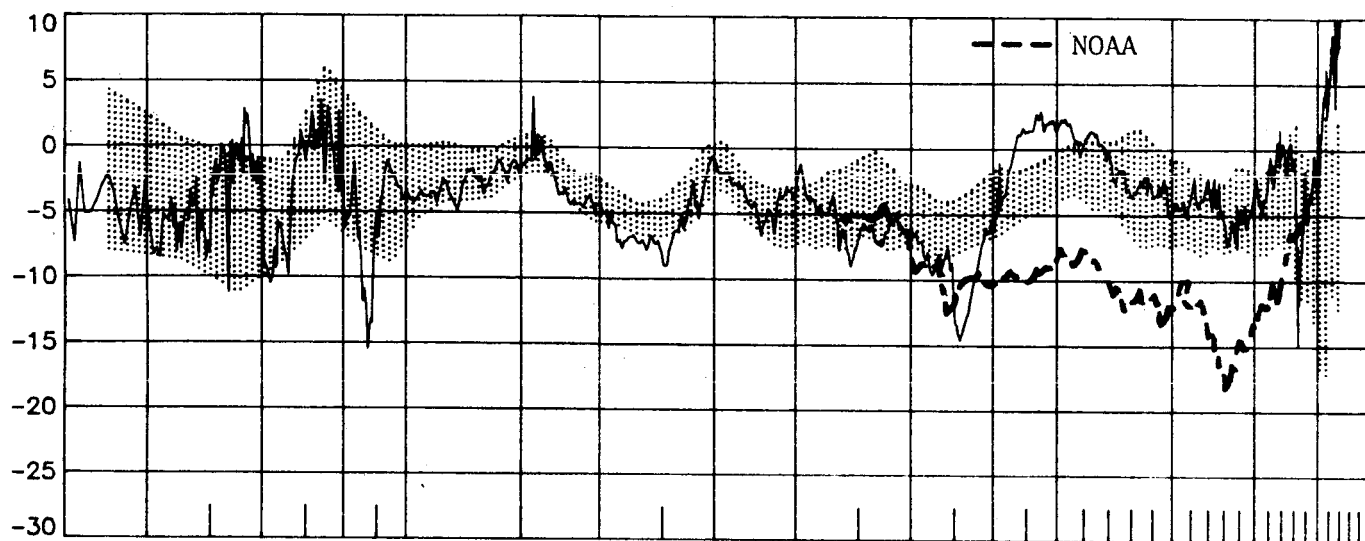


Figure L-3 STS-11 longitudinal performance comparisons
(shaded region defined by remaining ten flights)

ΔC_A , percent



ΔC_N , percent



ΔC_m , percent

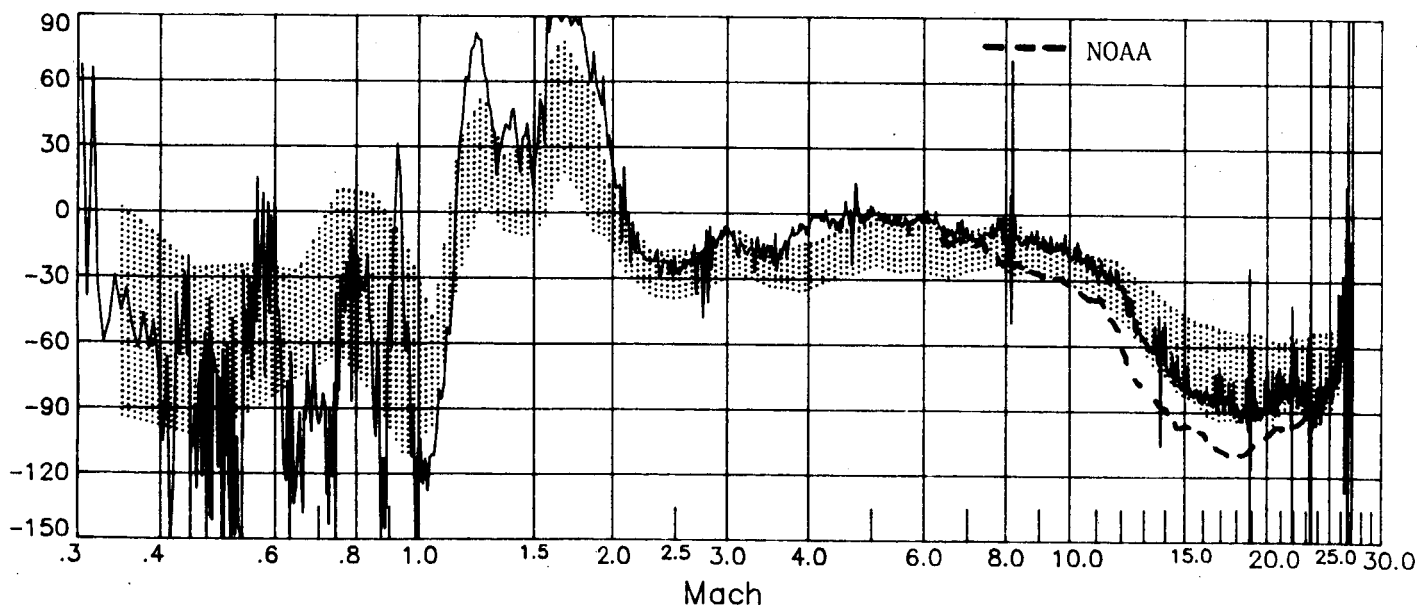


Figure L-3 (concluded)

(shaded region defined by remaining ten flights)

ORIGINAL DATA
OF POOR QUALITY

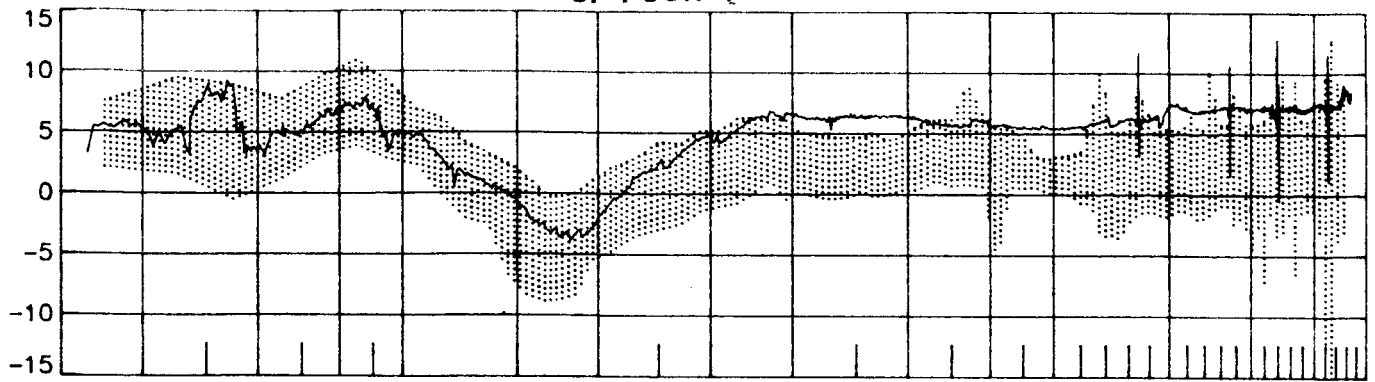


APPENDIX M.

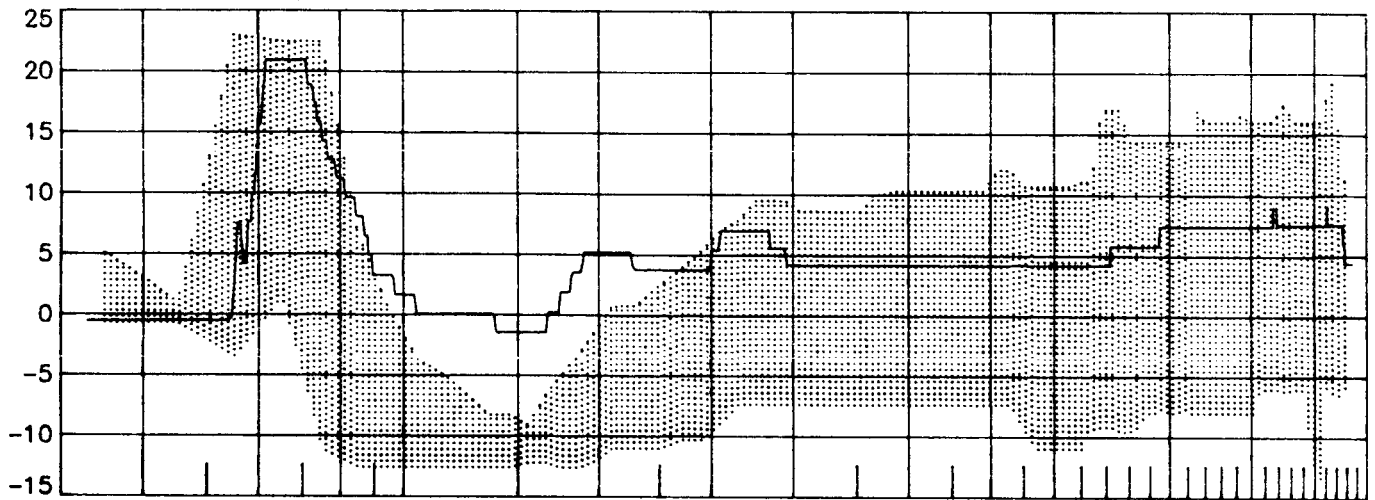
Summary of STS-13 (41-C) longitudinal results and comparisons.

ORIGINAL PAGE IS
OF POOR QUALITY

δ_E , deg



δ_{BF} , deg



δ_{SBA} , deg

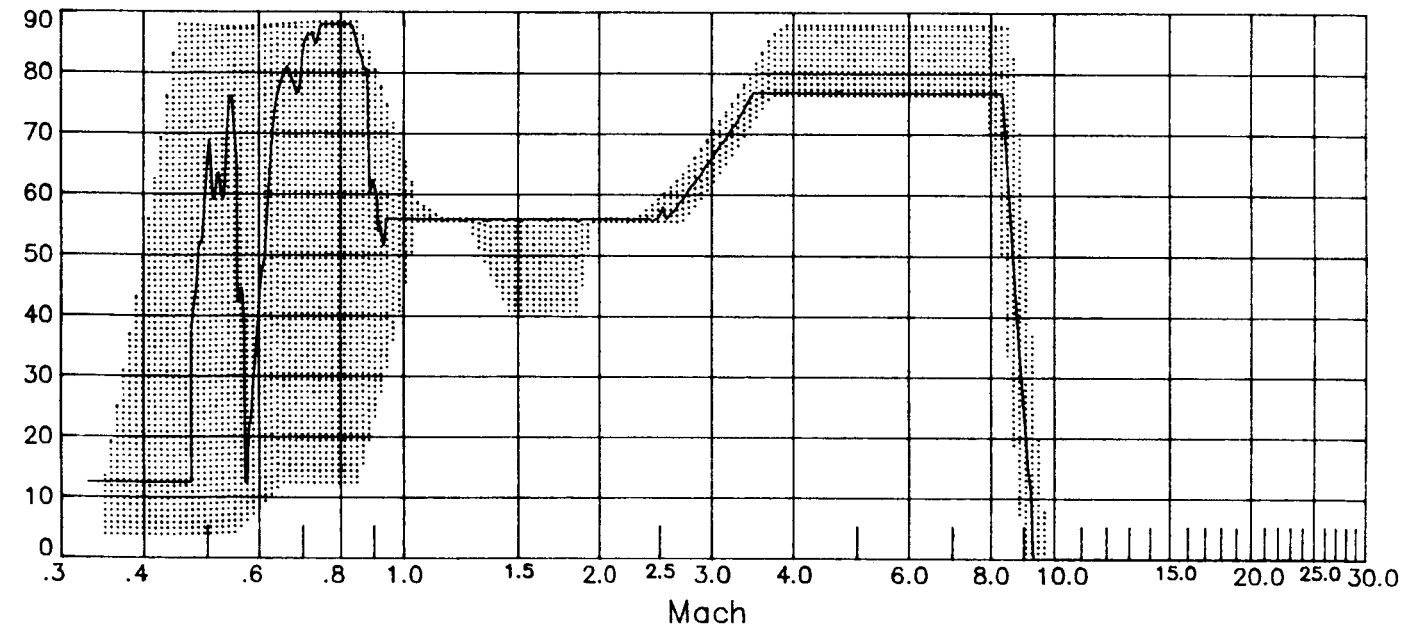
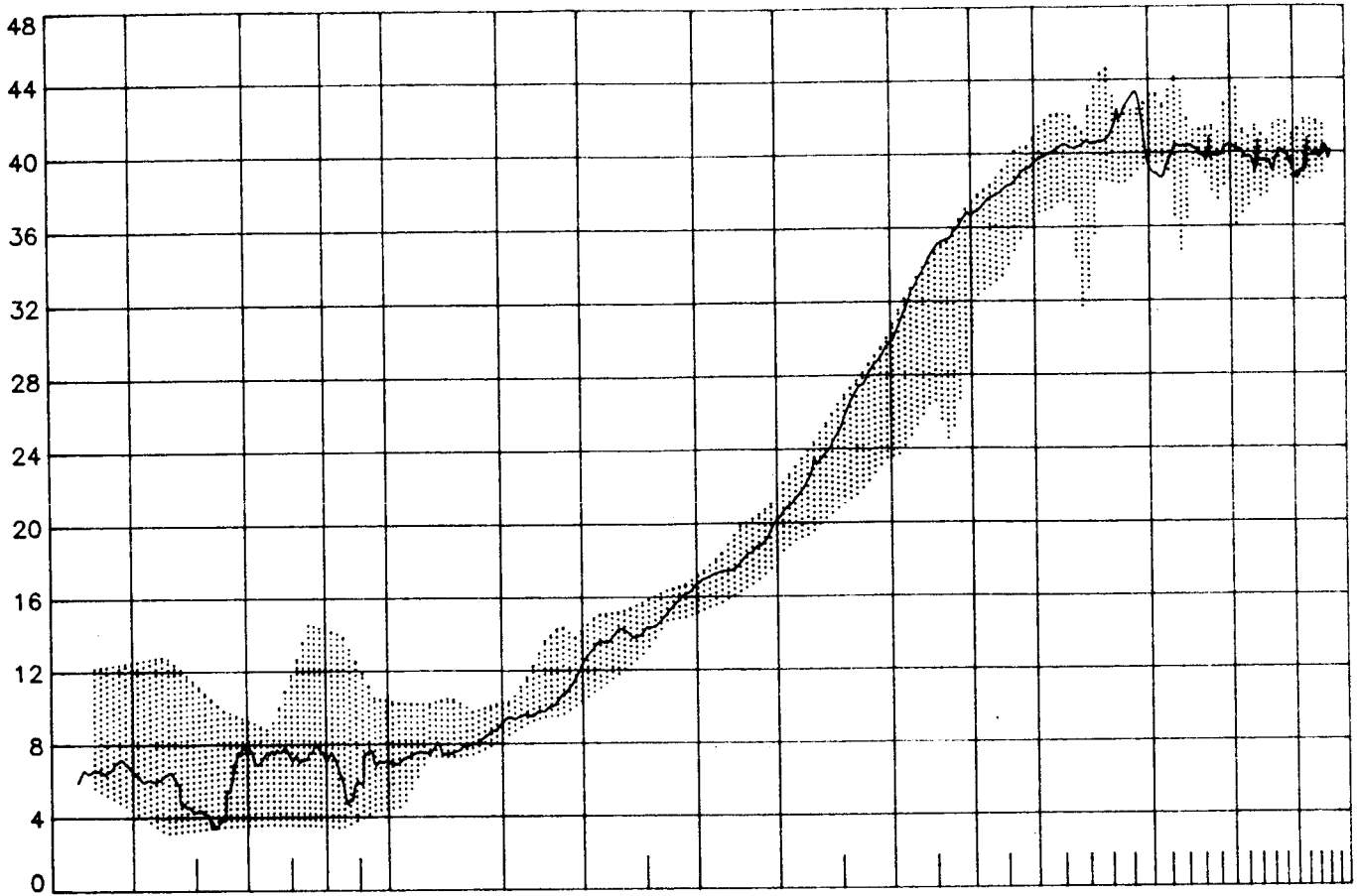
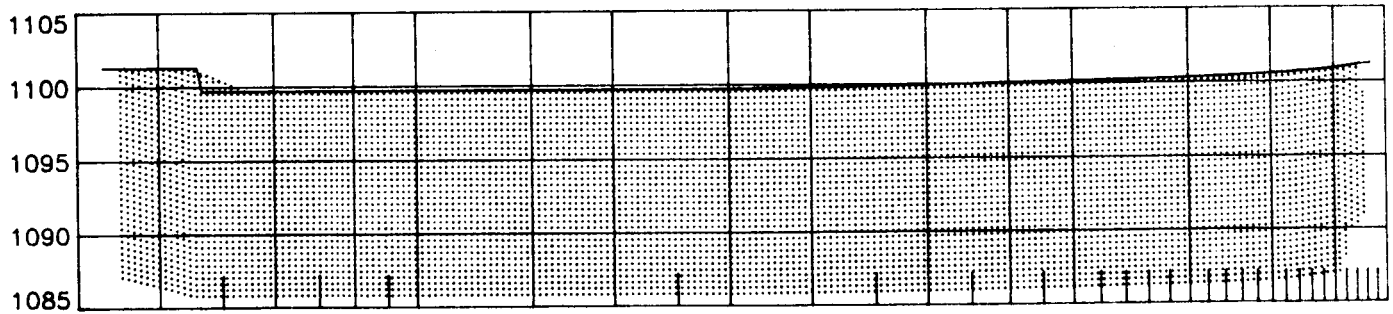


Figure M-1 STS-13 longitudinal control surface deflections
(shaded region defined by remaining ten flights)

α , deg



x_{cg} , in



z_{cg} , in

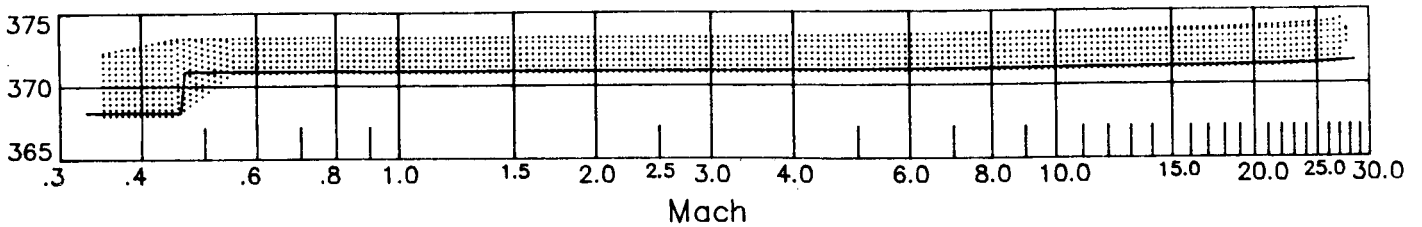
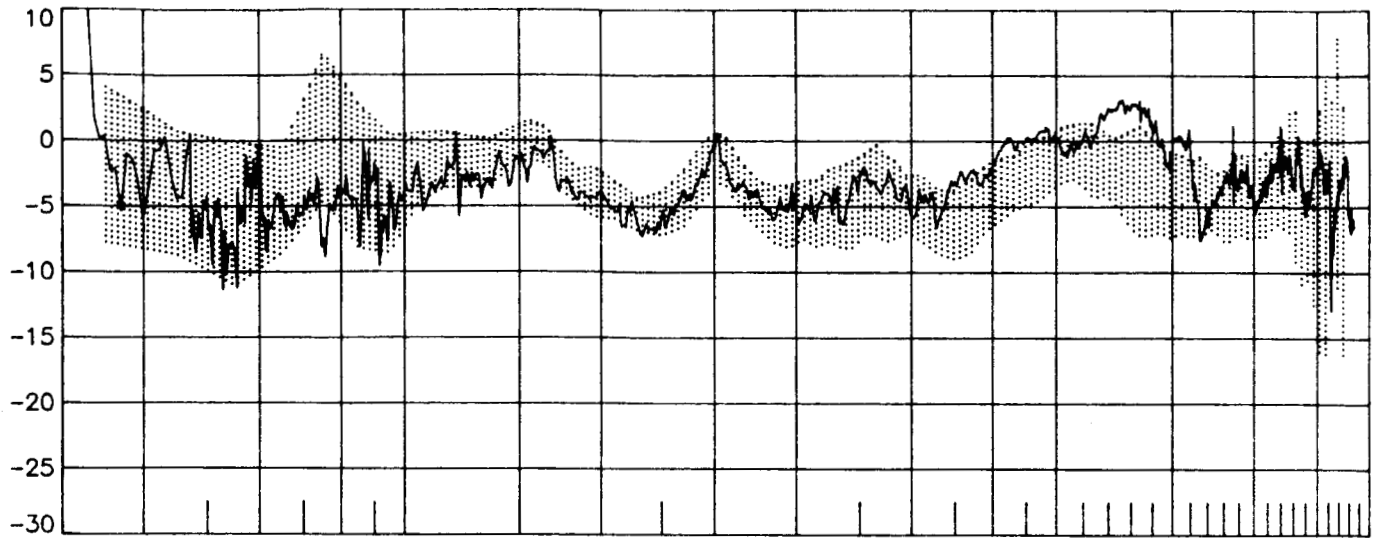
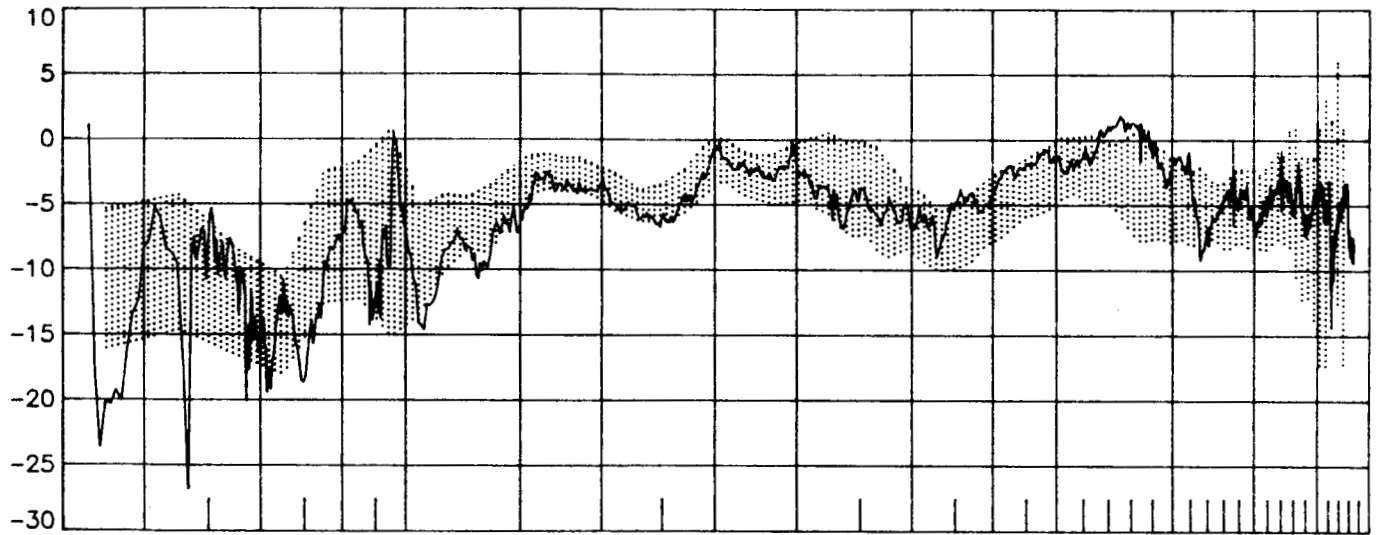


Figure M-2 STS-13 angle-of-attack and c.g. profiles
(shaded region defined by remaining ten flights)

ΔC_L , percent



ΔC_D , percent



$\Delta(L/D)$, percent

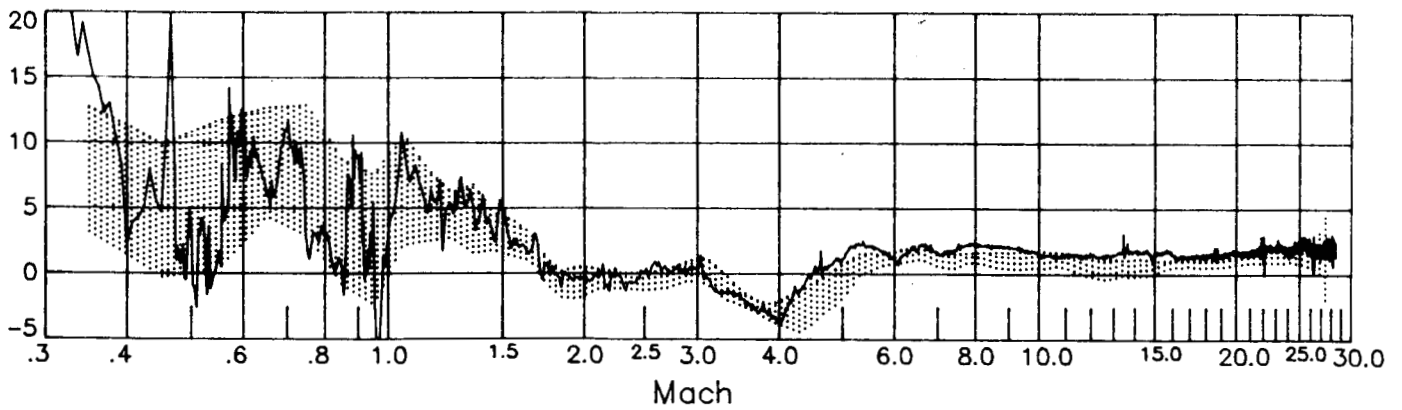
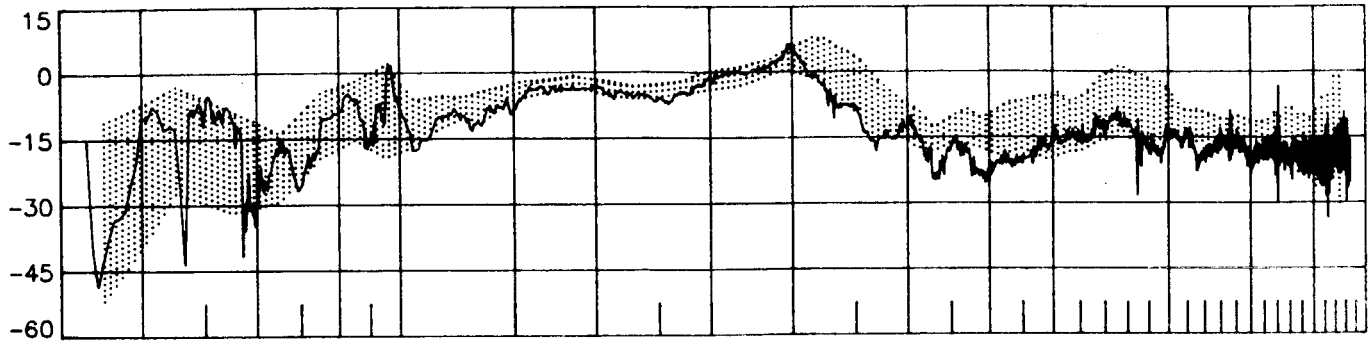


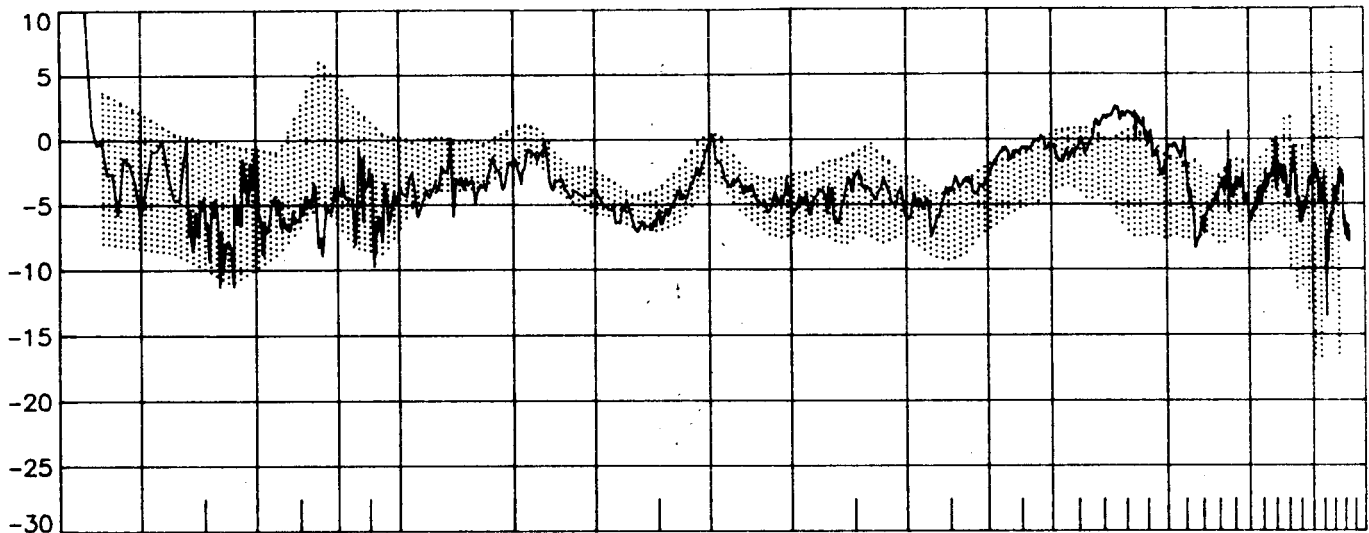
Figure M-3 STS-13 longitudinal performance comparisons
(shaded region defined by remaining ten flights)

ORIGINAL PAGE IS
OF POOR QUALITY

ΔC_A , percent



ΔC_N , percent



ΔC_m , percent

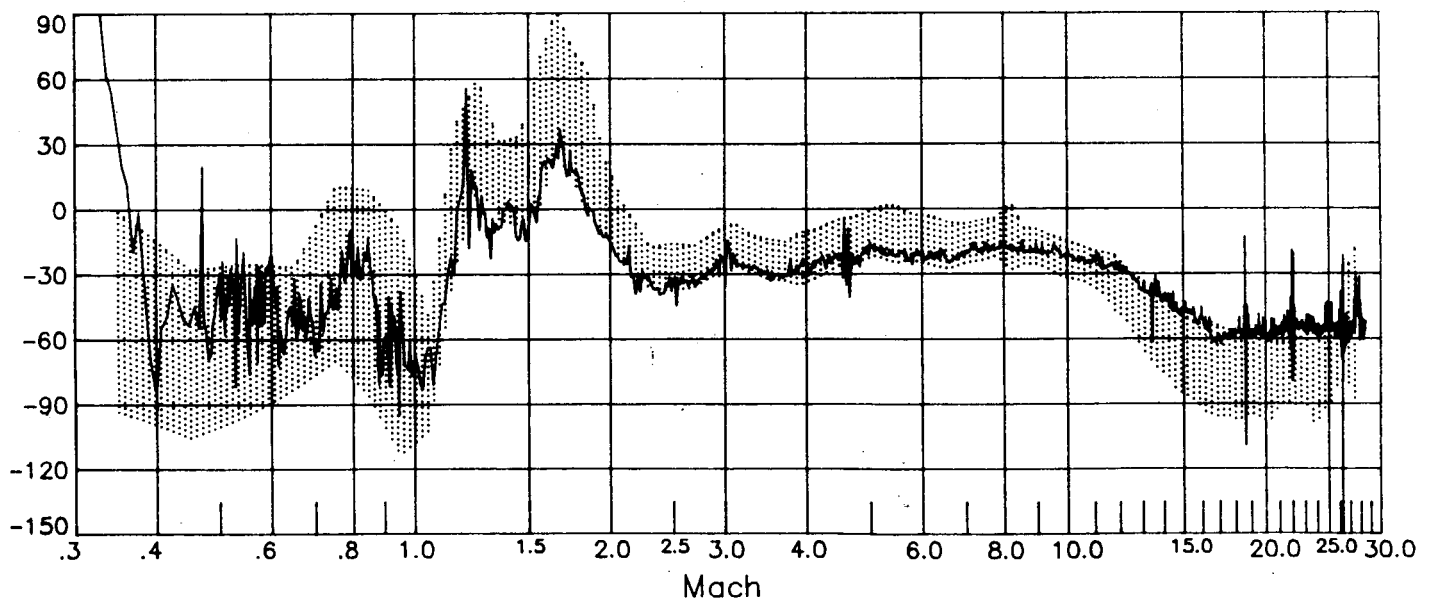
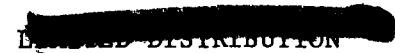




Figure M-3 (concluded)

(shaded region defined by remaining ten flights)

1. Report No. NASA CR-172440		2. Government Accession No.		3. Recipient's Catalog No.	
4. Title and Subtitle FINAL REPORT: Summary of Shuttle Data Processing and Aerodynamic Performance Comparisons for the First Eleven(11) Flights				5. Report Date September 1984	
				6. Performing Organization Code	
7. Author(s) John T. Findlay, G. Mel Kelly, Michael L. Heck, Judy G. McConnell				8. Performing Organization Report No. AMA Report No. 84-10	
9. Performing Organization Name and Address Analytical Mechanics Associates, Inc. 17 Research Road Hampton, VA. 23666				10. Work Unit No.	
				11. Contract or Grant No. NAS1-16087	
12. Sponsoring Agency Name and Address National Aeronautics and Space Administration Washington, DC 20546				13. Type of Report and Period Covered Contractor Report	
				14. Sponsoring Agency Code 506-51-13-06	
15. Supplementary Notes Langley Technical Monitor: Harold R. Compton					
16. Abstract <p>NASA Space Shuttle aerodynamic and aerothermodynamic research is but one part of the most comprehensive end-to-end flight test program ever undertaken considering: the extensive pre-flight experimental data base development; the multitude of spacecraft and remote measurements taken during entry flight; the complexity of the Orbiter aerodynamic configuration; the variety of flight conditions available across the entire speed regime; and the efforts devoted to flight data reduction throughout the aerospace community. Shuttle entry flights provide a wealth of research quality data, in essence a veritable "flying wind tunnel", for use by researchers to verify and improve the operational capability of the Orbiter and provide data for evaluations of experimental facilities as well as computational methods. This final report merely summarizes the major activities conducted by the AMA, Inc. under NASA Contract NAS1-16087 as part of that interesting research. Investigators desiring more detailed information can refer to the glossary of AMA publications attached herein as Appendix A. Section I provides a background discussion of software and methodology development to enable Best Estimate Trajectory (BET) generation. Actual products generated are summarized in Section II as tables which completely describe the post-flight products available from the first three-year Shuttle flight history. Summary results are presented in Section III, with longitudinal performance comparisons included as Appendices for each of the flights.</p>					
17. Key Words (Suggested by Author(s)) Space Shuttle STS, Best Estimate Trajectory, Atmospheric Data, Flight Extracted Aerodynamics, Predicted Aerodynamics, Performance and Configuration Comparisons, MMLE Input Files			18. Distribution Statement   		
19. Security Classif. (of this report) Unclassified		20. Security Classif. (of this page) Unclassified		21. No. of Pages 124	22. Price